UNIVERSIDAD DE EXTREMADURA

TESIS DOCTORAL / PHD THESIS

METAHEURÍSTICAS MULTIOBJETIVO PARA LA RESOLUCIÓN DEL PROBLEMA DEL POSICIONAMIENTO DE NODOS REPETIDORES EN REDES DE SENSORES INALÁMBRICOS

MULTIOBJECTIVE METAHEURISTICS FOR SOLVING THE RELAY NODE PLACEMENT PROBLEM IN WIRELESS SENSOR NETWORKS

José Manuel Lanza-Gutiérrez

DEPARTAMENTO DE TECNOLOGÍA DE LOS COMPUTADORES Y DE LAS COMUNICACIONES

DEPARTMENT OF TECHNOLOGIES OF COMPUTERS AND COMMUNICATIONS

2015

UNIVERSIDAD DE EXTREMADURA

TESIS DOCTORAL / PHD THESIS

Metaheurísticas Multiobjetivo para la Resolución del Problema del Posicionamiento de Nodos Repetidores en Redes de Sensores Inalámbricos

Multiobjective Metaheuristics for Solving the Relay Node Placement Problem in Wireless Sensor Networks

José Manuel Lanza-Gutiérrez

Departamento de Tecnología de los Computadores y de las Comunicaciones

Department of Technologies of Computers and Communications

Conformidad del director / Advisor's conformity:

Prof. Dr. Juan A. Gómez-Pulido

2015

SCORING SHEET

Ph.D. title: Multiobjective Metaheuristics for Solving the Relay Node Placement Problem in Wireless Sensor Networks

Affiliation: Department of Technologies of Computers and Communications

Author: José Manuel Lanza-Gutiérrez

Advisor: Prof. Dr. Juan A. Gómez-Pulido

Supervisory Committee

1. Reviewer:

Signature:

2. Reviewer:

Signature:

3. Reviewer:

Signature:

4. Reviewer:

Signature:

5. Reviewer:

Signature:

Day of the defense:

Score:

Ph.D. thesis: *Multiobjective Metaheuristics for Solving the Relay Node Placement Problem in Wireless Sensor Networks*

Author: José Manuel Lanza-Gutiérrez

Advisor: Prof. Dr. Juan A. Gómez-Pulido

Affiliation: Department of Technologies of Computers and Communications - Polytechnic School - University of Extremadura - Cáceres - Spain

Author's email: jmlanza@unex.es

Text printed in Madrid (Spain)

First edition, October 2015

Try to make sense of what you see and wonder about what makes the universe exist. Be curious, and however difficult life may seem, there is always something you can do, and succeed at. It matters that you do not just give up.

Stephen Hawking

Abstract

Nowadays, Wireless Sensor Networks (WSNs) are widely considered in many fields of application, such as intensive agriculture, industrial control, environmental monitoring, and robotics, among many others. Traditionally, a WSN is composed of a set of sensors, capturing information about the environment, and a sink node, which collects all the information provided by the network. The sensors have some interesting features, encouraging the use of this technology, e.g. they are small, power-autonomous, cheap, and wireless. These features allow considering WSNs in environments, where the deployment of other technologies would be impossible or really expensive. In fact, this is one of the great contributions of this technology.

Nevertheless, WSNs also have shortcomings, affecting critical features, such as energy consumption and quality of service. Traditionally, the sensors are powered by batteries to assume cheap devices and avoid wires. Thus, WSNs are particularly sensitive to energy cost. This problem is increased further if the network considers an usual multi-hop routing protocol, where the devices send data to each other's.

In recent years, a new device specialised in communication tasks and called Relay Node (RN) is added to traditional WSNs as a possible way to address this issue, resulting in the Relay Node Placement Problem (RNPP), which is defined as an NP-hard optimisation problem in the literature. In this thesis, we tackle three different approaches of the RNPP, divided into two groups: outdoor and indoor networks.

In the first approach, we study how to efficiently deploy energy-harvesting RNs in previously-established static outdoor WSNs for optimising average energy consumption and average coverage. The second approach is a more realistic version of the previous deployment problem, where we also optimise network reliability. Both approaches are solved by applying a wide range of MultiObjective (MO) metaheuristics. Specifically, we implement Non-dominated Sorting Genetic Algorithm II (NSGA-II), Strength Pareto Evolutionary Algorithm 2 (SPEA2), Multiobjective Variable Neighbourhood Search Algorithm (MO-VNS), Multiobjective Artificial Bee Colony Algorithm (MO-ABC), Multiobjective Firefly Algorithm (MO-FA), Multiobjective Gravitational Search Algorithm (MO-GSA), and Multiobjective Evolutionary Algorithm Based on Decomposition (MOEA/D).

In the third approach and based on the knowledge obtained from the outdoor problem, we propose a new line of research not considered before in the literature: the deployment of low-cost static indoor WSNs, trying to leverage existing infrastructure. This new MO problem derives from the need to deploy low-cost networks for providing indoor localisation services, e.g. for domestic and industrial robots.

Resumen

Hoy en día, las Redes de Sensores Inalámbricas (WSNs, del inglés Wireless Sensor Networks) son usualmente utilizadas en campos como la agricultura intensiva, el control industrial, la monitorización ambiental y la robótica, entre otros. Tradicionalmente, una WSN se compone de un conjunto de sensores, que capturan información sobre el entorno, y un nodo central, que recolecta toda la información proporcionada por la red. Los sensores presentan algunas interesantes características que incitan el uso de esta tecnología, ej. son pequeños, autónomos, baratos e inalámbricos. Estas características permiten que las WSNs puedan ser utilizadas en entornos, donde para otras tecnologías sería imposible o tendría un elevado coste. De hecho, ésta es una de las grandes contribuciones de esta tecnología.

No obstante, las WSNs también presentan inconvenientes, que afectan factores como el consumo energético y la calidad de servicio. Habitualmente, los sensores se alimentan mediante baterías para evitar el uso de cables y obtener dispositivos económicos. En consecuencia, las WSNs son particularmente sensibles al consumo energético. Este problema se acrecienta aún más al considerar protocolos de enrutado multi-salto, donde todos los dispositivos pueden comunicarse entre si.

Recientemente, un nuevo dispositivo especializado en tareas de comunicación y denominado Nodo Repetidor (RN, del inglés Relay Node), fue añadido a las WSNs tradicionales como una posible vía de abordar esta cuestión, dando lugar al Problema del Posicionamiento de Nodos Repetidores (RNPP, del inglés Relay Node Placement Problem), el cual es definido como un problema de optimización NP-completo en la literatura. En esta tesis abordamos tres diferentes versiones del RNPP, divididas en torno a dos grupos: WSNs exteriores y WSNs interiores.

En la primera versión estudiamos cómo desplegar RNs en WSNs exteriores estáticas previamente establecidas, con el objetivo de optimizar el consumo energético medio y la cobertura media. La segunda versión aporta un enfoque más realista sobre la primera, donde además optimizamos la robustez de la red. Ambas versiones se resuelven mediante múltiples metaheurísticas multiobjetivo: NSGA-II (del inglés, Non-dominated Sorting Genetic Algorithm II), SPEA2 (del inglés Strength Pareto Evolutionary Algorithm 2), MO-VNS (del inglés, Multiobjective Variable Neighbourhood Search Algorithm), MO-ABC (del inglés, Multiobjective Artificial Bee Colony Algorithm), MO-FA (del inglés, Multiobjective Firefly Algorithm), MO-GSA (del inglés, Multiobjective Gravitational Search Algorithm) y MOEA/D (del inglés Multiobjective Evolutionary Algorithm Based on Decomposition).

En la tercera versión y basándonos en el conocimiento adquirido, proponemos una novedosa línea de investigación: el despliegue de WSNs interiores estáticas de bajo coste, tratando de aprovechar la infraestructura existente. Este nuevo problema de optimización se deriva de la necesidad de desplegar redes interiores de bajo coste para proporcionar servicios de localización, ej. para robótica doméstica y del hogar.

Contents

List of Figures

List of Tables

List of Algorithms

Acronyms

ABC Artificial Bee Colony

ACO Ant Colony Optimisation

CHIM Convex Hull of Individual Minima

CPU Central Processing Unit

CUDA Compute Unified Device Architecture

EA Evolutionary Algorithm

FA Firefly Algorithm

GA Genetic Algorithm

GLS Guided Local Search

GPU Graphics Processing Unit

GRASP Adaptive Search Procedure

GSA Gravitational Search Algorithm

ILS Iterated Local Search

MIMD Multiple Instruction Multiple Data

MISD Multiple Instruction Single Data

MO MultiObjective

MO-ABC MultiObjective Artificial Bee Colony

MO-FA MultiObjective Firefly Algorithm

MO-GSA MultiObjective Gravitational Search Algorithm

MO-VNS MultiObjective Variable Neighbour Search Algorithm

MOEA/D MultiObjective Evolutionary Algorithm based on Decomposition

MOP Multiobjective Optimisation Problem

MPI Message Passing Interface

NBI Normal Boundary Intersection

NP-hard Non-deterministic Polynomial-time hard

NSGA-II Non-dominated Sorting Genetic Algorithm II

NUMA Non-Uniform Memory Access

PoI Point Of Interest

PSO Particle Swarm Optimisation

QoS Quality of Service

RN Relay Node

RNPP Relay Node Placement Problem

SIA Swarm Intelligence Algorithm

SIMD Single Instruction Multiple Data

SISD Single Instruction Single Data

SO Single Objective

SOP Singleobjective Optimisation Problem

SPEA2 Strength Pareto Evolutionary Algorithm 2

ST Single-Tiered

TA Trajectory Algorithm

UMA Uniform Memory Access

VNS Variable Neighbour Search Algorithm

WSA Weighted Sum Approach

WSN Wireless Sensor Network

WTA Weighted Tchebycheff Approach

CHAPTER

1

Introduction

In the last years, Wireless Sensor Networks (WSNs) are one of the most important emerging technologies, being considered in many different fields, such as forest fire detection, traffic monitoring, industrial control, military surveillance, intensive agriculture, and robotics [1]. Traditionally, these networks are composed of many autonomous low-cost sensing devices, capturing information about the environment, and a single sink node, collecting all this data.

In this thesis, we study a critical deployment problem for large-scale WSNs: the addition of Relay Nodes (RNs) to traditional WSNs as a way to optimise such networks, the so-called Relay Node Placement Problem (RNPP). This issue was defined as a complex optimisation problem in the literature [2][3]. This means that traditional exact techniques cannot be considered due to the computational effort required, when the complexity of the problem raises.

Most problems in the real world are defined as complex, because of the great amount of factors involved in their resolution. As a potential way to solve this issue, metaheuristics provide approximate solutions with a good balance between solution quality and computational effort required. The concept is that, in many cases, a good approximate solution could be almost as good as the result of the exact technique. This type of solving methodology has shown a good behaviour in many current state-of-the-art optimisation problems as detailed in [4].

Following this potential way, we propose to apply MultiObjective (MO) metaheuristics for solving the RNPP, i.e. metaheuristics optimising multiple criteria at the same time. Specifically, we study the behaviour of eight MO metaheuristics in two different approaches of the outdoor RNPP from lower to higher problem complexity: two objectives and three objectives. Next and based on the acquired knowledge, we propose a new line of research of the indoor RNPP for three objectives. This novel problem is studied by applying two standard MO metaheuristics.

Next we detail the major motivations which led us to tackle the thesis, the planning followed to conduct the research, and the organisation of the entire document.

1.1 Motivation

As detailed before, a traditional WSN is composed of a set of sensors and a sink node. The sensors have some features encouraging the use of this technology, e.g. they are small, power-autonomous, cheap, and able to capture different types of measures in a same device. In addition, the use of wireless technologies facilitates the network deployment, so reducing costs. These features, among others, allow considering WSNs in environments where the deployment of other technologies would be very expensive or impossible, such as wired networks [5].

Figure 1.1 compares two different approaches for covering a crop field by assuming Points of Interest (PoI), points where we are interested in getting a physical measure. In this case, we consider a PoI in each tree and a single sink node connected to the Internet. If we assume a traditional wired network as in Figure 1.1a, we need to deploy a sink node and a device including a sensor in each PoI, adding the wires needed for providing power supply and connectivity. On the other hand, if we consider a traditional WSN as in Figure 1.1b, we have to deploy the same number of devices, adding only additional sensors if needed for getting a connected network because of range limitations. The second approach is more interesting, because it is cheaper of deploying and upgrading without having a previous infrastructure. The inclusion of additional sensors is not a really serious issue, due to its current reduced price, about 10-20 euro each one.

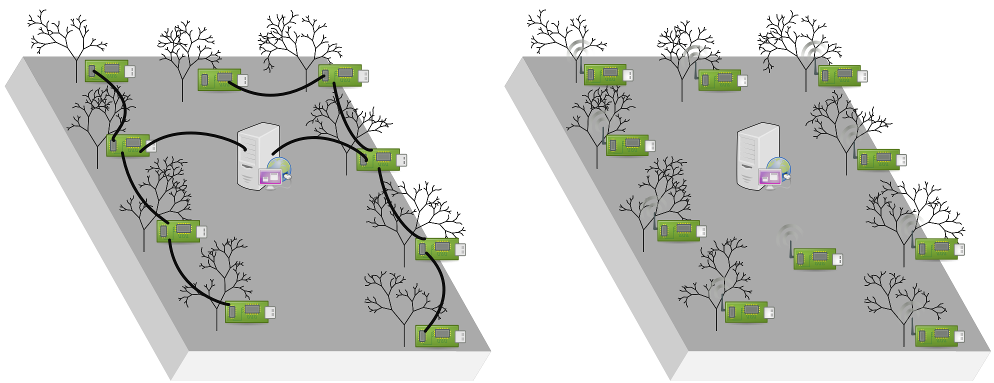

(a) Wired network. **(b)** WSN.

Figure 1.1: Comparing two different approaches for covering a crop field.

Nevertheless, WSNs also have unsolved shortcomings, affecting critical features for the industry, e.g. energy consumption, reliability, and Quality of Service (QoS). The sensors are powered by batteries to avoid wires and get cheaper devices. This means that WSNs are particularly sensitive to energy cost, affecting the network behaviour. If the sensors send data to the sink node by assuming a simple star topology, the energy cost distribution of all the sensors would be similar as in Figure 1.2a. However, if we assume a habitual multi-hop topology for larger networks, where the sensors relay data, the workload of all the devices could not be similar as in Figure 1.2b. This situation involves the existence of bottlenecks, i.e. sensors subject to higher energy cost than others, which means that the batteries drain faster.

In the last years and with the goal of reducing these bottlenecks, a new device specialised in communication tasks was added to traditional WSNs [6]. This device is called RN and forwards all the received information to the sink node, so reducing the communication workload of the sensors. The RNs have higher energy capacity than the sensors, e.g. they could be plugged into

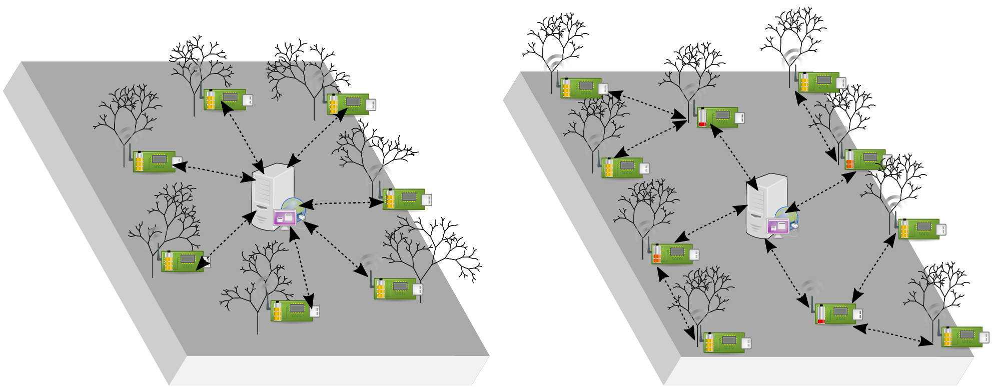

(a) Star topology. **(b)** Muti-hop topology.

Figure 1.2: Analysing energy cost in both single-hop and multi-hop WSNs.

the grid, have greater batteries, or be energy-harvesting devices. This way, they are more expensive than the sensors and their deployment must be carefully studied to ensure the investment. The efficient deployment of these RNs is the issue addressed in the RNPP.

As stated before, the efficient deployment of WSNs is defined as a complex optimisation problem in the literature, specifically a Non-deterministic Polynomial-time hard (NP-hard) problem [7]. Most papers in the literature solve the problem by assuming heuristics or Single-Objective (SO) metaheuristics, metaheuristics optimising a single criterion, but not through a more realistic MO focus. Based on this motivation, the major goal of this thesis is to propose and solve a more realistic formal statement of the RNPP for both indoor and outdoor scenarios, assuming to this end state-of-the-art MO metaheuristics. Moreover, this type of solving-methodologies usually provides a good behaviour solving such NP-hard problems, getting trade-off solutions, which facilitates the decision-making task in industrial settings.

1.2 Research Planning

As in any project, designing a good work strategy is crucial to ensure that the objectives proposed at the beginning of the project can be reached. Table 1.1 shows the initial milestone plan developed for this PhD thesis, where each task falls within one of the five main phases, i.e. A) Acquire knowledge, B) First approach: solving the outdoor RNPP for two objectives, C) Second approach: solving the outdoor RNPP for three objectives, D) Third approach: propose a more realistic indoor RNPP for three objectives, and E) Dissemination of the work done.

As Figure 1.3 shows, the project starts with the phase A, acquiring the initial knowledge needed for performing the work. Next in phase B, we assume the optimisation of an outdoor RNPP for two objectives. In phase C, we complete the model tackled in phase B by adding a new objective to optimise. In phase D and based on the previous models studied, we propose to solve a more realistic indoor approach of the RNPP for three objectives. Finally, in phase E, we disseminate the work done during all the research. As expected, phases A and E coexist for almost the entire duration of the project and phases B, C, and D are undertaken sequentially. Note that in phase A, we need to study parallel computing, because we consider this technology to reduce execute times, when running the algorithms, e.g. for adjusting the metaheuristics. In this dissertation, we do not include any analysis while considering parallel computing, because this is not the main aim of this thesis, instead we consider it as a tool.

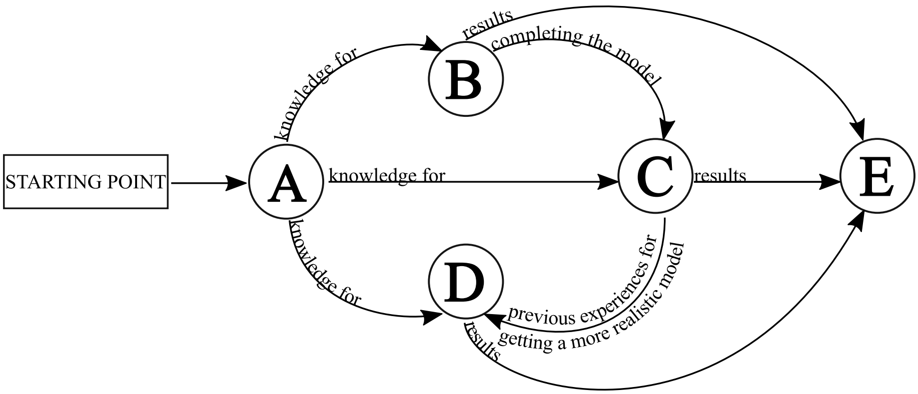

Figure 1.3: Relationship between project phases.

Table 1.1: Initial milestone plan.

Phase	Milestone	Milestone goal
A	Acquire knowledge of scientific method	Study the methodologies for getting a good research work
	Acquire knowledge of WSNs	Study the fundamentals of WSNs: technology, shortcomings, etc.
	Acquire knowledge of optimisation	Study the fundamentals of optimisation algorithms and quality metrics
	Acquire knowledge of parallelism	Study the fundamentals of parallelism for optimisation algorithms
	Study the RNPP for WSNs	Perform a current state-of-the-art review about the RNPP for WSNs
	Study state-of-the-art metaheuristics	Perform a current state-of-the-art review about MO metaheuristics
B	Define an outdoor RNPP for two objectives	Based on the current definitions of the RNPP, establish a new model including two relevant objectives for the industry
	Implement the RNPP for two objectives	Implement the problem definition for two objectives in C++ language
	Search data sets for benchmarking purposes	Search data sets fitting this problem definition in the literature. If they are not found, then define a new data set
	Search similar works for comparing purposes	Search works solving a similar approach to this new proposal
	Implement the two standard metaheuristics	Implement two well-known metaheuristics from the literature
	Test the approach for two objectives	Apply the standard algorithms for solving the RNPP for two objectives. Perform minor changes in algorithms and problem definition if needed
	Implement state-of-the-art metaheuristics	Implement current state-of-the-art metaheuristics not assumed to this end
	Conduct experiments for solving the approach	Solve the RNPP for two objectives through all the metaheuristics implemented, comparing to standard algorithms
C	Enhance the outdoor RNPP definition	Include a third objective from the current literature in the RNPP
	Implement the RNPP for three objectives	Implement the problem definition for three objectives in C++ language
	Update standard algorithms	Reimplement the standard algorithms by assuming the three objectives
	Test the approach for three objectives	Apply the standard algorithms for solving the RNPP for three objectives. Perform minor changes in algorithms and problem definition if needed
	Update the other metaheuristics	Reimplement all the metaheuristics including the third objective
	Conduct new experiments	Solve the RNPP for three objectives through all the metaheuristics implemented, comparing to standard algorithms
D	Define an indoor RNPP for three objectives	Based on the previous research, define a more realistic model for indoor WSNs including three relevant objectives for the industry
	Implement the new indoor RNPP	Implement the problem definition for three objectives in C++ language
	Update standard algorithms	Reimplement the standard algorithms for the new problem definition
	Test the indoor approach for three objectives	Apply the standard algorithms for solving the indoor RNPP. Perform changes in algorithms and problem definition if needed
E	Disseminate the results obtained	Write papers for relevant conferences and ISI-SCI journals with the goal of disseminating this research
	Write the PhD thesis	Write a full document, including all the details of this research for getting the degree of Doctor of Philosophy in Computer Science

1.3 Thesis Outline

This thesis is composed of the eight chapters described below:

Chapter 1: Introduction
This chapter introduces the issue tackled in this research work, providing the motivations which led us to start this task, the objectives to reach, and the research planning followed for getting the objectives proposed at the beginning.

Chapter 2: Background and Fundamentals
In this chapter, we discuss the background for the work assumed in this thesis. Including optimisation problems and solving methods, parallel computing, scientific methodology, WSN fundamentals, and a review of deployment strategies in WSNs.

Chapter 3: Multiobjective Metaheuristics
This chapter provides a general description of the MO metaheuristics assumed in this dissertation for solving the RNPP. We include the standard Non-dominated Sorting Genetic Algorithm II (NSGA-II) [8] and Strength Pareto Evolutionary Algorithm 2 (SPEA2) [9], the state-of-the-art MultiObjective Evolutionary Algorithm based on Decomposition (MOEA/D) [10], and MO variants of the SO Variable Neighbour Search Algorithm (VNS) [11], Gravitational Search Algorithm (GSA) [12], Firefly Algorithm (FA) [13], and Artificial Bee Colony (ABC) [14].

Chapter 4: Solving the RNPP: bi-objective Outdoor Approach
In this chapter, we propose and solve a bi-objective outdoor approach of the RNPP, where we optimise both Average Energy Cost (AEC) and Average Sensitivity Area (ASA). To this end, we consider the wide range of MO metaheuristics presented in Chapter 3. This chapter includes a description of the WSN model considered, a formal problem statement, a detailed description of the data set considered for solving the problem, specific considerations for implementing the metaheuristics, experimental results, and scientific achievements obtained from performing this research task.

Chapter 5: Solving the RNPP: three-objective Outdoor Approach
This chapter proposes and solve a three-objective outdoor approach of the RNPP, where we optimise AEC, ASA, and Network Reliability (NR). To this end, we consider the wide range of MO metaheuristics presented in Chapter 3. This chapter presents a similar structure to the bi-objective approach discussed in Chapter 4.

Chapter 6: Solving the RNPP: a Novel three-objective Indoor Approach
In this chapter, we propose a novel approach of the RNPP for indoor environments, where we try to leverage existing infrastructures, while three objectives are optimised: AEC, ASA, and Average Network Reliability (ANR). As an initial approach, we consider the two classic MO metaheuristics, NSGA-II and SPEA2, presented in Chapter 3. The structure of this chapter is similar to the bi-objective approach discussed in Chapter 4.

Chapter 7: Conclusions and Future Works
This chapter includes the conclusions obtained after performing this research task and the future lines of work. Moreover, a summary of the major contributions to the science is included at this point.

Chapter 8: Scientific Production

This thesis ends with a summary of all the scientific achievements obtained, directly and indirectly, while performing this PhD dissertation.

In addition to these seven main chapters, we incorporate three appendix, including additional information. They are described below:

Additional Information for Implementing MOEA/D

This appendix includes four mathematical developments needed for implementing MOEA/D in the two approaches: bi-objective and three-objective.

Additional Information for Solving the RNPP: bi-objective approach

This appendix incorporate all the p-values and set coverage metrics obtained, while comparing the metaheuristics in the bi-objective approach. A summary of this information is presented in Chapter 4.

Additional Information for Solving the RNPP: three-objective approach

This appendix includes all the p-values and set coverage metrics obtained, while comparing the metaheuristics in the three-objective approach. A summary of this information is presented in Chapter 5.

CHAPTER

2

Background and Fundamentals

In this chapter, we introduce the background and fundamentals for the research task assumed in this PhD thesis. This chapter is structured as follows. In Section 2.1, we discuss main concepts of optimisation problems and solving methods. Section 2.2 defines some important terms of parallel computing. In Section 2.3, we describe the scientific methodology considered in this work. WSN technology is introduced in Section 2.4. Finally, we provide a state-of-the-art in WSN deployment strategies in Section 2.5.

2.1 Optimisation Problems and Solving Methods

In this section, we start by providing a formal statement of optimisation problems regarding the number of objectives assumed, with particular emphasis on the most important MO concepts. Next, we discuss about the main types of solving methods based on the accuracy of the solutions obtained, including both exact and approximate techniques. Finally, we describe different performance tools for defining the quality of the solutions obtained in MO terms.

2.1.1 A Formal Statement: Multiobjective vs Singleobjective

There are two main types of optimisation problems regarding the number of objectives assumed, i.e. Singleobjective Optimisation Problems (SOPs) and Multiobjective Optimisation Problems (MOPs), optimising a single criterion and several ones, respectively. The definition of an SOP is straightforward, but not for an MOP. While in an SOP the optimal solution is usually clearly defined and unique, in a MOP the objectives are in conflict, and then they cannot be optimised simultaneously. Instead, a satisfactory optimal trade-off has to be found [15].

Definition 2.1.1 (**MOP**). *Let x and y be the decision vector and the objective vector, respectively, and let X and Y be the decision space and the objective space, respectively. A general*

MOP[1] *is composed of* k *conflicting objective functions* $f_1(x), f_2(x), \ldots, f_k(x)$ *,* n *decision variables, and* m *constraints* $e_1(x), e_2(x), \ldots, e_m(x)$*, where* y *is optimised as*

$$\begin{array}{ll} \textit{maximise} & y = f(x) = (f_1(x)\ ,\ f_2(x)\ ,\ \ldots\ ,\ f_k(x)) \\ \textit{subject to} & e(x) = (e_1(x)\ ,\ e_2(x)\ ,\ \ldots\ ,\ e_m(x)) \leq 0 \\ \textit{where} & x = (x_1\ ,\ x_2\ ,\ \ldots\ ,\ x_n) \in X \\ & y = (y_1\ ,\ y_2\ ,\ \ldots\ ,\ y_k) \in Y \end{array} .$$

Definition 2.1.2 (Feasible set). *The feasible set* X_f *is the set of decision vectors satisfying the* m *constraints, which is expressed as*

$$X_f = \{x \in X\ :\ e(x) \leq 0\}.$$

Definition 2.1.3 (Feasible region). *The image of* X_f *is the feasible region* Y_f *in the objective space, that is given by*

$$Y_f = f(X_f) = \bigcup_{x \in X_f} \{f(x)\}.$$

In an SOP, X_f is totally ordered according to the objective function $f(x)$. For any two decision vectors $a, b \in X_f$, it holds that $f(a) \geq f(b)$ or $f(a) \leq f(b)$ with the purpose of finding the solution or solutions maximising $f(x)$. However, if several objectives are considered, as in an MOP, X_f is partially ordered. We express this new situation by extending the relations $=$, $\geq$, and $>$ to objective vectors, analogously to the single-objective case.

Definition 2.1.4 ($\geq$ relation for MOPs). *Let* u, v *be any two objective vectors in* Y_f*. The relations* $=$*,* $\geq$*, and* $>$ *for a maximisation problem are given by*[2]

$$\begin{array}{lcl} u = v & \Longleftrightarrow & \forall i \in \{1, 2, \ldots, k\}\ :\ u_i = v_i \\ u \geq v & \Longleftrightarrow & \forall i \in \{1, 2, \ldots, k\}\ :\ u_i \geq v_i \\ u > v & \Longleftrightarrow & u \geq v \wedge u \neq v \end{array} .$$

According to this relation, if we analyse the solutions C, D, and E in Figure 2.1, it holds that $C > E$ and $D > E$. However, comparing C and D, neither can be considered superior, because of $C \not\geq D$ and $D \not\geq C$. Thus, we have three different situations with MOPs according to the $\geq$ relation in contrast to two with SOPs, i.e $f(a) \geq f(b)$, $f(a) \leq f(b)$, or $f(a) \not\geq f(b) \wedge f(b) \not\geq f(a)$. A new notation called Pareto dominance is included for a better relationship identification.

Definition 2.1.5 (Pareto dominance relation). *Let* a *and* b *be any two decision vectors in* X_f*. The Pareto dominance is denoted by*[3]

$$\begin{array}{lcl} a \succ b\ \textit{(a dominates b)} & \Longleftrightarrow & f(a) > f(b) \\ a \succeq b\ \textit{(a weakly dominates b)} & \Longleftrightarrow & f(a) \geq f(b) \\ a \sim b\ \textit{(a is indifferent to b)} & \Longleftrightarrow & f(a) \not\geq f(b) \wedge f(b) \not\geq f(a) \end{array} . \tag{2.1}$$

The optimality criterion for MOPs is based on the Pareto dominance. A solution is optimal if it cannot be improved in any objective without causing a degradation in at least one other objective. In such a case, it is called a Pareto-optimal solution.

[1] Without loss of generality, we assume a maximisation problem here. For minimisation or mixed maximisation/minimisation problems the definitions presented in this section are similar.

[2] For a minimisation problem it is similar ($=,\leq,<$).

[3] For a minimisation problem the definitions are analogous ($\prec,\preceq,\sim$).

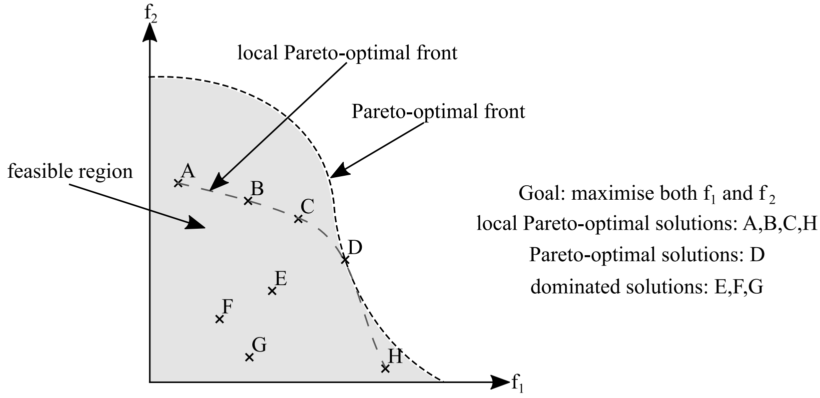

Figure 2.1: Concepts of MO optimisation.

Definition 2.1.6 (Pareto-optimal and local Pareto-optimal solutions). *Let x be a decision vector in X_f, such that it is non-dominated regarding a given set $A \subseteq X_f$, that is expressed as*

$$x \in X_f \text{ is non-dominated in } A \iff \nexists a \in A \ : \ a \succ x. \tag{2.2}$$

If A equals X_f, then x is a Pareto-optimal solution. Otherwise, x is a local Pareto-optimal solution in A.

Definition 2.1.7 (Pareto-optimal set, Pareto-optimal front, local Pareto-optimal set, and local Pareto-optimal front). *Let $p(A)$ be the function providing the set of non-dominated solutions in $A \subseteq X_f$, that is given by*

$$p(A) = \{a \in A \ : \ a \text{ is non-dominated in } A\}, \tag{2.3}$$

and let $f(p(A))$ be its image. If A equals X_f, then $p(X_f)$ is denoted as the Pareto-optimal set and $f(p(X_f))$ is called the Pareto-optimal front (or the optimal front). Otherwise, they are denoted as local Pareto-optimal set and local Pareto-optimal front (or simply front), respectively.

In practice, both the Pareto-optimal set and the Pareto-optimal front of an MOP are unknown. This way, when the problem is solved through any technique, we get a local Pareto-optimal set and its corresponding local Pareto-optimal front.

Below, we include a discrete MO optimisation problem example from [16], showing some of the previously discussed concepts. This example will be considered in the next sections.

Example 2.1.1. *Assume a maximisation problem having two objectives given by*

$$f_1(a, b) = a + b$$

and

$$f_2(a, b) = c - b + a,$$

where $c \in \mathbb{N}$ and $a, b \in 0, 1, \ldots, c$. Thus, the decision space consists of all pairs $(a, b) \in \{0, 1, \ldots, c\} \times \{0, 1, \ldots, c\}$. The Pareto-optimal set is denoted as

$$S_O = \{(c, b) : b \in 0, 1, \ldots, c\}$$

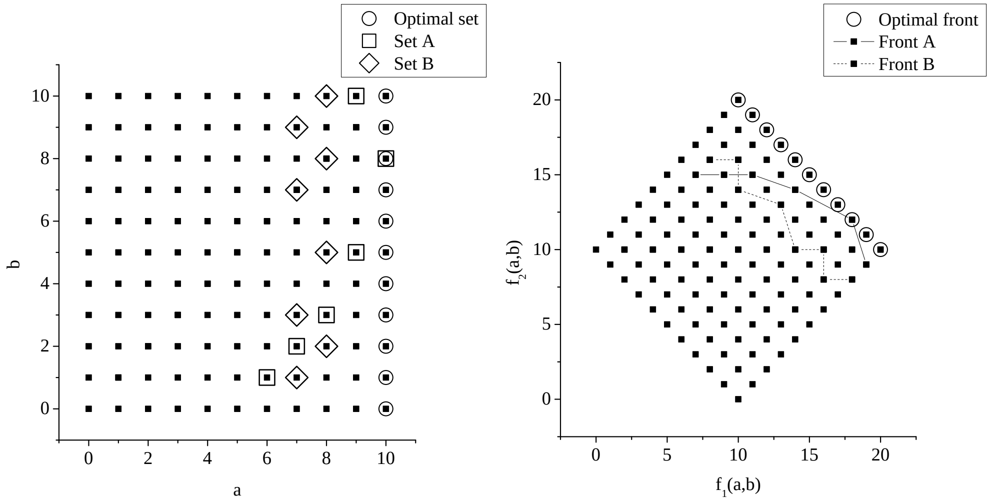

(a) Decision space. **(b)** Objective Space.

Figure 2.2: Decision and objective space of a bi-objective optimisation problem.

and the Pareto-optimal front is given by

$$F_O = \{(x, y) : x + y = 3 \cdot c \wedge x, y \in \{0, 1, \ldots, c\}.$$

Figure 2.2a shows the decision space for c equals 10*, including the Pareto-optimal set and two local Pareto-optimal sets* A *and* B*. On the other hand, Figure 2.2b shows the objective space and the corresponding images of the three sets.*

2.1.2 Solving Complex Problems: Complete vs Approximate Algorithms

There are two main types of solving methods regarding the accuracy of the solutions obtained, i.e. complete and approximate algorithms. Complete algorithms guarantee to find the optimal solution for every finite size instance in bounded time. This type of algorithms is not suitable for solving NP-hard optimisation problems, because no polynomial time algorithm exists, instead computation time raises in an exponential way, which is not appropriate for practical purposes. Some examples of complete algorithms are integer linear programming [17] and finite domain constraint programming [18]. On the contrary, approximate algorithms sacrifice finding optimal solutions for the sake of getting approximate ones in a significant reduced time. Such approximate algorithms are suited for tackling NP-hard optimisation problems [19].

We find two main traditional approximate algorithms, which are also called heuristics: constructive and local search methods. The first ones generate solutions from scratch by adding components to a solution until it is completed. This is the fastest approximate method, but the solution quality is often inferior compared to local search methods. Local search methods start from some initial solution, which is iteratively replaced by a better solution in its neighbourhood.

In the last decades, a more intelligent approximate method called metaheuristic has acquired a great relevance [20]. It combines basic heuristic methods and effectiveness exploring the search space. Next, we quote some of the definitions of metaheuristics in the literature:

> *"A metaheuristic is formally defined as an iterative generation process which guides a subordinate heuristic by combining intelligently different concepts for exploring and exploiting the search space, learning strategies are used to structure information in order to find efficiently near-optimal solutions."* [21].

> *"A metaheuristic is an iterative master process that guides and modifies the operations of subordinate heuristics to efficiently produce high-quality solutions. It may manipulate a complete (or incomplete) single solution or a collection of solutions at each iteration. The subordinate heuristics may be high (or low) level procedures, or a simple local search, or just a construction method."* [22].

> *"Metaheuristics are typically high-level strategies which guide an underlying, more problem specific heuristic, to increase their performance. The main goal is to avoid the disadvantages of iterative improvement and, in particular, multiple descent by allowing the local search to escape from local optima. This is achieved by either allowing worsening moves or generating new starting solutions for the local search in a more intelligent way than just providing random initial solutions. Many of the methods can be interpreted as introducing a bias such that high quality solutions are produced quickly. This bias can be of various forms and can be cast as descent bias (based on the objective function), memory bias (based on previously made decisions) or experience bias (based on prior performance). Many of the metaheuristic approaches rely on probabilistic decisions made during the search. But, the main difference to pure random search is that in metaheuristic algorithms randomness is not used blindly but in an intelligent, biased form."*[23].

> *"A metaheuristic is a set of concepts that can be used to define heuristic methods that can be applied to a wide set of different problems. In other words, a metaheuristic can be seen as a general algorithmic framework that can be applied to different optimization problems with relatively few modifications."* [24].

In general, the authors agree on some properties characterising most metaheuristics:

- They are non-deterministic and non-problem specific high level search strategies.
- The purpose is to efficiently explore the search space to find near-optimal solutions.
- They consider a wide range of different techniques from simple constructive methods to complex learning processes. It is possible to include domain-specific knowledge for designing these techniques, which are controlled by an upper level strategy.
- It is usual to include mechanisms to avoid getting trapped in local optima.
- It is increasingly common to assume memory for including search experience knowledge.
- They perform a dynamic balance between diversification[1] and intensification[2].
- The basic concepts of metaheuristics permit an abstract level description.

[1] Exploration of the search space.
[2] Exploitation of the accumulated search experience.

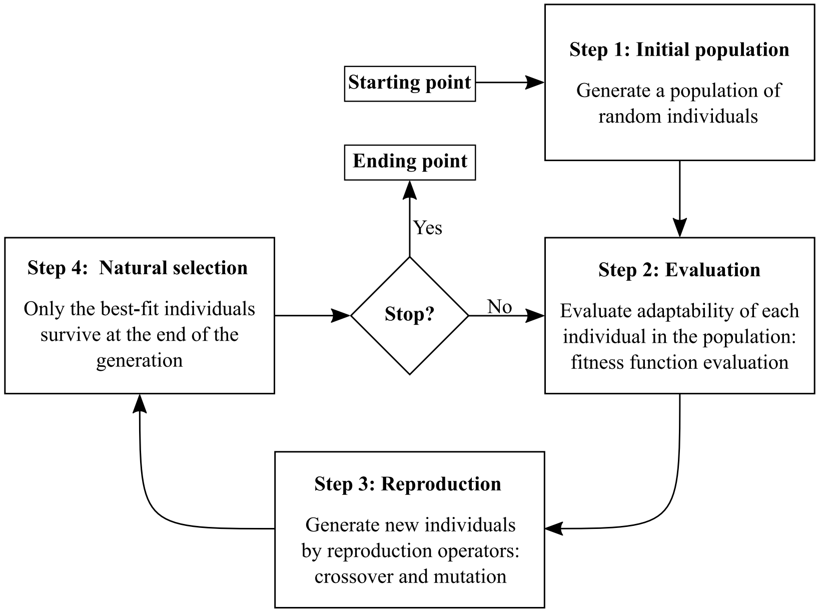

Figure 2.3: Traditional scheme followed by EAs.

2.1.3 Classification of Metaheuristics

There are a wide variety of metaheuristics because of its high level conception. Therefore, making a classification is not a trivial issue. In this thesis, we consider a usual classification splitting metaheuristics into three large groups:

Evolutionary Algorithms (EAs)

EAs are inspired by nature's capability to evolve adapting to the environment. Thus, they consider mechanisms from the Darwin's theory of evolution, such as crossover, mutation, and natural selection. EAs follow the well-known scheme shown in Figure 2.3. Initially, the algorithm starts from a population of random individuals, where each individual is a possible solution to the optimisation problem (step 1). In step 2, the fitness of each individual in the population is evaluated, getting its adaptability to the environment. Next, the best-fit individuals of the population are selected to be the parents of the next generation, resulting in a new offspring population through both crossover and mutation reproduction operators (step 3). Note that crossover is assumed to recombine two individuals in a new one and mutation is for including random changes in the new individual, increasing diversity. Then, only the strongest individuals survive at the end of the generation, i.e. the least-fit individuals are replaced by the best-fit ones (step 4). At this point, the algorithm returns to step 2. This loop ends when a stop condition is reached, such as a maximum number of generations or elapsed time [25].

There are two standard algorithms in EAs, NSGA-II and SPEA2. Both belong to a subtype of EAs called Generic Algorithms (GAs), which are characterised by encoding their individuals as chromosomes, where a chromosome is composed of several genes. These two standard GAs and a current state-of-the-art EA known as MOEA/D are considered in this thesis and will be discussed in the next section.

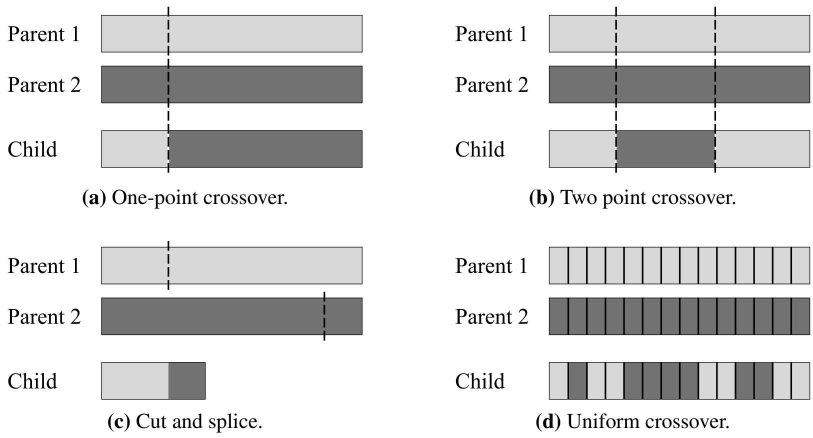

Figure 2.4: Crossover strategies assuming two parents of equal length as input.

Regarding reproduction operators, crossover is assumed to recombine two parents with the hope of creating a better individual. We find many different strategies in the literature [25]. Below, we describe some of them, assuming two parents of equal length as input:

- **One-point crossover:** A single crossover point is selected to generate a new child as follows. The data before that point is taken from the first parent, the remaining data after the point is taken from the second parent. See Figure 2.4a.
- **Two point crossover:** Two crossover points are selected to generate a new child as follows. The data before the first point is taken from the first parent, the data between the two points is taken from the second parent, and the data after the second point is taken from the fist parent again. See Figure 2.4b.
- **Cut and splice:** This strategy generates a new child of variable length as follows. A crossover point is selected in each parent. Then, the data before the point in the first parent is taken from such first parent and the data after the point in the second parent is taken from such second parent. See Figure 2.4c.
- **Uniform crossover:** For each gene of the new child, this strategy evaluates if the gene is taken from the first or the second parent with a given probability. Thus, with a probability of 0.5, the child will have about 50% of genes from the first parent and 50% of genes from the second parent. See Figure 2.4d.

On the other hand, mutation is considered to increase diversity. After generating a new individual through crossover, a mutation is performed in such new individual. The changes can be more or less pronounced regarding the strategy followed. The most common strategy is the uniform gene mutation: each gene is changed with a given probability. This change could be an inversion if a binary encoding is considered, as in Figure 2.5a, or replacing the previous value for a random number in an interval, as in Figure 2.5b.

Swarm Intelligence Algorithms (SIAs)

SIAs are inspired by the behaviour of self-organised systems, where individuals interact with each other and with the environment, such as colonies of ants, schools of fish, flocks

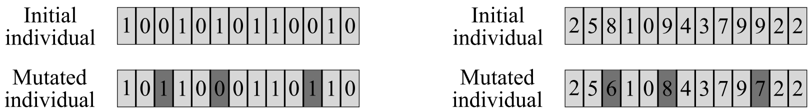

(a) Binary encoding. **(b)** Natural number encoding.

Figure 2.5: Uniform gene mutation for two types of encoding.

of birds, and herds of land animals. Typical SIAs are Particle Swarm Optimisation (PSO) [26] and Ant Colony Optimisation (ACO) [27]. In PSO a possible solution to the problem is represented by a particle in the search space. Each particle searches for better positions by modifying its velocity according to some rules inspired by the social behaviour of flocks of birds. In ACO, a set of agents, called artificial ants, search for better solutions. The ants generate solutions by moving for a weighted graph to find the best path by assuming the pheromone model, i.e. each time an ant traverses an edge, it deposits a small amount of pheromone. Subsequent ants consider the pheromone information as a guide towards more promising paths.

In this thesis, we consider some novel SIAs: GSA, FA, and ABC, which are based on the behaviour of gravitational forces, fireflies, and honey bees, respectively. These algorithms will be described in depth in the next section.

Trajectory Algorithms (TAs)

TAs are characterised by following a trajectory during the search. The optimisation starts from an initial solution, which dynamically describes a trajectory in the search space. This trajectory is more or less complex depending on the strategy of the algorithm.

We find three main traditional TAs. *Basic local search*, where a movement is only performed if the resulting solution is better than the current one, stopping if a local optimum is found. *Simulated annealing* [28], which follows an approach analogous to the annealing process of metals and glass. The fundamental idea of this algorithm is to allow moving to worse solutions to escape from local optima attending to a given probability, which is decreased during the search. And *tabu search* [29], which allows moving to worse solutions if no improvement is available. To this end, it includes the search history concept to avoid selecting previously visited solutions, which are marked as forbidden (*tabu*).

There are some recently proposed TAs assuming general explorative strategies. They are called *explorative local search methods*. Some of the most important are Greedy Randomised Adaptive Search Procedure (GRASP) [30], VNS, Guided Local Search (GLS) [31], and Iterated Local Search (ILS) [32]. GRASP combines greedy randomized heuristics and local search: assuming that a solution is composed of several elements, the algorithm generates a solution step-by-step by randomly adding elements from a list of candidates ranked by a greedy function. VNS applies a strategy based on dynamically changing the neighbourhood structures, which delimit how getting a neighbourhood solution, i.e. a solution which is similar to another except for some minor details. This algorithm will be studied in depth in the next section. GLS assumes a different strategy, which dynamically changes the landscape of the objective function with the purpose of moving away from local optima. ILS applies local search to an initial solution until a local optimum is found. Then, a small perturbation is performed and the procedure is restarted again.

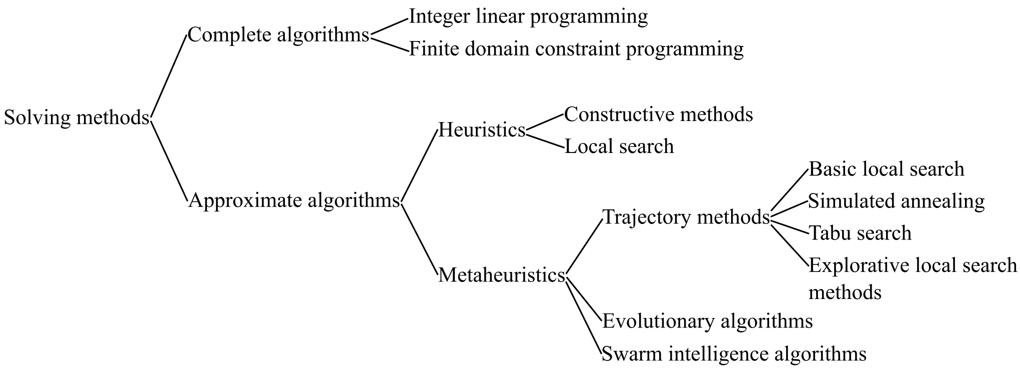

Figure 2.6: Classification of solving methods.

Figure 2.6 shows the classification of solving method discussed in Section 2.1.2, including the metaheuristics described before. There are many other different ways to classify metaheuristics depending on the features selected, see Figure 2.7. Below, we briefly summarize some of the most significant in the literature [33, 34, 35]:

Nature inspired vs. non-nature inspired

Nature inspired algorithms include all the metaheuristics, which are fully or partially inspired by a process found in nature. As may be expected, EAs and SIAs are part of nature inspired algorithms. Moreover, there are some algorithms from TAs, which are usually included in this group, such as tabu search and simulated annealing.

Population-based vs. single-solution

This classification is based on the number of solutions assumed at each step. Population-based algorithms perform search processes determining the evolution of a set of points in the search space. There are two main types EAs and SIAs. On the contrary, single-solution algorithms work on a unique solution to perform the process, such as TAs.

Dynamic vs. static objective function

This classification is according the way the objective functions are considered. Static algorithms keep the objective functions as they were given, while dynamic ones modify them during the search by adding information collected during the optimisation process. An example of dynamic algorithm is GLS.

One vs. various neighbourhood structures

Most metaheuristics do not change the fitness landscape in the curse of the optimisation. However, other algorithms, such as VNS, consider neighbourhood structures to dynamically swap between different fitness landscapes, giving the possibility of increasing the diversity of the results.

Serial vs. hybrid vs. parallel metaheuristics

In addition to the serial metaheuristics described above, there are hybrid and parallel algorithms. A hybrid metaheuristic combines a metaheuristic with other optimisation approaches, such machine learning, constraint programming, or even other metaheuristics. A parallel metaheuristic considers parallel tools to execute several metaheuristic processes in parallel, interacting among them to improve the overall solution.

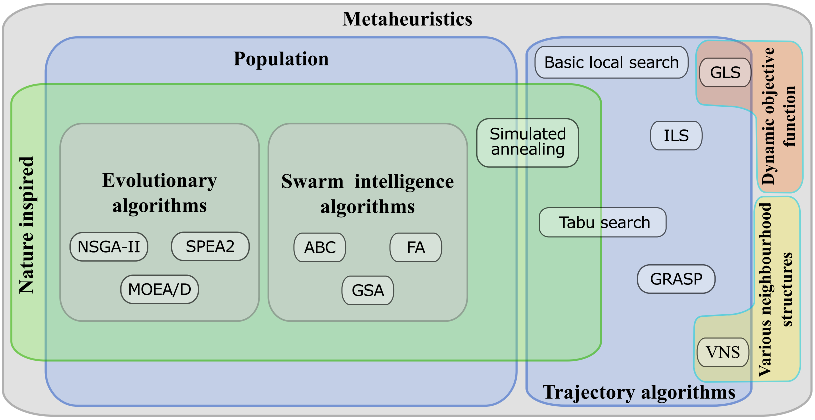

Figure 2.7: Classification of metaheuristics attending to several features.

2.1.4 Performance Assessment for Multiobjective Optimisation

The notion of performance assessment involves both quality of the solutions found and the time needed to obtain them. In the case of stochastic optimisers the relation between quality and time is not fixed, instead it is described by a probability density function. Consequently, the performance of a stochastic search algorithm is probabilistic in nature. Moreover, there is another difficulty in the case of MO optimisers, because the outcome is usually not a single solution, but a trade-off. Thus, we find two main issues: how to define quality and how to represent the outcome of several runs in terms of a probability density function [16].

There are two main approaches to tackle such issues: attainment functions and quality indicators. Given the outcome of an optimiser, an attainment function shows the outcome as a probability density function in the objective space. On the contrary, a quality indicator provides a quantitative measure of the outcome, which can be considered to perform a statistical analysis of the measure along executions. Statistical testing will be discussed in Section 2.3.1.

Definition 2.1.8 (Quality indicator). *A quality indicator I is defined as a mapping from the set of approximate results Ω to the set of real numbers, that is*

$$I : \Omega \mapsto \mathbb{R}.$$

Thus, given two sets of non-dominated solutions $Z, H \in \Omega$, the difference between the quality indicators of both sets $I(Z)$ and $I(H)$ reveals the difference in terms of quality.

Definition 2.1.9 (Pareto compliant). *A quality indicator I is Pareto compliant if and only if*

$$\forall Z, H \in \Omega : Z \succeq H \Rightarrow I(Z) \geq I(H)$$

for a maximisation problem[1]*. This means that I is an order-preserving function from $(\Omega, \succeq)$ to $(\mathbb{R}, \geq)$, which is a desirable feature for any quality indicator. However, many of them do not meet this requirement and are called Pareto non-compliant indicators [36].*

It is widely accepted to classify quality indicators based on if needed to know the Pareto-optimal front or not to calculate the measure. Firstly, we introduce some quality indicators

[1] For a minimisation problem the definition is similar $(\preceq, \leq)$.

which do not need the Pareto-optimal front. Note that we consider Example 2.1.1 to analyse the behaviour of the next tools by comparing the sets A and B.

Number of solutions

It is a simple Pareto non-compliant indicator, showing the number of non-dominated solutions provided by a Pareto-front. This way, given a front Z, the indicator is denoted as

$$I^1_{NS}(Z) = ||Z||,$$

where $||.||$ is the operator giving the cardinal of a set. In the example, $I^1_{NS}(A) = 6$ and $I^1_{NS}(B) = 8$. Hence, B is better than A.

Hypervolume

This Pareto compliant indicator was proposed by Zitzler and Thiele [37]. It measures the portion of the objective space weakly dominated by a front Z regarding a reference point, while solving a problem with k objectives. Before computing the metric, the front Z should be normalised so that all the objectives contribute equally to the indicator, resulting in a new front Z'. To this end, two k-dimensional points called ideal and nadir are considered, denoting the best and worst estimated values for each objective.

Let α_i^ζ be the value of the i-th fitness function of a solution ζ. Let β_i be the reference value of the i-th fitness function. Let f_i be the i-th fitness function. Given a normalised front Z' in the interval $[0, 1]$ and a reference point $\gamma = (\beta_1, \beta_2, \ldots, \beta_k)$ given by

$$\beta_i = \begin{cases} 1 \iff f_i \text{ is to maximise} \\ 0 \iff f_i \text{ is to minimise} \end{cases}; \qquad \beta_i \in \gamma, i \in 1, \ldots, k.$$

Then, each member of Z' has a hypercube given by

$$h(\zeta) = [\alpha_1^\zeta, \beta_1] \times [\alpha_2^\zeta, \beta_2] \times \ldots \times [\alpha_k^\zeta, \beta_k]; \qquad \zeta \in Z'.$$

The hypervolume of Z is calculated as the union of all the hypercubes of Z' by assuming the Lebesgue measure Λ, that is

$$I^1_H(Z) = I_H(Z', \gamma) = \Lambda\left(\bigcup_{\zeta \in Z'} h(\zeta)\right).$$

In the example, $I^1_H(A) = 66.00\%$ and $I^1_H(B) = 61.25\%$ by considering $\gamma = (1.00, 1.00)$ and $(20.00, 20.00)$ and $(0.00, 0.00)$ as the ideal and nadir points, respectively. Hence, A is better than B, providing A more hypervolume than B. If we modify the ideal and nadir points to be closer to the two fronts, the measure is more accurate, i.e. we get $I^1_H(A) = 65.63\%$ and $I^1_H(B) = 46.88\%$ by assuming $(19.00, 16.00)$ and $(7.00, 8.00)$ as the new bounding points, increasing the difference to 18.75%. This means that it is important to adjust the bounding points as close as possible to the data being analysed. Figure 2.8a shows an example of this quality indicator comparing the two fronts.

Binary epsilon

The Pareto compliant binary epsilon indicator was presented by Zitzler et al. [38], including a multiplicative and an additive version. Let $\succeq_{\epsilon\cdot}$ be the $\epsilon\cdot$-dominance relation for a maximisation problem given by[1]

$$\zeta \succeq_{\epsilon\cdot} \eta \iff \forall i \in 1 \ldots k : \zeta_i \cdot \epsilon \geq \eta_i; \qquad \epsilon \in \mathbb{R},$$

[1] For a minimisation problem the definitions are analogous ($\preceq_{\epsilon\cdot}, \leq$).

where ζ and η are two different solutions and ζ_i and η_i are the value of the i-th fitness function of ζ and η, respectively. Then, given two fronts Z and H, the multiplicative epsilon indicator $I_{\epsilon\cdot}(Z, H)$ calculates the minimum factor ϵ by which each point in Z has to be multiplied, such that the resulting set weakly dominates H, that is

$$I_{\epsilon\cdot}(Z, H) = \inf_{\epsilon \in \mathbb{R}} \{\forall \eta \in H \; \exists \zeta \in Z : \zeta \succeq_{\epsilon\cdot} \eta\}.$$

Analogously, the $\epsilon+$-dominance relation for a maximisation problem is defined as[1]

$$\zeta \succeq_{\epsilon+} \eta \iff \forall i \in 1 \ldots k : \zeta_i + \epsilon \geq \eta_i; \qquad \epsilon \in \mathbb{R}.$$

Then, the additive epsilon indicator $I_{\epsilon+}(Z, H)$ is expressed as

$$I_{\epsilon+}(Z, H) = \inf_{\epsilon \in \mathbb{R}} \{\forall \eta \in H \; \exists \zeta \in Z : \zeta \succeq_{\epsilon+} \eta\}.$$

As for hypervolume, the fronts should be normalised before calculating the indicator. In the example, we get $I_{\epsilon+}(A, B) = 0.05$ and $I_{\epsilon+}(B, A) = 0.10$ by assuming $(20.00, 20.00)$ and $(0.00, 0.00)$ as bounding points. Hence, A is better than B because the transformation needed is lower. As before, if we assume the closer bounding points $(19.00, 16.00)$ and $(7.00, 8.00)$, the accuracy increases obtaining $I_{\epsilon+}(A, B) = 0.13$ and $I_{\epsilon+}(B, A) = 0.25$.

Set coverage

The Pareto compliant binary set coverage indicator was developed by Zitzler [15], being based on the Pareto dominance concept. Given two fronts Z and H, the set coverage metric $I_{SC}(Z, H)$ calculates the percentage of solutions from H, which are weakly dominated by Z. That is,

$$I_{SC}(Z, H) = \frac{||\{\exists \zeta \in Z : \zeta \succeq \eta\}||}{||H||}; \qquad \eta \in H.$$

In the example, $I_{SC}(A, B) = 50.00\%$ and $I_{SC}(B, A) = 33.33\%$. Consequently, A is better than B.

The quality indicators needed the Pareto-optimal set or, on the contrary, a reference set of points are the following:

Number of optimal solutions

This simple Pareto non-compliant indicator is defined as the number of Pareto-optimal solutions which a front provides. Given a front Z, the indicator is expressed as

$$I_{NOS}(Z) = ||Z \cap f(p(X_f))||,$$

where X_f and $p(.)$ are given by Equations (2.2) and (2.3), respectively. In our example, $I_{NOS}(A) = 1$ and $I_{NOS}(B) = 0$. Hence, A is better than B.

Unary epsilon

On the basis of the definition of the binary epsilon indicator discussed before, the Pareto compliant unary multiplicative version for a front Z and a reference set Υ is given by [38]

$$I_{\epsilon\cdot}(Z)^1 = I_{\epsilon\cdot}(Z, \Upsilon).$$

[1] For a minimisation problem the definitions are analogous ($\preceq_{\epsilon+}$, $\leq$).

Analogously, the additive version is defined as

$$I_{\epsilon+}(Z)^1 = I_{\epsilon+}(Z, \Upsilon).$$

In our example, we get $I_{\epsilon+}(A)^1 = 0.20$ and $I_{\epsilon+}(B)^1 = 0.15$ by assuming $\Upsilon = f(p(X_f))$. If we consider the bounding points $(20.00, 20.00)$ and $(7.00, 8.00)$, we get $I_{\epsilon+}(A)^1 = 0.33$ and $I_{\epsilon+}(B)^1 = 0.25$. Hence, B is better than A. If we compare this conclusion to the one obtained through the binary epsilon indicator discussed before, we note that both are contradictory. This is due to this indicator is not adequate if minimum and maximum distances between the two sets compared are large. In such a case, the indicator could show an erratic behaviour. Figure 2.8b shows some details for calculating the metric.

Spread

This Pareto non-compliant indicator measures how the solutions are distributed in a front. Given an ordered front Z and the Pareto-optimal front $f(p(X_f))$, the spread metric proposed by Deb et al. [8] for two objectives is expressed as

$$I_S(Z)^1 = I_S(Z, d_o, d_l) = \frac{d_o + d_l + \sum_{i=1}^{||Z||-1} |d_i - \overline{d_Z}|}{d_o + d_l + (||Z|| - 1)\overline{d_Z}},$$

where d_o and d_l are the Euclidean distances between the extreme solutions of $f(p(X_f))$ and Z, d_i is the Euclidean distance between the i-th solution in Z and its consecutive $i+1$-th solution, $\overline{d_Z}$ is the average of all these consecutive distances, and $|.|$ is the operator giving the absolute value of a number. Note that with n solutions, there are $n-1$ consecutive distances (see Figure 2.8c). In the example, we get $I_S(A)^1 = 0.33$ and $I_S(B)^1 = 0.31$, assuming the default bounding points, and $I_S(A)^1 = 0.58$ and $I_S(B)^1 = 0.57$ for the closer ones. Hence, B is better distributed than A. There are other approaches for more than two objectives, e.g. the crowding distance, which will be discussed in Section 3.1.

Generational distance

This Pareto non-compliant indicator was proposed by Van Veldhuizen et al. [39] and computes the proximity in the objective space of a certain front from the Pareto-optimal front. Given a front Z and the Pareto-optimal front $f(p(X_f))$, the indicator is given by

$$I_{GD}(Z)^1 = I_{GD}(Z, f(p(X_f))) = \frac{\sum_{\zeta \in Z} d_{\zeta, f(p(X_f))}}{||Z||},$$

where $d_{\zeta, f(p(X_f))}$ is the Euclidean distance between $\zeta \in Z$ and its nearest solution in $f(p(X_f))$ (see Figure 2.8d) . In the example, we get $I_{GD}(A)^1 = 0.13$ and $I_{GD}(B)^1 = 0.18$, assuming default bounding points, and $I_{GD}(A)^1 = 0.21$ and $I_{GD}(B)^1 = 0.28$ through the closer ones. Hence, A is nearer to $f(p(X_f))$ than B.

Inverted generational distance

This Pareto non-compliant indicator developed by Coello et al. [40] follows a similar approach to generational distance. It computes how far is the Pareto-optimal front from a certain front. Given a front Z and the Pareto-optimal front $f(p(X_f))$, the indicator is expressed as

$$I_{IGD}(Z)^1 = I_{IGD}(Z, f(p(X_f))) = \frac{\sum_{\alpha \in f(p(X_f))} d_{\alpha, Z}}{||f(p(X_f))||},$$

Table 2.1: Main features of performance tools.

Performance tool	Is it Pareto compliant?	Does it require normalize?	Does It require a reference set?	Behaviour
I^1_{NS}	NO	NO	NO	More is better
I^1_H	YES	YES	NO	More is better
$I^2_{\epsilon\cdot}$	YES	YES	NO	Less is better
$I^2_{\epsilon+}$	YES	YES	NO	Less is better
I^2_{SC}	YES	NO	NO	More is better
I^1_{NOS}	NO	NO	YES	More is better
$I^1_{\epsilon\cdot}$	YES	YES	YES	Less is better
$I^1_{\epsilon+}$	YES	YES	YES	Less is better
I^1_S	NO	YES	YES	Less is better
I^1_{GD}	NO	YES	YES	Less is better
I^1_{IGD}	NO	YES	YES	Less is better
Attainment Surface	YES	NO	NO	Pareto dominance

where $d_{\alpha,Z}$ is the Euclidean distance between $\alpha \in f(p(X_f))$ and its nearest solution in Z (see Figure 2.9a). In our example, we obtain $I_{IGD}(A)^1 = 0.11$ and $I_{IGD}(B)^1 = 0.16$ for default bounding points, and $I_{IGD}(A)^1 = 0.18$ and $I_{IGD}(B)^1 = 0.25$ by assuming closer ones. Then, as for generational distance, $f(p(X_f))$ is nearer to A than B.

On the other hand, the attainment surface is a graphical tool for representing fronts. It draws a boundary in the objective space, separating those points which are dominated, from those which are non-dominated. This approach is useful when we want to display several fronts in a same plot, e.g. comparing different algorithms or analysing several runs of a same optimiser. This graphical tool is based on the attainment function, which studies the distribution of the data obtained in several runs according to the notion of goal-attainment, i.e. the probability that the optimiser attains a certain solution in a single run [41]. Figure 2.9b shows an example of this tool. Finally, Table 2.1 summarises the main features of the performance tools discussed before.

2.2 Parallel Computing

Traditionally, software has been written for serial computation. Following this approach, an algorithm is implemented as a serial stream of instructions, which are executed sequentially on a single Central Processing Unit (CPU). This means that only one instruction can be executed at any moment in time (see Figure 2.10a) [42]. Note that the terms processor, CPU, and core are used interchangeably throughout this dissertation to denote a single processing unit.

In the simple sense, parallel computing is the simultaneous use of multiple compute resources to solve a computational problem. Thus, an algorithm is broken into discrete sets of instructions, which can be executed concurrently on different processors under an overall control mechanism (see Figure 2.10b). The compute resources are typically an arbitrary number of single CPU computers connected by a network, a single computer with multiple CPUs, or a combination of both [42]. We find many reasons to consider parallel computing [43]:

- **The real work is massively parallel:** Parallel computing is better suited for simulating and modelling real world phenomena, compared to serial computing. This is because many real problems include interrelated events happening at the same time. Some examples of such problems are galaxy formation, planetary movements, and climate change.
- **Save time and/or money:** Allocating more resources to a task will shorten its time to completion. This implies potential cost savings.

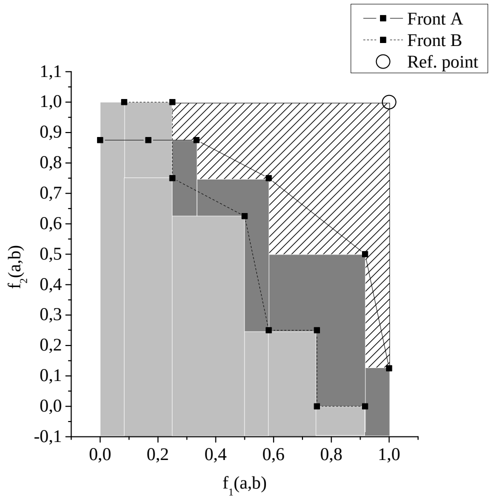

(a) Hypervolume.

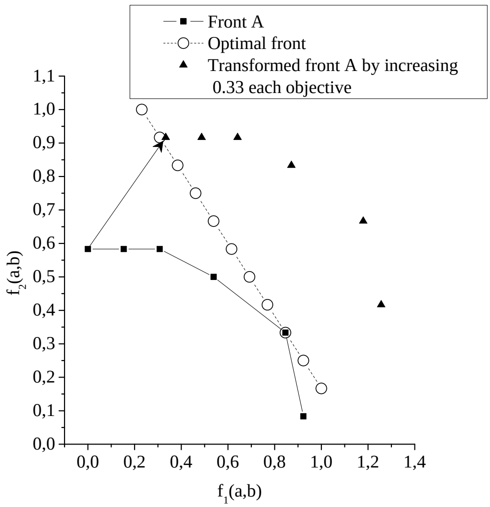

(b) Unary epsilon.

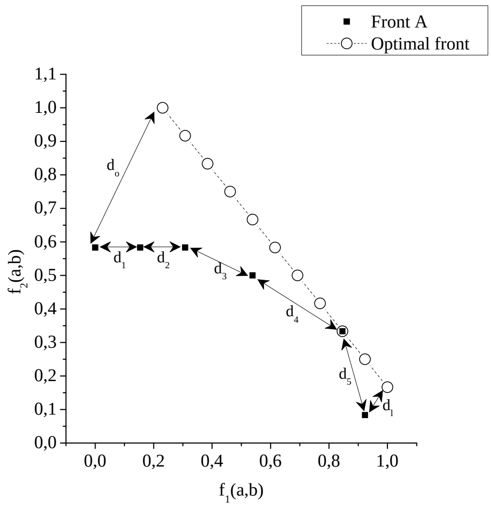

(c) Spread.

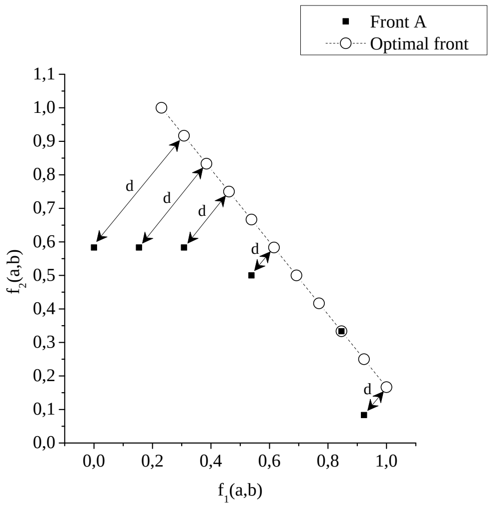

(d) Generational distance.

Figure 2.8: Example of Performance tools (Part 1/2).

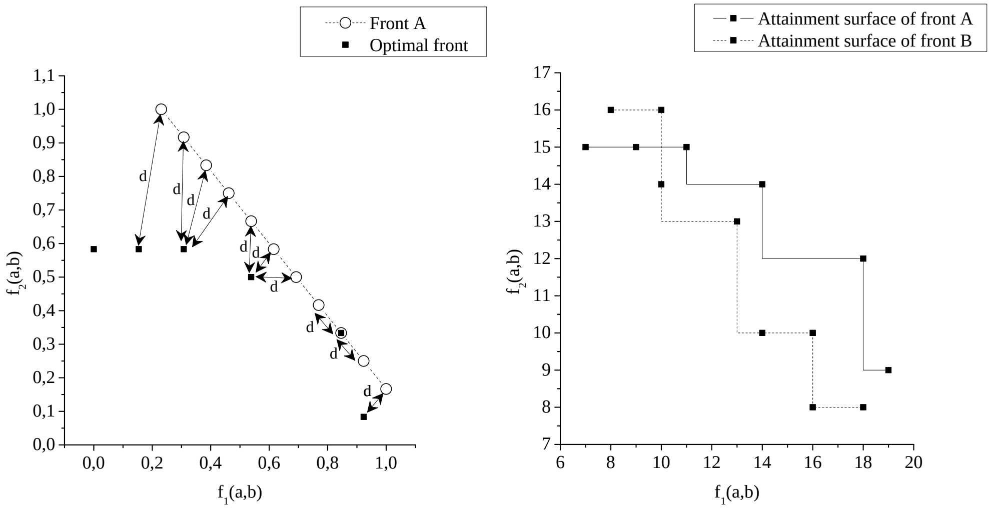

(a) Inverted generational distance.

(b) Attainment surface.

Figure 2.9: Example of Performance tools (Part 2/2).

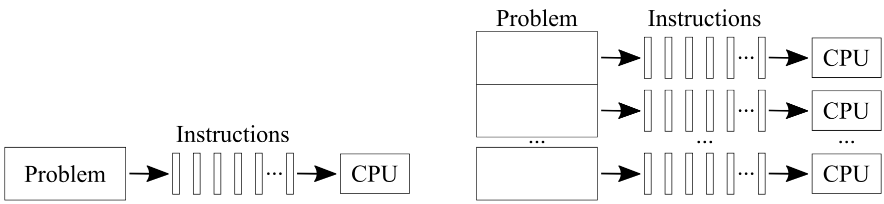

(a) Serial computation.

(b) Parallel computation.

Figure 2.10: Serial vs. parallel computation.

- **Solve larger/more complex problems:** Many problems are so complex and/or large that is impossible or impracticable to solve them on a single-core computer. Either because of restrictions on computing time or computer memory.

- **Provide concurrency:** A single-core computer can only execute one task at a time. Multiple compute resources can do many things at the same time. An example is a collaborative network for virtual working, where many users execute tasks at the same time.

- **Take advantage of non-local resources:** Sometimes local resources are insufficient for a given task. Then, the use of non-local resources on a wide area network or even the Internet is a good option. An example is BOINC for volunteer computing [1].

- **Make better use of underlying parallel hardware:** Most computers, even smartphones, are parallel in architecture with multiple processors/cores. In most cases, serial programs running on modern computers waste potential computing power.

[1] https://boinc.berkeley.edu/

Next, we describe some relevant classifications for parallel systems, as well as tools for performance assessment of parallel computation.

2.2.1 Flynn's Classification

This traditional classification was presented by Flynn in [44]. It classifies computers and programs by whether, during any one clock cycle, they assume a single set or multiple sets of instructions (instruction stream), and whether or not those instructions consider a single set or multiple sets of data as input (data stream). There are four possibilities according to Flynn:

Single Instruction stream, Single Data stream (SISD)
: This classification includes convectional serial computers, where only one instruction stream is executed during any one clock cycle and only one data stream is considered as input during any clock cycle (see Figure 2.11a).

Single Instruction stream, Multiple Data stream (SIMD)
: This is a type of parallel computer suited for specialised problems with a high degree of regularity, e.g. image processing. All CPUs execute the same instruction at any given clock cycle and each CPU operates on a different data element (see Figure 2.11b).

Multiple Instruction stream, Single Data stream (MISD)
: This is a rarely used classification, where all CPUs execute a different instruction stream considering the same single data stream as input. A conceivable use of this classification may be multiple frequency filters operating on a single signal stream (see Figure 2.11c).

Multiple Instruction stream, Multiple Data stream (MIMD)
: This is by far the most common type of classification. Each processor can execute a different instruction stream by assuming a different data stream at any given clock cycle. Most modern supercomputers fall into this category (see Figure 2.11d).

2.2.2 Structural Classification

Flynn's classification discusses the overall behaviour of parallel systems. However, such systems can also be classified based on their structure [45]. If CPUs communicate through global shared memories, then this organisation is called a shared memory system. On the other hand, if CPUs have their own local memories and communications between CPUs are performed by sending messages through a communication network, then this organisation is called a distributed memory system. Moreover, it is possible to have a combination of both approaches, which is called a hybrid distributed-shared memory system. Below, we discuss each of them:

Shared memory systems
: These systems have the ability to access all memory as global address space for all CPUs. Thus, CPUs work independently, but sharing the same memory resources, which is an advantage and a disadvantage at the same time. On the one hand, global address space provides a user-friendly programming perspective to memory and data sharing between CPUs is fast and uniform. On the other hand, an important disadvantage is the lack of scalability between memory and CPUs, because adding more CPUs can geometrically increase traffic on the shared memory. Another disadvantage is that global memory implies that synchronization between tasks is a programmer's responsibility.

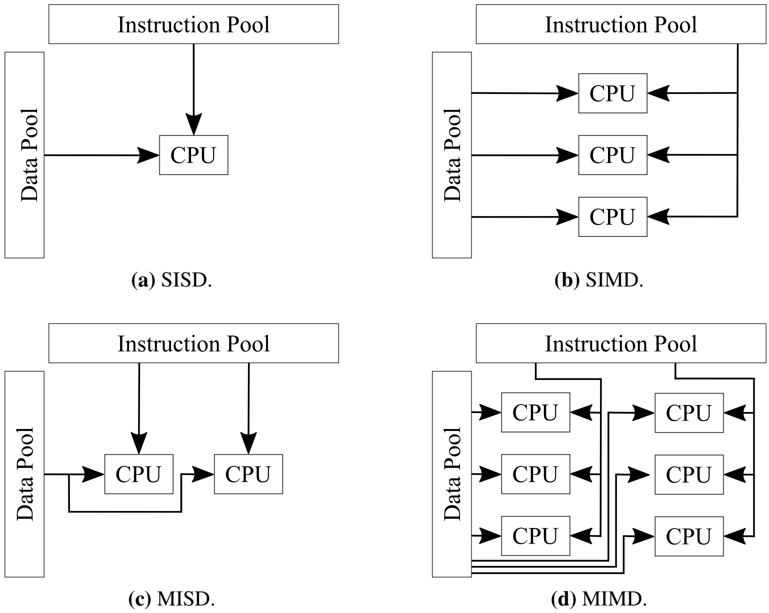

Figure 2.11: Flynn's classification.

Traditionally, we find two main shared memory systems: Uniform Memory Access systems (UMAs) and Non-Uniform Memory Access systems (NUMAs). UMAs have identical processors, allowing equal access time to memory (see Figure 2.12a). NUMAs are often made by physically linking two or more UMAs through a bus (see Figure 2.12b). Consequently, not all CPUs have equal access time to all memories.

There are two main parallel programming models for shared memory:

- The first one is a simple model, where processes/tasks read and write asynchronously in a common address space as Figure 2.13a shows. The incorporation of control mechanisms, such as semaphores, is usually to prevent race conditions and deadlocks, which makes this model difficult to use. This programming model is included in the UNIX specification[1] and the POSIX standard[2].
- The second one is a more advanced model, including the concept of thread: a process having local data, but also, accessing to global memory. In addition, a thread can also have associated multiple light-weight concurrent threads. As an example, in Fig 2.13b *Thread 1* is the parent of *Thread 1.1*. We find two different implementations of threads: POSIX threads and OpenMP[3]. The first one is a very explicit parallelism included in the POSIX standard, requiring significant programmer attention to detail. The second one is a simple and easy multi-platform industry standard, which is widely considered in the literature.

[1] http://www.unix.org/
[2] http://standards.ieee.org/develop/wg/POSIX.html
[3] http://openmp.org/wp/

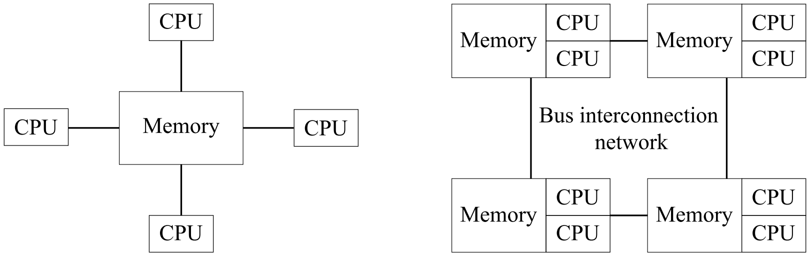

(a) UMA. **(b)** NUMA.

Figure 2.12: Shared memory systems.

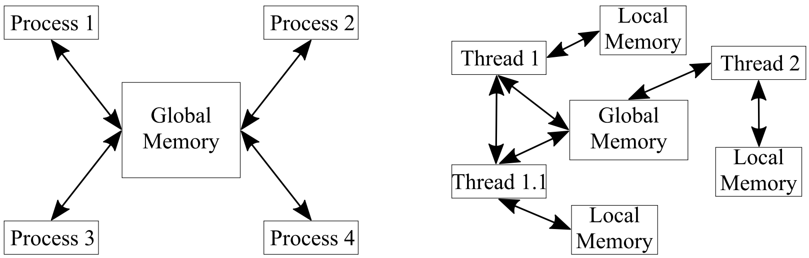

(a) Common address space model. **(b)** Thread model.

Figure 2.13: Parallel programming models for shared memory.

Distributed memory systems

These systems do not consider the concept of global address space. Instead, each processor has its own local memory operating independently as in Figure 2.14. This means that changes in the local memory do not have effect on the memory of the other processors. When a CPU needs to access to data in another CPU or memory, it considers a communication network interconnecting all the CPUs, such as an Ethernet network.

The use of distributed memory systems has some advantages. For example, memory is scalable with the number of processors and it has a good profitability (in theory, any type of device connected to the network can be used to compute). However, there are also shortcomings, such as non-uniform memory access times due to networking delay and the difficulty to map data structures based on global memory to this organisation.

Parallel programming models for distributed memory are based on message passing. Historically, we find a variety of message passing libraries. However, nowadays an industry standard called Message Passing Interface[1] (MPI) has replaced all other message passing implementations. Figure 2.15 shows an MPI example of two machines communicating through synchronous functions.

Hybrid distributed-shared memory systems

This is the most common architecture for supercomputers. It is a combination of the two previous approaches, where a shared memory component can be a shared memory

[1] http://www.mpi-forum.org/

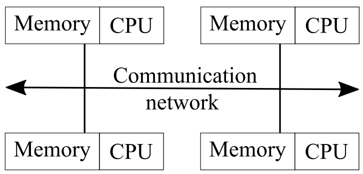

Figure 2.14: Distributed memory systems.

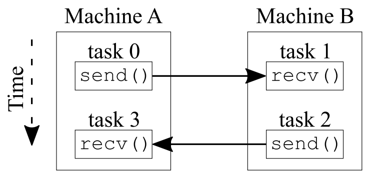

Figure 2.15: MPI example for distributed memory systems.

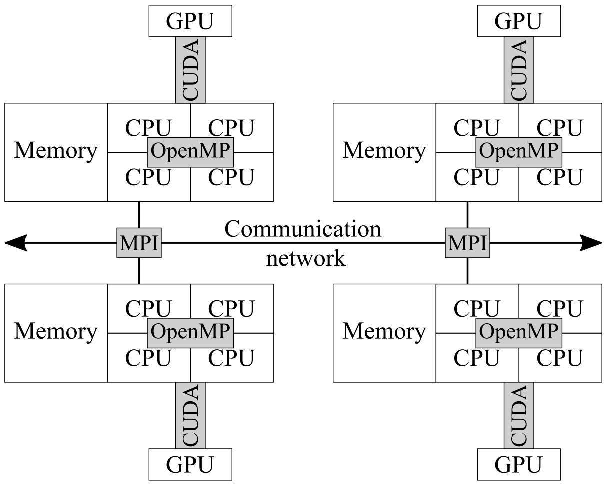

Figure 2.16: Hybrid distributed-shared memory systems.

machine and/or Graphics Processing Units (GPUs). This model provides scalability with a great ratio of power/profitability. However, programming complexity is increased.

Parallel programming models for hybrid memory systems are also a combination of the two previous approaches. As an example, in Figure 2.16 we assume OpenMP for shared memory machines and MPI for sending messages between them. As GPUs are also considered, Compute Unified Device Architecture (CUDA) is assumed for data exchanging between shared memory machine and GPU.

2.2.3 Classification Based on Grain Size

There is another classification, measuring the granularity of a parallel program, i.e. how often parallel tasks need to synchronize or communicate with each other, compared to the computing load [46]. There are three levels according to this classification:

- **Fine grain:** It assumes a high degree of communications. At this level, a reduced set of instructions or simple loops are executed in parallel. Usually, each parallel task has less than 20 instructions. This type of parallelism can be achieved through compilers.

- **Medium grain:** It assumes a medium degree of communications. At this level, procedures or subprograms are executed in parallel. Usually, each parallel task has less than 500 instructions. This level is exploited by programmers, but not through compilers.

- **Coarse grain:** It assumes a low degree of communications. At this level, independent programs are executed in parallel. Usually, each parallel task has more than 1000 instructions. Traditionally, this level is exploited through operating systems. If there is not any communication, then the application is considered embarrassingly parallel.

2.2.4 Performance Assessment for Parallel Computing

As for problem solving, it is interesting to define some metrics to establish the quality of a parallel implementation. One of the most important metrics is speedup. It was defined by Amdahl's law [47] and evaluates the improvement when executing a task.

Definition 2.2.1 (Speedup). *Let c be a section of code to analyse, let p be the number of CPUs for parallel computing, and let t_c^p be the execution time of code c by assuming p CPUs. Speedup or acceleration metric $I_{SU}(c,p)$ for a code c and p CPUs is given by*

$$I_{SU}(c,p) = \frac{t_c^1}{t_c^p}.$$

Optimally, if we parallelise an algorithm doubling the number of CPUs considered initially, then execution times should be halved. However, very few parallel algorithms get optimal speedup, i.e. linear speedup. Most of them achieve a near-linear speedup for a small number of CPUs, reducing the gain while the number of CPUs is increased, approximating to a constant for large numbers of CPUs. This is because the speedup of a parallel program is limited by how much of the program can be parallelised. As an example, Figure 2.17 shows speedup and number of CPUs for some parallel codes by assuming a logarithmic scale. Note that codes having a higher parallel percentage show a better speedup. In this figure, the code having 100% parallel percentage corresponds to ideal speedup.

Definition 2.2.2 (Theoretical speedup limit). *Given a code c and the percentage α_c of c suitable for being parallelised. Theoretical maximum speedup $I_{SU}^1(c)$ of c is expressed as*

$$I_{SU}^1(c) = \frac{1}{1-\alpha_c}.$$

Thus, if α_c equals 0.95, then the theoretical maximum speedup would be 20. Note that if α_c equals 1, then speedup is infinity, i.e. it is optimal.

An additional metric based on speedup is efficiency, estimating how well-utilised the processors are in the parallel implementation.

Definition 2.2.3 (Efficiency). *Given a code c and p CPUs. Efficiency $I_E(c,p)$ of c executed in p CPUs is expressed as*

$$I_E(c,p) = \frac{I_{SU}(c,p)}{p}.$$

Based on this efficiency metric, we get three different possibilities:

- **Efficiency equals 1:** It is the ideal situation showing a very good convergence.
- **Efficiency lower than 1:** It is the usual situation. Values closer to 1 are desirable.
- **Efficiency greater than 1:** It is an unusual situation called super-linear speedup. It happens when the theoretical maximum speedup is exceeded. One possible reason is the cache effect, resulting from the different memory hierarchies of a modern computer.

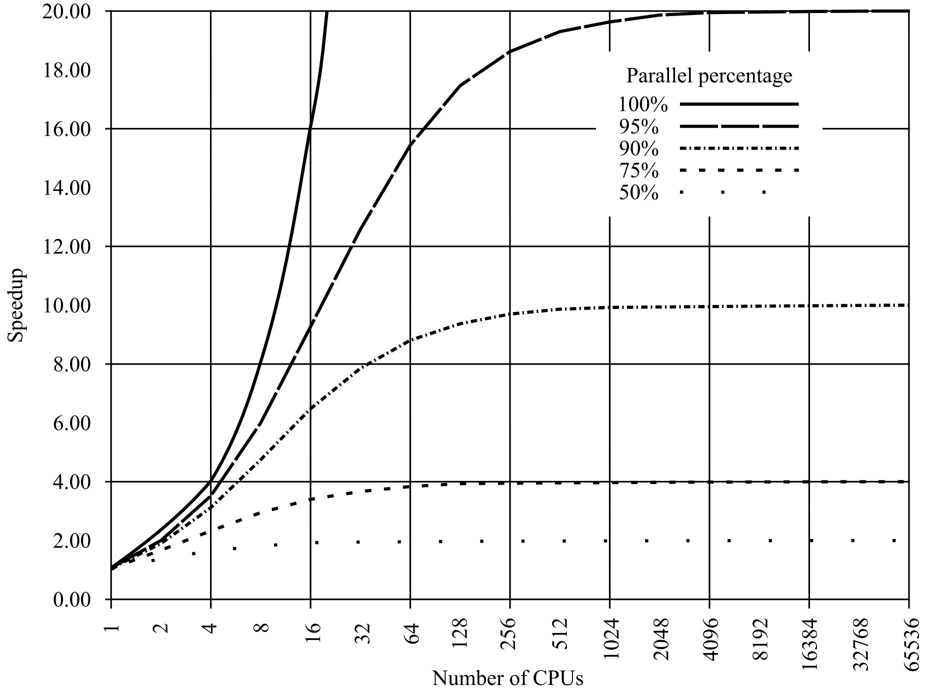

Figure 2.17: Amdahl's Law.

CHAPTER

3

Multiobjective Metaheuristics

In this chapter, we provide a general description of the MO metaheuristics considered in this dissertation to solve the RNPP. We include metaheuristics from the three main types:

- MO approaches of the three SO SIAs FA, ABC, and GSA.
- Three EAs, the standard NSGA-II and SPEA2 and the state-of-the-art MOEA/D.
- An MO approach of the TA VNS.

Next, we describe each one in depth.

3.1 Non-dominated Sorting Genetic Algorithm II

NSGA-II was proposed by Deb et al. in [8] as a revised version of NSGA ([48]). This improved metaheuristic is characterized by assuming two MO measures called rank and crowding:

- Given a set of solutions, rank is obtained by splitting the set into different Pareto fronts. Thus, the solutions in the non-dominated front have rank 0; the solutions in the non-dominated front in the absence of the previous one have rank 1, and so on. The authors proposed a sorting function called fast-non-dominated-sort to perform this task.
- The crowding distance provides density information. Given a solution in a Pareto front, the measure is calculated as the average perimeter of the cuboid formed by the nearest neighbours to such solution. Note that the cuboid assumes as many dimensions as objectives the problem considers.

Based on these two MO measures, the authors defined an elitist crowded-comparison operator $\prec_n$ to guide the selection process.

Algorithm 1 NSGA-II.

$P_g \leftarrow$ generateInitialPopulation(ps_n) ▷ g starts from 1
$Q_g \leftarrow \{\ \}$
$F_g \leftarrow P_g$
while not stop condition **do**
  $R_g \leftarrow P_g \cup Q_g$ ▷ Combine both parent and offspring populations
  $S_g \leftarrow$ fastNonDominatedSort(R_g) ▷ Sort R_g in fronts, $S_g = \{f_g^1, f_g^2, \ldots\}$
  $P_{g+1} \leftarrow \{\ \}$
  while $||P_{g+1}|| + ||f_g^i|| <= ps_n$ **do** ▷ i starts from 1
    crowdingDistanceAssignment(f_g^i) ▷ Calculate the crowding distance of solutions in f_g^i
    $P_{g+1} \leftarrow P_{g+1} \cup f_g^i$
    $i \leftarrow i + 1$
  end while
  if $||P_{g+1}|| < ps_n$ **then**
    $f_g^i \leftarrow$ sortCrowding(f_g^i) ▷ Sort f_g^i in descending order based on crowding
    $P_{g+1} \leftarrow P_{g+1} \cup f_g^i[1 : (ps_n - ||P_{g+1}||)]$ ▷ Choose the first $ps_n - ||P_{g+1}||$ elements of f_g^i
  end if
  $Q_{g+1} \leftarrow \{\ \}$
  while $||Q_{g+1}|| <= ps_n$ **do**
    $(\zeta, \zeta') \leftarrow$ binaryTournament(P_{g+1})
    $\eta \leftarrow$ crossover(ζ,ζ',$param\_cro_n$)
    $\eta \leftarrow$ mutation(η,$param\_mut_n$)
    $Q_{g+1} \leftarrow Q_{g+1} \cup \{\eta\}$
  end while
  $F_{g+1} \leftarrow$ getBestSolutions(F_g, Q_{g+1})
  $g \leftarrow g + 1$
end while

Definition 3.1.1 (Crowded-comparison operator). *Let ζ and η be two solutions to an optimisation problem. Let ζ_{rank} and η_{rank} be the rank of ζ and η, respectively. Let ζ_{crow} and η_{crow} be the crowding of ζ and η, respectively. Then, the crowded-comparison operator $\prec_n$ is given by*

$$\zeta \prec_n \eta \iff \Big[\zeta_{rank} < \eta_{rank}\Big] \vee \Big[(\zeta_{rank} = \eta_{rank}) \wedge (\zeta_{crow} > \eta_{crow})\Big],$$

i.e. ζ is better than η if any of the conditions holds.

As Algorithm 1 shows, NSGA-II assumes two populations P and Q of size ps_n, where at generation $g \geq 1$, P_g saves the parents of the current generation and Q_g contains the offspring generated by individuals in P_g. We propose to include another auxiliary population F with undefined size, where at generation g, F_g saves the best solutions found until g. This is particularly interesting when we want to save all the solutions found and the number of non-dominated individuals in P is greater than ps_n. Below, NSGA-II is described step by step:

Input:

- ps_n: size of the populations P and Q.
- $param\_cro_n \in [0, 1]$: probability that crossover is performed.
- $param\_mut_n \in [0, 1]$: probability that mutation is performed.

Output:

- F: a set of non-dominated individuals solving the problem.

Step 0: Initialisation (lines $1-3$)
In this first step, P_g is randomly generated and Q_g is empty, starting g from 1. F_g is initialised with the content of P_g.

Step 1: Generation of the parent population of the next generation (lines $5-16$)
Both populations P_g and Q_g are combined in a new one R_g with size $2\ ps_n$ (line 5). The best ps_n individuals from R_g are inserted into a new parent population P_{g+1}. To this end, R_g is sorted into Pareto fronts according to the sorting algorithm proposed by the authors. Next, full fronts are inserted into the new population in ascending order (from best to worst rank) until P_{g+1} is filled or the remaining free space is not enough (lines 6-12). If the latter case is fulfilled, the current front is sorted using the crowding distance and then only its best $ps_n - ||P_{g+1}||$ solutions are inserted into P_{g+1} (lines 13-16).

Step 2: Generation of the offspring population of the next generation (lines $17-23$)
In this step, a new Q_{g+1} is generated based on P_{g+1}. To this end and so long as Q_{g+1} is not filled, two individuals ζ and ζ' are selected from P_{g+1} by binary tournament[1](line 19). Then, a new individual is generated through crossover and mutation operators (lines $20-21$). Both operators usually assume a parameter determining the probability that the task is performed, $param\_cro_n$ and $param\_mut_n$, respectively. Finally, the new individual is inserted into Q_{g+1} (line 22).

Step 3: Next generation (lines 4 and $24-25$)
The algorithm goes to the next generation jumping to step 1. Before this, the best solutions found are saved in F_{g+1}. This procedure is repeated while a stop condition is not reached.

3.2 Strength Pareto Evolutionary Algorithm 2

SPEA2 was developed by Zitzler et al. [9] as an enhanced version of the previous SPEA [37]. This MO metaheuristic assumes two populations P and $\overline{P}$, where at generation $g \geq 1$, P_g is a regular population of size ps_s and $\overline{P}_g$ is an auxiliary population of size $\overline{ps}_s$, saving the best individuals found over generations. SPEA2 is characterised by assuming a selection process based on the Pareto dominance concept and additional density measure as fine assignment.

Each solution $\zeta \in \{P_g \cup \overline{P}_g\}$ is assigned a strength value $strength_s(\zeta)$, denoting the number of solutions dominated by ζ, that is[2]

$$strength_s(\zeta) = ||\{\eta : \eta \in \{P_g \cup \overline{P}_g\} \wedge \zeta \succ \eta\}||.$$

On the basis of the strength value, the raw fitness of ζ, denoted as $raw_s(\zeta)$, is defined as the strength of its dominators in both populations, which is given by[3]

$$raw_s(\zeta) = \sum_{\eta : \eta \in \{P_g \cup \overline{P}_g\} \wedge \eta \succ \zeta} strength_s(\eta),$$

[1]Two individuals are randomly selected from a set, choosing the best individual of both.
[2]This is for a maximisation problem. If a minimisation problem is assumed, the expression changes $\succ$ for $\prec$.
[3]This is for a maximisation problem. If a minimisation problem is assumed, the expression changes $\succ$ for $\prec$.

Algorithm 2 SPEA2.

1: $P_g \leftarrow$ generateInitialPopulation(ps_s) ▷ g starts from 1
2: $\overline{P}_g \leftarrow \{\,\}$
3: $F_g \leftarrow P_g$
4: **while** not stop condition **do**
5: $A_g \leftarrow$ fitnessAssignment(P_g,$\overline{P}_g$) ▷ Calculate SPEA2 fitness values
6: $\overline{P}_{g+1} \leftarrow$ environmentalSelection(A_g) ▷ Copy the best solutions from $P_g \cup \overline{P}_g$ to $\overline{P}_{g+1}$
7: $P_{g+1} \leftarrow$ makeNewPopulation($\overline{P}_{g+1}, param\_cro_s, param\_mut_s$) ▷ Generate a new P_{g+1}
8: $F_{g+1} \leftarrow$ getBestSolutions(F_g, P_{g+1})
9: $g \leftarrow g + 1$
10: **end while**

where $raw_s(\zeta)$ equalling 0 corresponds to a non-dominated individual and a high $raw_s(\zeta)$ value means that ζ is dominated by many individuals.

In case that most solutions are non-dominated, the raw fitness is lacking. To alleviate this issue, additional density information is added to guide the selection process. This density measure is based on the k-th nearest neighbour method: given a reference solution ζ, the distances (in the objective space) to all other individuals in both populations are calculated and sorted in increasing order. Next, the k-th element is taken, where k is given by

$$k = \sqrt{ps_s + \overline{ps}_s}.$$

Based on this neighbour method, the density measure of ζ, denoted as $dens_s(\zeta)$, is expressed as

$$dens_s(\zeta) = \frac{1}{\sigma_\zeta^k + 2},$$

where σ_ζ^k is the k-th element provided by the neighbour method, assuming ζ as the reference solution. Given ζ, the combination of both measures, the raw fitness and the density information, yields a fitness value $fitness_s(\zeta)$ guiding the selection process, that is

$$fitness_s(\zeta) = raw_s(\zeta) + dens_s(\zeta). \tag{3.1}$$

Algorithm 2 shows the overall behaviour of SPEA2. As for NSGA-II, we propose to include an auxiliary population F with undefined size. Below, the algorithm is described step by step:

Input:

- ps_s: size of the population P.
- $\overline{ps}_s$: size of the population $\overline{P}$.
- $param\_cro_s \in [0, 1]$: probability that crossover is performed.
- $param\_mut_s \in [0, 1]$: probability that mutation is performed.

Output:

- F: a set of non-dominated individuals solving the problem.

Step 0: Initialisation (lines $1 - 3$)

In this first step, P_g is randomly generated and $\overline{P}_g$ is empty, starting g from 1. F_g is initialised with the content of P_g.

Step 1: Fitness assignment (line 5)
Each solution in $P_g \cup \overline{P_g}$ is assigned a fitness value given by Equation (3.1).

Step 2: Environmental selection (line 6)
The best solutions from $P_g \cup \overline{P_g}$ are copied to $\overline{P}_{g+1}$. To this end, we get the number of non-dominated solutions in $P_g \cup \overline{P_g}$, denoted as nd_g. Note that non-dominated solutions have an SPEA2 fitness lower than one. According to nd_g, we could have three possibilities: i) nd_g equals $\overline{ps}_s$, then the non-dominated solutions are copied to $\overline{P}_{g+1}$. ii) nd_g is lower than $\overline{ps}_s$, then the solutions in $P_g \cup \overline{P_g}$ are sorted in increasing order according to the SPEA2 fitness, copying the first $\overline{ps}_s$ solutions to $\overline{P}_{g+1}$. iii) nd_g is greater than $\overline{ps}_s$, then a truncation procedure is performed based on the k-th nearest neighbour method, copying only the $\overline{ps}_s$ non-dominated individuals, which have greater distances among them.

Step 4: Generation of a new regular population (line 7)
A new P_{g+1} is generated based on $\overline{P}_{g+1}$, assuming binary tournament, crossover, and mutation as previously discussed in Section 3.1 for NSGA-II .

Step 5: Next generation (lines 4 and $8-9$)
The algorithm goes to the next generation jumping to step 1. Before this, the best solutions found are saved in F_{g+1}. This procedure is repeated while a stop condition is not reached.

3.3 Multiobjective Variable Neighbourhood Search Algorithm

MO-VNS was proposed by Geiger et al. [49] as an MO version of the traditional SO VNS [11]. This metaheuristic does not exactly follow a trajectory in the objective space as other TAs. Instead, given a solution to the optimisation problem, the algorithm explores the search space by generating new solutions in the surrounding of such initial solution. To this end, it considers a set of neighbourhood structures, determining how different could be a new solution from the initial one. This set is denoted as NS_v and is expressed as

$$NS_v = \{ns_v^1, ns_v^2, \ldots, ns_v^{param\_neigh_v}\},$$

where $param\_neigh_v$ is the number of neighbourhood structures. This set NS_v is partially ordered, for any two structures $ns_v^i, ns_v^{i+1} \in NS_v$ with $i \in 1, 2, \ldots, param\_neigh_v - 1$, ns_v^{i+1} could generate a more different solution than ns_v^i, regarding the initial solution.

The definition of the set of neighbourhood structures depends on the problem definition and should be carefully studied. If we consider Example 2.1.1, where we have two decision variables a and b, NS_v could be defined as

$$NS_v = \{1, 2, 3\}.$$

This way, a new solution could be generated by adding an integer random number between 0 and one of the three neighbourhood structures to a and b. For example, if we select the second neighbourhood structure ns_v^2, the random number will be generated in the interval $[0, 2]$.

As described in Algorithm 3, MO-VNS assumes two populations P and S with undefined size, where at generation $g \geq 1$, P_g is a regular population, keeping only non-dominated solutions, and S_g saves the solutions from P_g, which were considered during g to explore the search space. Below, the algorithm is described step by step:

Algorithm 3 MO-VNS.

1: $P_g \leftarrow$ generateRandomIndividual() ▷ g starts from 1
2: $S_g \leftarrow \{ \}$
3: $NS_v \leftarrow$ generateNeighborhoodStructures$(param_neigh_v, param_ns_v)$
4: **while** not stop condition **do**
5:     **while** $P_g \neq S_g$ **do** ▷ While there are non-considered solutions
6:         $\zeta \leftarrow$ selectNonConsideredSolution(P_g, S_g) ▷ A non-considered solution from P_g is selected
7:         $ns_v^i \leftarrow$ selectNeighborhoodStructure(NS_v) ▷ $i \in 1, 2, \ldots, param\_neigh_v$
8:         $S_g \leftarrow S_g \cup \{\zeta\}$ ▷ The solution is marked as studied
9:         **do**
10:             $\overline{\zeta} \leftarrow$ generateNeighborhoodSolution(ζ, ns_v^i)
11:             $P_g \leftarrow P_g \cup \{\overline{\zeta}\}$
12:             $(P_g, S_g) \leftarrow$ update(P_g, S_g) ▷ Only non-dominated solutions are saved
13:             **if** $\overline{\zeta} \in P_g$ **then**
14:                 $\zeta \leftarrow \overline{\zeta}$ ▷ The new solution is considered to explore the search space
15:                 $ns_v^i \leftarrow ns_v^1$ ▷ The first neighbourhood structure is selected
16:                 $S_g \leftarrow S_g \cup \{\zeta\}$ ▷ The solution is marked as studied
17:             **else**
18:                 **if** $ns_v^i \neq ns_v^{param\_neigh_v}$ **then**
19:                     $ns_v^i \leftarrow ns_v^{i+1}$ ▷ The next neighbourhood structure is considered if possible
20:                 **end if**
21:             **end if**
22:         **while** $ns_v^i \neq ns_v^{param\_neigh_v}$
23:     **end while**
24:     **if** perturbation mechanism **then**
25:         $P_{g+1} \leftarrow$ performPerturbation$(P_g, param_per_v)$
26:     **else**
27:         $P_{g+1} \leftarrow P_g$
28:     **end if**
29:     $S_{g+1} \leftarrow \{ \}$
30:     $g \leftarrow g + 1$
31: **end while**

Input:

- $param\_neigh_v$: number of neighbourhood structures.
- $param\_ns_v$: it determines how the neighbourhood structures are generated.
- $param\_per_v$: it determines how the perturbation mechanism is performed.

Output:

- P: a set of non-dominated individuals solving the problem.

Step 0: Initialisation (lines $1 - 3$)
In this first step, a random solution is inserted into P_g and S_g is empty, starting g from 1. Next, the set of neighbourhood structures is generated. It is usual that the generation of this set is based on any parameter related to the problem definition. In this case, we include a parameter called $param\_ns_v$ to show this behaviour.

Step 1: Select non-considered solutions (lines $6 - 8$)
A non-considered solution $\zeta \in P_g \wedge \zeta \notin S_g$ and a neighbourhood structure $ns_v^i \in NS_v$

with $i \in 1, 2, \ldots, param\_neigh_v$ are randomly selected to explore the search space (lines $6 - 7$). ζ is inserted into S_g to avoid being selected again over g (line 8).

Step 2: Explore neighbourhood solutions (lines $10 - 22$)
A new solution $\overline{\zeta}$ is generated in the neighbourhood of ζ based on ns_v^i (line 10). The new solution $\overline{\zeta}$ is added to P_g (line 11). Next, P_g is updated, removing all the dominated solutions (line 12). Note that if a solution from P_g is removed, it is also removed from S_g. If after this procedure $\overline{\zeta}$ is in P_g, this means that the exploration provided a good performance. Hence, the search is repeated again, but assuming $\overline{\zeta}$ as base solution and considering $ns_v^{i=1}$ as neighbourhood structure (lines $13 - 16$). Otherwise, the next structure is taken so long as ns_v^i equals $ns_v^{param\_neigh_v}$ (lines $17 - 22$).

If the latter case is fulfilled and ns_v^i equals $ns_v^{param\_neigh_v}$, then the algorithm goes to step 1 if there is any non-considered solution in P_g. Otherwise, it goes to step 3 (line 5).

Step 3: Next generation (lines $24 - 30$)
At this point, some authors consider a perturbation mechanism [49], modifying the solutions in P_g to avoid local minima. For example, by assuming a mutation operator as discussed for NSGA-II and SPEA2 (lines $24 - 25$). We include a parameter called $param\_per_v$, which could be considered to determine the behaviour of this procedure. After this, the algorithm goes to the next generation jumping to step 1 (lines $26 - 30$). This procedure is repeated so long as a stop condition is not reached.

3.4 Multiobjective Artificial Bee Colony Algorithm

ABC was proposed by Karaboga and Basturk [14]. This is an SO SIA based on the behaviour of honey bees. According to the authors, there are three essential components in a real honey bee swarm, i.e. food sources, employed foragers, and unemployed foragers:

- Food sources are set of flowers in the surrounding of the hive.
- Employed foragers are the bees exploiting known food sources. Each time an employed forager exploits a food source, it returns to the nest to upload the nectar and shares quality information about the source.
- Unemployed foragers are the bees looking out for new food sources. There are two types: onlookers and scouts. Onlookers wait in the nest to define new food sources based on the quality information provided by employed foragers. Scouts search new food sources without considering any previous experience.

The authors considered some assumptions to design the metaheuristic:

- A food source is a solution to the optimisation problem.
- The colony consists of two groups of artificial bees: employed foragers and onlookers.
- Each employed forager is assigned to a food source, which is exploited by generating new solutions in its surrounding. The algorithm includes a parameter called $param\_limit_a$ to detect if a food source is exhausted. Thus, if the bee does not get a better solution after $param\_limit_a$ times, the employed forager considers that the source is exhausted. Then, the bee becomes a scout, choosing a new food source through a low cost search.

Algorithm 4 MO-ABC.

```
P_g ← generateInitialPopulation(ps_a)                      ▷ g starts from 1
F_g ← { }
while not stop condition do
    (Se_g, So_g) ← selectBees(P_g,param_Se_a)              ▷ Divide population
    Se_{g+1} ← { }                                          ▷ Employed forager process
    for each ζ ∈ Se_g do
        ζ̄ ← generateEmployedForagerSolution(ζ)
        if ζ is better than ζ̄ then
            ζ.attemptCounter + +
        end if
        Se_{g+1} ← Se_{g+1} ∪ greedySelection(ζ,ζ̄)
    end for
    So_{g+1} ← { }                                          ▷ Onlooker process
    ProbSe_{g+1} ← generateProbabilities(Se_{g+1})
    for each η ∈ So_g do
        ζ ← selectEmployedForager(ProbSe_{g+1},Se_{g+1})
        η̄ ← generateOnlookerSolution(η,ζ)
        So_{g+1} ← So_{g+1} ∪ greedySelection(η,η̄)
    end for
    for each ζ ∈ Se_{g+1} do                                ▷ Scout process
        if ζ.attemptCounter > param_limit_a then
            ζ̄ ← generateScoutSolution()
            Se_{g+1} ← replaceSolution(Se_{g+1},ζ,ζ̄)
        end if
    end for
    P_{g+1} ← Se_{g+1} ∪ So_{g+1}                           ▷ Next generation
    F_{g+1} ← getBestSolutions(F_g,P_{g+1})
    g ← g + 1
end while
```

- As stated before, onlookers establish new food sources based on the information shared by employed foragers. This information quality is shared with a probability proportional to the profitability of the food source.

In this dissertation, we propose an MO approach of this SIA called MO-ABC. As given in Algorithm 4, MO-ABC assumes a population P of size ps_a and an auxiliary population F of undefined size, where at generation $g \geq 1$, P_g saves the non-exhausted food sources known at g and F_g saves the best food sources found until g. Below, the algorithm is described step by step:

Input:

- ps_a: size of the population P.
- $param\_Se_a \in [0, 1]$: percentage of employed foragers in P.
- $param\_limit_a \in 0, 1, \ldots$: number of attempts to determine if a food source is exhausted.

Output:

- F: a set of non-dominated individuals solving the problem.

Step 0: Initialisation (line $1-2$)
In this first step, P_g is randomly generated and F_g is empty, starting g from 1.

Step 1: Select group of bees (line 4)
Based on $param\_Se_a$, P_g is divided into two groups Se_g and So_g, i.e. the set of employed foragers and onlookers at generation g, respectively.

Step 2: Employed forager process (lines $5-12$)
Each employed forager $\zeta \in Se_g$ generates a new solution $\overline{\zeta}$ in its surrounding. Next, a greedy selection between both solutions is performed, increasing the attempt counter of ζ if the previous solution is better than the one generated. The resulting solution is inserted into a new Se_{g+1}. Note that a new solution has an attempt counter value equalling 0.

Step 3: Onlooker process (lines $13-19$)
The original SO ABC considers a probability based selection process to generate new solutions based on Se_{g+1}. It establishes selection probabilities based on the value of the objective to optimise. Here, we propose an MO version of ABC. To this end, Se_{g+1} is sorted according to the elitist crowded-comparison operator $\prec_n$ discussed for NSGA-II in Section 3.1. Thus, after the sorting, the best solution of Se_{g+1} is twice as likely as the second one, the second solution is twice as likely as the third one, and so on (line 14).

Each onlooker $\eta \in So_g$ takes an employed forager $\zeta \in Se_{g+1}$ according to the selection probabilities $ProbSe_{g+1}$. Then, a new solution $\overline{\eta}$ is generated based on the information provided by ζ. Next, a greedy selection is performed between both. The resulting solution is added to a new So_{g+1} (lines $15-19$).

Step 4: Scout process (lines $20-25$)
For each employed forager $\zeta \in Se_{g+1}$, we check if its solution is exhausted. In such a case, a new solution $\overline{\zeta}$ is generated by a low-cost local search. This procedure is characterised by a low average in food source quality. However, scouts occasionally discover rich unknown food sources. The new solution is replaced by the exhausted one.

Step 5: Next generation (lines $26-28$)
The new P_{g+1} is generated by combining both Se_{g+1} and So_{g+1}. F_{g+1} saves the best solutions found until now. Next, the algorithm goes to the next generation jumping to step 1. This procedure is repeated so long as a stop condition is not reached.

3.5 Multiobjective Firefly Algorithm

Fireflies are a type of nocturnal beetle, which produces flashing lights by a process of bioluminescence, with the main purpose of attracting mating partners and potential prey. As is well known, light intensity decreases with the distance from its source and the media absorbs light. Hence, flashing lights of fireflies are only visible to a limited distance.

The original SO FA was proposed by Yang [13]. This algorithm is based on the idealised behaviour of fireflies by following three basic rules:

- All fireflies are unisex. Hence, a firefly can be attracted to another, regardless of its sex.
- Attractiveness is proportional to light intensity. Given any two fireflies, the less bright one will move towards the brighter one.

- The light intensity of a firefly is determined by the landscape of the objective function to be optimised. As this is an SO metaheuristic, light intensity could be proportional to the value of the fitness function, in case that a maximisation problem is assumed.

There are two important aspects in the formulation of FA, i.e. the variation of brightness and the formulation of attractiveness:

- A firefly is a possible solution to the optimisation problem. Hence, the brightness of a firefly is determined by its solution quality. In this dissertation, we propose an MO approach of this SIA called MO-FA. To this end, we consider the elitist crowded-comparison operator $\prec_n$ previously discussed for NSGA-II in Section 3.1. Thus, let ζ and η be any two fireflies, ζ is brighter than η if $\zeta \prec_n \eta$.

- Attractiveness is defined based on the distance between fireflies. Let n be the number of decision variables of the optimisation problem. Let ζ and η be any two fireflies, where ζ_i and η_i are the values of the i-th decision variable of ζ and η, with $i \in 1, 2, \ldots, n$. Let $d^s_{fa}(\zeta, \eta)$ be the Cartesian distance between ζ and η in the solution space denoted as

$$d^s_{fa}(\zeta, \eta) = \sqrt{\sum_{i=1}^{n} (\zeta_i - \eta_i)^2}.$$

Suppose that $\zeta \prec_n \eta$. Then, the attractiveness that ζ applies to η causes a movement in η expressed as

$$\eta_i = \eta_i + \beta_{0_f} e^{-\gamma_f \ d^s_{fa}(\zeta,\eta)^2} (\zeta_i - \eta_i) + r_f \ (\alpha - \frac{1}{2}); \quad \forall i \in 1, 2, \ldots, n, \tag{3.2}$$

where $r_f \in [0, 1]$ is the randomisation parameter, α is a random number in the interval $[0, 1]$, $\beta_{0_f} \in [0, 1]$ is the attractiveness at $d^s_{fa}(\zeta, \eta)$ equalling 0, and $\gamma_f \in [0, \infty)$ is the light absorption coefficient. The value of γ is crucial, due to it determines the convergence speed of the algorithm. In practice, this value is limited by the characteristics of the optimisation problem. Most applications assume values varying from 0.01 to 100.

The original formulation of attractiveness given by Equation (3.2) presents some limitations, due to the exponential function e. If the distance between two fireflies is large, the value provided by the exponential function will be huge. This formulation limits the applicability of the algorithm in certain problems. To solve this, we propose to change distances to the interval $[0, 1]$ by assuming a bounding distance, that is

$$bd^s_{fa}(\zeta, \eta) = \frac{d^s_{fa}(\zeta, \eta)}{\sqrt{n \sum_{i=1}^{n} (max\_x_i - min\_x_i)^2}},$$

where max_x_i and min_x_i are the maximum and minimum values of the decision variable x_i, respectively. These maximum and minimum values could be theoretical or practical ones. Thus, the new formulation of attractiveness is expressed as

$$\eta_i = \eta_i + \beta_{0_f} e^{-\gamma_f \ bd^s_{fa}(\zeta,\eta)^2} (\zeta_i - \eta_i) + r_f \ (\alpha - \frac{1}{2}); \quad \forall i \in 1, 2, \ldots, n. \tag{3.3}$$

Algorithm 5 MO-FA.

1: $P_g \leftarrow$ generateInitialPopulation(ps_f) ▷ g starts from 1
2: $Q_g \leftarrow \{\ \}$
3: $F_g \leftarrow P_g$
4: **while** not stop condition **do**
5: $\quad I_g \leftarrow$ calculateLightIntensity(P_g)
6: $\quad$ **for each** $\zeta \in P_g$ **do**
7: $\quad\quad \overline{\zeta} \leftarrow$ copyFirefly($\zeta, \overline{\zeta}$) ▷ Copy ζ to a new firefly $\overline{\zeta}$
8: $\quad\quad$ **for each** $\eta \in P_g : \zeta \neq \eta$ **do**
9: $\quad\quad\quad$ **if** getLightIntensity(I_g, η) $>$ getLightIntensity(I_g, ζ) **then** ▷ If η is brighter than ζ
10: $\quad\quad\quad\quad \overline{\zeta} \leftarrow$ moveFirefly($\overline{\zeta}, \eta, r_f, \beta_{0_f}, \lambda_f$) ▷ Move firefly $\overline{\zeta}$ towards η
11: $\quad\quad\quad$ **end if**
12: $\quad\quad$ **end for**
13: $\quad\quad Q_g \leftarrow Q_g \cup \{\overline{\zeta}\}$
14: $\quad$ **end for**
15: $\quad \overline{\zeta} \leftarrow$ moveBrightestFirefly(P_g) ▷ The brightest firefly in P_g is randomly moved
16: $\quad Q_g \leftarrow Q_g \cup \{\overline{\zeta}\}$
17: $\quad Q_g \leftarrow$ calculateFitnessValues(Q_g) ▷ Evaluate fireflies in Q_g
18: $\quad Q_{g+1} \leftarrow \{\ \}$
19: $\quad P_{g+1} \leftarrow$ selectBestIndividuals(P_g, Q_g) ▷ The best ps_f fireflies of $P_g \cup Q_g$ are inserted into P_{g+1}
20: $\quad P_{g+1} \leftarrow$ stagnationControl($P_{g+1}, P_g, Q_g, param\_how\_sc_f, param\_when\_sc_f$)
21: $\quad F_{g+1} \leftarrow$ getBestSolutions(F_g, P_{g+1})
22: $\quad g \leftarrow g + 1$
23: **end while**

As stated before, we propose an MO approach of FA called MO-FA. As given in Algorithm 5, MO-FA assumes two populations P and Q of size ps_f, where at generation $g \geq 1$, P_g saves the fireflies at the beginning of g, before attractiveness, and Q_g contains the resulting population after moving the fireflies in P_g. As for NSGA-II and SPEA2, we propose to include an auxiliary population F with undefined size. Below, the algorithm is described step by step:

Input:

- ps_f: size of the populations P and Q.
- $r_f \in [0, 1]$: randomisation parameter.
- $\beta_{0_f} \in [0, 1]$: attractiveness at distance 0.
- $\lambda_f \in [0, \infty)$: light absorption coefficient.
- $param\_how\_sc_f$: it determines how the stagnation control is performed.
- $param\_when\_sc_f$: it determines when the stagnation control is performed.

Output:

- F: a set of non-dominated individuals solving the problem.

Step 0: Initialisation (lines $1 - 3$)
In this first step, P_g is randomly generated and Q_g is empty, starting g from 1. F_g is initialised with the content of P_g.

Step 1: Calculate light intensity of fireflies (line 5)
Light intensity of fireflies in P_g is calculated attending to $\prec_n$. The values are saved in I_g.

Step 2: Attractiveness (lines $6-14$)
Each solution in P_g is attracted to others, having greater light intensity. This attractiveness causes a movement described by Equation (3.3). The resulting fireflies are saved in Q_g.

Step 3: Move the brightest firefly (lines $15-16$)
The brightest firefly in P_g is randomly moved, because it was not attracted to any other solution. The resulting firefly is inserted into Q_g.

Step 4: Next generation (lines $17-22$)
After movements, the fitness functions of each solution in Q_g are calculated. Next, Q_{g+1} is initialised to empty and a new P_{g+1} is generated by combining both P_g and Q_g, saving only its best ps_f solutions according to $\prec_n$. After this, a stagnation control is performed to ensure that the algorithm escapes from local minima. To this end, if the condition in $param\_when\_sc_f$ holds, then this procedure will include changes in P_{g+1} attending to $param\_how\_sc_f$. We include this mechanism due to the algorithm does not have any procedure to ensure this aspect. Next, the best solutions found are saved in F_{g+1}. This procedure is repeated, jumping to step 1, so long as a stop condition is not reached.

3.6 Multiobjective Gravitational Search Algorithm

GSA was developed by Rashedi et al [12]. This SO SIA is considered as an isolated system of masses, where agents are objects and their performance is measured by their masses. All these objects are mutually attracted by the Newtonian gravity force, causing a global movement of all objects towards heavier masses, which correspond to good solutions. Heavier masses move slowly than lighter ones, guaranteeing the exploitation of the solution space.

There are five important aspects in the formulation of GSA, i.e. position of agents, masses of agents, gravitational forces, acceleration of agents, velocity of agents, and movement of agents:

- **Position of agents:** Let n be the number of decision variables of the problem. Let ps_{gsa} be the number of agents in the system. Let $x_i^d(g)$ be the value of the d-th decision variable of the i-th agent $x_i(d)$ at generation g, with $d \in 1, 2, \ldots, n$, $g \in 1, 2, \ldots$, $i \in 1, 2, \ldots, ps_{gsa}$. The position in the system of the i-th agent at g is given by

$$x_i(g) = (x_i^1(g), x_i^2(g), \ldots, x_i^n(g)).$$

- **Masses of agents:** They are calculated according to the solution quality. Following the original SO approach, the individual mass $m_i(g)$ of agent $x_i(g)$ is given by

$$m_i(g) = \frac{f(x_i(g)) - worst(g)}{best(g) - worst(g)}, \tag{3.4}$$

where $f(x_i(g))$ is the fitness value of $x_i(g)$ and $best(g)$ and $worst(g)$ are defined as[1]

$$best(g) = \max_{j \in 1,2,\ldots,ps_{gsa}} f(x_j(g)) \tag{3.5}$$

and

$$worst(g) = \min_{j \in 1,2,\ldots,ps_{gsa}} f(x_j(g)), \tag{3.6}$$

[1] This is for a minimisation problem. If a maximisation problem is assumed, the definitions will be opposite and then Equation (3.5) will be for $worst(g)$ and Equation (3.6) will be for $best(g)$.

respectively. Based on this individual mass, the total mass $mm_i(g)$ of agent $x_i(g)$ is calculated regarding all other masses in the system, that is

$$mm_i(g) = \frac{m_i(g)}{\displaystyle\sum_{j=1}^{ps_{gsa}} m_j(g)}. \tag{3.7}$$

As stated before, we propose an MO approach of GSA called MO-GSA. Consequently, individual masses cannot be calculated assuming Equation (3.4), because we have more than one objective. To solve this, we consider the elitist crowded-comparison operator $\prec_n$ discussed for NSGA-II in Section 3.1. Thus, we sort the ps_{gsa} agents in decreasing order at g. After this sorting, the $x_i(g)$ agent corresponds to the i-th best solution in the system at g. This order is assumed to formulate a new expression for calculating individual masses, that is

$$m_i = m_i(g) = \frac{i - ps_{gsa}}{1 - ps_{gsa}}. \tag{3.8}$$

Note that this expression is constant over time. Consequently, Equation (3.7) is also constant over time. Following this MO approach, both individual and total masses are calculated by assuming Equations (3.8) and (3.7), respectively.

- **Gravitational forces:** They are calculated for each decision variable. Given any two agents $x_i(g)$ and $x_j(g)$, the individual force $f^d_{i,j}(g)$ acting on agent $x_i(g)$ from $x_j(g)$ at g is defined as

$$f^d_{i,j}(g) = c(g)\,\frac{mm_i(g)\; mm_j(g)}{d(x_i(g), x_j(g)) + \varepsilon}\,(x^d_j(g) - x^d_i(g)), \tag{3.9}$$

where ε is a very small constant, $d(\cdot)$ provides the n-dimensional Euclidean distance between any two agents, $c(g)$ is a gravitational constant described by an increasing function of g. Based on this individual force, the total force $ff^d_i(g)$ acting on agent $x_i(g)$ is expressed as a randomly weighted sum of the individual forces exerted from the $kbest(g)$ agents at g, that is

$$ff^d_i(g) = \sum_{j=1, j\neq i}^{kbest(g)} (f^d_{i,j}(g)\;\alpha), \tag{3.10}$$

where α is a random number in the interval $[0, 1]$ and $kbest(g)$ is a decreasing function of g, providing values in the range $1, 2, \ldots, ps_{gsa}$.

- **Acceleration of agents:** It is calculated for each decision variable. The acceleration $a^d_i(g)$ of agent $x_i(g)$ is calculated attending to the total forces acting on it, that is

$$a^d_i(g) = \frac{ff^d_i(g)}{mm_i}. \tag{3.11}$$

- **Velocity of agents:** It is calculated for each decision variable. The velocity of agent $x_i(g+1)$ is calculated by assuming its acceleration and velocity in the previous instant g, that is

$$v^d_i(g+1) = a^d_i(g) + v^d_i(g)\;\alpha, \tag{3.12}$$

where α is a random number in the interval $[0, 1]$.

Algorithm 6 MO-GSA.

$(P_g, V_g) \leftarrow$ generateInitialPopulation(ps_{gsa}) ▷ g starts from 1
$Q_g \leftarrow \{\,\}$
$F_g \leftarrow P_g$
$IM \leftarrow$ calculateIndividualMasses(ps_{gsa})
$TM \leftarrow$ calculateTotalMasses(IM)
$c_g \leftarrow param\_cInitial$
$kbest_g \leftarrow param\_kbestInitial$
while not stop condition **do**
    $(P_g, V_g) \leftarrow$ sortPopulation(P_g, V_g)
    $IF_g \leftarrow$ calculateIndividualForces(P_g, c_g, TM)
    $TF_g \leftarrow$ calculateTotalForces($IF_g, kbest_g$)
    $A_g \leftarrow$ calculateAcceleration(TF_g, TM)
    $V_{g+1} \leftarrow$ calculateVelocity(A_g, V_g)
    $Q_g \leftarrow$ moveAgents(P_g, V_{g+1})
    $P_{g+1} \leftarrow$ selectBestIndividuals(P_g, Q_g)
    $P_{g+1} \leftarrow$ stagnationControl($P_{g+1}, P_g, Q_g, param\_how\_sc_{gsa}, param\_when\_sc_{gsa}$)
    $c_{g+1} \leftarrow$ updateC(g)
    $kbest_{g+1} \leftarrow$ updateKbest(g)
    $F_{g+1} \leftarrow$ getBestSolutions(F_g, P_{g+1})
    $g \leftarrow g + 1$
end while

- **Movement of agents:** It is calculated for each decision variable. The position of agent $x_i(g+1)$ is calculated attending to its velocity at such generation and its position in the previous instant g, that is

$$x_i^d(g+1) = x_i^d(g) + v_i^d(g+1). \tag{3.13}$$

As Algorithm 6 shows, MO-GSA assumes two populations P and Q of size ps_{gsa}, where at generation $g \geq 1$, P_g saves the agents at the beginning of g, before acting gravitational forces, and Q_g contains the resulting agents after acting the forces in P_g. As for NSGA-II, SPEA2, and MO-FA, we propose to include an auxiliary population F with undefined size. Below, the algorithm is described step by step:

Input:

- ps_{gsa}: size of the populations P and Q.
- $param\_cInitial_{gsa} \in \mathbb{R}$: value of $c(g)$ at the beginning of the algorithm.
- $param\_cFinal_{gsa} \in \mathbb{R}$: value of $c(g)$ at the end of the algorithm.
- $param\_kbestInitial_{gsa} \in 1, 2, \ldots, ps_{gsa}$: value of $kbest(g)$ at the beginning of the algorithm.
- $param\_kbestFinal_{gsa} \in 1, 2, \ldots, ps_{gsa}$: value of $kbest(g)$ at the end of the algorithm.
- $param\_how\_sc_{gsa}$: it determines how the stagnation control is performed.
- $param\_when\_sc_{gsa}$: it determines when the stagnation control is performed.

Output:

- F: a set of non-dominated individuals solving the problem.

Step 0: Initialisation. Population (lines $1-3$)
In this first step, P_g is randomly generated and Q_g is empty, starting g from 1. F_g is initialised with the content of P_g. Note that when a new solution is generated, its velocity is initialised to zero, that is

$$x_i(g) \in P_g,\ v_i^d(g) = 0 \in V_g; \quad g = 1,\ \forall i \in 1, 2, \ldots, ps_{gsa} \text{ and } \forall d \in 1, 2, \ldots, n.$$

Step 1: Initialisation. Masses (lines $4-5$)
As stated before, for our MO approach the mass of an agent depends on its order position in P_g and the mass for each position is constant over time. Thus, individual and total masses are calculated based on Equations (3.8) and (3.7), that is

$$m_i \in IM,\ mm_i \in TM; \quad \forall i \in 1, 2, \ldots, ps_{gsa}.$$

Step 2: Initialisation. Functions (lines $6-7$)
Initialise $c(g)$ and $kbest(g)$ to the values in $param\_cInitial$ and $param\_kbestInitial$, respectively. Note that according to the notation assumed in the other algorithms, $c(g)$ and $kbest(g)$ are denoted as c_g and $kbest_g$ in Algorithm 6.

Step 3: Evaluate agents (line 9)
P_g is sorted according to $\prec_n$ in decreasing order. Note that V_g is also reorganised to fit the new order of P_g.

Step 4: Calculate gravitational forces (lines $10-11$)
Individual and total forces are calculated for each agent in P_g according to Equations (3.9) and (3.10), respectively. This way,

$$f_{i,j}^d(g) \in IF_g,\ ff_i^d(g) \in TF_g; \quad \forall i, j \in 1, 2, \ldots, ps_{gsa} \text{ and } \forall d \in 1, 2, \ldots, n.$$

Step 5: Calculate acceleration and velocity (lines $12-13$)
Acceleration at g and velocity at $g+1$ are calculated for each agent in P_g according to Equations (3.11) and (3.12), respectively. Thus,

$$a_i^d(g) \in A_g,\ v_i^d(g+1) \in V_{g+1}; \quad \forall i \in 1, 2, \ldots, ps_{gsa} \text{ and } \forall d \in 1, 2, \ldots, n.$$

Step 6: Move agents (line 14)
The agents in P_g are moved because of gravitational forces at g according to Equation (3.13). The new agents are saved in Q_g.

Step 7: Next generation (lines $15-20$)
A new P_{g+1} is generated by selecting the best ps_{gsa} agents according to $\prec_n$ (line 15). A stagnation control is performed as for MO-FA in line 16, according to the parameters $param\_how\_sc_{gsa}$ and $param\_when\_sc_{gsa}$. Next, we calculate c_{g+1} and $kbest_{g+1}$ (lines $17-18$). To this end, we should estimate how many generations the algorithm will execute. The purpose is that the distribution of the values provided by both functions is uniform over generations. Note that maximum and minimum values of such functions are parameters of MO-GSA. Then, the best solutions found are saved in F_{g+1} (line 19). This procedure is repeated, jumping to step 1, so long as a stop condition is not reached.

3.7 Multiobjective Evolutionary Algorithm Based on Decomposition

MOEA/D was proposed by Qingfu Zhang and Hui Liu [10]. In contrast to the majority of the current state-of-the-art MOEAs, which treat MOPs as a whole. MOEA/D decomposes a given MOP into several SO optimisation subproblems, solving each one by considering only information from neighbouring subproblems.

Two decomposition methods are common in MOEA/D: Weighted Sum Approach (WSA) and Weighted Tchebycheff Approach (WTA) [10]. The first one works out well on convex problems, but not for non-convex ones. The second method is able to deal with both types of problems. However, both are very sensitive to the scale of the objectives.

A decomposition method independent of the scales of the objectives is Normal Boundary Intersection (NBI) [50]. This approach tries to find the intersection points between the solutions in the Pareto front and a number of straight lines, which are defined by both a set of uniformly-distributed reference points in the Convex Hull of Individual Minima (CHIM) and a normal vector to the CHIM. Due to NBI has several constraints applied to MOEA/D [51], the authors in [52] proposed to take the advantages of the NBI approach and the Tchebycheff approach, defining the NBI-Tchebycheff approach for decomposing three-objective optimisation problems.

In this dissertation, we assume MOEA/D with this NBI-Tchebycheff approach for optimising problems with two and three objectives. Below, we describe the way in which the subproblems are defined for each case:

- **For two objectives:** Suppose an MOP, maximising f_1 and f_2. Let $F^1 = (\text{maxF}(f_1), \text{minF}(f_2))$, $F^2 = (\text{minF}(f_1), \text{maxF}(f_2))$ be the two extreme points delimiting the objective space. Note that $\text{maxF}(\cdot)$ and $\text{minF}(\cdot)$ denote the maximum and minimum possible values of a fitness function. These values could be theoretical or practical ones. Let $\Upsilon = \{r^1, r^2, \ldots, r^{ps_m}\}$ be a set of points evenly distributed on the plane I (CHIM), where ps_m is the cardinal of the set. Both F^1 and F^2 are included in Υ. Let $\hat{n} = (n_1, n_2)$ be the normal vector to the plane I. Then, the bi-objective optimisation problem is decomposed into ps_m SO minimisation subproblems, according to the NBI-Tchebycheff approach. Each i-th subproblem optimises the fitness function given by[1]

$$g(x : r^i, \hat{n}) = \max\left\{ \begin{array}{l} n_1\ (f_1(x) - r_1^i), \\ n_2\ (f_2(x) - r_2^i) \end{array} \right\}; \quad r^i = (r_1^i, r_2^i) \in \Upsilon, i \in 1, 2, \ldots, ps_m, \tag{3.14}$$

  where x is a possible solution to the optimisation problem.

- **For three objectives:** Suppose an MOP, maximising f_1, f_2, and f_3. Let $F^1 = (\text{maxF}(f_1), \text{minF}(f_2), \text{minF}(f_3))$, $F^2 = (\text{minF}(f_1), \text{maxF}(f_2), \text{minF}(f_3))$, and $F^3 = (\text{minF}(f_1), \text{minF}(f_2), \text{maxF}(f_3))$ be the three extreme points delimiting the objective space. Let $\Upsilon = \{r^1, r^2, \ldots, r^{ps_m}\}$ be a set of points evenly distributed on the plane II (CHIM), where ps_m is the cardinal of the set. Note that F^1, F^2, and F^3 are included in Υ. Let $\hat{n} = (n_1, n_2, n_3)$ be the normal vector to the plane II. Then, the three-objective optimisation problem is decomposed into ps_m SO minimisation subproblems, according to the

[1] If f_1 is to minimise, the definition would be similar, changing $n_1(f_1(x) - r_1^i)$ for $n_1(r_1^i - f_1(x))$.

Algorithm 7 Distribution of the reference points on the CHIM for two objectives.

1: $\Upsilon \leftarrow \{\}$
2: $ps_m \leftarrow 0$
3: $(E^1, E^2) \leftarrow$ scaleExtremePointsCHIM($F^1, F^2, param\_CHIMinc_m$)
4: $n_{E^1,E^2} \leftarrow \frac{d(E^1,E^2)}{param\_crow_m}$
5: **for** $m \leftarrow 0$ **to** n_{E^1,E^2} **do**
6: $\quad \Upsilon \leftarrow \Upsilon \cup \{E^1 + m \, \frac{E^2 - E^1}{n_{E^1,E^2}}\}$
7: $\quad ps_m \leftarrow ps_m + 1$
8: **end for**

NBI-Tchebycheff approach. Each i-th subproblem optimises the fitness function given by

$$g(x : r^i, \hat{n}) = \max\{ \begin{array}{l} n_1\,(f_1(x) - r_1^i), \\ n_2\,(f_2(x) - r_2^i), \\ n_3\,(f_3(x) - r_3^i)\ \} \end{array} \quad ; \quad r^i = (r_1^i, r_2^i, r_3^i) \in \Upsilon, i \in 1, 2, \ldots, ps_m, \tag{3.15}$$

where x is a possible solution to the optimisation problem.

Another important aspect of MOEA/D is the distribution of the reference points Υ on the CHIM. Following the same NBI-Tchebycheff approach, we assume two different algorithms according to whether the problem considers two or three objectives:

- **For two objectives:** As Algorithm 7 shows, the reference points are distributed following a straight line between F^1 and F^2. Below, the procedure is described step by step:

  Input:

  - F^1 and F^2: extreme points of the CHIM.
  - $param\_CHIMinc_m \in [1, \infty)$: increment of the CHIM.
  - $param\_crow_m \in (0, \infty)$: distance between reference points.

  Output:

  - The set of reference points Υ is distributed on the CHIM.

  Step 0: Initialisation (lines $1-3$)
  At this step, Υ is initialised to empty. Next the new extreme points E^1 and E^2 of the CHIM are calculated by solving the equation given by

  $$d(E^1, E^2) = d(F^1, F^2)\, param\_CHIMinc_m,$$

  where $d(\cdot)$ provides the Euclidean distance between any two points. Because we did not find any work providing the mathematical development needed to perform this scaling task, which is not trivial, we provide this information in Appendix A, specifically in Section A.1.

  Step 1: Obtaining the number of divisions (line 4)
  Calculate the number of divisions n_{E^1,E^2} in the segment $\overline{E^1E^2}$.

  Step 2: Generate reference points (lines $5-8$)
  Generate new reference points in the segment $\overline{E^1E^2}$.

Algorithm 8 Distribution of the reference points on the CHIM for three objectives.

1: $\Upsilon \leftarrow \{\,\}$
2: $ps_m \leftarrow 0$
3: $(E^1, E^2, E^3) \leftarrow$ scaleExtremePointsCHIM($F^1, F^2, F^3, param\_CHIMinc_m$)
4: **while** $true$ **do**
5: $\quad (E^1, E^2, E^3) \leftarrow$ reassignExtremePointsCHIM(E^1, E^2, E^3)
6: $\quad n_{E^1,E^2} \leftarrow \frac{d(E^1,E^2)}{param\_crow_m}$
7: $\quad n_{E^1,E^3} \leftarrow \frac{d(E^1,E^3)}{param\_crow_m}$
8: $\quad$ **if** $n_{E^1,E^2} \leq 1.0$ **then**
9: $\quad\quad$ **stop algorithm**
10: $\quad$ **end if**
11: $\quad$ **for** $m \leftarrow 0$ **to** n_{E^1,E^3} **do**
12: $\quad\quad a \leftarrow E^1 + m\ \frac{E^2-E^1}{n_{E^1,E^2}}$
13: $\quad\quad b \leftarrow E^1 + m\ \frac{E^3-E^1}{n_{E^1,E^3}}$
14: $\quad\quad n_{ab} \leftarrow \frac{d(a,b)}{param\_crow_m}$
15: $\quad\quad$ **for** $n \leftarrow 0$ **to** n_{ab} **do**
16: $\quad\quad\quad \Upsilon \leftarrow \Upsilon \cup \{a + n\ \frac{b-a}{n_{ab}}\}$
17: $\quad\quad\quad ps_m \leftarrow ps_m + 1$
18: $\quad\quad$ **end for**
19: $\quad$ **end for**
20: $\quad E^1 \leftarrow E^1 + n_{E^1,E^3}\ \frac{E^2-E^1}{n_{E^1,E^2}}$
21: **end while**

- **For three objectives:** As Algorithm 8 shows, the reference points are distributed in the area enclosed by F^1, F^2, and F^3. Below, the procedure is described step by step:

  Input:

  - F^1, F^2, and F^3: extreme points of the CHIM.
  - $param\_CHIMinc_m \in [1, \infty)$: increment of the CHIM.
  - $param\_crow_m \in (0, \infty)$: distance between reference points.

  Output:

  - The set of reference points Υ is distributed on the CHIM.

  Step 0: Initialisation (lines $1-3$)
  Υ is initialised to empty. Next the new extreme points E^1, E^2, and E^3 of the CHIM are calculated by solving the system of equations given by

$$\left.\begin{array}{l} d(E^1, E^2) = d(F^1, F^2)\ param\_CHIMinc_m \\ d(E^1, E^3) = d(F^1, F^3)\ param\_CHIMinc_m \\ d(E^2, E^3) = d(F^2, F^3)\ param\_CHIMinc_m \end{array}\right\} .$$

  As for two objectives, we provide the mathematical development needed to perform this scaling task in Appendix A, specifically in Section A.3.

Algorithm 9 MOEA/D with NBI-Tchebycheff approach.

$\Upsilon \leftarrow$ distributeReferenceSet($F^1, F^2, F^3, param\_CHIMinc_m, param\_crow_m$)
$P_g \leftarrow$ generateInitialPopulation(ps_m) ▷ g starts from 1
$F_g \leftarrow \{\ \}$
$N \leftarrow$ computeNeighbourhood(Υ,$param\_neigh_m$)
while not stop condition **do**
  for each $r^i \in \Upsilon$ **do**
    $k \leftarrow$ getRandomNeighbourhood(N,r^i)
    $l \leftarrow$ getRandomNeighbourhood(N,r^i)
    $\eta \leftarrow$ generateNewSolution($p_g[N_{i,k}], p_g[N_{i,l}]$)
    $F_g \leftarrow F_g \cup \{\eta\}$
    for $j = 1 \rightarrow param\_neigh_m$ **do** ▷ Update neighbouring solutions
      if $g(\eta : r^{N_{i,j}}, \hat{n}) \leq g(p_g[N_{i,j}] : r^{N_{i,j}}, \hat{n})$ **then**
        $P_g[N_{i,j}] \leftarrow \eta$
      end if
    end for
  end for
  $F_{g+1} \leftarrow$ updateNonDominatedSet(F_g)
  $P_{g+1} \leftarrow P_g$
end while

Step 1: Reassignment of extreme points (line 5)
The extreme points E^1, E^2, and E^3 are reassigned among them to satisfy: $d(E^1, E^2) \geq d(E^1, E^3) \geq d(E^2, E^3)$. For example, E^1 and E^2 could exchange their positions to satisfy the condition.

Step 2: Obtaining the number of divisions (lines $6 - 10$)
Calculate the number of divisions in the two largest segments $\overline{E^1E^2}$ and $\overline{E^1E^3}$, denoted as n_{E^1,E^2} and n_{E^1,E^3}, respectively. In case of $n_{E^1,E^2} \leq 1.0$, it is not possible to add new reference points, and then, the algorithm ends.

Step 3: Generate reference points (lines $11 - 19$)
Generate new reference points in the area delimited by E^1, E^2, and E^3.

Step 4: Going to the next area (line 20)
Not all the surface delimited by the tree extreme points E^1, E^2, and E^3 was studied in step 3. To solve this, E^1 is moved to a new position, delimiting a new area to study for the next iteration.

As Algorithm 9 shows, MOEA/D assumes a regular population P of size ps_m and an auxiliary population F of undefined size. At generation $g \geq 1$, P_g is considered to generate new solutions in g and F_g saves the non-dominated solutions found until g. Note that this implementation is for two or three objectives. Below, the algorithm is described step by step:

Input:

- F^1 and F^2 (and F^3 if there is three objectives): extreme points of the CHIM.
- $param\_CHIMinc_m \in [1, \infty)$: increment of the CHIM.
- $param\_crow_m \in (0, \infty)$: distance between reference points.
- $param\_neigh_m \in 1, 2, \ldots$: number of neighbourhoods for each reference point.
- $param\_cro_m \in [0, 1]$: probability that crossover is performed.
- $param\_mut_m \in [0, 1]$: probability that mutation is performed.

Output:

- F: a set of non-dominated individuals solving the problem.

Step 0: Initialisation. Reference points (line 1)
In this first step, Υ is generated by distributing the ps_m reference points on the CHIM as Algorithm 7 and 8 show. Note that F_1 and F_2 are the extreme points if a bi-objective problem is assumed and F_1, F_2, and F_3 if it is a three-objective problem. Note that in Algorithm 9, we assume three objectives.

Step 1: Initialisation. Population (lines $2 - 3$)
P_g is randomly generated and F_g is empty, starting g from 1. To this end, each solution in P_g is associated with a different reference point in Υ, i.e. given a point $r^i \in \Upsilon$, r^i is associated with the solution in P_g denoted as $P_g[i]$, with $i \in 1, 2, \ldots, ps_m$.

Step 2: Initialisation. Neighbourhood (line 4)
In this step, the neighbourhood of the reference points in Υ is calculated. To this end, the Euclidean distance between each pair of points in Υ is obtained, including itself. Next, we get the $param\_neigh_m$ closest reference points to each reference point, generating a N matrix of size $ps_m \times param\_neigh_m$. Given a reference point $r^i \in \Upsilon$, $N_{i,j} \in 1, 2, \ldots, ps_m$ is the index in Υ of its j-th closest reference point, with $i \in 1, 2, \ldots, ps_m$, $j \in 1, 2, \ldots, param\_neigh_m$. As an example, suppose $N_{i,j}$ equalling 4, this means that the j-th closest reference point to r^i is r^4.

Step 3: Generation of new solutions (lines $6 - 16$)
For each reference point r^i in Υ, two neighbouring reference points $N_{i,k}$ and $N_{i,l}$ of r^i are randomly selected, with $k, l \in 1, 2, \ldots, param\_neigh_m$. Then, based on the solutions associated to such points in P_g, i.e. $P_g[N_{i,k}]$ and $P_g[N_{i,l}]$ a new solution η is generated through binary tournament, crossover, and mutation according to $param\_cro_m$ and $param\_mut_m$, as previously discussed in Section 3.1 for NSGA-II. This new solution is added to F_g (lines $7 - 10$).

Next, for each neighbourhood of r^i, we check if the new solution η is better suited than the solutions associated to such reference points, according to Equations (3.14) and (3.15). In that case, the new solution replaces the previous one (lines $11 - 15$).

Step 4: Next generation (lines $17 - 18$)
F_{g+1} is generated by removing all the dominated solutions from F_g. The algorithm goes to the next generation jumping to step 3. This procedure is repeated so long as a stop condition is not reached.

CHAPTER

4

Solving the RNPP: bi-objective Outdoor Approach

In this chapter, we define and solve the first approach of the RNPP by applying the previously mentioned MO metaheuristics. This chapter is structured as follows. The WSN model considered in this work is presented in Section 4.1. Based on this model, we define the optimisation problem in Section 4.2. Section 4.3 presents the data set considered for comparing the metaheuristics while solving the problem. Chromosome definition and specific considerations for implementing the metaheuristics are detailed in Sections 4.5 and 4.6, respectively. Experimental results are presented in Section 4.7. Finally, we discuss the scientific achievements from solving this first optimisation problem in Section 4.8.

4.1 The Wireless Sensor Network Model Assumed

This section describes the WSN model considered in the bi-objective unconstrained RNPP outdoor approach. The notation assumed is listed in Section 4.1.1. The general assumptions of the model are presented in Section 4.1.2. Finally, we discuss energy expenditure, sensitivity area, and network lifetime in Sections 4.1.3, 4.1.4, and 4.1.5, respectively.

4.1.1 Notation

The following notation is considered for modelling the WSN definition:

α	path loss exponent, $\alpha \in [2, 4]$;
β	transmission quality parameter, $\beta > 0$;
τ	set of time periods, $\tau = \{0, 1, 2, \ldots\}$;

$A(t)$	sensitivity area provided by the WSN at time $t > 0 \in \tau$;
$a_p(t)$	variable assuming 1 if there is at least one sensor $i \in S_s(t)$ at a distance to the demand point $p \in \tilde{D}_p(t)$ lower than r_s;
amp	energy cost per bit of the power amplifier, $amp > 0$;
c	sink coordinates, $c = (x, y)$ where $x \in [0, d_x]$ and $y \in [0, d_y]$;
co_{th}	coverage threshold, $co_{th} \in [0, 1]$;
$\tilde{D}_p(t)$	set of demand points at time $t > 0$, $\forall p \in \tilde{D}_p,\ p = (x, y)$ where $x \in [0, d_x]$ and $y \in [0, d_y]$;
$\tilde{d}_p(t)$	number of demand points. It is the cardinal of $\tilde{D}_p(t)$;
d_{pn}	distance between two neighbouring demand points;
d_x	width of the surface, $d_x > 0$;
d_y	height of the surface, $d_y > 0$;
$Ec_i(t)$	energy charge of a sensor $i \in S_s(t)$ at time t;
$Ee_i(t)$	energy expenditure of a sensor $i \in S_s(t)$ at time $t > 0$;
f_1	AEC of the sensors over the network lifetime;
f_2	ASA provided by the WSN over the network lifetime;
iec	initial energy charge of the sensors, $iec > 0$;
k	information packet size in bits, $k > 0$;
$P_i(t)$	number of packets sent by the sensor $i \in S_s(t)$ at time $t > 0$;
r_c	communication radius, $r_c > 0$;
$Rp_i(t)$	number of relayed packets sent by the sensor $i \in S_s(t)$ at time $t > 0$;
r_s	sensitivity radius, $r_s > 0$;
$\tilde{S}_r$	set of RN coordinates, $\forall r \in \tilde{S}_r,\ r = (x, y)$ where $x \in [0, d_x]$ and $y \in [0, d_y]$;
$\tilde{s}_r$	number of RNs. It is the cardinal of $\tilde{S}_r$;
$\tilde{S}_s$	set of initial sensor coordinates, $\forall i \in \tilde{S}_s$, $i = (x, y)$, where $x \in [0, d_x]$ and $y \in [0, d_y]$;
$\tilde{s}_s$	number of initial sensors. It is the cardinal of $\tilde{S}_s$;
$S_s(t)$	set of sensor coordinates, holding that the energy charge is greater than 0 and that there is any path to the sink node, both at time $t > 0$, $S_s(t) \subseteq \tilde{S}_s$;
$s_s(t)$	number of sensors, holding that the energy charge is greater than 0 and that there is any path to the sink node, both at time $t > 0$. It is the cardinal of $S_s(t)$, $s_s(t) \leq \tilde{s}_s$;
t_n	network lifetime of the WSN based on the coverage threshold co_{th};
$w_i^c(t)$	variable which provides the next device in the minimum path between $i \in S_s(t)$ and the sink node at $t > 0$, $w_i^c(t) \in \{S_s(t) \cup \tilde{S}_r\} + c - i$;
$z_{j,i}^c(t)$	variable assuming 1 if $i \in S_s(t)$ is in the minimum path between $j \in S_s(t)$ and the sink node at $t > 0$, and 0 otherwise.

4.1.2 Assumptions of the Wireless Aensor Network Model

The general assumptions of the network model are:

1. The network is composed of three types of wireless static devices: a sink node, $\tilde{s}_s$ sensors, and $\tilde{s}_r$ RNs. They send messages by following a ST approach.

2. All the devices are placed on a same outdoor 2D-surface of size d_x x d_y, where there is not any relevant obstacle nor interferences from other electronic devices.

3. We suppose that there are not prohibited areas. Hence, all the devices can be placed on anywhere of the surface, i.e. we follow an unconstrained approach of the RNPP.

4. The sensors are powered by batteries. On the contrary, the sink node and the RNs are energy-harvesting devices. Thus, we consider that they have enough energy capacity for operating over the network lifetime, not as the sensors.

5. Initially, at time $t = 0$, all the sensors start with the same energy capacity iec in their batteries. If during operation, $t > 0$, a sensor is exhausted, it cannot be linked again.

6. The sink node is the only connection point of the network to the outside.

7. The sensors capture information about the environment on a regular basis and with a sensitivity radius r_s, i.e. each sensor covers a circumference of radius r_s. Once the information is captured, it is immediately sent to the sink node.

8. The RNs are low-cost devices, which only forward all the information received to the sink node, i.e. they do not capture information.

9. Any two devices can be linked, if they are at a distance lower than the communication radius r_c and have enough energy capacity in their batteries.

10. All the devices consider the same multi-hop routing protocol provided by Dijsktra's Algorithm [53], for minimum path length among devices.

11. We suppose a perfect synchronisation among devices and the use of an efficient MAC protocol, such as S-MAC [54], which allows reducing energy cost on idle time.

4.1.3 Energy Expenditure

As stated before, the sensors are the only devices powered by batteries. Hence, if we want to optimise energy cost, we need to simulate the energy consumption of such devices during operation. To this end, we consider the energy model proposed by Konstantinidis et al. [55], where the energy expenditure is only due to the sending task. Consequently, processing, receiving, and sensing tasks are considered negligible.

Following this energy model, a sensor i, with $i \in S_s(t)$, sends a number of data packets $P_i(t)$ at time $t \in \tau$ and $t > 0$ given by

$$P_i(t) = 1 + Rp_i(t). \tag{4.1}$$

This means that Equation (4.1) is given by the sum of the number of data packets generated by i at t (in this case, we consider that each sensor captures a data packet per time period) and the number of relayed packets because of the multi-hop routing approach, which is denoted as

$$Rp_i(t) = \sum_{j \in \{S_s(t) - i\}} z^c_{j,i}(t).$$

Note that control packets from routing and MAC protocols were not simulated, because this is not the aim of this dissertation.

Based on this expression, the energy cost $Ee_i(t)$ of a sensor i at time $t > 0$ is given by

$$Ee_i(t) = P_i(t)\,\beta\; amp\; k\; (\|i - w^c_i(t)\|_d)^\alpha, \tag{4.2}$$

where $||\cdot||_d$ is the Euclidean distance between any two devices. This way, the energy charge of a sensor i at time t is given by

$$Ec_i(t) = \begin{cases} Ec_i(t-1) - Ee_i(t) & \text{if } t > 0 \\ iec & \text{if } t = 0 \end{cases}.$$

If this value equals zero, the sensor is out of energy; otherwise, it is active.

4.1.4 Sensitivity Area

As stated before, a sensor covers a circumference of radius r_s and area $\pi\, r_s^2$. Hence, at time t, the total sensitivity area of a WSN is calculated as the union of its $s_s(t)$ areas by assuming possible overlaps between circles. The intersection of two circles is straightforward, even three circles is not a really complex computational problem. However, the computational effort increases exponentially when the number of circles increases [56].

As a possible way to approximate this calculation, some authors assume a set of demand points uniformly distributed on the surface. Then, they count the number of demand points, which have an active sensor at a distance lower than r_s [57]. Based on this idea, the sensitivity area provided by a WSN at time $t > 0$ is given by

$$A(t) = \frac{\sum_{p \in \tilde{D}_p(t)} a_p(t)}{\tilde{d}_p(t)}, \tag{4.3}$$

where $a_p(t)$ is the indicator function expressed as

$$a_p(t) = \begin{cases} 1 & \text{if } \exists i \in \tilde{S}_s(t) : ||p - i||_d < r_s \\ 0 & \text{otherwise} \end{cases},$$

i.e. $a_p(t)$ equals 1 if there is a sensor i such that the distance between the demand point p and i is lower than r_s, and 0 otherwise.

In this dissertation, we consider that the demand points follow a grid distribution, with d_{pn} distance between neighbouring points. Thus, the number of demand points is given by

$$\tilde{d}_p(t) = \frac{d_x\, d_y}{d_{pn}}.$$

We express the accuracy of this metric according to the upper bound of the relative error of calculating the area of a single circumference, regarding the total area of the surface. To this

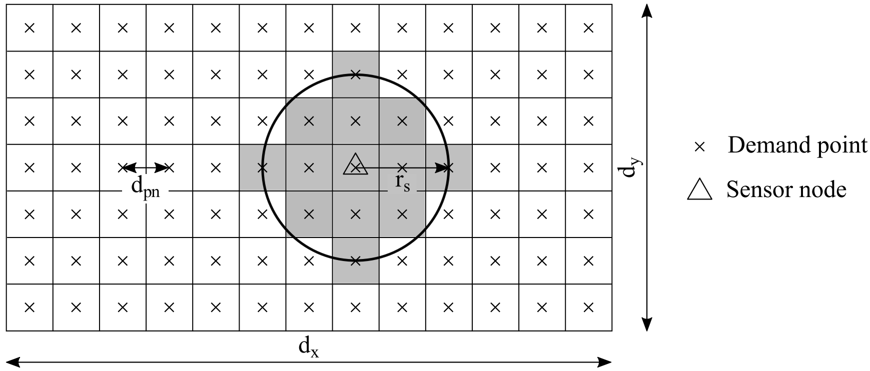

Figure 4.1: Approximate method for calculating the area of the circumference.

end, we consider a circumference, whose center is placed in a demand point and its r_s is a multiple of d_{pn}, see Figure 4.1. In such a case, the approximate area of the circumference is calculated according to a number of demand points given by

$$n_d = \left\lceil \frac{2\, r_s}{d_{pn}} \right\rceil + \sum_{i=0}^{\left\lceil \frac{2\, r_s}{d_{pn}} \right\rceil} 2(2i+1).$$

In Figure 4.1, the cells having the demand points considered for calculating the area are shaded.

Let e be the upper bound of the error defined as the difference between the real and the estimated areas. That is,

$$e = \pi\, r_s^2 - n_d\, d_{pn}\, d_{pn}.$$

Then, the upper bound for the relative error e_r is expressed as

$$e_r = \frac{e}{d_x\, d_y}.$$

If this quantity is multiplied by 100, the result is expressed in percentage. As an example, we get an error of 0.3176% by assuming $d_x = 300$m, $d_y = 300$m, $d_{pn} = 1$m, and $r_s = 15$m. Note that the error decreases when d_{pn} also decreases. However, the number of demand points increases exponentially when d_{pn} decreases, affecting the computational cost.

4.1.5 Network Lifetime

The network lifetime is defined as the number of time periods over which a WSN is useful. We find several approaches to check this requirement in the literature, e.g. the time until all the nodes are exhausted or the time until the first node dies [58]. In this dissertation, we assume a coverage threshold method. This way, the network lifetime is defined according to the time until the information provided by the network is not enough, that is

$$t_n = ||\{t > 0 \in \tau : A(t) > co_{th}\}||. \tag{4.4}$$

This criterion is better than others, because it fits most WSN applications.

4.2 Problem Formulation

Let f_1 be the AEC of the sensors over the network lifetime. That is expressed as

$$f_1 = \frac{\sum_{t=1}^{t_n} \left(\sum_{i \in S_s(t)} \frac{Ee_i(t)}{s_s(t)} \right)}{t_n}, \tag{4.5}$$

where $f_1 \in \mathbb{R}^+$ and both $Ee_i(t)$ and t_n are given by Equations (4.2) and (4.4), respectively.

Let f_2 be the ASA provided by the network, which is expressed as

$$f_2 = \frac{\sum_{t=1}^{t_n} A(t)}{t_n}, \tag{4.6}$$

where $f_2 \in [0, 1]$ and $A(t)$ is given by Equation (4.3).

This way, we define the unconstrained outdoor RNPP as a bi-objective optimisation problem, where given a previously-established traditional WSN, i.e. $\tilde{s}_s$ sensors and a sink node, the objective is to place $\tilde{s}_r$ RNs by assuming an ST network model to

$$\min(f_1) \text{ and } \max(f_2),$$

subject to

$$\forall r \in \tilde{S}_r,\ r = (x, y) : x \in [0, d_x] \text{ and } y \in [0, d_y].$$

These objectives are related to two important problems in the WSN literature: i) Energy efficiency problem [59], whose aim is to reduce the energy cost, increasing the network lifetime and balancing the energy distribution. ii) Coverage problem [60], its purpose is to optimise the amount and diversity of the information provided by the network.

It is well-known that one fundamental requirement for a problem to be considered as an MOP is that the objectives should be conflicting [15]. Other authors checked that both energy cost and coverage were conflicting objectives in WSNs [55] [61] [62] [63] [64].

4.3 Description of the Dataset

We did not find any data set fitting the problem definition discussed in Section 4.2, or instead, providing enough information for replicating the experiments from other authors. This situation led us to define a new data set, with the purpose of providing a common framework for studying the outdoor RNPP in future works. This data set is freely available in [65].

This data set is composed of four different scenarios of sizes 50x50m, 100x100m, 200x200m, and 300x300m. A traditional WSN is deployed in each scenario, i.e. a set of sensors and a sink node, considering the minimum number of sensors to cover the whole surface. Thus, if the area of the surface is $d_x\ d_y$ and a sensor covers a circumference of radius r_s, then the lower bound of the minimum number of sensors is given by

$$\tilde{s}_s = \left\lceil \frac{d_x\ d_y}{\pi\ r_s^2} \right\rceil.$$

Thus, for each scenario, we deploy $\tilde{s}_s$ sensors by assuming an SO GA, which optimises the sensitivity area provided by the WSN according to Equation (4.3) and subject to all the sensors can be linked to the sink node via one or more hops. This means that the resulting traditional WSN is fully functional without including RNs.

As stated before, this WSN model includes several parameters. We consider $\alpha = 2.00$, $\beta = 1.00$, $co_{th} = 0.70\%$, $k = 128$KB, $r_s = 15.00$m, $iec = 5$J, and $amp = 100$pJ/bit/m^2, from [66] and [61]. Two r_c values are assumed to simulate sensors with different communication capacities, 30m and 60m, respectively. Thus, we define two instances for each scenario by following the notation d_x x $d_y\_r_c$. Figures 4.2, 4.3, 4.4, and 4.5 show detailed information of these four scenarios according to three criteria:

- **a) Main features:** We show the instance name, the position of the sink node, the fitness values f_1 and f_2 without deploying any RN, the reference points for calculating the hypervolume metric, which were obtained experimentally, and the test cases. Note that we consider that a test case is the number or RNs, which we deploy in a traditional WSN as a way to optimise it. Being as adding RNs increases the network cost, we do not include more than 20% of these devices regarding the total number of sensors. Thus, we define one test case for 50x50_30 and 50x50_60 instances, two for 100x100_30 and 100x100_-60 instances, four for 200x200_30 and 200x200_60 instances, and four for 300x300_30 and 300x300_60 instances.

- **b) Deployment details:** We include a table with all the sensor coordinates and a plot, showing the positions of all the devices in the scenario.

- **c) Energy charge distribution:** For each instance and without including any RN ($\tilde{s}_r = 0$), we analyse the energy charge distribution at the end of the network lifetime, i.e. the remaining energy charge for each sensor once the lifetime is ended. For all the cases, we check that the energy distribution is really unbalanced: there are many sensors having energy charge, while others are exhausted. This means that the active sensors cannot send data to the sink node, because there is not any available path, resulting in a bottleneck situation. Consequently, these instances are candidates to be optimised by deploying RNs.

4.4 Problem Example

We propose an illustrative example of this problem definition by adding a RN in one of the previously discussed instances. In this case, we consider the instance 100x100_60. Before adding the RN, we analyse in depth this WSN to identify possible improvements. Table 4.1 shows fitness functions, sensitivity area, and energy charge of the sensors over simulation time. Notice that when $A(t)$ is lower than co_{th}, the network lifetime is ended. In this case, when t equals 25. In Table 4.1, $\sim$0.0000 means that the energy charge is near to zero, but enough for transmitting this time. As stated before, its energy charge distribution is in Figure 4.3.

Table 4.2 and Figure 4.6 show the same information mentioned above, but for the instance 100x100_60 including a RN in coordinate (20.00,20.00), i.e. test case 100x100_60(1). We check that the network lifetime was increased and the energy cost of the sensors in the surrounding of the RN is lower than shown in Table 4.1, affecting the sensitivity area. Thus, sensors #1, #9, and #12 have more energy charge at the end of the network lifetime. In Figure 4.6, $R1$ denotes the position of the RN and C is the position of the sink node.

Instance name	Sink node	Fitness values ($\tilde{s}_r = 0$)		Reference points (f_1, f_2)		Test cases ($\tilde{s}_r$)
($d_x \times d_y\_r_c$)	(x-coordinate, y-coordinate)	f_1	f_2	ideal	nadir	
50x50_30	(25.00,25.00)	0.035	91.75%	(0.02,100.00)	(0.04,60.00)	1
50x50_60	(25.00,25.00)	0.035	91.75%	(0.02,100.00)	(0.04,60.00)	1

(a) Main features.

($\tilde{S}_s$) Sensor coordinates: sensorID , (x-coordinate, y-coordinate)							
#1	(8,34)	#2	(37,38)	#3	(36,9)	#4	(14,12)

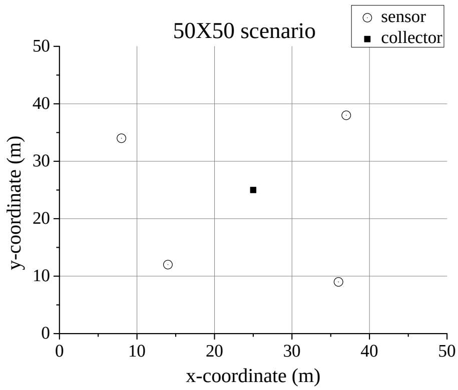

(b) Deployment details.

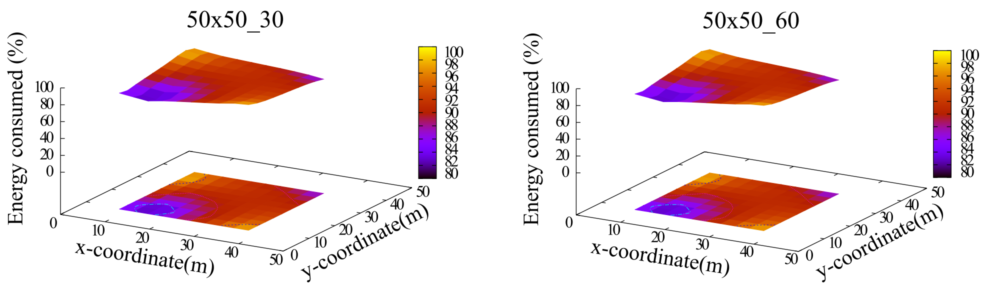

(c) Energy charge distribution.

Figure 4.2: Instace 50x50.

Instance name	Sink node	Fitness values ($\tilde{s}_r = 0$)		Reference points (f_1, f_2)		Test cases ($\tilde{s}_r$)
($d_x \times d_y\_r_c$)	(x-coordinate, y-coordinate)	f_1	f_2	ideal	nadir	
100x100_30	(50.00,50.00)	0.1091	89.24%	(0.02,100.00)	(0.10,60.00)	2, 3
100x100_60	(50.00,50.00)	0.1482	86.63%	(0.02,100.00)	(0.10,60.00)	2, 3

(a) Main features.

($\tilde{S}_s$) Sensor coordinates: sensorID , (x-coordinate, y-coordinate)							
#1	(17,10)	#5	(76,13)	#9	(13,34)	#13	(85,87)
#2	(63,66)	#6	(59,90)	#10	(13,88)	#14	(38,55)
#3	(88,59)	#7	(65,40)	#11	(40,30)	#15	(13,59)
#4	(38,84)	#8	(89,35)	#12	(47,10)		

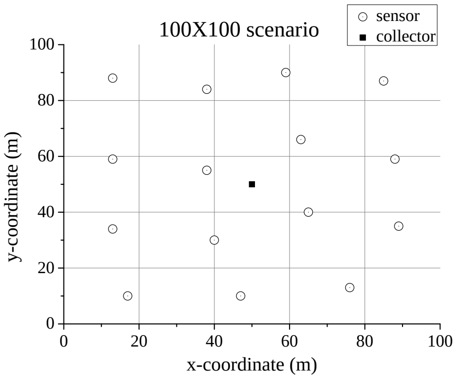

(b) Deployment details.

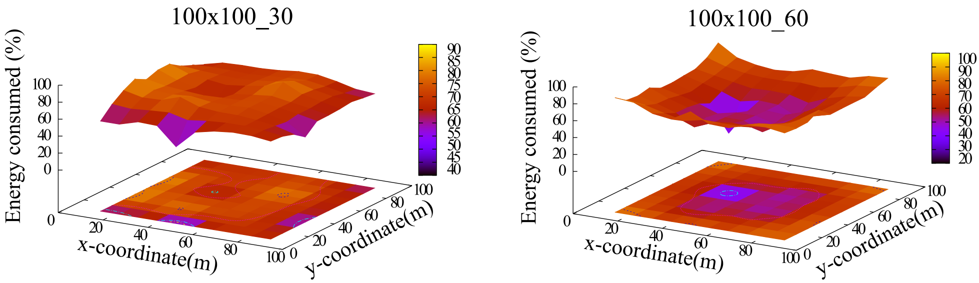

(c) Energy charge distribution.

Figure 4.3: Instace 100x100.

Instance name	Sink node	Fitness values ($\tilde{s}_r = 0$)		Reference points (f_1, f_2)		Test cases ($\tilde{s}_r$)
$(d_x \times d_y\_r_c)$	(x-coordinate, y-coordinate)	f_1	f_2	ideal	nadir	
200x200_30	(100.00,100.00)	0.2791	87.10%	(0.10,100.00)	(0.30,60.00)	2, 4, 6, 9
200x200_60	(100.00,100.00)	0.3871	82.43%	(0.10,100.00)	(0.30,60.00)	2, 4, 6, 9

(a) Main features.

($\tilde{S}_s$) Sensor coordinates: sensorID , (x-coordinate, y-coordinate)											
#1	(87,14)	#11	(26,120)	#21	(135,80)	#31	(144,13)	#41	(139,164)	#51	(9,68)
#2	(185,187)	#12	(188,159)	#22	(161,118)	#32	(29,67)	#42	(121,59)	#52	(186,46)
#3	(161,92)	#13	(83,62)	#23	(69,86)	#33	(106,128)	#43	(117,101)	#53	(14,189)
#4	(158,143)	#14	(158,63)	#24	(80,134)	#34	(10,140)	#44	(136,112)	#54	(69,186)
#5	(61,13)	#15	(103,78)	#25	(55,64)	#35	(189,16)	#45	(125,188)	#55	(13,96)
#6	(62,112)	#16	(185,132)	#26	(41,94)	#36	(61,158)	#46	(35,153)	#56	(186,104)
#7	(165,167)	#17	(86,161)	#27	(89,104)	#37	(167,13)	#47	(70,39)	#57	(115,12)
#8	(100,38)	#18	(52,132)	#28	(111,162)	#38	(12,13)	#48	(185,75)		
#9	(14,41)	#19	(155,189)	#29	(13,167)	#39	(157,39)	#49	(129,38)		
#10	(131,139)	#20	(96,187)	#30	(41,182)	#40	(41,41)	#50	(37,14)		

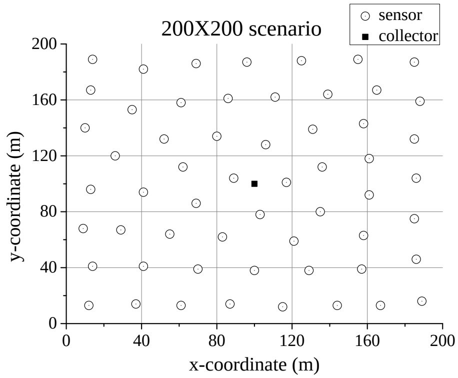

(b) Deployment details.

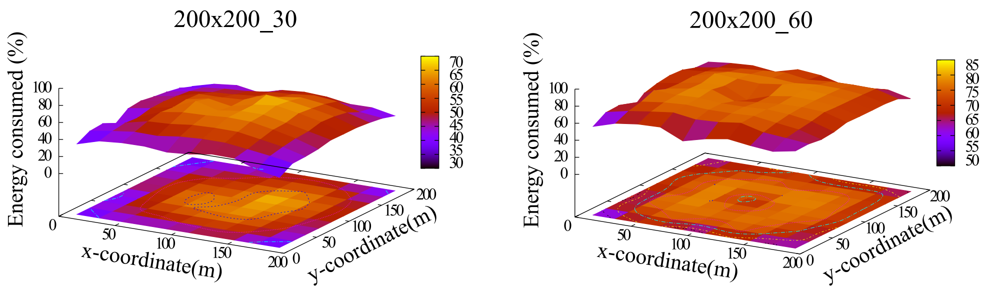

(c) Energy charge distribution.

Figure 4.4: Instace 200x200.

Instance name	Sink node	Fitness values ($\tilde{s}_r = 0$)		Reference points (f_1, f_2)		Test cases ($\tilde{s}_r$)
($d_x \times d_y\_r_c$)	(x-coordinate, y-coordinate)	f_1	f_2	ideal	nadir	
300x300_30	(150.00,150.00)	0.4225	76.44%	(0.04,100.00)	(0.50,60.00)	6, 12, 18, 24
300x300_60	(150.00,150.00)	0.6295	81.22%	(0.04,100.00)	(0.50,60.00)	6, 12, 18, 24

(a) Main features.

($\tilde{S}_s$) Sensor coordinates: sensorID , (x-coordinate, y-coordinate)											
#1	(131,223)	#23	(285,30)	#45	(197,247)	#67	(63,132)	#89	(39,93)	#111	(39,226)
#2	(64,71)	#24	(173,264)	#46	(169,12)	#68	(185,178)	#90	(119,11)	#112	(72,153)
#3	(37,255)	#25	(111,82)	#47	(195,286)	#69	(56,204)	#91	(226,55)	#113	(61,103)
#4	(126,57)	#26	(147,36)	#48	(266,262)	#70	(263,107)	#92	(121,243)	#114	(231,211)
#5	(254,288)	#27	(167,288)	#49	(86,113)	#71	(93,281)	#93	(278,171)	#115	(16,208)
#6	(13,234)	#28	(225,287)	#50	(90,12)	#72	(218,157)	#94	(119,290)	#116	(13,87)
#7	(190,86)	#29	(149,247)	#51	(175,235)	#73	(121,138)	#95	(163,99)	#117	(285,226)
#8	(261,46)	#30	(102,224)	#52	(65,265)	#74	(179,39)	#96	(12,59)	#118	(212,107)
#9	(147,15)	#31	(63,241)	#53	(240,262)	#75	(74,226)	#97	(68,42)	#119	(212,264)
#10	(13,10)	#32	(286,58)	#54	(173,129)	#76	(230,182)	#98	(181,206)	#120	(202,132)
#11	(144,275)	#33	(278,12)	#55	(86,178)	#77	(85,200)	#99	(155,216)	#121	(38,122)
#12	(64,14)	#34	(219,81)	#56	(13,287)	#78	(14,32)	#100	(225,238)	#122	(139,112)
#13	(208,35)	#35	(221,10)	#57	(160,185)	#79	(268,79)	#101	(290,95)	#123	(249,160)
#14	(193,14)	#36	(260,135)	#58	(85,88)	#80	(256,188)	#102	(40,40)	#124	(236,33)
#15	(39,14)	#37	(138,164)	#59	(93,134)	#81	(288,121)	#103	(286,150)	#125	(152,43)
#16	(117,264)	#38	(191,153)	#60	(13,110)	#82	(138,194)	#104	(112,201)	#126	(37,67)
#17	(186,110)	#39	(207,193)	#61	(124,34)	#83	(41,151)	#105	(251,13)	#127	(34,184)
#18	(138,83)	#40	(13,161)	#62	(112,108)	#84	(285,197)	#106	(69,290)	#128	(285,283)
#19	(115,174)	#41	(9,185)	#63	(100,157)	#85	(246,75)	#107	(14,136)		
#20	(253,236)	#42	(239,103)	#64	(41,285)	#86	(164,69)	#108	(58,176)		
#21	(97,39)	#43	(231,132)	#65	(91,61)	#87	(163,156)	#109	(91,250)		
#22	(289,254)	#44	(12,261)	#66	(197,61)	#88	(260,212)	#110	(203,221)		

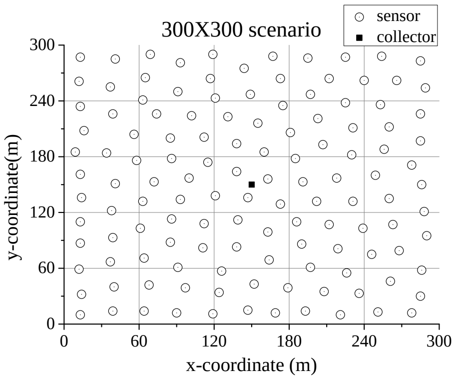

(b) Deployment details.

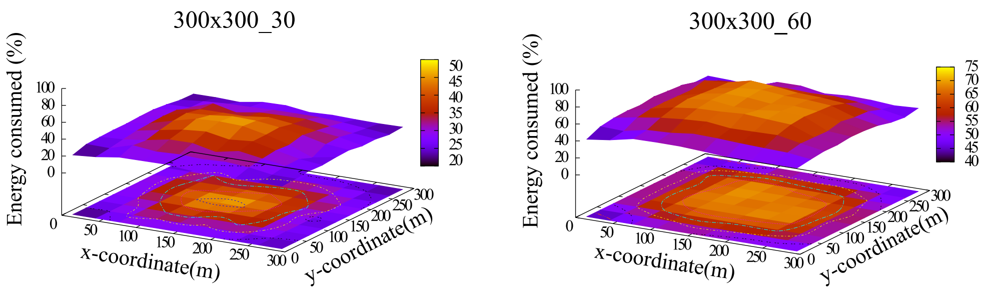

(c) Energy charge distribution.

Figure 4.5: Instace 300x300.

Table 4.1: Example of the bi-objective outdoor RNPP based on instance 100x100_60 without assuming any RN.

Evolution of the energy charge of the sensors over time (J)																		
#1	#2	#3	#4	#5	#6	#7	#8	#9	#10	#11	#12	#13	#14	#15	f_1	f_2	A(t)	t
4.7180	4.9554	4.8401	4.8637	4.7856	4.8237	4.9659	4.8169	4.8296	4.7050	4.9476	4.8313	4.7280	4.9823	4.8480	0.1573	0.9194	0.9194	1
4.4361	4.9109	4.6802	4.7274	4.5711	4.6475	4.9318	4.6338	4.6592	4.4101	4.8951	4.6626	4.4560	4.9646	4.6959	0.1573	0.9194	0.9194	2
4.1541	4.8663	4.5203	4.5911	4.3567	4.4712	4.8978	4.4508	4.4888	4.1151	4.8427	4.4939	4.1840	4.9468	4.5439	0.1573	0.9194	0.9194	3
3.8722	4.8217	4.3604	4.4547	4.1423	4.2949	4.8637	4.2677	4.3184	3.8201	4.7903	4.3251	3.9120	4.9291	4.3918	0.1573	0.9194	0.9194	4
3.5902	4.7772	4.2005	4.3184	3.9278	4.1187	4.8296	4.0846	4.1480	3.5252	4.7379	4.1564	3.6400	4.9114	4.2398	0.1573	0.9194	0.9194	5
3.3082	4.7326	4.0406	4.1821	3.7134	3.9424	4.7955	3.9015	3.9776	3.2302	4.6854	3.9877	3.3680	4.8937	4.0877	0.1573	0.9194	0.9194	6
3.0263	4.6880	3.8806	4.0458	3.4990	3.7661	4.7614	3.7184	3.8072	2.9352	4.6330	3.8190	3.0960	4.8760	3.9357	0.1573	0.9194	0.9194	7
2.7443	4.6435	3.7207	3.9095	3.2845	3.5899	4.7274	3.5353	3.6369	2.6403	4.5806	3.6503	2.8240	4.8582	3.7837	0.1573	0.9194	0.9194	8
2.4623	4.5989	3.5608	3.7732	3.0701	3.4136	4.6933	3.3523	3.4665	2.3453	4.5281	3.4816	2.5520	4.8405	3.6316	0.1573	0.9194	0.9194	9
2.1804	4.5544	3.4009	3.6369	2.8557	3.2373	4.6592	3.1692	3.2961	2.0504	4.4757	3.3128	2.2800	4.8228	3.4796	0.1573	0.9194	0.9194	10
1.8984	4.5098	3.2410	3.5005	2.6412	3.0611	4.6251	2.9861	3.1257	1.7554	4.4233	3.1441	2.0080	4.8051	3.3275	0.1573	0.9194	0.9194	11
1.6165	4.4652	3.0811	3.3642	2.4268	2.8848	4.5911	2.8030	2.9553	1.4604	4.3709	2.9754	1.7360	4.7873	3.1755	0.1573	0.9194	0.9194	12
1.3345	4.4207	2.9212	3.2279	2.2124	2.7085	4.5570	2.6199	2.7849	1.1655	4.3184	2.8067	1.4640	4.7696	3.0234	0.1573	0.9194	0.9194	13
1.0525	4.3761	2.7613	3.0916	1.9979	2.5323	4.5229	2.4369	2.6145	0.8705	4.2660	2.6380	1.1920	4.7519	2.8714	0.1573	0.9194	0.9194	14
0.7706	4.3315	2.6014	2.9553	1.7835	2.3560	4.4888	2.2538	2.4441	0.5755	4.2136	2.4693	0.9200	4.7342	2.7193	0.1573	0.9194	0.9194	15
0.4886	4.2870	2.4415	2.8190	1.5691	2.1798	4.4547	2.0707	2.2737	0.2806	4.1611	2.3005	0.6480	4.7165	2.5673	0.1573	0.9194	0.9194	16
0.2066	4.2424	2.2816	2.6826	1.3546	2.0035	4.4207	1.8876	2.1033	~0.0000	4.1087	2.1318	0.3760	4.6987	2.4153	0.1573	0.9194	0.9194	17
~0.0000	4.1978	2.1217	2.5463	1.1402	1.8272	4.3866	1.7045	1.9329	0.0000	4.0563	1.9631	0.1040	4.6810	2.2632	0.1567	0.9161	0.8595	18
0.0000	4.1533	1.9618	2.4100	0.9258	1.6510	4.3525	1.5215	1.7625	0.0000	4.0039	1.7944	~0.0000	4.6633	2.1112	0.1557	0.9101	0.8021	19
0.0000	4.1087	1.8018	2.2737	0.7113	1.4747	4.3184	1.3384	1.5921	0.0000	3.9514	1.6257	0.0000	4.6456	1.9591	0.1542	0.9015	0.7386	20
0.0000	4.0641	1.6419	2.1374	0.4969	1.2984	4.2843	1.1553	1.4217	0.0000	3.8990	1.4570	0.0000	4.6279	1.8071	0.1528	0.8937	0.7386	21
0.0000	4.0196	1.4820	2.0011	0.2825	1.1222	4.2503	0.9722	1.2513	0.0000	3.8466	1.2883	0.0000	4.6101	1.6550	0.1516	0.8867	0.7386	22
0.0000	3.9750	1.3221	1.8648	0.0680	0.9459	4.2162	0.7891	1.0809	0.0000	3.7941	1.1195	0.0000	4.5924	1.5030	0.1505	0.8803	0.7386	23
0.0000	3.9305	1.1622	1.7284	~0.0000	0.7696	4.1821	0.6060	0.9106	0.0000	3.7417	0.9508	0.0000	4.5747	1.3510	0.1495	0.8744	0.7386	24
0.0000	3.8859	1.0023	1.5921	0.0000	0.5934	4.1480	0.4230	0.7402	0.0000	3.6893	0.7821	0.0000	4.5570	1.1989	0.1482	0.8664	0.6745	25

Table 4.2: Example of the bi-objective outdoor RNPP based on instance 100x100_60 by assuming a RN in coordinate (20.00,20.00).

Evolution of the energy charge of the sensors over time (J)																		
#1	#2	#3	#4	#5	#6	#7	#8	#9	#10	#11	#12	#13	#14	#15	f_1	f_2	A(t)	t
4.9886	4.9554	4.8401	4.8637	4.7856	4.8237	4.9659	4.8169	4.9743	4.7050	4.9476	4.9131	4.7280	4.9823	4.8480	0.1241	91.94%	91.94%	1
4.9771	4.9109	4.6802	4.7274	4.5711	4.6475	4.9318	4.6338	4.9486	4.4101	4.8951	4.8261	4.4560	4.9646	4.6959	0.1241	91.94%	91.94%	2
4.9657	4.8663	4.5203	4.5911	4.3567	4.4712	4.8978	4.4508	4.9229	4.1151	4.8427	4.7392	4.1840	4.9468	4.5439	0.1241	91.94%	91.94%	3
4.9543	4.8217	4.3604	4.4547	4.1423	4.2949	4.8637	4.2677	4.8972	3.8201	4.7903	4.6523	3.9120	4.9291	4.3918	0.1241	91.94%	91.94%	4
4.9429	4.7772	4.2005	4.3184	3.9278	4.1187	4.8296	4.0846	4.8715	3.5252	4.7379	4.5654	3.6400	4.9114	4.2398	0.1241	91.94%	91.94%	5
4.9314	4.7326	4.0406	4.1821	3.7134	3.9424	4.7955	3.9015	4.8459	3.2302	4.6854	4.4784	3.3680	4.8937	4.0877	0.1241	91.94%	91.94%	6
4.9200	4.6880	3.8806	4.0458	3.4990	3.7661	4.7614	3.7184	4.8202	2.9352	4.6330	4.3915	3.0960	4.8760	3.9357	0.1241	91.94%	91.94%	7
4.9086	4.6435	3.7207	3.9095	3.2845	3.5899	4.7274	3.5353	4.7945	2.6403	4.5806	4.3046	2.8240	4.8582	3.7837	0.1241	91.94%	91.94%	8
4.8971	4.5989	3.5608	3.7732	3.0701	3.4136	4.6933	3.3523	4.7688	2.3453	4.5281	4.2177	2.5520	4.8405	3.6316	0.1241	91.94%	91.94%	9
4.8857	4.5544	3.4009	3.6369	2.8557	3.2373	4.6592	3.1692	4.7431	2.0504	4.4757	4.1307	2.2800	4.8228	3.4796	0.1241	91.94%	91.94%	10
4.8743	4.5098	3.2410	3.5005	2.6412	3.0611	4.6251	2.9861	4.7174	1.7554	4.4233	4.0438	2.0080	4.8051	3.3275	0.1241	91.94%	91.94%	11
4.8628	4.4652	3.0811	3.3642	2.4268	2.8848	4.5911	2.8030	4.6917	1.4604	4.3709	3.9569	1.7360	4.7873	3.1755	0.1241	91.94%	91.94%	12
4.8514	4.4207	2.9212	3.2279	2.2124	2.7085	4.5570	2.6199	4.6660	1.1655	4.3184	3.8700	1.4640	4.7696	3.0234	0.1241	91.94%	91.94%	13
4.8400	4.3761	2.7613	3.0916	1.9979	2.5323	4.5229	2.4369	4.6403	0.8705	4.2660	3.7830	1.1920	4.7519	2.8714	0.1241	91.94%	91.94%	14
4.8286	4.3315	2.6014	2.9553	1.7835	2.3560	4.4888	2.2538	4.6146	0.5755	4.2136	3.6961	0.9200	4.7342	2.7193	0.1241	91.94%	91.94%	15
4.8171	4.2870	2.4415	2.8190	1.5691	2.1798	4.4547	2.0707	4.5890	0.2806	4.1611	3.6092	0.6480	4.7165	2.5673	0.1241	91.94%	91.94%	16
4.8057	4.2424	2.2816	2.6826	1.3546	2.0035	4.4207	1.8876	4.5633	~0.0000	4.1087	3.5222	0.3760	4.6987	2.4153	0.1241	91.94%	91.94%	17
4.7943	4.1978	2.1217	2.5463	1.1402	1.8272	4.3866	1.7045	4.5376	0.0000	4.0563	3.4353	0.1040	4.6810	2.2632	0.1234	91.61%	85.95%	18
4.7828	4.1533	1.9618	2.4100	0.9258	1.6510	4.3525	1.5215	4.5119	0.0000	4.0039	3.3484	~0.0000	4.6633	2.1112	0.1228	91.31%	85.95%	19
4.7714	4.1087	1.8018	2.2737	0.7113	1.4747	4.3184	1.3384	4.4862	0.0000	3.9514	3.2615	0.0000	4.6456	1.9591	0.1217	90.72%	79.60%	20
4.7600	4.0641	1.6419	2.1374	0.4969	1.2984	4.2843	1.1553	4.4605	0.0000	3.8990	3.1745	0.0000	4.6279	1.8071	0.1206	90.19%	79.60%	21
4.7486	4.0196	1.4820	2.0011	0.2825	1.1222	4.2503	0.9722	4.4348	0.0000	3.8466	3.0876	0.0000	4.6101	1.6550	0.1197	89.71%	79.60%	22
4.7371	3.9750	1.3221	1.8648	0.0680	0.9459	4.2162	0.7891	4.4091	0.0000	3.7941	3.0007	0.0000	4.5924	1.5030	0.1188	89.27%	79.60%	23
4.7257	3.9305	1.1622	1.7284	~0.0000	0.7696	4.1821	0.6060	4.3834	0.0000	3.7417	2.9138	0.0000	4.5747	1.3510	0.1180	88.87%	79.60%	24
4.7143	3.8859	1.0023	1.5921	0.0000	0.5934	4.1480	0.4230	4.3577	0.0000	3.6893	2.8268	0.0000	4.5570	1.1989	0.1169	88.24%	73.19%	25
4.7028	3.8413	0.8424	1.4558	0.0000	0.4171	4.1140	0.2399	4.3321	0.0000	3.6369	2.7399	0.0000	4.5393	1.0469	0.1158	87.66%	73.19%	26
4.6914	3.7968	0.6825	1.3195	0.0000	0.2408	4.0799	0.0568	4.3064	0.0000	3.5844	2.6530	0.0000	4.5215	0.8948	0.1149	87.13%	73.19%	27
4.6800	3.7522	0.5226	1.1832	0.0000	0.0646	4.0458	~0.0000	4.2807	0.0000	3.5320	2.5660	0.0000	4.5038	0.7428	0.1140	86.63%	73.19%	28
4.6685	3.7076	0.3627	1.0469	0.0000	~0.0000	4.0117	0.0000	4.2550	0.0000	3.4796	2.4791	0.0000	4.4861	0.5907	**0.1129**	**85.99%**	**68.13%**	**29**

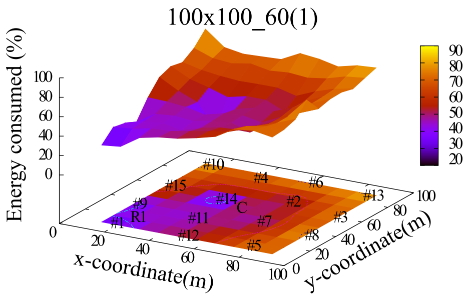

Figure 4.6: Energy charge distribution of instance 100x100_60(1) by assuming a RN in coordinate (20.00,20.00).

r_1	r_2		$r_{\tilde{s}_r}$
(x_1,y_1)	(x_2,y_2)	$\cdots$	$(x_{\tilde{s}_r},y_{\tilde{s}_r})$

$r_z \in S_r$, $r_z=(x_z,y_z)$, for $z=1,2,\ldots,\tilde{s}_r$, where $x_z \in [0,d_x]$ and $y_z \in [0,d_y]$

(a) Formal definition.

r_1	r_2	r_3
(25.02,30.28)	(10.85,78.65)	(98.41,73.24)

(b) Example.

Figure 4.7: Chromosome Statement.

4.5 Chromosome Definition

We consider a same chromosome structure for all the metaheuristics. As stated before, a chromosome is a possible solution to the optimisation problem and the objective of the RNPP defined in Section 4.2 is to place $\tilde{s}_r$ RNs. This way, as Figure 4.7a shows, we assume that a chromosome is composed of s_r genes, where a gene is a bi-dimensional coordinate of a RN. We include an example of this encoding in Figure 4.7b by assuming $\tilde{s_r} = 3$, $d_x = 100$, and $d_y = 100$m.

4.6 Considerations for Implementing the Metaheuristics

In this section, we discuss some specific details assumed for implementing the metaheuristics according to this problem definition. Before this, we include an important common aspects to all the metaheuristics: the generation of random individuals.

- **Random individuals:**
  The generation of random individuals is detailed in Algorithm 10, where *random(a,b)* $a, b \in \mathbb{R}$ is a function providing random numbers in the interval [a,b]. evaluateSolution(ζ) calculates the fitness functions of ζ according to the problem definition. Note that $\zeta[i].x$ and $\zeta[i].y$ are the x-coordinate and y-coordinate of the i-th gene (RN) of ζ, respectively. This procedure is considered for generating the initial population of all the metaheuristics.

Non-dominated Sorting Genetic Algorithm II

Next, we discuss the crossover and mutation strategies considered in NSGA-II:

- **Crossover operator:** ($\eta \leftarrow$ crossover($\zeta, \zeta', param\_cro_n$), line 20 of Algorithm 1)
  We consider the standard one-point crossover described in Section 2.1.3, taking two input individuals (ζ and ζ') and giving a new one (η) based on them. This operator depends on the crossover probability ($param\_cro_n$), determining if the crossover is performed, or otherwise, the best individual of the incoming pair is returned.

Algorithm 10 Generation of random individuals.

for $i = 1$ to $\tilde{s}_r$ **do**
    $\zeta[i].x \leftarrow \text{random}(0, d_x)$
    $\zeta[i].y \leftarrow \text{random}(0, d_y)$
end for
$\zeta \leftarrow$ evaluateSolution(ζ)
return ζ

Algorithm 11 Mutation operator for NSGA-II.

$\zeta' \leftarrow \zeta$ ▷ Backup of the initial individual
for $i = 0 \rightarrow \tilde{s}_r$ **do** ▷ Modify coordinates for each RN
    if $\text{random}(0, 1) < param\_mut_n$ **then**
        $\zeta[i].x \leftarrow \text{random}(0, d_x)$
        $\zeta[i].y \leftarrow \text{random}(0, d_y)$
        $\zeta \leftarrow$ evaluateSolution(ζ)
        if $\zeta' \succ \zeta$ **then**
            $\zeta \leftarrow \zeta'$ ▷ Restore backup
        else
            $\zeta' \leftarrow \zeta$ ▷ Accept changes
        end if
    end if
end for
return ζ

- **Mutation operator:** ($\eta \leftarrow$ mutation($\zeta, param\_mut_n$) in line 21 of Algorithm 1)
  This operator generates a new individual (η) by performing random changes in the input chromosome (ζ), attending to the mutation probability ($param\_mut_n$). In this approach, $param\_mut_n$ is the probability that each gene of the chromosome is mutated. As detailed in Algorithm 11, we follow a greedy strategy, where each time a gene is mutated, the individual is evaluated, and then, only if the mutated individual is not dominated by the previous one, the change is accepted. Otherwise, the gene takes the previous value.

Strength Pareto Evolutionary Algorithm 2

We consider the same crossover and mutation operators described for NSGA-II.

Multiobjective Variable Neighbour Search algorithm

Next, we discuss the generation of the neighbourhood structures, the generation of neighbourhood solutions, and the perturbation mechanism:

- **Neighbourhood structures:** ($NS_v \leftarrow$ generateNeighborhoodStructures (*param_neigh*$_v$, $param\_ns_v$), line 3 of Algorithm 3)
  We assume that a neighbourhood structure is the maximum displacement, that the RNs of a solution could experience during the local search, regarding the initial position. Thus, the set of neighbourhood structures NS_v is given by

$$NS_v = \left\{ ns_v^i \in \mathbb{R} : ns_v^i = \frac{\min(d_x, d_y)\ i}{param\_ns_v\ param\_neigh_v} \right\}, \qquad (4.7)$$

for $i = 1, 2, \ldots, param\_neigh_v$, where $ns_v^i < ns_v^{i+1}$, $param\_neigh_v$ is the number of neighbourhood structures, i.e. the cardinal of NS_v, $\min(d_x, d_y)$ is the minimum value between d_x and d_y, and $param\_ns_v$ is a factor delimiting the displacement. Accordingly, if i equals $param\_neigh_v$ and $param\_ns_v$ equals j, $j \in \mathbb{N}$, the maximum displacement is $\min(d_x, d_y)$ divided by j.

- **Neighbourhood solutions:** ($\overline{\zeta} \leftarrow$ generateNeighborhoodSolution(ζ, ns_v^i), line 10 of Algorithm 3)
  A new solution $\overline{\zeta}$ is generated in the neighbourhood of ζ, according to the neighbourhood structure $ns_v^i \in NS_v$, $i \in 1, 2, \ldots, param\_neigh_v$, by assuming the expression given by

$$\overline{\zeta}[j].x = \zeta[j].x + \left(\frac{ns_v^i}{2} - \text{random}(0, ns_v^i)\right); \quad \forall j \in 1, 2, \ldots, param\_neigh_v.$$

  Note that this expression is for the x-coordinate. For the y-coordinate it is similar.
- **Perturbation mechanism:** ($P_{g+1} \leftarrow$ performPerturbation($P_g, param_per_v$), line 25 of Algorithm 3)
  The perturbation is performed by applying the previously discussed mutation operator to each individual in P_g, resulting in a new P_{g+1}. In this case, the mutation probability is $param\_per_v$.

Multiobjective Artificial Bee Colony

We describe the generation of employed, onlooker, and scout solutions:

- **Employed forager solutions:** ($\overline{\zeta} \leftarrow$ generateEmployedForagerSolution(ζ), line 7 of Algorithm 4)
  It generates a new solution $\overline{\zeta}$ in the surrounding of a given employed forager $\zeta \in Se_g$ by following the expression given by

$$\overline{\zeta}[i].x = \zeta[i].x + random(-1, 1)(\zeta[i].x - \zeta'[i].x); \quad \forall i \in 1, 2, \ldots, \tilde{s}_r,$$

  where $\zeta' \in Se_g$ is a randomly selected solution. Note that this expression is for the x-coordinate. For the y-coordinate it is similar.
- **Onlooker solutions:** ($\overline{\eta} \leftarrow$ generateOnlookerSolution(η, ζ), line 17 of Algorithm 4)
  The onlooker bee $\eta \in So_g$ generates a new solution $\overline{\eta}$ based on the employed forager $\zeta \in Se_{g+1}$, according to the expression given by

$$\overline{\eta}[i].x = \eta[i].x + random(-1, 1)(\eta[i].x - \zeta[i].x); \quad \forall i \in 1, 2, \ldots, \tilde{s}_r.$$

  Note that this expression is for the x-coordinate. For the y-coordinate it is similar.
- **Scout solutions:** ($\overline{\zeta} \leftarrow$ generateScoutSolution(), line 22 of Algorithm 4)

  A employed solution $\zeta \in Se_{g+1}$ is randomly selected from the first two Pareto fronts of Se_{g+1}, according to rank measure. Next, we get the Euclidean distance between ζ and all other solutions in $Se_{g+1} \cup So_{g+1} - \{\zeta\}$. Finally, the k-nearest solutions to ζ are combined to generate a new one, which replaces the exhausted one, where k is a random number in the interval [2,11]. That is

$$\overline{\zeta}[i].x = \frac{\displaystyle\sum_{bee \in KS} bee[i].x}{k}; \quad \forall i \in 1, 2 \ldots, \tilde{s}_r, \tag{4.8}$$

where KS is the set of k-nearest solutions to ζ. Note that this expression is for the x-coordinate. For the y-coordinate it is similar.

Multiobjective Firefly Algorithm

The original algorithm describes how the solutions are generated. Consequently, we do not need to discuss this aspect. Next, we describe the stagnation control:

- **Stagnation control:** (P_{g+1} $\leftarrow$ stagnationControl(P_{g+1},P_g,Q_g,$param\_how\_sc_f$, $param\_when\_sc_f$), line 20 of Algorithm 5)
  In case that the percentage of non-dominated solutions in Q_g, regarding P_g, is lower than $param\_when\_sc_f \in [0, 1]$, then we apply the mutation operator discussed before for NSGA-II, attending to $param\_how\_sc_f$, to individuals in P_{g+1}.

Multiobjective Gravitational Search Algorithm

The original algorithm describes how the solutions are generated. Consequently, we do not need to discuss this aspect. The stagnation control (line 16 of Algorithm 6) is the same as described before for MO-FA. The definition of both $c(g)$ and $kbest(g)$ decreasing functions were inspired by the original proposal of the authors of GSA. We assume that $param\_kbestInitial_{gsa}$ is ps_{gsa} and $param\_kbestFinal_{gsa}$ is 1. We consider that $c(g)$ is given by

$$c(g) = 100e^{-h} \tag{4.9}$$

for 50x50 and 100x100 instances and

$$c(g) = 100e^{-2-h} \tag{4.10}$$

for larger displacements, i.e. 200x200 and 300x300 instances, where $h \in [0, 7]$. Thus, $param\_cInitial_{gsa}$ is the value obtained by considering Equations (4.9) or (4.10) with h equalling 0. $param\_cFinal_{gsa}$ is the value obtained by considering Equations (4.9) or (4.10) with h equalling 7.

Multiobjective Evolutionary Algorithm based on Decomposition

The generation of new solutions (line 9 of Algorithm 9) considers the same crossover and mutation operators as described before for NSGA-II. We consider that the extreme points of the CHIM correspond to the reference points defined for calculating the hypervolume metric in Section 4.3.

4.7 Solving the Problem

In this section, we discuss the results obtained by solving the bi-objective outdoor RNPP through a wide range of MO metaheuristics, assuming hypervolume, set coverage, and attainment surface as MO tools. To this end, we consider the data set described in Section 4.3 and several stop conditions based on the number of evaluations, i.e. 50 000, 100 000, 200 000, 300 000, and 400 000. The purpose is to determine which of them provide better significant performance, according to several criteria and not only to one, while convergence speed is analysed.

This section is structured as follows. Firstly, we adjust the algorithms in Section 4.7.1. We provide a statistical analysis based on the hypervolume metric in Section 4.7.2. A convergence study based on this same metric is discussed in Section 4.7.3 Another analysis based on the set coverage metric is provided in Section 4.7.4 Pareto fronts and attainment surfaces are shown in Section 4.7.5. We study the impact of the optimisation on the fitness functions in Section 4.7.6. Finally, comparisons to other approaches are discussed in Section 4.7.7.

Table 4.3: Parametric sweep.

NSGA-II

Parameter	Selected	Range
ps_n	**100**	-
$param\_cro_n$	**0.50**	[0.05,0.1,0.15,...,0.95]
$param\_mut_n$	**0.50**	[0.05,0.1,0.15,...,0.95]

SPEA2

Parameter	Selected	Range
ps_s	**100**	-
$\overline{ps}_s$	**100**	-
$param\_cro_s$	**0.50**	[0.05,0.1,0.15,...,0.95]
$param\_mut_s$	**0.50**	[0.05,0.1,0.15,...,0.95]

MO-VNS

Parameter	Selected	Range
$param\_neigh_v$	**7**	[4,5,6,...,14]
$param\_ns_v$	**2**	[1,2,3,4,5]

MO-VNS*

Parameter	Selected	Range
$param\_neigh_v$	**11**	[4,5,6,...,14]
$param\_ns_v$	**3**	[1,2,3,4,5]
$param\_per_v$	**0.10**	[0.05,0.1,0.15,...,0.95]

MO-ABC

Parameter	Selected	Range
ps_a	**100**	-
$param\_Se_a$	**0.50**	[0.30,0.35,0.40,...,0.70]
$param\_limit_a$	**30**	[10,15,20,...,60]

MO-FA

Parameter	Selected	Range
ps_f	**100**	-
r_f	**0.50**	[0.05,0.1,0.15,...,0.95]
β_{0_f}	**0.75**	[0.05,0.1,0.15,...,0.95]
γ_f	**0.05**	[0.05,0.1,0.15,...,0.95]
$param\_how\_sc_f$	**0.60**	[0.05,0.1,0.15,...,0.95]
$param\_when\_sc_f$	**0.30**	[0.05,0.1,0.15,...,0.95]

MO-GSA

Parameter	Selected	Range
ps_{gsa}	**100**	-
$param\_how\_sc_{gsa}$	**0.40**	[0.05,0.1,0.15,...,0.95]
$param\_when\_sc_{gsa}$	**0.05**	[0.05,0.1,0.15,...,0.95]

MOEA/D

Parameter	Selected	Range
$param\_CHIMinc_m$	**1.30**	[1.00,1.05,...,2.00]
$param\_crow_m$	**0.015**	[0.010,0.015,...,0.050]
$param\_neigh_m$	**0.55**	[0.05,0.10,...,0.95]
$param\_cro_m$	**0.15**	[0.05,0.10,...,0.95]
$param\_mut_m$	**0.25**	[0.05,0.10,...,0.95]

4.7.1 Parametric Swap

As stated before, the first step before executing the algorithms is to adjust their parameters. To this end, we consider the methodology discussed in Section 2.3.2 by assuming all the test cases, a reduced stop condition of 50 000 evaluations, and the hypervolume indicator as quality metric. The resulting configurations are in Table 4.3, showing for each parameter the range of values studied and the resulting value selected. Note that population size parameters were not studied, such as ps_n, instead we consider a widely accepted value of 100 individuals. In the next chapter, we will incorporate this aspect to the research.

Observing this table, we notice that we obtained mutation parameters close to 0.5, instead of expected values close to 0.0. E.g. $param\_mut_n$ and $param\_mut_s$ equal 0.5, This is because we consider a greedy strategy as discussed in Section 4.6, allowing to assume such level of mutation without penalising its behaviour. Otherwise, the level of novelty in the chromosome would be inadequate for generating good solutions.

4.7.2 Statistical Analysis Based on the Hypervolume Metric

Tables 4.4, 4.5, 4.6, and 4.7 shows median hypervolume ($\overline{Hyp}$) and InterQuartile Range (IQR) for each metaheuristic, test case, and stop condition, where higher hypervolumes are shaded. These median hypervolumes were obtained by running 31 independent runs for each metaheuristic and test case. Note that one run provides results for the five stop conditions. Analysing these tables according to the shaded cells, some algorithms seem to provide better results than others. However, these differences could not be significant, and then, we should check this by following the statistical methodology discussed in Section 2.3.1.

With this purpose, we study if hypervolume distributions come from a normal distribution through Kolmogorov-Smirnov-Lilliefor's [67] and Shapiro-Wilk's [68] tests, considering the hypothesis: H_0 if data follow a normal distribution and H_1 otherwise. P-values lower than 0.05 were obtained for all the cases. Hence, we cannot assume H_1. Consequently, we cannot assume that hypervolume distributions follow a normal distribution, and then, we should assume median and IQR as average value and statistical dispersion metric, respectively. Note that Tables 4.4, 4.5, 4.6, and 4.7 were developed after performing this study.

Next, we analyse if there are significant differences among the algorithms. To this end, as samples are independent and data do not follow a normal distribution, we assume the Wilcoxon-Mann-Whitney's [69] test with hypothesis: H_0 if $\overline{Hyp_i} <= \overline{Hyp_j}$, with $i = 1, 2, \ldots, 8$, $j = 2, 3, \ldots, 8$, $i < j$, 1=NSGA-II, 2=SPEA2, 3=MO-VNS, 4=MO-VNS*, 5=MO-ABC, 6=MOFA, 7=MO-GSA, and 8=MOEA/D. MO-VNS is the algorithm without perturbation mechanism and MO-VNS* includes this procedure. The p-values obtained are in Section B.1 of Appendix B, specifically in Tables B.1, B.2, B.3, B.4, B.5, B.6, and B.7. These p-values were analysed by assuming a widely accepted significance level of 0.05. Thus, if we compare any two algorithms i and j, we could reach three different situations for a given study case (a test case and a stop condition):

- The p-value is lower than 0.05: i is significant better than j.
- The p-value is higher than 0.95: j is significant better than i.
- The p-value is between 0.05 and 0.95: there are not significant differences between both.

Based on these p-values, Table 4.8 shows which algorithms provide the best significant performance for each study case. Note that it is possible that more than one algorithm provides the best significant performance, i.e. they are better than the remaining algorithms, but there is not significant differences among them. In such a case, more than one algorithm appears in a same cell of this table, e.g. MO-FA and MO-VNS for 100x100_30(2) and 100 000 evaluations.

In addition to study which algorithms provide a significant better performance for a given study case as before. It is also interesting to compare all the algorithms two by two, with the purpose of determining which metaheuristics provide the best average behaviour. Thus, Table 4.9 shows the percentage of study cases in which the metaheuristics are better and worse than others, considering all the instances, 50x50 instances, 100x100 instances, 200x200 instances, and 300x300 instances. In this table, better average values in *Percentage* field are shaded from darker to lighter tone, i.e. from better to worse average behaviour.

Analysing this table, we reach that MO-FA provides the best average behaviour for all the instances, followed by MO-ABC, MO-VNS*, and MO-VNS. For 50x50 instances, we find that MO-ABC, MO-FA, MO-GSA, and MOEA/D provides a similar behaviour, followed by MO-VNS and MO-VNS*. For 100x100 instances, MO-VNS provides the best behaviour, followed by MO-FA and MO-ABC. In case of 200x200 instances, MO-FA is the best algorithm, followed by MO-VNS* and MO-VNS. For 300x300 instances, MO-FA provides the best behaviour, followed by MO-ABC and MO-VNS*.

Based on this analysis, we can conclude that MO-FA is the best algorithm in average term. However, and according to the instance size, we recommend to consider MO-FA for solving this problem in large instances (200x200 and 300x300) and MO-VNS for small instances (50x50 and 100x100). Note that the behaviour of MO-VNS and MO-VNS* is really different and deserves special mention. MO-VNS provides a good behaviour for solving small instances, while

Table 4.4: Median hypervolume metric for each test case and stop condition, where higher hipervolumes obtained are shaded by considering all the metaheuristics. Part 1 of 4.

	NSGA-II($\overline{Hyp}\,\%, IQR$)				
	Evaluations (Stop condition)				
Instance($\tilde{s}_r$)	**50 000**	**100 000**	**200 000**	**300 000**	**400 000**
50x50_30(1)	64.61% , 0.0000	64.61% , 0.0000	64.61% , 0.0000	64.61% , 0.0000	64.61% , 0.0000
50x50_60(1)	64.61% , 0.0000	64.61% , 0.0000	64.61% , 0.0000	64.61% , 0.0000	64.61% , 0.0000
100x100_30(2)	42.40% , 0.0041	42.45% , 0.0038	42.67% , 0.0002	42.69% , 0.0003	42.69% , 0.0002
100x100_30(3)	55.02% , 0.0067	55.37% , 0.0045	55.53% , 0.0035	55.55% , 0.0031	55.66% , 0.0005
100x100_60(2)	31.60% , 0.0030	31.80% , 0.0023	31.82% , 0.0022	31.86% , 0.0020	31.94% , 0.0001
100x100_60(3)	58.97% , 0.0053	59.25% , 0.0048	59.69% , 0.0030	59.73% , 0.0038	59.91% , 0.0024
200x200_30(2)	34.39% , 0.0302	35.39% , 0.0213	36.33% , 0.0221	37.06% , 0.0102	37.54% , 0.0080
200x200_30(4)	43.41% , 0.0704	44.46% , 0.0660	46.45% , 0.0912	47.22% , 0.1052	47.48% , 0.1085
200x200_30(6)	53.70% , 0.1648	58.70% , 0.0988	64.61% , 0.0155	65.01% , 0.0154	65.26% , 0.0164
200x200_30(9)	73.47% , 0.0227	76.04% , 0.0197	77.56% , 0.0154	78.14% , 0.0176	78.47% , 0.0155
200x200_60(2)	22.40% , 0.0073	22.92% , 0.0060	23.32% , 0.0049	23.57% , 0.0034	23.68% , 0.0042
200x200_60(4)	56.14% , 0.0113	57.63% , 0.0095	58.94% , 0.0085	59.38% , 0.0077	59.65% , 0.0060
200x200_60(6)	71.79% , 0.0145	73.96% , 0.0123	75.33% , 0.0127	75.93% , 0.0159	76.37% , 0.0141
200x200_60(9)	85.98% , 0.0179	88.38% , 0.0137	90.05% , 0.0115	90.51% , 0.0122	90.94% , 0.0115
300x300_30(6)	38.22% , 0.0182	39.41% , 0.0136	40.31% , 0.0121	40.77% , 0.0153	41.11% , 0.0179
300x300_30(12)	44.36% , 0.0232	46.27% , 0.0195	47.65% , 0.0155	48.11% , 0.0191	48.51% , 0.0175
300x300_30(18)	47.01% , 0.0353	50.02% , 0.0290	52.34% , 0.0255	53.17% , 0.0203	53.90% , 0.0229
300x300_30(24)	48.00% , 0.0323	52.75% , 0.0374	56.67% , 0.0653	58.86% , 0.0770	59.99% , 0.0792
300x300_60(6)	33.77% , 0.0151	35.35% , 0.0130	36.34% , 0.0098	36.87% , 0.0131	37.22% , 0.0111
300x300_60(12)	53.14% , 0.0176	55.24% , 0.0118	57.09% , 0.0114	57.80% , 0.0115	58.31% , 0.0090
300x300_60(18)	61.23% , 0.0109	63.32% , 0.0113	65.13% , 0.0105	66.12% , 0.0101	66.67% , 0.0100
300x300_60(24)	65.21% , 0.0094	66.96% , 0.0064	68.71% , 0.0128	70.03% , 0.0104	70.85% , 0.0092

	SPEA2($\overline{Hyp}\,\%, IQR$)				
	Evaluations (Stop condition)				
Instance($\tilde{s}_r$)	**50 000**	**100 000**	**200 000**	**300 000**	**400 000**
50x50_30(1)	64.61% , 0.0000	64.61% , 0.0000	64.61% , 0.0000	64.61% , 0.0000	64.61% , 0.0000
50x50_60(1)	64.61% , 0.0000	64.61% , 0.0000	64.61% , 0.0000	64.61% , 0.0000	64.61% , 0.0000
100x100_30(2)	42.11% , 0.0055	42.45% , 0.0034	42.66% , 0.0002	42.66% , 0.0002	42.66% , 0.0001
100x100_30(3)	53.71% , 0.0117	53.78% , 0.0096	53.94% , 0.0105	54.24% , 0.0090	53.93% , 0.0094
100x100_60(2)	31.27% , 0.0039	31.57% , 0.0028	31.75% , 0.0026	31.78% , 0.0021	31.87% , 0.0009
100x100_60(3)	57.96% , 0.0101	58.63% , 0.0081	58.97% , 0.0121	58.84% , 0.0128	59.30% , 0.0069
200x200_30(2)	34.08% , 0.0221	34.35% , 0.0228	34.72% , 0.0195	34.85% , 0.0143	34.99% , 0.0144
200x200_30(4)	44.14% , 0.0608	44.71% , 0.0586	45.31% , 0.0581	45.49% , 0.0631	45.63% , 0.0580
200x200_30(6)	58.30% , 0.0285	61.29% , 0.0208	62.99% , 0.0254	63.34% , 0.0254	63.60% , 0.0256
200x200_30(9)	70.75% , 0.0140	74.49% , 0.0154	75.63% , 0.0179	75.97% , 0.0141	76.35% , 0.0148
200x200_60(2)	22.91% , 0.0047	23.29% , 0.0062	23.62% , 0.0048	23.76% , 0.0037	23.85% , 0.0030
200x200_60(4)	57.43% , 0.0108	58.57% , 0.0081	59.30% , 0.0066	59.74% , 0.0082	59.88% , 0.0061
200x200_60(6)	71.38% , 0.0086	72.69% , 0.0087	73.67% , 0.0094	74.13% , 0.0140	74.35% , 0.0166
200x200_60(9)	84.30% , 0.0076	86.50% , 0.0049	88.28% , 0.0171	89.27% , 0.0167	89.71% , 0.0122
300x300_30(6)	39.13% , 0.0176	40.15% , 0.0157	40.89% , 0.0201	41.12% , 0.0215	41.21% , 0.0205
300x300_30(12)	45.56% , 0.0278	47.03% , 0.0170	47.99% , 0.0149	48.39% , 0.0120	48.63% , 0.0113
300x300_30(18)	48.81% , 0.0184	50.81% , 0.0092	52.18% , 0.0087	52.99% , 0.0130	53.68% , 0.0167
300x300_30(24)	52.39% , 0.0492	56.93% , 0.0655	59.44% , 0.0639	60.34% , 0.0619	60.86% , 0.0657
300x300_60(6)	35.40% , 0.0117	36.42% , 0.0138	37.11% , 0.0122	37.35% , 0.0131	37.56% , 0.0127
300x300_60(12)	55.55% , 0.0122	56.98% , 0.0063	57.95% , 0.0065	58.40% , 0.0041	58.56% , 0.0039
300x300_60(18)	63.20% , 0.0076	64.50% , 0.0075	65.79% , 0.0083	66.57% , 0.0088	67.02% , 0.0080
300x300_60(24)	66.83% , 0.0081	68.14% , 0.0077	69.78% , 0.0062	70.73% , 0.0048	71.30% , 0.0051

Table 4.5: Median hypervolume metric for each test case and stop condition, where higher hipervolumes obtained are shaded by considering all the metaheuristics. Part 2 of 4.

	MO-VNS without perturbation($\overline{Hyp}$ %, IQR)				
	Evaluations (Stop condition)				
Instance($\bar{s}_r$)	**50 000**	**100 000**	**200 000**	**300 000**	**400 000**
50x50_30(1)	63.08% , 0.1408	67.03% , 0.0000	67.03% , 0.0000	67.03% , 0.0000	67.03% , 0.0000
50x50_60(1)	67.03% , 0.0000	67.03% , 0.0000	67.03% , 0.0000	67.03% , 0.0000	67.03% , 0.0000
100x100_30(2)	43.62% , 0.0188	44.67% , 0.0003	44.69% , 0.0000	44.69% , 0.0000	44.69% , 0.0000
100x100_30(3)	58.33% , 0.0023	58.65% , 0.0038	58.85% , 0.0067	59.09% , 0.0077	59.24% , 0.0077
100x100_60(2)	34.55% , 0.0005	34.58% , 0.0005	34.60% , 0.0006	34.61% , 0.0002	34.63% , 0.0000
100x100_60(3)	61.41% , 0.0169	62.05% , 0.0029	62.17% , 0.0021	62.25% , 0.0016	62.33% , 0.0005
200x200_30(2)	37.63% , 0.0613	38.82% , 0.0284	39.93% , 0.0173	40.75% , 0.0048	41.07% , 0.0022
200x200_30(4)	51.99% , 0.0430	53.29% , 0.0274	54.31% , 0.0176	54.74% , 0.0196	54.96% , 0.0202
200x200_30(6)	64.36% , 0.0332	65.47% , 0.0342	66.31% , 0.0378	66.63% , 0.0293	66.87% , 0.0266
200x200_30(9)	74.57% , 0.0414	75.84% , 0.0344	77.12% , 0.0290	77.75% , 0.0229	78.28% , 0.0260
200x200_60(2)	24.43% , 0.0068	24.55% , 0.0067	24.65% , 0.0069	24.68% , 0.0049	24.72% , 0.0048
200x200_60(4)	61.28% , 0.0114	61.68% , 0.0061	61.95% , 0.0074	62.17% , 0.0055	62.29% , 0.0067
200x200_60(6)	75.95% , 0.0126	76.75% , 0.0118	77.22% , 0.0166	77.61% , 0.0175	77.86% , 0.0148
200x200_60(9)	89.42% , 0.0106	90.21% , 0.0047	91.02% , 0.0089	91.39% , 0.0062	91.59% , 0.0081
300x300_30(6)	39.85% , 0.0155	40.57% , 0.0202	41.22% , 0.0158	41.67% , 0.0224	41.89% , 0.0250
300x300_30(12)	45.28% , 0.0174	46.39% , 0.0147	47.45% , 0.0127	47.97% , 0.0147	48.33% , 0.0146
300x300_30(18)	48.49% , 0.0138	49.51% , 0.0081	50.47% , 0.0092	51.04% , 0.0134	51.59% , 0.0090
300x300_30(24)	50.54% , 0.0105	51.88% , 0.0128	52.92% , 0.0179	53.75% , 0.0172	54.28% , 0.0167
300x300_60(6)	35.79% , 0.0237	36.39% , 0.0176	37.26% , 0.0182	37.69% , 0.0187	38.11% , 0.0172
300x300_60(12)	53.68% , 0.0235	54.99% , 0.0148	55.95% , 0.0162	56.51% , 0.0154	56.86% , 0.0147
300x300_60(18)	61.69% , 0.0162	62.75% , 0.0139	63.79% , 0.0175	64.26% , 0.0161	64.57% , 0.0177
300x300_60(24)	66.52% , 0.0109	67.44% , 0.0100	68.28% , 0.0093	68.69% , 0.0088	68.95% , 0.0092

	MO-VNS with perturbation($\overline{Hyp}$ %, IQR)				
	Evaluations (Stop condition)				
Instance($\bar{s}_r$)	**50 000**	**100 000**	**200 000**	**300 000**	**400 000**
50x50_30(1)	66.79% , 0.0026	66.84% , 0.0020	66.88% , 0.0019	66.94% , 0.0021	66.98% , 0.0019
50x50_60(1)	66.57% , 0.0060	66.79% , 0.0040	66.92% , 0.0020	66.96% , 0.0020	67.00% , 0.0011
100x100_30(2)	41.90% , 0.0489	42.73% , 0.0410	43.49% , 0.0376	44.69% , 0.0000	44.69% , 0.0000
100x100_30(3)	58.17% , 0.0063	58.48% , 0.0006	58.53% , 0.0018	58.52% , 0.0022	58.57% , 0.0025
100x100_60(2)	34.46% , 0.0017	34.56% , 0.0001	34.56% , 0.0001	34.58% , 0.0005	34.59% , 0.0005
100x100_60(3)	60.74% , 0.0286	61.29% , 0.0214	61.62% , 0.0168	62.20% , 0.0021	62.32% , 0.0011
200x200_30(2)	35.44% , 0.0544	37.35% , 0.0742	38.35% , 0.0763	38.66% , 0.0608	39.03% , 0.0375
200x200_30(4)	48.64% , 0.0944	50.13% , 0.0720	51.56% , 0.0654	52.88% , 0.0354	53.71% , 0.0252
200x200_30(6)	66.48% , 0.0258	67.06% , 0.0231	67.47% , 0.0226	67.70% , 0.0176	67.80% , 0.0181
200x200_30(9)	77.99% , 0.0259	78.97% , 0.0225	79.63% , 0.0177	80.06% , 0.0185	80.31% , 0.0161
200x200_60(2)	23.43% , 0.0195	24.26% , 0.0094	24.51% , 0.0088	24.59% , 0.0063	24.66% , 0.0061
200x200_60(4)	61.83% , 0.0061	61.95% , 0.0071	62.16% , 0.0072	62.27% , 0.0071	62.39% , 0.0067
200x200_60(6)	76.83% , 0.0093	77.42% , 0.0089	77.84% , 0.0117	78.06% , 0.0103	78.30% , 0.0064
200x200_60(9)	89.74% , 0.0113	90.46% , 0.0111	91.08% , 0.0130	91.37% , 0.0127	91.43% , 0.0132
300x300_30(6)	41.09% , 0.0225	41.66% , 0.0289	42.18% , 0.0308	42.42% , 0.0276	42.56% , 0.0286
300x300_30(12)	47.31% , 0.0114	47.95% , 0.0083	48.50% , 0.0051	48.77% , 0.0064	48.87% , 0.0052
300x300_30(18)	51.31% , 0.0124	52.08% , 0.0166	52.78% , 0.0134	53.28% , 0.0136	53.51% , 0.0165
300x300_30(24)	55.94% , 0.0251	57.58% , 0.0297	58.86% , 0.0173	59.26% , 0.0152	59.64% , 0.0160
300x300_60(6)	37.45% , 0.0119	37.89% , 0.0113	38.31% , 0.0129	38.57% , 0.0131	38.73% , 0.0146
300x300_60(12)	56.61% , 0.0119	57.35% , 0.0052	57.87% , 0.0105	58.18% , 0.0075	58.32% , 0.0061
300x300_60(18)	63.11% , 0.0079	63.67% , 0.0078	64.08% , 0.0080	64.34% , 0.0060	64.48% , 0.0045
300x300_60(24)	67.86% , 0.0099	68.47% , 0.0118	69.00% , 0.0130	69.25% , 0.0099	69.46% , 0.0069

Table 4.6: Median hypervolume metric for each test case and stop condition, where higher hipervolumes obtained are shaded by considering all the metaheuristics. Part 3 of 4.

	MO-ABC($\overline{Hyp}\,\%, IQR$)				
	Evaluations (Stop condition)				
Instance($\tilde{s}_r$)	**50 000**	**100 000**	**200 000**	**300 000**	**400 000**
50x50_30(1)	67.07% , 0.0000	67.07% , 0.0000	67.07% , 0.0000	67.07% , 0.0000	67.07% , 0.0000
50x50_60(1)	67.07% , 0.0000	67.07% , 0.0000	67.07% , 0.0000	67.07% , 0.0000	67.07% , 0.0000
100x100_30(2)	44.64% , 0.0003	44.64% , 0.0004	44.65% , 0.0003	44.66% , 0.0003	44.66% , 0.0003
100x100_30(3)	58.79% , 0.0060	59.11% , 0.0050	59.15% , 0.0038	59.16% , 0.0038	59.18% , 0.0039
100x100_60(2)	34.39% , 0.0023	34.40% , 0.0024	34.41% , 0.0024	34.41% , 0.0023	34.41% , 0.0021
100x100_60(3)	61.57% , 0.0044	61.95% , 0.0020	62.02% , 0.0017	62.04% , 0.0019	62.06% , 0.0018
200x200_30(2)	37.62% , 0.0145	37.98% , 0.0143	37.98% , 0.0143	37.99% , 0.0143	37.99% , 0.0143
200x200_30(4)	48.41% , 0.0446	49.89% , 0.0324	52.59% , 0.0179	53.21% , 0.0152	53.28% , 0.0150
200x200_30(6)	59.69% , 0.0279	62.60% , 0.0215	65.80% , 0.0228	67.74% , 0.0200	68.27% , 0.0202
200x200_30(9)	73.07% , 0.0241	75.35% , 0.0199	77.40% , 0.0121	78.79% , 0.0150	80.08% , 0.0128
200x200_60(2)	24.73% , 0.0018	24.82% , 0.0009	24.83% , 0.0011	24.84% , 0.0010	24.85% , 0.0009
200x200_60(4)	59.82% , 0.0088	61.88% , 0.0050	62.45% , 0.0032	62.50% , 0.0039	62.55% , 0.0043
200x200_60(6)	73.92% , 0.0164	75.29% , 0.0112	77.00% , 0.0090	78.19% , 0.0058	78.70% , 0.0087
200x200_60(9)	87.02% , 0.0118	88.66% , 0.0113	90.19% , 0.0090	91.19% , 0.0111	92.09% , 0.0072
300x300_30(6)	40.24% , 0.0067	41.45% , 0.0064	42.51% , 0.0080	43.09% , 0.0070	43.46% , 0.0063
300x300_30(12)	47.46% , 0.0090	49.40% , 0.0070	50.52% , 0.0073	51.04% , 0.0064	51.38% , 0.0054
300x300_30(18)	51.90% , 0.0068	54.31% , 0.0056	56.07% , 0.0080	56.79% , 0.0054	57.41% , 0.0051
300x300_30(24)	55.41% , 0.0112	59.05% , 0.0189	61.93% , 0.0144	63.46% , 0.0125	64.24% , 0.0129
300x300_60(6)	34.55% , 0.0115	35.89% , 0.0108	37.86% , 0.0095	39.17% , 0.0103	39.94% , 0.0064
300x300_60(12)	52.61% , 0.0139	54.36% , 0.0098	55.75% , 0.0109	56.63% , 0.0104	57.30% , 0.0108
300x300_60(18)	62.55% , 0.0096	63.96% , 0.0094	65.31% , 0.0101	65.93% , 0.0104	66.37% , 0.0105
300x300_60(24)	67.46% , 0.0081	68.78% , 0.0055	69.86% , 0.0062	70.41% , 0.0073	70.78% , 0.0074

	MO-FA($\overline{Hyp}\,\%, IQR$)				
	Evaluations (Stop condition)				
Instance($\tilde{s}_r$)	**50 000**	**100 000**	**200 000**	**300 000**	**400 000**
50x50_30(1)	67.07% , 0.0000	67.07% , 0.0000	67.07% , 0.0000	67.07% , 0.0000	67.07% , 0.0000
50x50_60(1)	67.07% , 0.0000	67.07% , 0.0000	67.07% , 0.0000	67.07% , 0.0000	67.07% , 0.0000
100x100_30(2)	44.66% , 0.0003	44.68% , 0.0002	44.69% , 0.0000	44.69% , 0.0000	44.69% , 0.0000
100x100_30(3)	58.47% , 0.0003	58.59% , 0.0034	58.74% , 0.0031	58.83% , 0.0003	58.84% , 0.0003
100x100_60(2)	33.99% , 0.0024	34.10% , 0.0025	34.25% , 0.0021	34.36% , 0.0022	34.41% , 0.0021
100x100_60(3)	61.54% , 0.0034	61.84% , 0.0027	62.00% , 0.0014	62.08% , 0.0011	62.14% , 0.0010
200x200_30(2)	38.06% , 0.0629	38.60% , 0.0409	41.02% , 0.0016	41.03% , 0.0013	41.05% , 0.0017
200x200_30(4)	49.95% , 0.0747	50.63% , 0.0838	50.95% , 0.0868	51.20% , 0.0869	51.16% , 0.0834
200x200_30(6)	66.70% , 0.0300	67.29% , 0.0174	67.52% , 0.0172	67.71% , 0.0178	67.68% , 0.0173
200x200_30(9)	78.92% , 0.0323	80.26% , 0.0238	80.76% , 0.0184	81.19% , 0.0193	81.30% , 0.0194
200x200_60(2)	24.38% , 0.0089	24.52% , 0.0055	24.61% , 0.0045	24.70% , 0.0034	24.74% , 0.0035
200x200_60(4)	61.61% , 0.0036	61.73% , 0.0034	61.79% , 0.0033	61.83% , 0.0026	61.86% , 0.0021
200x200_60(6)	76.38% , 0.0172	76.99% , 0.0156	77.19% , 0.0132	77.24% , 0.0127	77.34% , 0.0128
200x200_60(9)	90.84% , 0.0093	91.30% , 0.0075	91.51% , 0.0069	91.64% , 0.0069	91.71% , 0.0062
300x300_30(6)	40.68% , 0.0224	41.15% , 0.0257	41.40% , 0.0273	41.58% , 0.0247	41.65% , 0.0276
300x300_30(12)	49.20% , 0.0170	50.25% , 0.0164	51.06% , 0.0155	51.25% , 0.0165	51.41% , 0.0148
300x300_30(18)	54.15% , 0.0117	56.56% , 0.0163	58.06% , 0.0186	58.72% , 0.0201	59.13% , 0.0201
300x300_30(24)	59.68% , 0.0385	63.40% , 0.0308	65.98% , 0.0125	66.58% , 0.0138	66.90% , 0.0130
300x300_60(6)	38.09% , 0.0146	38.57% , 0.0118	38.83% , 0.0115	38.90% , 0.0129	38.99% , 0.0161
300x300_60(12)	58.28% , 0.0074	58.97% , 0.0074	59.40% , 0.0035	59.55% , 0.0069	59.64% , 0.0071
300x300_60(18)	65.19% , 0.0056	66.47% , 0.0065	66.93% , 0.0087	67.21% , 0.0092	67.30% , 0.0094
300x300_60(24)	69.25% , 0.0069	70.59% , 0.0086	71.34% , 0.0054	71.59% , 0.0049	71.69% , 0.0049

Table 4.7: Median hypervolume metric for each test case and stop condition, where higher hipervolumes obtained are shaded by considering all the metaheuristics. Part 4 of 4.

	MO-GSA($\overline{Hyp}\,\%, IQR$)				
	Evaluations (Stop condition)				
Instance($\bar{s}_r$)	**50 000**	**100 000**	**200 000**	**300 000**	**400 000**
50x50_30(1)	67.07% , 0.0000	67.07% , 0.0000	67.07% , 0.0000	67.07% , 0.0000	67.07% , 0.0000
50x50_60(1)	67.07% , 0.0000	67.07% , 0.0000	67.07% , 0.0000	67.07% , 0.0000	67.07% , 0.0000
100x100_30(2)	43.51% , 0.0092	44.10% , 0.0041	44.46% , 0.0023	44.53% , 0.0022	44.64% , 0.0003
100x100_30(3)	55.57% , 0.0153	56.21% , 0.0150	57.32% , 0.0079	58.03% , 0.0047	58.24% , 0.0045
100x100_60(2)	33.59% , 0.0040	33.85% , 0.0041	34.20% , 0.0030	34.33% , 0.0031	34.39% , 0.0025
100x100_60(3)	60.47% , 0.0133	61.07% , 0.0104	61.61% , 0.0035	61.81% , 0.0025	61.89% , 0.0023
200x200_30(2)	37.36% , 0.0166	37.46% , 0.0148	37.92% , 0.0201	38.51% , 0.0186	38.87% , 0.0201
200x200_30(4)	47.42% , 0.0327	48.89% , 0.0328	51.24% , 0.0469	52.56% , 0.0248	53.02% , 0.0271
200x200_30(6)	60.76% , 0.0338	63.50% , 0.0236	65.13% , 0.0246	65.90% , 0.0222	66.44% , 0.0198
200x200_30(9)	72.35% , 0.0340	74.83% , 0.0246	76.78% , 0.0197	77.69% , 0.0185	78.48% , 0.0158
200x200_60(2)	22.69% , 0.0221	23.38% , 0.0120	24.28% , 0.0051	24.37% , 0.0062	24.57% , 0.0028
200x200_60(4)	58.79% , 0.0132	60.20% , 0.0071	61.16% , 0.0052	61.41% , 0.0052	61.66% , 0.0054
200x200_60(6)	72.31% , 0.0151	74.04% , 0.0085	75.77% , 0.0121	76.58% , 0.0140	77.02% , 0.0154
200x200_60(9)	83.86% , 0.0189	86.74% , 0.0248	89.78% , 0.0116	90.54% , 0.0102	91.09% , 0.0085
300x300_30(6)	37.70% , 0.0234	38.89% , 0.0170	39.95% , 0.0161	40.52% , 0.0152	40.89% , 0.0150
300x300_30(12)	43.71% , 0.0338	45.79% , 0.0289	47.68% , 0.0175	48.44% , 0.0164	49.04% , 0.0125
300x300_30(18)	48.67% , 0.0206	51.12% , 0.0130	54.09% , 0.0359	55.25% , 0.0417	56.38% , 0.0271
300x300_30(24)	56.82% , 0.0402	60.25% , 0.0241	62.50% , 0.0206	63.56% , 0.0135	64.47% , 0.0156
300x300_60(6)	33.80% , 0.0217	35.10% , 0.0133	36.81% , 0.0103	37.57% , 0.0104	37.99% , 0.0131
300x300_60(12)	54.37% , 0.0156	56.14% , 0.0167	57.33% , 0.0130	57.97% , 0.0095	58.54% , 0.0050
300x300_60(18)	62.37% , 0.0079	63.81% , 0.0046	65.78% , 0.0077	66.70% , 0.0089	67.36% , 0.0083
300x300_60(24)	66.15% , 0.0106	67.92% , 0.0063	70.01% , 0.0096	71.17% , 0.0085	71.72% , 0.0091

	MOEA/D($\overline{Hyp}\,\%, IQR$)				
	Evaluations (Stop condition)				
Instance($\bar{s}_r$)	**50 000**	**100 000**	**200 000**	**300 000**	**400 000**
50x50_30(1)	67.07% , 0.0000	67.07% , 0.0000	67.07% , 0.0000	67.07% , 0.0000	67.07% , 0.0000
50x50_60(1)	67.07% , 0.0000	67.07% , 0.0000	67.07% , 0.0000	67.07% , 0.0000	67.07% , 0.0000
100x100_30(2)	44.22% , 0.0001	44.25% , 0.0003	44.32% , 0.0018	44.34% , 0.0019	44.35% , 0.0023
100x100_30(3)	58.30% , 0.0011	58.39% , 0.0007	58.41% , 0.0003	58.43% , 0.0002	58.43% , 0.0002
100x100_60(2)	33.33% , 0.0150	33.61% , 0.0138	33.76% , 0.0123	33.92% , 0.0110	34.04% , 0.0049
100x100_60(3)	57.79% , 0.0169	58.09% , 0.0182	58.40% , 0.0146	58.65% , 0.0153	58.81% , 0.0153
200x200_30(2)	37.25% , 0.0228	37.57% , 0.0216	37.86% , 0.0292	37.97% , 0.0319	38.25% , 0.0329
200x200_30(4)	48.08% , 0.0804	48.71% , 0.0793	49.68% , 0.0631	50.01% , 0.0557	50.63% , 0.0453
200x200_30(6)	60.91% , 0.0421	63.55% , 0.0299	63.35% , 0.0305	63.57% , 0.0347	63.98% , 0.0342
200x200_30(9)	74.45% , 0.0388	75.41% , 0.0266	76.25% , 0.0336	76.56% , 0.0347	76.78% , 0.0281
200x200_60(2)	23.82% , 0.0060	23.98% , 0.0063	24.11% , 0.0074	24.17% , 0.0084	24.18% , 0.0084
200x200_60(4)	57.01% , 0.0314	57.68% , 0.0296	58.15% , 0.0291	58.32% , 0.0313	58.42% , 0.0313
200x200_60(6)	70.97% , 0.0207	71.72% , 0.0187	72.19% , 0.0183	72.50% , 0.0222	72.83% , 0.0231
200x200_60(9)	84.15% , 0.0233	84.71% , 0.0229	85.28% , 0.0204	85.58% , 0.0220	85.74% , 0.0219
300x300_30(6)	37.78% , 0.0162	38.41% , 0.0142	38.95% , 0.0138	39.21% , 0.0152	39.41% , 0.0155
300x300_30(12)	46.02% , 0.0313	46.68% , 0.0417	47.38% , 0.0370	47.84% , 0.0397	48.04% , 0.0380
300x300_30(18)	53.29% , 0.0233	54.00% , 0.0299	54.65% , 0.0291	55.09% , 0.0296	55.30% , 0.0352
300x300_30(24)	58.03% , 0.0289	59.22% , 0.0322	60.05% , 0.0363	60.44% , 0.0313	60.70% , 0.0315
300x300_60(6)	36.51% , 0.0171	36.86% , 0.0161	37.40% , 0.0137	37.56% , 0.0154	37.65% , 0.0151
300x300_60(12)	55.13% , 0.0206	56.01% , 0.0151	56.61% , 0.0119	56.80% , 0.0119	56.96% , 0.0119
300x300_60(18)	62.97% , 0.0086	63.60% , 0.0099	64.27% , 0.0118	64.56% , 0.0143	64.77% , 0.0164
300x300_60(24)	67.65% , 0.0141	68.27% , 0.0140	68.79% , 0.0119	69.11% , 0.0145	69.31% , 0.0135

Table 4.8: Algorithms providing the best significant performance for each test case and stop condition, based on the hypervolume metric and the Wilcoxon-Mann-Whitney's test.

Instance($\bar{s}_r$)	Evaluations (Stop condition) 50 000	100 000	200 000	300 000	400 000
50x50_30(1)	MO-ABC,MO-FA, MOEAD,MO-ABC	MO-ABC,MO-FA, MOEAD,MO-ABC	MO-ABC,MO-FA, MOEAD,MO-ABC	MO-ABC,MO-FA, MOEAD,MO-ABC	MO-ABC,MO-FA, MOEAD,MO-ABC
50x50_60(1)	MO-ABC,MO-FA MOEAD,MO-ABC	MO-ABC,MO-FA MOEAD,MO-ABC	MO-ABC,MO-FA MOEAD,MO-ABC	MO-ABC,MO-FA MOEAD,MO-ABC	MO-ABC,MO-FA MOEAD,MO-ABC
100x100_30(2)	MO-FA	MO-FA,VNS	MO-FA	MO-FA	MO-FA
100x100_30(3)	MO-FA	MO-FA,VNS	MO-FA,VNS	MO-FA,VNS	VNS
100x100_60(2)	VNS	VNS	VNS	VNS	VNS
100x100_60(3)	MO-ABC,MO-FA, VNS*,VNS	VNS	VNS*,VNS	VNS*,VNS	VNS*,VNS
200x200_30(2)	MO-FA,VNS	MO-FA,VNS	MO-FA	MO-FA,VNS	MO-FA,VNS
200x200_30(4)	VNS	VNS	VNS	VNS	VNS
200x200_30(6)	MO-FA,VNS*	MO-FA,VNS*	MO-FA,VNS*	MO-ABC,MO-FA, VNS*	MO-ABC,MO-FA, VNS*
200x200_30(9)	MO-FA	MO-FA	MO-FA	MO-FA	MO-FA
200x200_60(2)	MO-ABC	MO-ABC	MO-ABC,VNS	MO-ABC,MO-FA, VNS	MO-ABC,MO-FA, VNS,VNS*
200x200_60(4)	VNS*	MO-ABC,VNS*	MO-ABC	MO-ABC	MO-ABC
200x200_60(6)	VNS*	VNS*	VNS*	MO-ABC,VNS*	MO-ABC
200x200_60(9)	MO-FA	MO-FA	MO-FA,VNS*	MO-FA,VNS*	MO-ABC
300x300_30(6)	MO-FA,VNS*	MO-ABC,MO-FA VNS*	MO-ABC,VNS*	MO-ABC,VNS*	MO-ABC,VNS*
300x300_30(12)	MO-FA	MO-FA	MO-FA	MO-ABC,MO-FA	MO-ABC,MO-FA
300x300_30(18)	MO-FA	MO-FA	MO-FA	MO-FA	MO-FA
300x300_30(24)	MO-FA	MO-FA	MO-FA	MO-FA	MO-FA
300x300_60(6)	MO-FA	MO-FA	MO-FA	MO-ABC,MO-FA	MO-ABC
300x300_60(12)	MO-FA	MO-FA	MO-FA	MO-FA	MO-FA
300x300_60(18)	MO-FA	MO-FA	MO-FA	MO-FA	MO-GSA,MO-FA
300x300_60(24)	MO-FA	MO-FA	MO-FA	MO-FA	MO-GSA,MO-FA

MO-VNS* is better for solving larger ones. The difference between them is the perturbation mechanism. In small instances, the perturbation mechanism penalises the exploitation of the search space, because of it consumes many evaluations if it is performed. On the other hand, in general, the optimisation of larger instances need further exploration of the search space, this is the reason why MO-VNS* provides better behaviour in such cases.

4.7.3 Convergence Study Based on the Hypervolume Metric

Tables 4.8, 4.9, and 4.10 show a converge study based on the hypervolume metric. We notice that most of the algorithms show an homogeneous growth over stop conditions and an asymptotic trend when 400 000 evaluations are reached. This means that the set of stop criteria is representative to analyse the behaviour of the algorithms, because we do not expect large improvements by assuming more evaluations.

MO-GSA is the only algorithm having an uneven trend, e.g. in 100x100_30(3), 200x200_30(6). Perhaps, this is due to the way of working of the algorithm: if it finds a good solution, it is able to generate many solutions in its surrounding by moving the other planets. However, it is not really good at generating new solutions (fresh solutions), the main way is through the anti-stagnation mechanism. Thus, it falls in local minima many times, penalising its performance.

Through this convergence analysis, we notice that the best algorithm according to the hypervolume metric, i.e. MO-FA, it shows an homogeneous growth. Hence, it could be considered irrespective of the stop criterion. This behaviour is similar for MO-VNS with small instances.

Table 4.9: Based on the hypervolume metric, percentage of test cases in which the metaheuristics are significant better and worse, for all the test cases, 50x50 instances, 100x100 instances, 200x200 instances, and 300x300 instances.

A is worse than B (all the instances)

A is better than B

A \ B	NSGA-II	SPEA2	MO-VNS	MO-VNS*	MO-ABC	MO-FA	MO-GSA	MOEA/D	Percentage
NSGA-II	0,00%	0,79%	0,37%	0,10%	0,12%	0,00%	0,14%	0,66%	2,17%
SPEA2	0,74%	0,00%	0,43%	0,19%	0,27%	0,00%	0,31%	0,58%	2,52%
MO-VNS	1,59%	1,43%	0,00%	0,62%	0,68%	0,37%	1,28%	1,20%	7,16%
MO-VNS*	1,82%	1,68%	1,01%	0,00%	0,72%	0,39%	1,37%	1,41%	8,40%
MO-ABC	1,84%	1,82%	1,12%	0,93%	0,00%	0,45%	1,28%	1,45%	8,88%
MO-FA	2,11%	2,07%	1,24%	1,30%	1,12%	0,00%	1,76%	1,90%	11,49%
MO-GSA	1,59%	1,51%	0,68%	0,48%	0,31%	0,00%	0,00%	1,01%	5,57%
MOEA/D	1,20%	1,04%	0,58%	0,39%	0,23%	0,00%	0,37%	0,00%	3,81%
Percentage	10,87%	10,35%	5,42%	4,01%	3,44%	1,20%	6,50%	8,20%	100,00%

A is worse than B (50x50 instances)

A is better than B

A \ B	NSGA-II	SPEA2	MO-VNS	MO-VNS*	MO-ABC	MO-FA	MO-GSA	MOEA/D	Percentage
NSGA-II	0,00%	0,00%	0,00%	0,00%	0,00%	0,00%	0,00%	0,00%	0,00%
SPEA2	0,00%	0,00%	0,00%	0,00%	0,00%	0,00%	0,00%	0,00%	0,00%
MO-VNS	2,43%	2,43%	0,00%	1,46%	0,00%	0,00%	0,00%	0,00%	6,31%
MO-VNS*	2,43%	2,43%	0,00%	0,00%	0,00%	0,00%	0,00%	0,00%	4,85%
MO-ABC	2,43%	2,43%	2,43%	2,43%	0,00%	0,00%	0,00%	0,00%	9,71%
MO-FA	2,43%	2,43%	2,43%	2,43%	0,00%	0,00%	0,00%	0,00%	9,71%
MO-GSA	2,43%	2,43%	2,43%	2,43%	0,00%	0,00%	0,00%	0,00%	9,71%
MOEA/D	2,43%	2,43%	2,43%	2,43%	0,00%	0,00%	0,00%	0,00%	9,71%
Percentage	14,56%	14,56%	9,71%	11,17%	0,00%	0,00%	0,00%	0,00%	100,00

A is worse than B (100x100 instances)

A is better than B

A \ B	NSGA-II	SPEA2	MO-VNS	MO-VNS*	MO-ABC	MO-FA	MO-GSA	MOEA/D	Percentage
NSGA-II	0,00%	1,86%	0,00%	0,00%	0,00%	0,00%	0,00%	0,49%	2,35%
SPEA2	0,00%	0,00%	0,00%	0,00%	0,00%	0,00%	0,00%	0,29%	0,29%
MO-VNS	1,96%	1,96%	0,00%	1,27%	1,27%	0,98%	1,96%	1,96%	11,37%
MO-VNS*	1,76%	1,76%	0,00%	0,00%	0,88%	0,69%	1,67%	1,76%	8,53%
MO-ABC	1,96%	1,96%	0,29%	0,59%	0,00%	0,88%	1,76%	1,96%	9,41%
MO-FA	1,96%	1,96%	0,49%	0,98%	0,59%	0,00%	1,67%	1,86%	9,51%
MO-GSA	1,96%	1,96%	0,00%	0,00%	0,00%	0,00%	0,00%	1,08%	5,00%
MOEA/D	1,47%	1,47%	0,00%	0,00%	0,00%	0,00%	0,59%	0,00%	3,53%
Percentage	11,08%	12,94%	0,78%	2,84%	2,75%	2,55%	7,65%	9,41%	100,00%

A is worse than B (200x200 instances)

A is better than B

A \ B	NSGA-II	SPEA2	MO-VNS	MO-VNS*	MO-ABC	MO-FA	MO-GSA	MOEA/D	Percentage
NSGA-II	0,00%	1,17%	0,00%	0,00%	0,05%	0,00%	0,27%	0,96%	2,44%
SPEA2	0,53%	0,00%	0,00%	0,00%	0,00%	0,00%	0,00%	0,58%	1,11%
MO-VNS	1,91%	2,12%	0,00%	0,69%	0,96%	0,48%	1,91%	1,96%	10,03%
MO-VNS*	2,07%	2,07%	0,80%	0,00%	0,96%	0,53%	1,75%	1,86%	10,03%
MO-ABC	1,80%	2,12%	0,69%	0,48%	0,00%	0,53%	1,38%	1,54%	8,55%
MO-FA	2,12%	2,12%	0,69%	0,74%	1,11%	0,00%	1,91%	2,07%	10,77%
MO-GSA	1,38%	1,86%	0,00%	0,05%	0,16%	0,00%	0,00%	1,27%	4,72%
MOEA/D	1,01%	1,01%	0,00%	0,00%	0,16%	0,00%	0,16%	0,00%	2,34%
Percentage	10,83%	12,47%	2,18%	1,96%	3,40%	1,54%	7,38%	10,24%	100,00%

A is worse than B (300x300 instances)

A is better than B

A \ B	NSGA-II	SPEA2	MO-VNS	MO-VNS*	MO-ABC	MO-FA	MO-GSA	MOEA/D	Percentage
NSGA-II	0,00%	0,00%	1,03%	0,27%	0,27%	0,00%	0,11%	0,59%	2,27%
SPEA2	1,51%	0,00%	1,19%	0,54%	0,76%	0,00%	0,86%	0,86%	5,72%
MO-VNS	0,86%	0,22%	0,00%	0,00%	0,22%	0,00%	0,54%	0,27%	2,11%
MO-VNS*	1,46%	1,08%	2,00%	0,00%	0,54%	0,16%	1,13%	1,08%	7,45%
MO-ABC	1,67%	1,30%	1,73%	1,24%	0,00%	0,22%	1,19%	1,40%	8,75%
MO-FA	2,11%	2,00%	1,94%	1,78%	1,67%	0,00%	2,05%	2,16%	13,71%
MO-GSA	1,40%	0,70%	1,35%	0,76%	0,70%	0,00%	0,00%	0,92%	5,83%
MOEA/D	0,97%	0,54%	1,08%	0,54%	0,49%	0,00%	0,54%	0,00%	4,16%
Percentage	9,99%	5,83%	10,31%	5,13%	4,64%	0,38%	6,43%	7,29%	100,00%

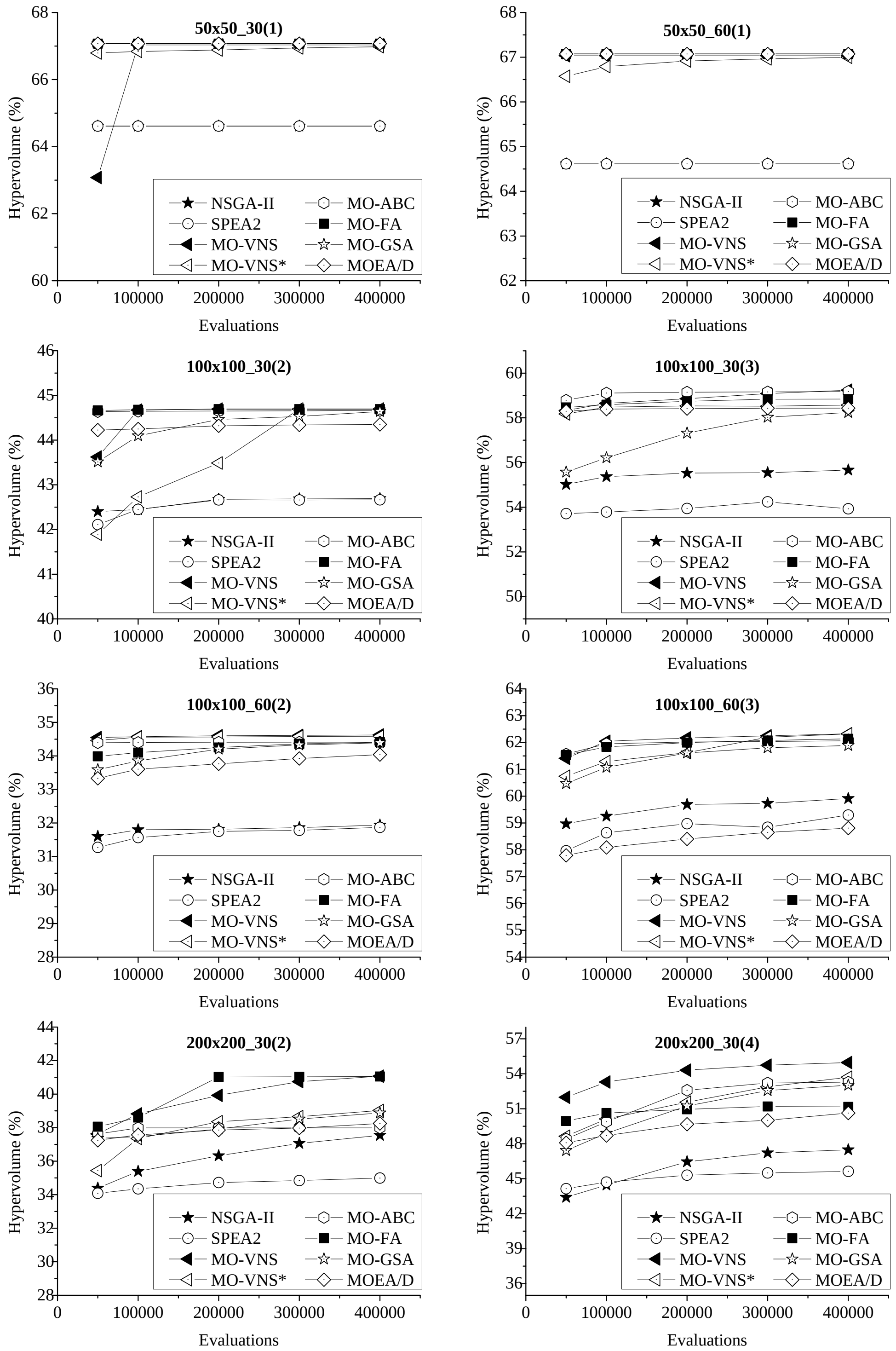

Figure 4.8: Convergence study based on the hypervolume metric. Part 1 of 3.

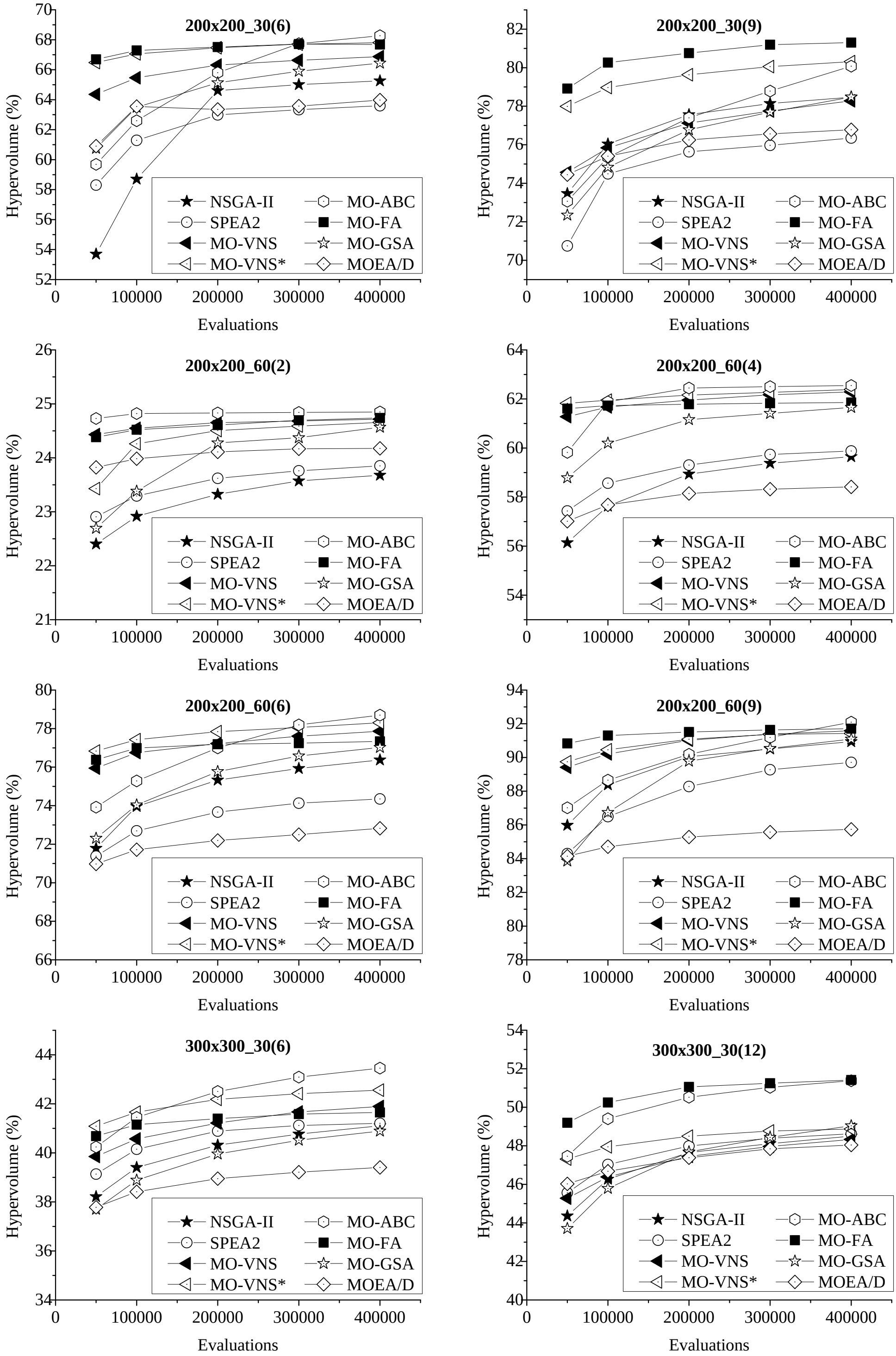

Figure 4.9: Convergence study based on the hypervolume metric. Part 2 of 3.

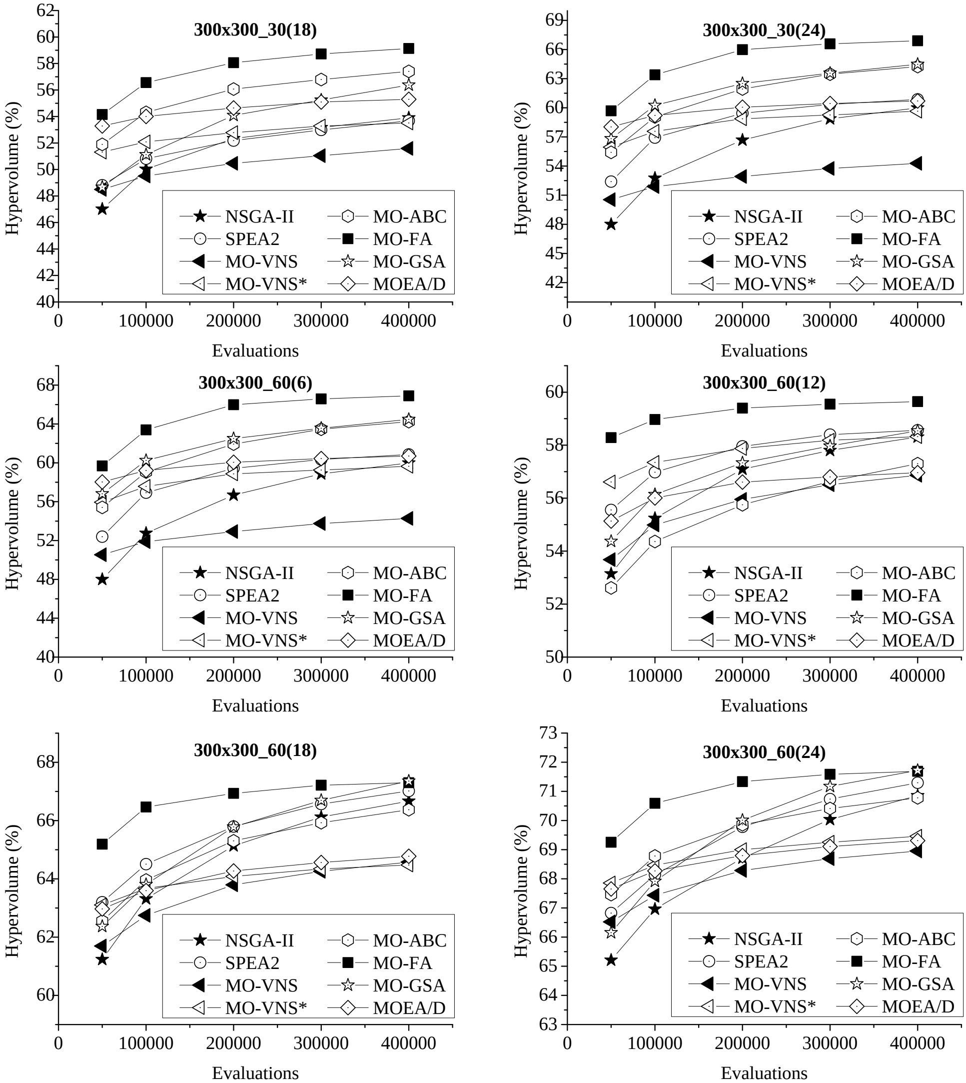

Figure 4.10: Convergence study based on the hypervolume metric. Part 3 of 3.

4.7.4 Set Coverage Analysis

In addition to hypervolume, in this study we include the set coverage metric as another MO quality indicator. Table 4.10 shows the set coverage metric comparing all the metaheuristics two by two for all the instances, 50x50 instances, 100x100 instances, 200x200 instances, and 300x300 instances. The Percentage field of this table shows the average set coverage regarding all other metaheuristics, where better average values are shaded from darker to lighter tone, i.e. from better to worse average behaviour.

The set coverage metric was calculated by assuming the median Pareto fronts from the distribution of 31 samples previously considered for hypervolume. Note that the values shown in Table 4.10 are the average set coverage for all the stop conditions, full values are in Section C.2 of Appendix B, specifically in Tables B.8, B.9, B.10, B.11, B.12, B.13, B.14, B.15, B.16, B.17, B.18, B.19, B.20, and B.21.

Analysing Table 4.10, we notice that MO-FA is the best algorithm for all the instances, followed by MO-VNS* and MO-ABC. For 50x50 instances, we reach that MO-ABC, MO-FA, and MO-GSA provides a same behaviour, followed by MOEA/D and MO-VNS. In case of 100x100 instances, MO-VNS is the best algorithm, followed by MO-VNS* and MO-FA. For 200x200 instances, MO-FA provides the best behaviour, followed by MO-VNS* and MO-VNS. Finally, for 300x300 instances, MO-FA is the best algorithm from far, followed by MO-VNS*.

Comparing both hypervolume and set converage analyses, we notice that the conclusions are similar. MO-FA is the algorithm providing the best average behaviour for all the instances. Attending to the instance size, MO-VNS is the best algorithm for small instances and MO-FA is the best for large instances.

4.7.5 Median Pareto Fronts and Attainment Surface

Figures 4.14, 4.15, 4.16 compare the median Pareto fronts obtained for 400 000 evaluations, by assuming the attainment surface representation. Through this methodology, we can observe in a clear way, which area of the objective space is considered for a given algorithm. Thus, we can see the differences in terms of performance for each test case and algorithm. We notice that the conclusions are the same as previously discussed for hypervolume and set coverage.

This representation is useful for graphically comparing several Pareto fronts. However, we cannot analyse the distribution of the points in the objective space nor the shape of the fronts. Figure 4.11, 4.12, and 4.13 show the median Pareto fronts obtained for 400 000 evaluations. We check that, in general, there are zones in the objective space, which are not covered by any algorithm. This means that maybe there are not solutions for this problem in this zone. On the contrary, we find fronts full of points, such as in 100x100_60(2). In this case, we notice that while MO-FA find many points, MOEA/D provides a non-continuous front.

4.7.6 Impact of the Optimisation on the Fitness Functions

In this subsection, we discuss the impact provided by the addition of RNs to traditional WSNs. Table 4.11 shows extreme values of the median Pareto front obtained by MO-FA for 400 000 evaluations. Each solution is associated with two quality metrics: I_G and I_{EF}. I_G denotes the percentage in which a fitness function is increased or decreased, regarding the use of a traditional WSN (see Section 4.3). On the other hand, I_{EF} measures the efficiency of the optimisation by dividing the gain obtained between the number of RNs assumed. According to this table, AEC is decreased up to 92.03% in 300x300_60(24), and ASA is increased up to 18.25% in 300x300_-30(24). Analysing this table, we note that as the number of RNs increases, the efficiency of the

Table 4.10: Set coverage metric among all the metaheuristics, for all the test cases, 50x50 instances, 100x100 instances, 200x200 instances, and 300x300 instances.

A dominates B (all the test cases)

A is dominated by B

A \ B	NSGA-II	SPEA2	MO-VNS	MO-VNS*	MO-ABC	MO-FA	MO-GSA	MOEA/D	Percentage
NSGA-II	#####	52,27%	25,07%	11,09%	15,82%	3,15%	21,95%	35,39%	23,54%
SPEA2	56,25%	######	28,48%	16,82%	18,87%	3,64%	24,08%	37,79%	26,56%
MO-VNS	65,21%	56,53%	######	35,93%	48,62%	30,25%	64,46%	70,80%	53,12%
MO-VNS*	74,32%	72,32%	70,51%	######	59,23%	32,82%	66,75%	70,81%	63,82%
MO-ABC	73,96%	70,65%	54,04%	42,22%	######	31,88%	66,95%	72,73%	58,92%
MO-FA	90,82%	84,29%	77,30%	71,17%	72,64%	######	88,80%	85,30%	81,47%
MO-GSA	68,32%	59,64%	36,13%	23,07%	29,19%	16,50%	######	60,71%	41,94%
MOEA/D	39,86%	39,46%	28,89%	14,07%	20,32%	15,14%	32,73%	######	27,21%
Percentage	66,96%	62,17%	45,77%	30,63%	37,81%	19,05%	52,25%	61,93%	

A dominates B (50x50 test cases)

A is dominated by B

A \ B	NSGA-II	SPEA2	MO-VNS	MO-VNS*	MO-ABC	MO-FA	MO-GSA	MOEA/D	Percentage
NSGA-II	######	100,00%	20,00%	9,09%	11,11%	11,11%	11,11%	20,00%	26,06%
SPEA2	100,00%	######	20,00%	41,05%	11,11%	11,11%	11,11%	20,00%	30,63%
MO-VNS	88,89%	88,89%	######	83,52%	88,89%	88,89%	88,89%	90,00%	88,28%
MO-VNS*	52,22%	52,22%	48,00%	######	38,89%	38,89%	38,89%	43,33%	44,63%
MO-ABC	100,00%	100,00%	100,00%	100,00%	######	100,00%	100,00%	100,00%	100,00%
MO-FA	100,00%	100,00%	100,00%	100,00%	100,00%	######	100,00%	100,00%	100,00%
MO-GSA	100,00%	100,00%	100,00%	100,00%	100,00%	100,00%	######	100,00%	100,00%
MOEA/D	90,00%	90,00%	90,00%	90,00%	90,00%	90,00%	90,00%	######	90,00%
Percentage	90,16%	90,16%	68,29%	74,81%	62,86%	62,86%	62,86%	67,62% %	

A dominates B (100x100 test cases)

A is dominated by B

A \ B	NSGA-II	SPEA2	MO-VNS	MO-VNS*	MO-ABC	MO-FA	MO-GSA	MOEA/D	Percentage
NSGA-II	######	79,08%	0,78%	0,29%	2,35%	1,76%	6,85%	13,49%	14,94%
SPEA2	51,76%	######	0,65%	0,63%	1,46%	1,93%	3,68%	10,26%	10,05%
MO-VNS	88,72%	92,56%	######	78,86%	80,80%	83,12%	93,22%	95,65%	87,56%
MO-VNS*	88,30%	90,45%	76,25%	######	79,90%	76,17%	84,08%	86,61%	83,11%
MO-ABC	94,03%	95,11%	51,78%	59,47%	######	64,15%	81,78%	84,98%	75,90%
MO-FA	88,09%	87,75%	59,49%	62,93%	70,12%	######	78,78%	84,38%	75,93%
MO-GSA	83,97%	91,44%	14,05%	19,17%	33,34%	22,60%	######	53,61%	45,45%
MOEA/D	52,70%	63,75%	19,13%	21,44%	29,90%	21,77%	31,44%	######	34,30%
Percentage	78,22%	85,73%	31,73%	34,68%	42,55%	38,79%	54,26%	61,28%	

A dominates B (200x200 test cases)

A is dominated by B

A \ B	NSGA-II	SPEA2	MO-VNS	MO-VNS*	MO-ABC	MO-FA	MO-GSA	MOEA/D	Percentage
NSGA-II	######	53,40%	6,81%	5,18%	13,70%	2,04%	18,45%	40,03%	19,95%
SPEA2	42,04%	######	2,89%	3,00%	7,54%	1,92%	10,00%	36,92%	14,90%
MO-VNS	83,41%	82,90%	######	43,27%	64,12%	30,77%	77,79%	84,06%	66,62%
MO-VNS*	79,43%	83,90%	59,72%	######	61,65%	34,67%	78,77%	84,33%	68,92%
MO-ABC	83,39%	84,67%	31,04%	24,58%	######	17,94%	69,18%	72,64%	54,78%
MO-FA	90,42%	85,22%	63,53%	59,39%	70,00%	######	87,21%	86,85%	77,52%
MO-GSA	77,90%	69,42%	8,39%	12,51%	21,21%	6,08%	######	60,54%	36,58%
MOEA/D	40,70%	38,49%	5,60%	5,02%	13,87%	4,42%	20,53%	######	18,38%
Percentage	71,04%	71,14%	25,43%	21,85%	36,01%	13,98%	51,70%	66,48%	

A dominates B (300x300 test cases)

A is dominated by B

A \ B	NSGA-II	SPEA2	MO-VNS	MO-VNS*	MO-ABC	MO-FA	MO-GSA	MOEA/D	Percentage
NSGA-II	######	25,79%	56,74%	22,91%	25,85%	2,97%	35,71%	45,55%	30,79%
SPEA2	61,78%	######	70,11%	32,68%	40,84%	4,36%	51,61%	56,87%	45,46%
MO-VNS	35,27%	12,16%	######	7,14%	17,02%	3,29%	30,66%	40,31%	20,83%
MO-VNS*	62,21%	51,68%	84,05%	######	46,46%	9,29%	53,04%	56,26%	51,86%
MO-ABC	47,97%	37,06%	66,67%	36,78%	######	12,65%	49,04%	59,87%	44,29%
MO-FA	92,60%	81,63%	94,30%	87,07%	76,53%	######	92,60%	80,52%	86,47%
MO-GSA	50,92%	33,96%	58,93%	35,59%	35,09%	3,00%	######	54,61%	38,87%
MOEA/D	32,60%	28,29%	41,78%	19,44%	21,98%	3,82%	31,25%	######	25,59%
Percentage	54,76%	38,65%	67,51%	34,51%	37,68%	5,63%	49,13%	56,29%	

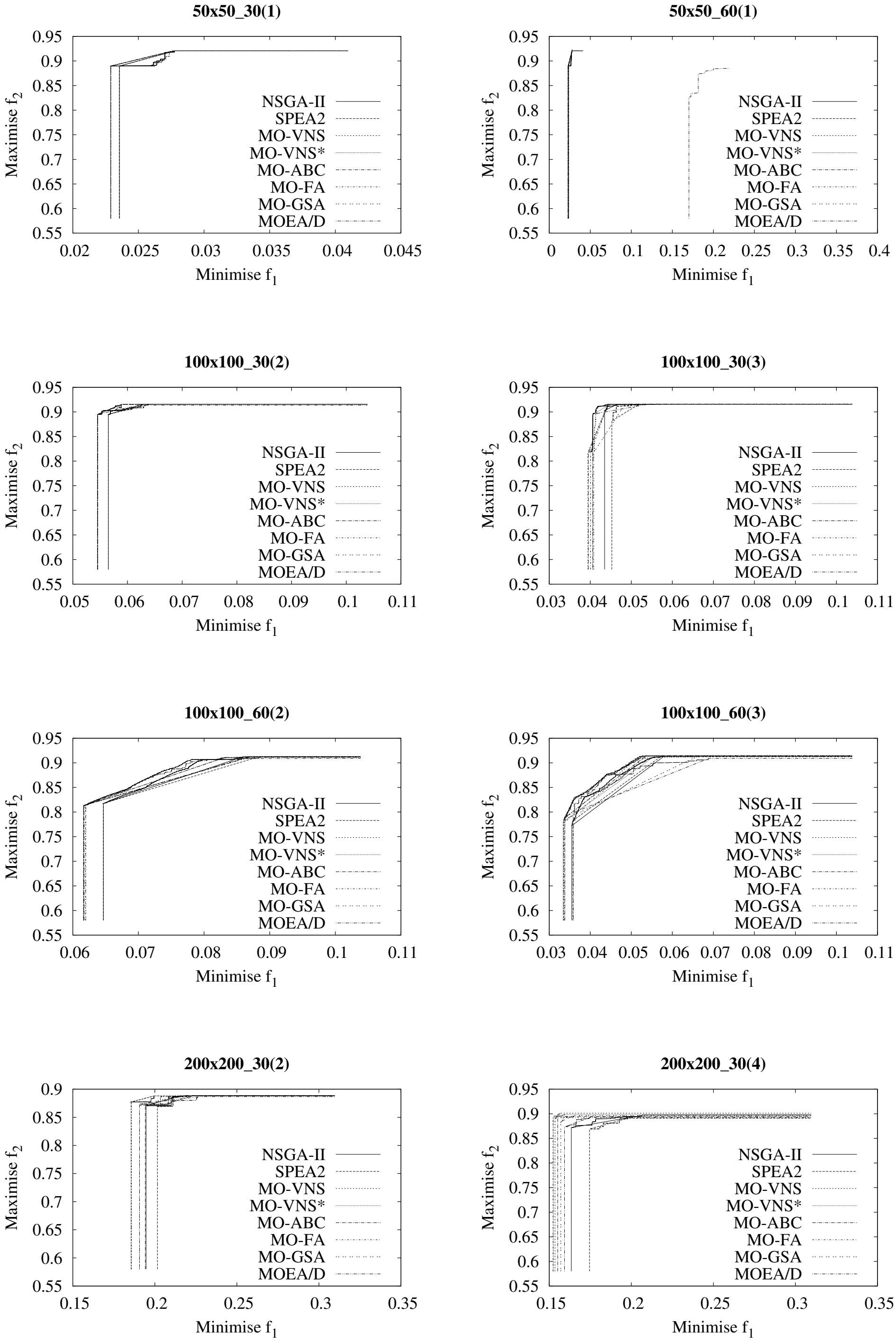

Figure 4.11: Comparing the metaheuristics through attainment surface. Part 1 of 3.

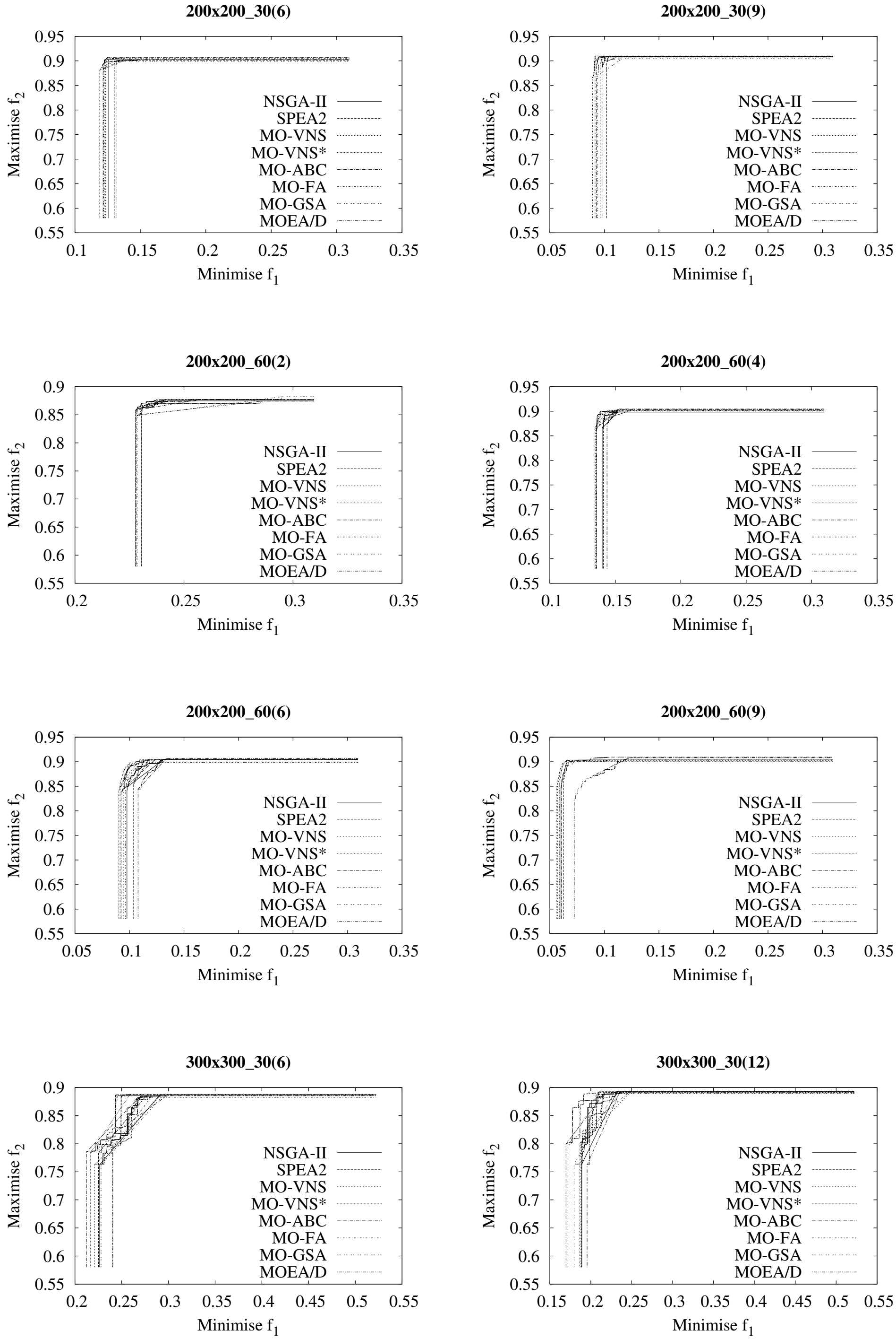

Figure 4.12: Comparing the metaheuristics through attainment surface. Part 2 of 3.

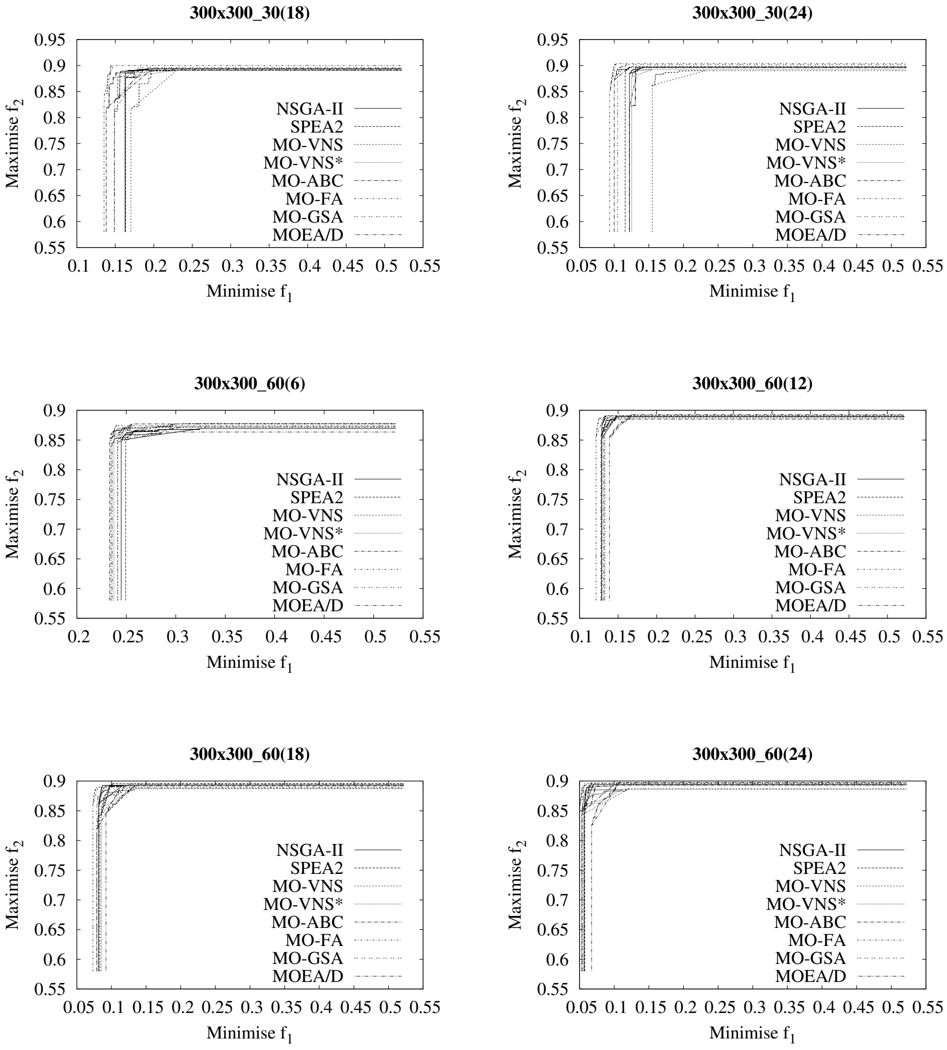

Figure 4.13: Comparing the metaheuristics through attainment surface. Part 3 of 3.

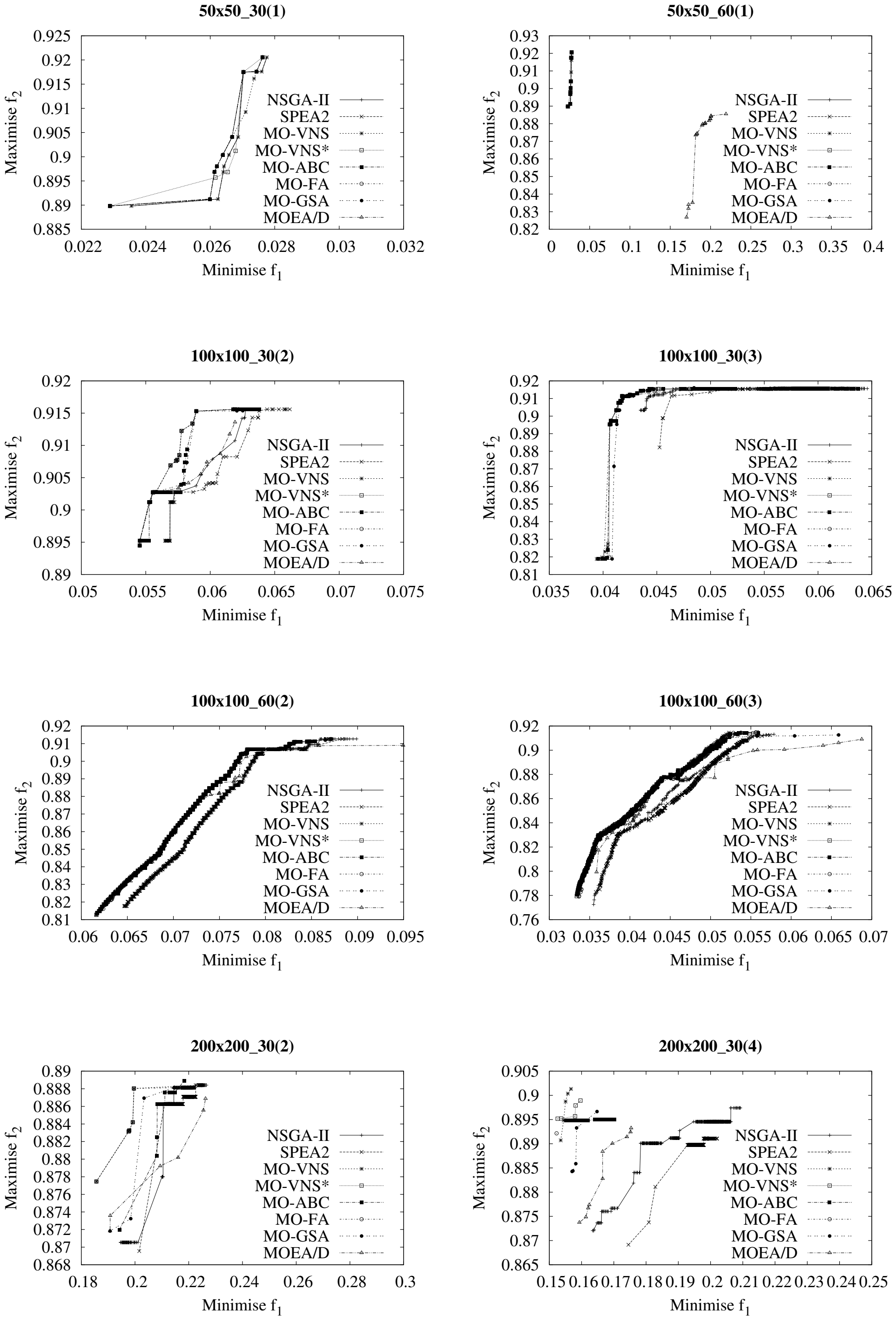

Figure 4.14: Comparing the metaheuristics through attainment surface. Part 1 of 3.

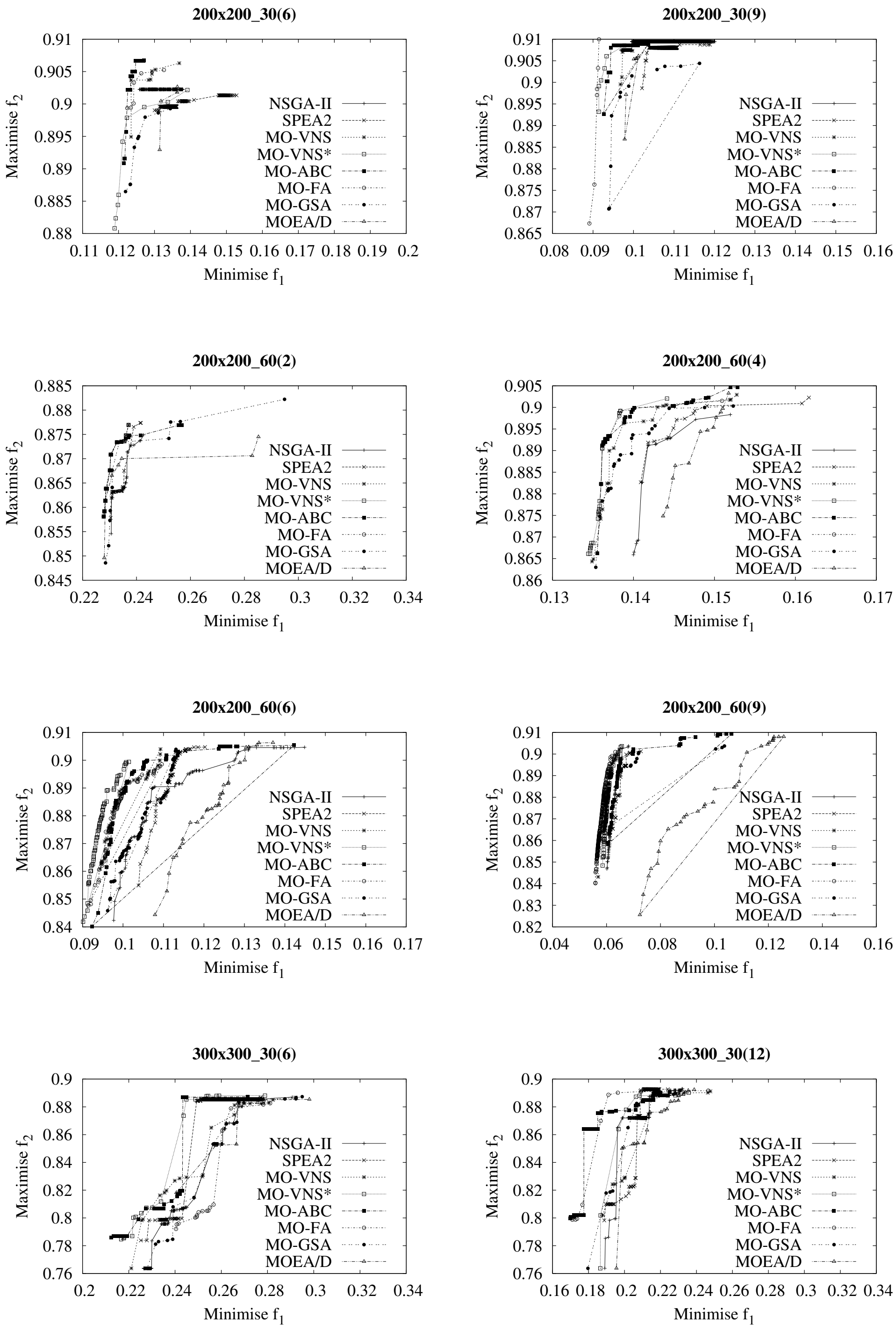

Figure 4.15: Comparing the metaheuristics through attainment surface. Part 2 of 3.

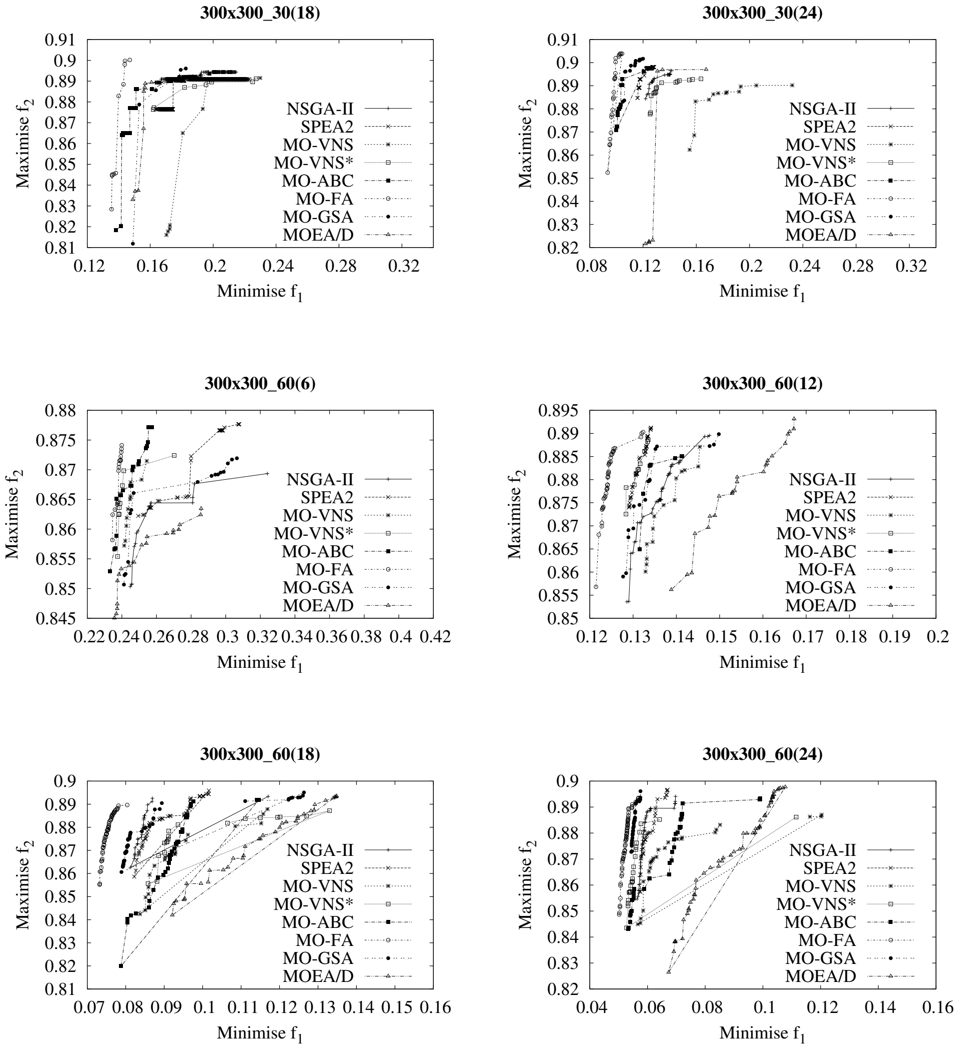

Figure 4.16: Comparing the metaheuristics through attainment surface. Part 3 of 3.

Table 4.11: Extreme values of the median Pareto fronts obtained by MO-FA for 400 000 evaluations, including efficiency and gain metrics.

	max(f_1 : AEC)		**min**(f_1 : AEC)		**max**(f_2 : ASA)		**min**(f_2 : ASA)	
Instance($\tilde{s}_r$)	**value**	I_G,I_{EF}	**value**	I_G,I_{EF}	**value**	I_G,I_{EF}	**value**	I_G,I_{EF}
50x50_30(1)	0,0229	-34,60%,**-34,60%**	0,0276	-21,08%,-21,08%	0,9205	0,33%,0,33%	0,8898	-3,02%,-3,02%
50x50_60(1)	0,0229	-34,60%,**-34,60%**	0,0276	-21,08%,-21,08%	0,9205	0,33%,0,33%	0,8898	-3,02%,-3,02%
100x100_30(2)	0,0545	-50,02%,-25,01%	0,0622	-42,99%,-21,49%	0,9156	2,60%,1,30%	0,8945	0,23%,0,12%
100x100_30(3)	0,0401	-63,25%,-21,08%	0,0622	-42,99%,-14,33%	0,9156	2,60%,0,87%	0,8195	-8,16%,-2,72%
100x100_60(2)	0,0619	-58,21%,-29,10%	0,0871	-41,23%,-20,61%	0,9126	5,35%,**2,67%**	0,8149	-5,94%,-2,97%
100x100_60(3)	0,0337	-77,28%,-25,76%	0,0556	-62,49%,-20,83%	0,9145	5,57%,1,86%	0,7790	-10,07%,-3,36%
200x200_30(2)	0,1856	-33,49%,-16,75%	0,2146	-23,10%,-11,55%	0,8881	1,97%,0,98%	0,8775	0,74%,0,37%
200x200_30(4)	0,1522	-45,45%,-11,36%	0,1522	-45,45%,-11,36%	0,8922	2,43%,0,61%	0,8922	2,43%,0,61%
200x200_30(6)	0,1224	-56,13%,-9,35%	0,1326	-52,48%,-8,75%	0,9052	3,93%,0,66%	0,8994	3,26%,0,54%
200x200_30(9)	0,0891	-68,08%,-7,56%	0,0915	-67,23%,-7,47%	0,9100	4,47%,0,50%	0,8673	-0,42%,-0,05%
200x200_60(2)	0,2279	-41,14%,-20,57%	0,2371	-38,76%,-19,38%	0,8769	6,39%,3,19%	0,8581	4,10%,2,05%
200x200_60(4)	0,1358	-64,92%,-16,23%	0,1509	-61,01%,-15,25%	0,9015	9,37%,2,34%	0,8752	6,18%,1,54%
200x200_60(6)	0,0914	-76,39%,-12,73%	0,1096	-71,69%,-11,95%	0,8985	9,01%,1,50%	0,8477	2,84%,0,47%
200x200_60(9)	0,0559	-85,57%,-9,51%	0,0632	-83,66%,-9,30%	0,9010	9,30%,1,03%	0,8402	1,93%,0,21%
300x300_30(6)	0,2404	-43,09%,-7,18%	0,2811	-33,46%,-5,58%	0,8826	15,46%,2,58%	0,7921	3,62%,0,60%
300x300_30(12)	0,1710	-59,53%,-4,96%	0,2466	-41,64%,-3,47%	0,8917	16,65%,1,39%	0,7987	4,49%,0,37%
300x300_30(18)	0,1354	-67,95%,-3,77%	0,1470	-65,20%,-3,62%	0,9002	17,76%,0,99%	0,8284	8,38%,0,47%
300x300_30(24)	0,0934	-77,89%,-3,25%	0,1042	-75,33%,-3,14%	0,9039	**18,25%**,0,76%	0,8524	11,52%,0,48%
300x300_60(6)	0,2345	-62,75%,-10,46%	0,2399	-61,89%,-10,31%	0,8741	7,62%,1,27%	0,8582	5,66%,0,94%
300x300_60(12)	0,1214	-80,71%,-6,73%	0,1323	-78,98%,-6,58%	0,8903	9,61%,0,80%	0,8568	5,49%,0,46%
300x300_60(18)	0,0732	-88,37%,-4,91%	0,0804	-87,23%,-4,85%	0,8896	9,54%,0,53%	0,8551	5,29%,0,29%
300x300_60(24)	0,0502	**-92,03%**,-3,83%	0,0569	-90,96%,-3,79%	0,8935	10,01%,0,42%	0,8487	4,49%,0,19%

optimisation decreases. This way, the maximum efficiency for AEC is 34.60% in both 50x50_-30(1) and 50x50_60(1). For ASA, the maximum efficiency is 2.62% in 100x100_60(2).

In summary, the addition of RNs seems to be a good way to optimise traditional WSNs. However, the efficiency of this approach could be reduced if many RNs are considered.

4.7.7 Comparisons to Other Approaches

We started this work assuming an important limitation: we did not find any paper fitting this problem definition. Hence, we cannot directly compare the results obtained to other author approaches. To alleviate this fact, we selected a paper from the current literature considering a similar approach: Hou et al [6] implemented a heuristic called SPINDS, which optimises the network lifetime by adding routers to TT-WSNs.

The network model assumed by Hou et al. is composed of several clusters and a Base Station (BS). Each cluster consists of a set of MicroSensor Nodes (MSNs) and one Aggregation and Forwarding Node (AFN). MSNs capture and send information via single-hop transmission to the local AFN. Each AFN relays all the received information to the BS via multi-hop routing. Finally, the RNs are additional devices, forwarding all the information received from AFNs to the BS. In this model, all the devices are powered by batteries, excepting the BS. In addition, each device can assume a different initial energy charge.

As both network models are different, we assume some assumptions to adapt this model to our problem definition:

- We consider that a cluster is a sensor node. This way, MSNs are not included and AFNs are the new sensors.
- In the original model, the amount of information relayed by an AFN is given by the number of MSNs in its cluster. Now, we assume that all the AFNs send an information packet of size k per time unit.

Table 4.12: Solutions obtained by SPINDS heuristic, including efficiency and gain metrics.

	$f_1 : AEC$			$f_2 : ASA$		
Instance($\tilde{s}_r$)	**value**	I_G	I_{EF}	**value**	I_G	I_{EF}
50x50_30(1)	0,0247	-29,29%	**-29,29%**	0,8898	-3,02%	-3,02%
50x50_60(1)	0,0247	-29,29%	**-29,29%**	0,8898	-3,02%	-3,02%
100x100_30(2)	0,0610	-44,11%	-22,06%	0,8946	0,25%	0,12%
100x100_30(3)	0,0534	-51,06%	-17,02%	0,8880	-0,49%	-0,16%
100x100_60(2)	0,0642	-56,65%	-28,32%	0,8209	-5,24%	-2,62%
100x100_60(3)	0,0492	**-66,81%**	-22,27%	0,8316	-4,00%	-1,33%
200x200_30(2)	0,2655	-4,89%	-2,44%	0,8645	-0,75%	-0,37%
200x200_30(4)	0,1851	-33,69%	-8,42%	0,8622	-1,01%	-0,25%
200x200_30(6)	0,1653	-40,77%	-6,80%	0,8568	-1,63%	-0,27%
200x200_30(9)	0,1171	-58,05%	-6,45%	0,8615	-1,09%	-0,12%
200x200_60(2)	0,2545	-34,24%	-17,12%	0,8333	1,09%	0,54%
200x200_60(4)	0,1598	-58,72%	-14,68%	0,8675	**5,24%**	**1,31%**
200x200_60(6)	0,1108	-71,37%	-11,90%	0,8488	2,97%	0,49%
200x200_60(9)	0,0716	-81,51%	-9,06%	0,8204	-0,48%	-0,05%
300x300_30(6)	0,3853	-8,80%	-1,47%	0,8038	5,16%	0,86%
300x300_30(12)	0,3853	-8,80%	-0,73%	0,8038	5,16%	0,43%
300x300_30(18)	0,3301	-21,86%	-1,21%	0,7804	2,10%	0,12%
300x300_30(24)	0,3301	-21,86%	-0,91%	0,7804	2,10%	0,09%
300x300_60(6)	0,5765	-8,42%	-1,40%	0,8031	-1,12%	-0,19%
300x300_60(12)	0,5765	-8,42%	-0,70%	0,8031	-1,12%	-0,09%
300x300_60(18)	0,5765	-8,42%	-0,47%	0,8031	-1,12%	-0,06%
300x300_60(24)	0,5765	-8,42%	-0,35%	0,8031	-1,12%	-0,05%

- All the AFNs have a same initial energy charge in their batteries. Having RNs and BS an unlimited power supply.
- We assume the energy model described in our work.

We implemented the SPINDS algorithm following these assumptions. The results obtained optimising our data set appear in Table 4.12, where the value of the fitness functions have associated both I_G and I_{EF} metrics previously defined in Section 4.7.6. Comparing Tables 4.11 and 4.12, we note that MO-FA provides a better behaviour for all the test cases. In fact, all the results provided by SPINDS are dominated by MO-FA. In addition, we check that SPINDS does not provide a good behaviour for large instances.

4.8 Scientific Achievements

In this chapter, we proposed and solved a bi-objetive RNPP by considering a wide range of MO metaheuristics. The following scientific achievements were obtained from performing this task:

International journals (ISI-SCI):

- Jose M. Lanza-Gutierrez and Juan A. Gomez-Pulido. A gravitational search algorithm for solving the relay node placement problem in wireless sensor networks. *International Journal of Communication Systems*, page n/a (on-line), 2015. Impact factor of 1.106 ($Q3$, $T2$). In [70], we apply NSGA-II, SPEA2, and MO-GSA for optimising 100x100 and 200x200 instances.
- Jose M. Lanza-Gutierrez and Juan A. Gomez-Pulido. Studying the multiobjective variable neighbourhood search algorithm when solving the relay node placement problem in wireless sensor networks. Soft Computing, page n/a (on-line), 2015.

Impact factor of 1.271 ($Q3$, $T2$). In [71], we apply NSGA-II, SPEA2, MO-VNS, and MO-VNS* for optimising all the instances.

- Jose M Lanza-Gutierrez, Juan A Gomez-Pulido, and Miguel A Vega-Rodriguez. Intelligent relay node placement in heterogeneous wireless sensor networks for energy efficiency. *International Journal of Robotics and Automation*, 29:1–13, 2014. Impact factor of 0.408 ($Q4$, $T3$). In [72], we apply NSGA-II, SPEA2, and MO-ABC for optimising 100x100, 200x200, and 300x300 instances.

International book chapters:

- Jose M. Lanza-Gutierrez, Juan A. Gomez-Pulido, and Miguel A. Vega-Rodriguez. A trajectory algorithm to solve the relay node placement problem in wireless sensor networks. In *Theory and Practice of Natural Computing*, volume 8273 of *Lecture Notes in Computer Science*, pages 145–156. Springer Berlin Heidelberg, 2013. In [73], we apply NSGA-II, SPEA2, and MO-VNS* for optimising 100x100, 200x200, and 300x300 instances.
- Jose M. Lanza-Gutierrez, Juan A. Gomez-Pulido, Miguel A. Vega-Rodriguez, and Juan M. Sanchez-Perez. Relay node positioning in wireless sensor networks by means of evolutionary techniques. In *Autonomous and Intelligent Systems*, volume 7326 of *Lecture Notes in Computer Science*, pages 18–25. Springer Berlin / Heidelberg, 2012. In [74], we apply NSGA-II and SPEA2 for optimising 100x100 and 200x200 instances. This is our first work exactly fitting this problem approach.
- Jose M. Lanza-Gutierrez, Juan A. Gomez-Pulido, Miguel A. Vega-Rodriguez, and Juan M. Sanchez-Perez. Optimizing energy consumption in heterogeneous wireless sensor networks by means of evolutionary algorithms. In *Applications of Evolutionary Computation*, volume 7248 of *Lecture Notes in Computer Science*, pages 1–10. Springer Berlin Heidelberg, 2012. In [75], we apply NSGA-II and SPEA2 for optimising 100x100 and 200x200 instances with 50 000 evaluations. In this contribution, we do not assume that the number of RNs should be significantly lower than the number of sensors. This paper can be considered as a very preliminary approach of the work in [74].

International conferences:

- Jose M. Lanza-Gutierrez, Juan A. Gomez-Pulido, Miguel A. Vega-Rodriguez, and Juan M. Sanchez- Perez. A parallel evolutionary approach to solve the relay node placement problem in wireless sensor networks. In *Proceeding of GECCO*, pages 1157–1164, 2013. ACM conference. In [76], we apply NSGA-II and SPEA2 for solving the problem with 100x100 and 200x200 instances by OpenMP with 32 cores.
- Jose M Lanza-Gutierrez, Juan Gomez-Pulido, Miguel Vega-Rodriguez, Juan M Sanchez -Perez. Multi-objective evolutionary algorithms for energy-efficiency in heterogeneous wireless sensor networks. IEEE conference. In *IEEE Sensors Applications Symposium (SAS)*, pages 1–6, 2012. In [77], we apply NSGA-II and SPEA2 for solving a less realistic approach of work presented in this chapter. This contribution can be considered as one of our first steps in this research line and is a continuation of the work in [78].

National conferences:

- Jose M. Lanza-Gutierrez, Juan A. Gomez-Pulido, Miguel A. Vega-Rodriguez, and Juan M. Sanchez-Perez. Optimizando la eficiencia energética en redes de sensores inalámbricos mediante computación evolutiva paralela. In *Actas de las XXIII Jornadas de Paralelismo (JP 2012), Servicio de Publicaciones. Universidad Miguel Hernández*, pages 163–168, 2012. In [79], we apply NSGA-II, SPEA2 for optimising 100x100 and 200x200 instances through OpenMP with 8 cores.
- Jose M. Lanza-Gutierrez, Juan A. Gomez-Pulido, Miguel A. Vega-Rodriguez, and Juan M. Sanchez-Perez. Posicionando routers en redes de sensores inalámbricos mediante algoritmos evolutivos para el incremento de la eficiencia energética. In *Actas de las III Jornadas de Computación Empotrada (JCE 2012), Servicio de Publicaciones. Univ. Miguel Hernandez*, pages 95–100, 2012. In [80], we apply NSGA-II and SPEA2 for optimising 100x100 and 200x200 instances with 50 000 evaluations. This is a very preliminary work before [74].
- Jose M Lanza-Gutierrez, Juan A Gomez-Pulido, Oscar Gutierrez-Blanco, Miguel A Vega- Rodriguez, and Juan M Sanchez. Diseño eficiente de redes heterogéneas de sensores inalámbricos mediante computación evolutiva multi-objetivo. In *Actas del VIII Congreso Español sobre Metaheurísticas, Algoritmos Evolutivos y Bioinspirados, Universidad de Castilla-La Mancha*, pages 337–344, 2012. In [78], we apply NSGA-II and SPEA2 for solving a less realistic approach of work performed in this chapter. This contribution can be considered as one of our first steps in this line.

CHAPTER

5

Solving the RNPP: three-objective Outdoor Approach

In this chapter, we define and solve the three-objective RNPP outdoor approach. This new three-objective approach is based on the work performed for two objectives in Chapter 4. Thus, chromosome definition and considerations for implementing the metaheuristics are the same as discussed before in Sections 4.5 and 4.6, respectively. This chapter is structured as follows. The WSN model considered in this work is presented in Section 5.1. The optimisation problem is defined in Section5.2. The data set considered for comparing the metaheuristics, while solving the problem is discussed in Section 5.3. Experimental results are presented in Section 5.4. Finally, scientific achievements from solving the problem are included in Section 5.5.

5.1 The Wireless Sensor Network Model assumed

This section describes the WSN model considered in the three-objective unconstrained RNPP outdoor approach. This model is based on the one described before in Section 4.1. This section is structured as follows. Section 5.1.1 presents additional notation and Section 5.1.2 discuss the concept of NR, related to the third objective of the RNPP.

5.1.1 Notation

The following notation is considered for modelling the WSN definition:

α	path loss exponent, $\alpha \in [2, 4]$;
β	transmission quality parameter, $\beta > 0$;
τ	set of time periods, $\tau = \{0, 1, 2, \ldots\}$;

$A(t)$	sensitivity area provided by the WSN at time $t > 0 \in \tau$;
$a_p(t)$	variable assuming 1 if there is at least one sensor $i \in S_s(t)$ at a distance to the demand point $p \in \tilde{D}_p(t)$ lower than r_s;
amp	energy cost per bit of the power amplifier, $amp > 0$;
c	sink coordinates, $c = (x, y)$ where $x \in [0, d_x]$ and $y \in [0, d_y]$;
co_{th}	coverage threshold, $co_{th} \in [0, 1]$;
$\tilde{D}_p(t)$	set of demand points at time $t > 0$, $\forall p \in \tilde{D}_p,\ p = (x, y)$ where $x \in [0, d_x]$ and $y \in [0, d_y]$;
$\tilde{d}_p(t)$	number of demand points. It is the cardinal of $\tilde{D}_p(t)$;
d_{pn}	distance between two neighbouring demand points;
djp_i^c	number of disjoint paths between the sensor $i \in \tilde{S}_s$ and the sink node;
d_x	width of the surface, $d_x > 0$;
d_y	height of the surface, $d_y > 0$;
$Ec_i(t)$	energy charge of a sensor $i \in S_s(t)$ at time t;
$Ee_i(t)$	energy expenditure of a sensor $i \in S_s(t)$ at time $t > 0$;
err	local channel error, $err \in [0, 1]$;
f_1	AEC of the sensors over the network lifetime;
f_2	ASA provided by the WSN over the network lifetime;
f_3	NR provided by the WSN at the beginning of the network lifetime;
$h_l^{i,c}$	number of hops in the l-th disjoint path between $i \in \tilde{S}_s$ and the sink node;
iec	initial energy charge of the sensors, $iec > 0$;
k	information packet size in bits, $k > 0$;
$P_i(t)$	number of packets sent by the sensor $i \in S_s(t)$ at time $t > 0$;
re_i	reliability of the sensor $i \in \tilde{S}_s$;
r_c	communication radius, $r_c > 0$;
$Rp_i(t)$	number of relayed packets sent by the sensor $i \in S_s(t)$ at time $t > 0$;
r_s	sensitivity radius, $r_s > 0$;
$\tilde{S}_r$	set of RN coordinates, $\forall r \in \tilde{S}_r,\ r = (x, y)$ where $x \in [0, d_x]$ and $y \in [0, d_y]$;
$\tilde{s}_r$	number of RNs. It is the cardinal of $\tilde{S}_r$;
$\tilde{S}_s$	set of initial sensor coordinates, $\forall i \in \tilde{S}_s$, $i = (x, y)$, where $x \in [0, d_x]$ and $y \in [0, d_y]$;
$\tilde{s}_s$	number of initial sensors. It is the cardinal of $\tilde{S}_s$;
$S_s(t)$	set of sensor coordinates, holding that the energy charge is greater than 0 and that there is any path to the sink node, both at time $t > 0$, $S_s(t) \subseteq \tilde{S}_s$;

$s_s(t)$	number of sensors, holding that the energy charge is greater than 0 and that there is any path to the sink node, both at time $t > 0$. It is the cardinal of $S_s(t)$, $s_s(t) \leq \tilde{s}_s$;
t_n	network lifetime of the WSN based on the coverage threshold co_{th};
$w_i^c(t)$	variable which provides the next device in the minimum path between $i \in S_s(t)$ and the sink node at $t > 0$, $w_i^c(t) \in \{S_s(t) \cup \tilde{S}_r\} + c - i$;
$z_{j,i}^c(t)$	variable assuming 1 if $i \in S_s(t)$ is in the minimum path between $j \in S_s(t)$ and the sink node at $t > 0$, and 0 otherwise.

5.1.2 Network Reliability

We assume that reliability is defined as in [81], where it is given according to the number of disjoint paths between a given sensor and the sink node. Thus, given a sensor $i \in \tilde{S}_s$, the reliability re_i of i is denoted as

$$re_i = 1 - \prod_{l=1}^{djp_i^c} \left(1 - (1 - err)^{h_l^{i,c}}\right),$$

where djp_i^c is the number of disjoint paths between i and the sink node, $h_l^{i,c}$ is the number of hops in the l-th disjoint path between both devices, and err is the local channel error. The disjoint paths are calculated through Suurballe's Algorithm [82].

5.2 Problem Formulation

Let f_1 be the AEC of the sensors over the network lifetime. That is expressed as

$$f_1 = \frac{\sum_{t=1}^{t_n} \left(\sum_{i \in S_s(t)} \frac{Ee_i(t)}{s_s(t)} \right)}{t_n}, \tag{5.1}$$

where $f_1 \in \mathbb{R}^+$ and both $Ee_i(t)$ and t_n are given by Equations (4.2) and (4.4), respectively.

Let f_2 be the ASA provided by the network, which is expressed as

$$f_2 = \frac{\sum_{t=1}^{t_n} A(t)}{t_n}, \tag{5.2}$$

where $f_2 \in [0, 1]$ and $A(t)$ is given by Equation (4.3).

Let f_3 be the NR, showing the probability that the sensors successfully send information to the sink node. That is

$$f_3 = \sum_{i \in \tilde{S}_s} \left(\frac{re_i}{\tilde{s}_s} \right), \tag{5.3}$$

where $f_3 \in [0, 1]$ and re_i is given by Equation (5.1.2).

Table 5.1: Trade-off study among the fitness functions.

case	f_1	f_2	f_3
#1	Increase	Decrease	**Increase**
#2	Increase	**Increase**	**Increase**
#3	**Decrease**	Decrease	Decrease
#4	**Decrease**	**Increase**	Decrease

This way, we define the unconstrained outdoor RNPP as a three-objective optimisation problem, where given a previously-established traditional WSN, i.e. $\tilde{s}_s$ sensors and a sink node, the objective is to place $\tilde{s}_r$ RNs by assuming an ST network model to

$$\min(f_1), \max(f_2), \text{ and } \max(f_3),$$

subject to

$$\forall r \in \tilde{S}_r,\ r = (x, y) : x \in [0, d_x] \text{ and } y \in [0, d_y].$$

These objectives are related to three important problems in the WSN literature: i) Energy efficiency problem [59], whose aim is to reduce the energy cost, increasing the network lifetime and balancing the energy distribution. ii) Coverage problem [60], its purpose is to optimise the amount and diversity of the information provided by the network. ii) Reliability problem [83], the objective is to deploy a reliable WSN, this means that the network is able to recover from the failure of nodes, which is crucial to reduce maintenance costs. Although these problems are widely considered in the literature, these objectives were not considered all together for the deployment of ST-WSNs, applied to the unconstrained RNPP.

It is well-known that one fundamental requirement for a problem to be considered as an MO optimisation problem is that the objectives should be conflicting [15]. Other authors assumed that both energy cost and coverage were conflicting objectives in WSNs [55] [61] [62] [63] [64], where [61] and [63] also tackled the connectivity issue. With the purpose of showing that our definition of the RNPP is an MO problem, we analyse the trade-off among the fitness functions in Table 5.1, where *Increase* implies that the value of the fitness function is increased and *Decrease* otherwise. Note that *Increase* and *Decrease* are in boldface if the behaviour of the fitness function fits with the purpose of the optimization problem, i.e. it appears in boldface if the fitness function is increased for a maximisation problem or decreased for a minimisation one, respectively.

According to this trade-off study, we find four different cases in which at least one of the objectives is optimised:

- Case #1: on the basis of Eq. (5.3), a high reliability implies the existence of many disjoint paths between the sink node and the sensors, which allows that the network is able to recover from the collapse of nodes, avoiding that sensors having energy in their batteries are disconnected from the WSN. This means that more sensors can send packets over the network lifetime. As shown in Eq. (5.1), the energy consumption depends on the number of packets sent by the sensors, including forwards. Hence, more sensors implies more packets, increasing the energy cost. The average coverage is low due to the coverage is decreasing slowly over the network lifetime. As detailed in Eq. (5.2), this value depends on the number of sensors that can be connected to the sink node over the lifetime. A bad distribution of the energy cost (which is high) could mean that the network loses coverage. However, as the reliability is high, the other sensors can reach the sink node and the coverage decreases slowly, instead of reaching the co_{th}.

Table 5.2: Main features of the data set by adding the third objective to the RNPP.

Instance name	Fitness values ($\tilde{s}_r = 0$)			Reference points (f_1, f_2, f_3)	
($d_x \times d_y\_r_c$)	f_1	f_2	f_3	ideal	nadir
50x50_30	0.0350	0.9175	0.9964	(0.02,1.00,1.00)	(0.04,0.60,0.50)
100x100_30	0.1091	0.8924	0.9567	(0.02,1.00,1.00)	(0.10,0.60,0.50)
200x200_30	0.2791	0.8710	0.9323	(0.10,1.00,1.00)	(0.30,0.60,0.50)
300x300_30	0.4225	0.7644	0.8528	(0.04,1.00,1.00)	(0.50,0.60,0.50)

- Case #2: it is similar to the previous case. The difference is that the deployment of the RNs is more efficient in energy terms, i.e. the energy distribution is homogeneous. Consequently, the coverage is not decreasing slowly, instead the sensors are exhausted at the same time, reaching the co_{th}.
- Case #3: a network with a low reliability implies that sensors having energy can be disconnected from the WSN, because other sensors are exhausted. This situation decreased the number of packets sent over the network lifetime, decreasing the energy cost. A bad distribution of this energy cost means that the network loses sensors slowly, decreasing the average coverage, as in case #1.
- Case #4: it is similar to #3. As in case #2, a better deployment of the RNs allows that the energy distribution is homogeneous. Hence, the sensors are exhausted at the same time, increasing the average coverage.

Analysing the behaviour of the fitness functions, we reach the following conclusions: we cannot optimise an objective without degrading at least one of the other two, and on the other hand, enhancing an objective does not necessarily imply that another is optimised. Thus, we conclude that the objectives are in conflict. Hence, this is an MO optimisation problem.

5.3 Description of the Dataset

We consider the same dataset as described before in Section 4.3, which is composed of four scenarios, i.e. 50x50, 100x100, 200x200, and 300X300. In Figures 4.2, 4.3, 4.4, and 4.5, we presented detailed information of such scenarios according to three criteria: main features, deployment details, and energy charge distribution. Both deployment details and energy charge distribution are the same for this new problem definition. However, this is not the case for main features, specifically the fitness values without deploying RN, the reference points for calculating the hypervolume metric, and the communication radius.

Table 5.2 shows this new information. Note that we only consider an r_c value of 30m, this is because the number of disjoint paths for 60m is really high, and then NR is also high for all the test cases. Consequently, it is not necessary to optimise this objective for 60m.

5.4 Solving the Problem

In this section, we expose the experimental results obtained, while solving the three-objective RNPP through the MO metaheuristics. To this end, we consider the data set exposed in Section 5.3 and five stop conditions based on the number of evaluations: 50 000, 100 000, 200 000, 300 000, and 400 000. This section is structured as follows. The algorithms are adjusted in Section 5.4.1. A detailed statistical analysis based on the hypervolume metric is provided in Section

Table 5.3: Parametric sweep.

NSGA-II

Parameter	Selected	Range
ps_n	**50**	[25,50,...,300]
$param\_cro_n$	**0.80**	[0.05,0.10,...,0.95]
$param\_mut_n$	**0.80**	[0.05,0.10,...,0.95]

SPEA2

Parameter	Selected	Range
ps_s	**50**	[25,50,...,300]
$\overline{ps}_s$	**50**	-
$param\_cro_s$	**0.60**	[0.05,0.10,...,0.95]
$param\_mut_s$	**0.70**	[0.05,0.10,...,0.95]

MO-VNS

Parameter	Selected	Range
$param\_neigh_v$	**9**	[4,5,...,14]
$param\_ns_v$	**2**	[1,2,3,4,5]

MO-VNS*

Parameter	Selected	Range
$param\_neigh_v$	**10**	[4,5,...,14]
$param\_ns_v$	**2**	[1,2,3,4,5]
$param\_per_v$	**0.10**	[0.05,0.10,...,0.95]

MO-ABC

Parameter	Selected	Range
ps_a	**50**	[25,50,...,300]
$param\_Se_a$	**0.25**	[0.30,0.35,...,0.70]
$param\_limit_a$	**15**	[5,10,...,60]

MO-FA

Parameter	Selected	Range
ps_f	**100**	[25,50,...,300]
r_f	**0.85**	[0.05,0.10,...,0.95]
β_{0_f}	**0.70**	[0.05,0.10,...,0.95]
γ_f	**0.60**	[0.05,0.10,...,0.95]
$param\_how\_sc_f$	**0.10**	[0.05,0.10,...,0.95]
$param\_when\_sc_f$	**0.25**	[0.05,0.10,...,0.95]

MO-GSA

Parameter	Selected	Range
ps_{gsa}	**25**	[25,50,...,300]
$param\_how\_sc_{gsa}$	**0.20**	[0.05,0.10,...,0.95]
$param\_when\_sc_{gsa}$	**0.05**	[0.05,0.10,...,0.95]

MOEA/D

Parameter	Selected	Range
$param\_CHIMinc_m$	**1.30**	[1.00,1.05,...,2.00]
$param\_crow_m$	**0.015**	[0.010,0.015,...,0.050]
$param\_neigh_m$	**0.05**	[0.05,0.10,...,0.95]
$param\_cro_m$	**0.15**	[0.05,0.10,...,0.95]
$param\_mut_m$	**0.25**	[0.05,0.10,...,0.95]

5.4.2. We study the convergence of the algorithms according to hypervolume in Section 5.4.3. We analyse the results obtained through set coverage in Section 5.4.4. Pareto fronts obtained are shown in Section 5.4.5. The impact of the optimisation on the fitness functions is discussed in Section 5.4.6. Finally, comparisons to other approaches are included in Section 5.4.7.

5.4.1 **Parametric Swap**

As in the previous chapter, we consider the methodology exposed in Section 2.3.2 to adjust the algorithms. To this end, we assume all the test cases, 50 000 evaluations, and the hypervolume metric as quality indicator. The resulting configurations are in Table 5.3. Note that population size parameters were also studied, not as in the previous approach (see Section 4.7.1).

5.4.2 **Statistical Analysis Based on the Hypervolume Metric**

Tables 5.4, 5.5, and 5.6 show median hypervolume ($\overline{Hyp}$) and IQR for each algorithm, test case, and stop condition, where higher hypervolumes obtained are shaded. As in the previous chapter, these values were obtained by executing 31 independent runs for each metaheuristic and test case. Analysing these tables, some algorithms seem to provide better performance than others. However, we should determine if such differences are significant. To this end, we follow the statistical methodology described in Section 2.3.1.

To this end, the fist step is to remove possible outliers from the hypervolume distributions. Next, we determine if such hypervolumes follow a normal distribution or not. With this pur-

Table 5.4: Median hypervolume metric for each test case and stop condition, where higher hipervolumes obtained are shaded by considering all the metaheuristics. Part 1 of 3.

	NSGA-II($\overline{Hyp}\,\%, IQR$)				
	Evaluations (Stop condition)				
Instance($\bar{\mathbf{s}}_\mathbf{r}$)	**50 000**	**100 000**	**200 000**	**300 000**	**400 000**
50x50_30(1)	64.52%, 0.0000	64.52%, 0.0000	64.52%, 0.0000	64.52%, 0.0000	64.52%, 0.0000
100x100_30(2)	40.99%, 0.0052	41.28%, 0.0032	41.36%, 0.0033	41.47%, 0.0002	41.48%, 0.0002
100x100_30(3)	53.78%, 0.0040	54.18%, 0.0043	54.49%, 0.0026	54.60%, 0.0013	54.60%, 0.0015
200x200_30(2)	32.40%, 0.0125	33.01%, 0.0066	33.44%, 0.0063	33.58%, 0.0042	33.66%, 0.0036
200x200_30(4)	43.40%, 0.0243	44.54%, 0.0257	45.53%, 0.0223	46.08%, 0.0217	46.41%, 0.0221
200x200_30(6)	54.07%, 0.0188	56.14%, 0.0220	57.43%, 0.0167	58.15%, 0.0200	58.58%, 0.0183
200x200_30(9)	63.42%, 0.0254	65.83%, 0.0232	68.04%, 0.0204	68.93%, 0.0123	69.48%, 0.0134
300x300_30(6)	30.03%, 0.0078	30.91%, 0.0081	31.40%, 0.0107	31.71%, 0.0098	31.90%, 0.0111
300x300_30(12)	33.09%, 0.0134	34.32%, 0.0164	35.32%, 0.0165	35.90%, 0.0186	36.37%, 0.0212
300x300_30(18)	34.66%, 0.0096	36.38%, 0.0171	37.67%, 0.0194	38.46%, 0.0201	38.92%, 0.0200
300x300_30(24)	37.55%, 0.0126	38.88%, 0.0146	40.44%, 0.0173	41.30%, 0.0187	41.58%, 0.0167

	SPEA2($\overline{Hyp}\,\%, IQR$)				
	Evaluations (Stop condition)				
Instance($\bar{\mathbf{s}}_\mathbf{r}$)	**50 000**	**100 000**	**200 000**	**300 000**	**400 000**
50x50_30(1)	64.52%, 0.0000	64.52%, 0.0000	64.52%, 0.0000	64.52%, 0.0000	64.52%, 0.0000
100x100_30(2)	41.18%, 0.0033	41.28%, 0.0030	41.45%, 0.0002	41.45%, 0.0002	41.46%, 0.0003
100x100_30(3)	54.05%, 0.0063	54.43%, 0.0033	54.71%, 0.0036	54.77%, 0.0047	54.87%, 0.0045
200x200_30(2)	32.54%, 0.0090	33.03%, 0.0076	33.23%, 0.0068	33.38%, 0.0063	33.43%, 0.0061
200x200_30(4)	43.11%.0.0196	44.25%, 0.0283	45.34%, 0.0222	45.74%, 0.0176	46.00%, 0.0190
200x200_30(6)	54.71%, 0.0199	56.72%, 0.0162	58.00%, 0.0197	58.71%, 0.0177	59.17%, 0.0161
200x200_30(9)	64.93%. 0.0294	67.56%, 0.0242	69.21%, 0.0224	70.08%, 0.0138	70.62%, 0.0133
300x300_30(6)	30.37%, 0.0132	31.21%, 0.0141	31.86%, 0.0139	32.20%, 0.0138	32.35%, 0.0148
300x300_30(12)	33.90%, 0.0145	35.25%, 0.0202	36.54%, 0.0121	37.23%, 0.0123	37.75%, 0.0130
300x300_30(18)	36.01%, 0.0154	37.81%, 0.0127	39.07%, 0.0145	39.84%, 0.0139	40.36%, 0.0167
300x300_30(24)	38.51%, 0.0107	40.08%, 0.0123	41.77%, 0.0101	42.72%, 0.0137	43.31%, 0.0168

	MO-VNS($\overline{Hyp}\,\%, IQR$)				
	Evaluations (Stop condition)				
Instance($\bar{\mathbf{s}}_\mathbf{r}$)	**50 000**	**100 000**	**200 000**	**300 000**	**400 000**
50x50_30(1)	64.58%, 0.0000	64.58%, 0.0001	64.59%, 0.0002	64.59%, 0.0001	64.60%, 0.0001
100x100_30(2)	41.73%, 0.0008	41.77%, 0.0004	41.81%, 0.0004	41.81%, 0.0003	41.82%, 0.0002
100x100_30(3)	54.87%, 0.0053	55.19%, 0.0025	55.45%, 0.0053	55.55%, 0.0057	55.59%, 0.0060
200x200_30(2)	31.98%, 0.0334	33.18%, 0.0173	34.41%, 0.0180	35.37%, 0.0066	35.84%, 0.0031
200x200_30(4)	41.94%, 0.0255	43.76%, 0.0224	45.09%, 0.0281	45.60%, 0.0280	46.05%, 0.0354
200x200_30(6)	52.49%, 0.0543	54.94%, 0.0407	57.05%, 0.0323	58.10%, 0.0186	58.74%, 0.0155
200x200_30(9)	63.30%, 0.0331	65.41%, 0.0306	67.30%, 0.0311	68.39%, 0.0278	69.13%, 0.0239
300x300_30(6)	30.37%, 0.0103	30.97%, 0.0132	31.61%, 0.0121	31.97%, 0.0124	32.18%, 0.0106
300x300_30(12)	34.06%, 0.0185	35.13%, 0.0161	36.08%, 0.0154	36.75%, 0.0194	37.13%, 0.0149
300x300_30(18)	36.62%, 0.0143	37.80%, 0.0119	38.95%, 0.0116	39.58%, 0.0123	40.09%, 0.0116
300x300_30(24)	39.59%, 0.0138	40.96%, 0.0129	42.20%, 0.0123	42.90%, 0.0104	43.45%, 0.0111

Table 5.5: Median hypervolume metric for each test case and stop condition, where higher hipervolumes obtained are shaded by considering all the metaheuristics. Part 2 of 3.

	MO-VNS*($\overline{Hyp}\,\%, IQR$)				
	Evaluations (Stop condition)				
Instance($\tilde{s}_r$)	**50 000**	**100 000**	**200 000**	**300 000**	**400 000**
50x50_30(1)	64.60%, 0.0002	64.61%, 0.0001	64.62%, 0.0002	64.62%, 0.0001	64.63%, 0.0001
100x100_30(2)	41.75%, 0.0005	41.79%, 0.0004	41.81%, 0.0003	41.81%, 0.0002	41.82%, 0.0001
100x100_30(3)	54.96%, 0.0062	55.17%, 0.0039	55.45%, 0.0071	55.56%, 0.0063	55.61%, 0.0065
200x200_30(2)	31.76%, 0.0451	34.00%, 0.0078	34.60%, 0.0180	35.22%, 0.0149	35.49%, 0.0135
200x200_30(4)	42.81%, 0.0232	44.38%, 0.0284	45.24%, 0.0245	45.78%, 0.0213	46.14%, 0.0198
200x200_30(6)	54.27%, 0.0300	56.20%, 0.0192	56.80%, 0.0208	57.13%, 0.0219	57.47%, 0.0208
200x200_30(9)	63.48%, 0.0225	64.30%, 0.0198	65.33%, 0.0143	65.87%, 0.0195	66.45%, 0.0179
300x300_30(6)	30.39%, 0.0067	30.93%, 0.0105	31.23%, 0.0082	31.34%, 0.0079	31.40%, 0.0079
300x300_30(12)	33.88%, 0.0110	34.56%, 0.0113	35.31%, 0.0110	35.68%, 0.0096	35.83%, 0.0099
300x300_30(18)	37.04%, 0.0101	37.83%, 0.0107	38.48%, 0.0080	38.77%, 0.0066	39.01%, 0.0078
300x300_30(24)	40.14%, 0.0159	40.85%, 0.0126	41.48%, 0.0099	41.79%, 0.0084	41.95%, 0.0068

	MO-ABC($\overline{Hyp}\,\%, IQR$)				
	Evaluations (Stop condition)				
Instance($\tilde{s}_r$)	**50 000**	**100 000**	**200 000**	**300 000**	**400 000**
50x50_30(1)	64.60%, 0.0000	64.60%, 0.0000	64.60%, 0.0000	64.60%, 0.0000	64.60%, 0.0001
100x100_30(2)	41.40%, 0.0068	41.40%, 0.0053	41.50%, 0.0055	41.50%, 0.0049	41.50%, 0.0048
100x100_30(3)	54.70%, 0.0070	55.00%, 0.0082	55.10%, 0.0098	55.10%, 0.0099	55.10%, 0.0099
200x200_30(2)	32.40%, 0.0103	32.70%, 0.0105	32.80%, 0.0079	32.90%, 0.0082	32.90%, 0.0083
200x200_30(4)	39.80%, 0.0289	40.70%, 0.0230	41.40%, 0.0246	41.40%, 0.0256	41.40%, 0.0256
200x200_30(6)	47.00%, 0.0509	49.20%, 0.0429	50.80%, 0.0430	51.00%, 0.0426	51.20%, 0.0413
200x200_30(9)	60.20%, 0.0443	62.30%, 0.0426	63.30%, 0.0337	63.50%, 0.0403	63.70%, 0.0408
300x300_30(6)	30.00%, 0.0103	31.00%, 0.0142	31.50%, 0.0110	31.70%, 0.0108	31.80%, 0.0127
300x300_30(12)	34.80%, 0.0150	36.50%, 0.0136	37.70%, 0.0115	38.20%, 0.0119	38.40%, 0.0118
300x300_30(18)	39.20%, 0.0130	41.10%, 0.0136	42.60%, 0.0120	43.50%, 0.0145	44.00%, 0.0118
300x300_30(24)	42.90%, 0.0164	44.90%, 0.0127	46.80%, 0.0114	47.70%, 0.0115	48.30%, 0.0121

	MO-FA($\overline{Hyp}\,\%, IQR$)				
	Evaluations (Stop condition)				
Instance($\tilde{s}_r$)	**50 000**	**100 000**	**200 000**	**300 000**	**400 000**
50x50_30(1)	64.63%, 0.0000	64.63%, 0.0000	64.63%, 0.0000	64.63%, 0.0000	64.63%, 0.0000
100x100_30(2)	41.66%, 0.0013	41.71%, 0.0010	41.75%, 0.0005	41.77%, 0.0003	41.78%, 0.0004
100x100_30(3)	54.79%, 0.0055	55.19%, 0.0013	55.29%, 0.0011	55.35%, 0.0014	55.38%, 0.0014
200x200_30(2)	35.05%, 0.0155	35.57%, 0.0049	35.98%, 0.0019	36.00%, 0.0020	36.06%, 0.0019
200x200_30(4)	43.65%, 0.0272	44.58%, 0.0231	45.21%, 0.0162	45.56%, 0.0117	45.91%, 0.0173
200x200_30(6)	55.22%, 0.0346	56.54%, 0.0383	57.89%, 0.0358	58.38%, 0.0409	58.96%, 0.0358
200x200_30(9)	65.87%, 0.0400	67.83%, 0.0269	69.82%, 0.0250	70.50%, 0.0239	70.94%, 0.0261
300x300_30(6)	30.28%, 0.0130	31.39%, 0.0202	32.59%, 0.0251	32.90%, 0.0173	33.02%, 0.0168
300x300_30(12)	34.63%, 0.0228	36.24%, 0.0238	37.76%, 0.0215	38.25%, 0.0192	39.17%, 0.0064
300x300_30(18)	37.97%, 0.0188	39.63%, 0.0187	41.18%, 0.0190	41.90%, 0.0189	42.54%, 0.0196
300x300_30(24)	40.83%, 0.0313	42.88%, 0.0207	44.35%, 0.0200	45.13%, 0.0217	45.59%, 0.0176

Table 5.6: Median hypervolume metric for each test case and stop condition, where higher hiper-volumes obtained are shaded by considering all the metaheuristics. Part 3 of 3.

	MO-GSA($\overline{Hyp}\,\%, IQR$)				
	Evaluations (Stop condition)				
Instance($\tilde{s}_r$)	**50 000**	**100 000**	**200 000**	**300 000**	**400 000**
50x50_30(1)	64.56%, 0.0000	64.56%, 0.0000	64.56%, 0.0000	64.56%, 0.0000	64.56%, 0.0000
100x100_30(2)	39.70%, 0.0090	40.24%, 0.0082	40.77%, 0.0058	41.08%, 0.0046	41.21%, 0.0041
100x100_30(3)	52.40%, 0.0074	53.15%, 0.0070	53.75%, 0.0040	54.05%, 0.0041	54.18%, 0.0028
200x200_30(2)	32.53%, 0.0104	32.82%, 0.0095	33.21%, 0.0062	33.50%, 0.0047	33.59%, 0.0058
200x200_30(4)	41.03%, 0.0178	42.97%, 0.0268	44.66%, 0.0151	45.62%, 0.0136	45.96%, 0.0136
200x200_30(6)	50.75%, 0.0368	52.58%, 0.0264	55.82%, 0.0151	57.24%, 0.0176	57.98%, 0.0142
200x200_30(9)	61.53%, 0.0253	63.79%, 0.0196	67.15%, 0.0210	69.10%, 0.0215	69.64%, 0.0201
300x300_30(6)	29.05%, 0.0090	29.82%, 0.0105	30.81%, 0.0095	31.27%, 0.0071	31.47%, 0.0077
300x300_30(12)	33.49%, 0.0131	34.74%, 0.0118	36.40%, 0.0115	37.68%, 0.0097	38.00%, 0.0092
300x300_30(18)	37.57%, 0.0214	38.85%, 0.0193	41.62%, 0.0208	43.18%, 0.0241	43.72%, 0.0213
300x300_30(24)	42.37%, 0.0313	44.51%, 0.0248	47.76%, 0.0220	49.86%, 0.0184	50.33%, 0.0132

	MOEA/D($\overline{Hyp}\,\%, IQR$)				
	Evaluations (Stop condition)				
Instance($\tilde{s}_r$)	**50 000**	**100 000**	**200 000**	**300 000**	**400 000**
50x50_30(1)	64.62%, 0.0001	64.62%, 0.0000	64.63%, 0.0000	64.63%, 0.0000	64.63%, 0.0000
100x100_30(2)	41.07%, 0.0027	41.20%, 0.0021	41.31%, 0.0016	41.35%, 0.0015	41.39%, 0.0010
100x100_30(3)	54.82%, 0.0047	55.12%, 0.0046	55.36%, 0.0063	55.42%, 0.0069	55.48%, 0.0068
200x200_30(2)	32.32%, 0.0180	32.76%, 0.0186	33.27%, 0.0147	33.54%, 0.0116	33.71%, 0.0127
200x200_30(4)	43.85%, 0.0451	44.82%, 0.0383	46.18%, 0.0234	46.72%, 0.0213	46.69%, 0.0198
200x200_30(6)	57.48%, 0.0160	58.62%, 0.0155	59.56%, 0.0192	60.01%, 0.0180	60.38%, 0.0171
200x200_30(9)	69.60%, 0.0167	70.96%, 0.0163	72.16%, 0.0177	72.87%, 0.0155	73.35%, 0.0150
300x300_30(6)	30.54%, 0.0057	31.25%, 0.0077	31.82%, 0.0074	32.08%, 0.0069	32.26%, 0.0053
300x300_30(12)	36.39%, 0.0152	37.56%, 0.0174	38.48%, 0.0174	38.85%, 0.0159	39.11%, 0.0154
300x300_30(18)	40.53%, 0.0257	42.22%, 0.0266	43.92%, 0.0219	44.74%, 0.0168	45.21%, 0.0178
300x300_30(24)	45.09%, 0.0202	47.51%, 0.0187	49.82%, 0.0242	51.04%, 0.0308	51.75%, 0.0275

Table 5.7: Algorithms providing the best significant performance for each test case and stop condition, based on the hypervolume metric and the Wilcoxon-Mann-Whitney's test.

	Evaluations (Stop condition)				
Instance($\tilde{s}_r$)	**50 000**	**100 000**	**200 000**	**300 000**	**400 000**
50x50(1)	FA	FA	FA	FA	FA
100x100(2)	VNS, VNS*	VNS, VNS*	VNS, VNS*	VNS, VNS*	VNS, VNS*
100x100(3)	FA,VNS, VNS*,MOEA/D	ABC,FA, VNS,VNS*	MOEA/D,VNS, VNS*	VNS, VNS*	VNS, VNS*
200x200(2)	FA	FA	FA	FA	FA
200x200(4)	MOEA/D,FA, NSGA-II,SPEA2	MOEA/D,FA,VNS*, NSGA-II,SPEA2	MOEA/D,VNS*, NSGA-II,SPEA2	MOEA/D,VNS*, NSGA-II	MOEA/D,VNS, VNS*,NSGA-II
200x200(6)	MOEA/D,FA	MOEA/D,FA	MOEA/D,FA	MOEA/D,FA	MOEA/D,FA
200x200(9)	MOEA/D	MOEA/D	MOEA/D	MOEA/D	MOEA/D
300x300(6)	FA,VNS, VNS*,SPEA2	ABC,FA, VNS*,SPEA2	FA	FA	FA
300x300(12)	MOEA/D	MOEA/D	MOEA/D,FA	MOEA/D,FA	MOEA/D,FA
300x300(18)	MOEA/D	MOEA/D	MOEA/D	MOEA/D	MOEA/D
300x300(24)	MOEA/D	MOEA/D	MOEA/D	MOEA/D	MOEA/D

pose, we consider both Kolmogorov-Smirnov-Lilliefor's [67] and Shapiro-Wilk's [68] tests with hypothesis H_0: data follow a normal distribution and H_1: data do not follow a normal distribution. Since all the p-values obtained were lower or equal than 0.05, we cannot assume H_0. Consequently, hypervolume distributions are not modelled under a normal distribution and we should consider the median and IQR as average value and statistical dispersion metric, respectively. As expected, Tables 5.4, 5.5, and 5.6 were developed after performing this study.

The next step is to analyse if there are significant differences among the algorithms. To this end, as samples are independent and data do not follow a normal distribution, we consider the Wilcoxon-Mann-Whitney's [69] test with hypothesis H_0: $\overline{Hyp_i} \leq \overline{Hyp_j}$ and H_1: $\overline{Hyp_i} > \overline{Hyp_j}$, with $i, j = 1, 2, \ldots, 8$, 1=NSGA-II, 2=SPEA2, 3=MO-VNS, 4=MO-VNS*, 5=MO-ABC, 6=MOFA, 7=MO-GSA, and 8=MOEA/D. MO-VNS is the algorithm without perturbation mechanism and MO-VNS* includes this procedure. The p-values obtained are in Section C.1 of Appendix C, specifically in Tables C.1, C.2, C.3, C.4, and C.5.

According to these p-values and a significance level of 0.05, Table 5.7 shows which algorithms provide the best significant performance for each study case, i.e. a test case and a stop condition. As stated in Section 4.7.2, it is possible that two algorithms appear in a same cell of this table, meaning that there are not significant differences among them, but they are significant better than the remaining ones. Note that in this table, the name of some of the metaheuristics was shortened to reduce the size of the table. This way, MO-ABC, MO-GSA, MO-FA, MO-VNS, and MO-VNS* were renamed to ABC, GSA, FA, VNS, and VNS*, respectively.

In addition to identify which algorithms provide the best significant performance for each study case, it is also interesting to determine which metaheuristics provide the best average behaviour attending to the instance size. To this end, we compare the algorithms two by two in Table 5.8, showing the percentage of study cases in which the metaheuristics are better and worse than others. Note that average values in *Percentage* field are shaded from darker to lighter tone, i.e. from better to worse average behaviour.

Analysing this table, we note that MO-FA provides the best behaviour for 50x50 instances, followed by MOEA/D and MO-ABC. For 100x100 instances, we check that MO-VNS provides the best behaviour, followed by MO-VNS* and MO-FA. In case of 200x200 instances, MO-FA is the best algorithm, followed by MO-VNS* and MO-FA. For 300x300 instances, we find that MO-FA is the best algorithm, followed by MOEA/D and MO-ABC. Regarding all the instances, we reach that MO-FA is the algorithm providing the best average behaviour, followed by MOEA/D and MO-VNS.

According to this analysis, we conclude that MO-FA is the best algorithm in average term. However and based on the instance size, we recommend to consider MO-FA for small and large instances, i.e. 50x50, 200x200, and 300x300 instances, and MO-VNS for medium size instances, i.e. 100x100 instances. Thus, we notice that MO-FA is good to explore large search spaces, such as 200x200 and 300x300 instances, and MO-VNS is good for medium size search spaces (100x100 instances) because of neighbouring search procedures. The exception is for small search spaces (50x50 instances), where most of the algorithms reach solutions near to the optimal, falling into local optima. In such a case, MO-FA is able to avoid this situation.

5.4.3 Convergence Study Based on the Hypervolume Metric

Figures 5.3 and 5.4 show a convergence study based on the hypervolume metric. We note that most of the algorithms have an homogeneous grown over stop conditions and an asymptotic trend for 400 000 evaluations. This means that the set of stop conditions is representative to analyse the behaviour of the algorithms, as discussed before in Section 4.7.3.

Table 5.8: Based on the hypervolume metric. percentage of test cases in which the metaheuristics are significant better and worse. for all the test cases. 50x50 instances. 100x100 instances. 200x200 instances. and 300x300 instances.

A is worse than B (all the instances) — rows: A is better than B

A \ B	MOEA/D	MO-FA	MO-VNS*	MO-ABC	NSGA-II	SPEA2	MO-VNS	MO-GSA	Percentage
MOEA/D	0.00%	0.76%	1.20%	1.48%	1.40%	1.52%	1.36%	2.00%	9.74%
MO-FA	0.92%	0.00%	1.56%	1.36%	1.96%	1.72%	1.56%	2.52%	11.62%
MO-VNS*	0.48%	0.28%	0.00%	1.12%	1.12%	0.88%	0.40%	1.12%	5.41%
MO-ABC	0.28%	0.40%	0.76%	0.00%	1.20%	1.20%	0.80%	1.00%	5.65%
NSGA-II	0.24%	0.00%	0.36%	0.76%	0.00%	0.16%	0.04%	1.12%	2.68%
SPEA2	0.32%	0.00%	0.80%	0.92%	1.28%	0.00%	0.40%	1.16%	4.89%
MO-VNS	0.48%	0.32%	0.76%	1.16%	1.40%	0.92%	0.00%	1.32%	6.37%
MO-GSA	0.00%	0.28%	0.60%	0.84%	0.80%	0.64%	0.48%	0.00%	3.65%
Percentage	2.72%	2.04%	6.05%	7.65%	9.17%	7.05%	5.05%	10.26%	100.00%

A is worse than B (50x50 instances) — rows: A is better than B

A \ B	MOEA/D	MO-FA	MO-VNS*	MO-ABC	NSGA-II	SPEA2	MO-VNS	MO-GSA	Percentage
MOEA/D	0.00%	0.00%	1.53%	0.76%	1.91%	1.91%	1.91%	1.91%	9.92%
MO-FA	1.91%	0.00%	1.91%	1.91%	1.91%	1.91%	1.91%	1.91%	13.36%
MO-VNS*	0.00%	0.00%	0.00%	0.00%	1.91%	1.91%	1.91%	1.91%	7.63%
MO-ABC	0.76%	0.00%	1.15%	0.00%	1.91%	1.91%	1.91%	1.91%	9.54%
NSGA-II	0.00%	0.00%	0.00%	0.00%	0.00%	0.00%	0.00%	0.00%	0.00%
SPEA2	0.00%	0.00%	0.00%	0.00%	0.00%	0.00%	0.00%	0.00%	0.00%
MO-VNS	0.00%	0.00%	0.00%	0.00%	1.91%	1.91%	0.00%	1.91%	5.73%
MO-GSA	0.00%	0.00%	0.00%	0.00%	1.91%	1.91%	0.00%	0.00%	3.82%
Percentage	2.67%	0.00%	4.58%	2.67%	11.45%	11.45%	7.63%	9.54%	100.00%

A is worse than B (100x100 instances) — rows: A is better than B

A \ B	MOEA/D	MO-FA	MO-VNS*	MO-ABC	NSGA-II	SPEA2	MO-VNS	MO-GSA	Percentage
MOEA/D	0.00%	0.00%	0.00%	0.42%	1.05%	1.05%	0.00%	2.10%	4.62%
MO-FA	1.26%	0.00%	0.00%	1.05%	2.10%	2.10%	0.00%	2.10%	8.61%
MO-VNS*	1.47%	1.47%	0.00%	1.68%	2.10%	2.10%	0.00%	2.10%	10.92%
MO-ABC	1.05%	0.00%	0.00%	0.00%	2.10%	2.10%	0.00%	2.10%	7.35%
NSGA-II	0.63%	0.00%	0.00%	0.00%	0.00%	0.42%	0.00%	2.10%	3.15%
SPEA2	0.63%	0.00%	0.00%	0.00%	1.05%	0.00%	0.00%	2.10%	3.78%
MO-VNS	1.68%	1.68%	0.00%	1.89%	2.10%	2.10%	0.00%	2.10%	11.55%
MO-GSA	0.00%	0.00%	0.00%	0.00%	0.00%	0.00%	0.00%	0.00%	0.00%
Percentage	6.72%	3.15%	0.00%	5.04%	10.50%	9.87%	0.00%	14.71%	100.00%

A is worse than B (200x200 instances) — rows: A is better than B

A \ B	MOEA/D	MO-FA	MO-VNS*	MO-ABC	NSGA-II	SPEA2	MO-VNS	MO-GSA	Percentage
MOEA/D	0.00%	0.88%	1.38%	2.25%	1.25%	1.63%	1.75%	1.88%	11.00%
MO-FA	0.88%	0.00%	1.88%	2.50%	1.88%	1.25%	2.00%	2.13%	12.50%
MO-VNS*	0.50%	0.00%	0.00%	2.38%	0.50%	0.50%	0.38%	1.25%	5.50%
MO-ABC	0.00%	0.00%	0.00%	0.00%	0.00%	0.00%	0.00%	0.00%	0.00%
NSGA-II	0.00%	0.00%	0.75%	2.38%	0.00%	0.25%	0.13%	1.63%	5.13%
SPEA2	0.00%	0.00%	1.00%	2.38%	1.00%	0.00%	1.00%	1.63%	7.00%
MO-VNS	0.50%	0.00%	0.75%	2.38%	0.50%	0.50%	0.00%	1.50%	6.13%
MO-GSA	0.00%	0.00%	0.38%	2.25%	0.00%	0.13%	0.00%	0.00%	2.75%
Percentage	1.88%	0.88%	6.13%	16.50%	5.13%	4.25%	5.25%	10.00%	100.00%

A is worse than B (300x300 instances) — rows: A is better than B

A \ B	MOEA/D	MO-FA	MO-VNS*	MO-ABC	NSGA-II	SPEA2	MO-VNS	MO-GSA	Percentage
MOEA/D	0.00%	1.25%	1.57%	1.57%	1.57%	1.57%	1.57%	2.09%	11.17%
MO-FA	0.52%	0.00%	1.98%	0.42%	1.98%	1.88%	1.88%	3.24%	11.90%
MO-VNS*	0.10%	0.00%	0.00%	0.10%	0.94%	0.31%	0.21%	0.31%	1.98%
MO-ABC	0.00%	1.04%	1.67%	0.00%	1.57%	1.57%	1.57%	1.04%	8.46%
NSGA-II	0.31%	0.00%	0.31%	0.00%	0.00%	0.00%	0.00%	0.52%	1.15%
SPEA2	0.52%	0.00%	1.25%	0.42%	1.98%	0.00%	0.21%	0.63%	5.01%
MO-VNS	0.00%	0.00%	1.36%	0.10%	1.67%	0.42%	0.00%	0.63%	4.18%
MO-GSA	0.00%	0.73%	1.25%	0.31%	1.57%	1.04%	1.25%	0.00%	6.16%
Percentage	1.46%	3.03%	9.39%	2.92%	11.27%	6.78%	6.68%	8.46%	100.00%

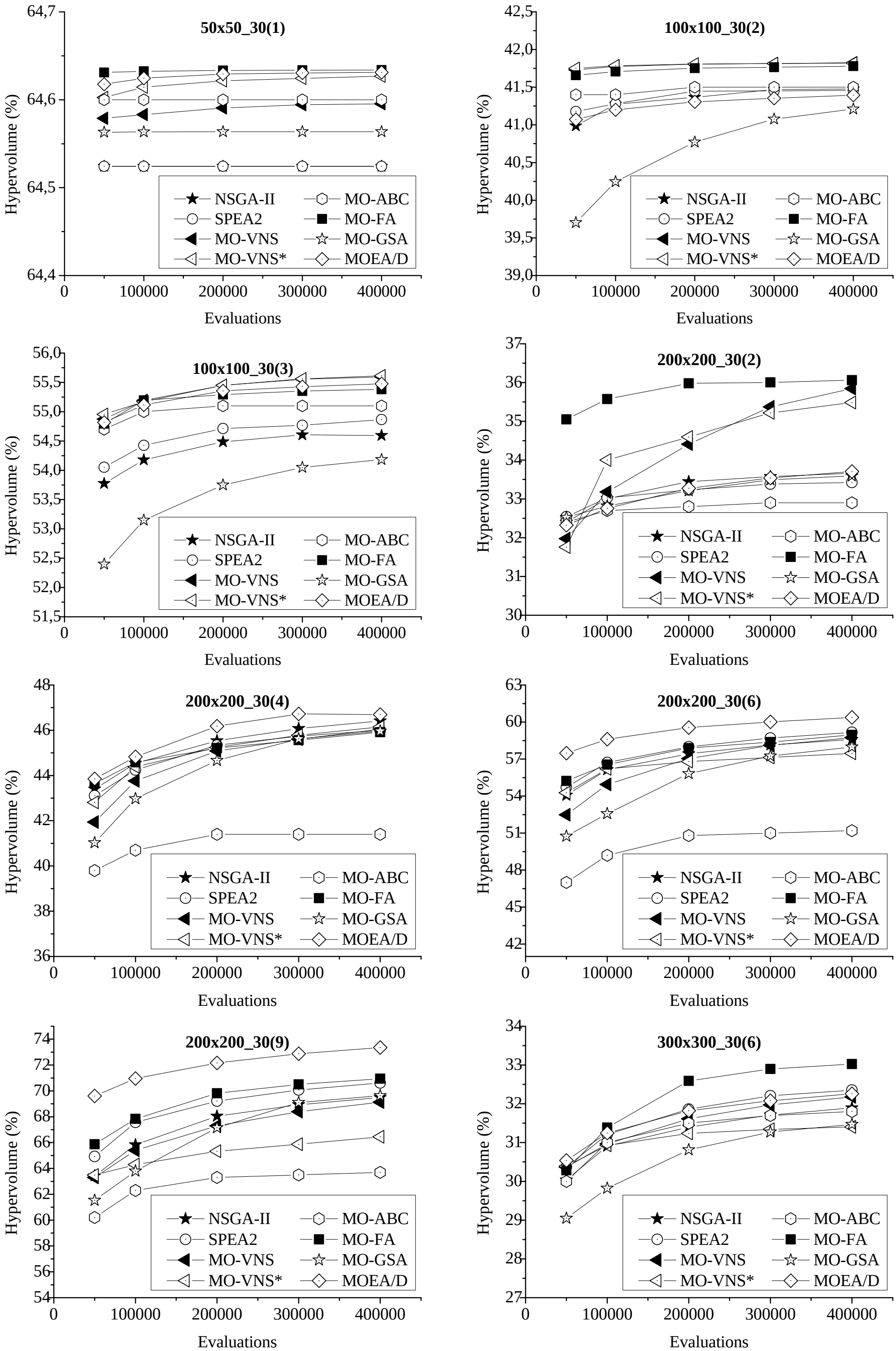

Figure 5.1: Convergence study based on the hypervolume metric. Part 1 of 2.

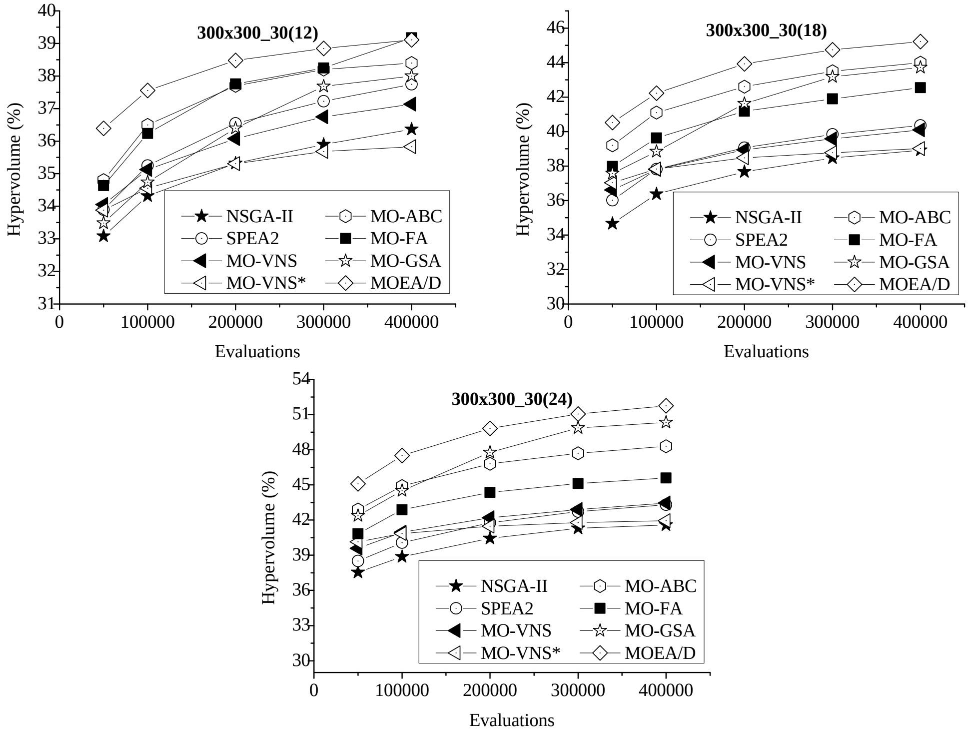

Figure 5.2: Convergence study based on the hypervolume metric. Part 2 of 2.

As noticed in Section 4.7.3, MO-GSA is the algorithm having an uneven trend, because of the way of working of this metaheuristic, e.g. in 100x100_30(2), 100x100_30(3), and 200x200_30(6). On the other hand, both MO-VNS and MO-VNS* show an uneven trend in 200x200_30(2), but only in this test case.

As discussed before, MO-FA and MOEA/D show a similar behaviour for large instances, being MO-FA the best in average term. Analysing this convergence study, MOEA/D seems to provide a better behaviour than MO-FA, when the number of RN is increased in such instances. For example in 200x200_30(9), 300x300_30(18) and 300x300_30(24).

From this convergence study, we can conclude that the stop conditions are representative to analyse the algorithms, the three better metaheuristics for all the instances (MO-FA, MO-VNS, and MOEA/D) show an homogeneous grown over stop conditions, and MOEA/D seems to outperform MO-FA in large instances, when the number of RNs is increased.

5.4.4 **Set Coverage Analysis**

In addition to hypervolume, we consider set coverage to analyse the behaviour of the algorithms. Table 5.9 shows the set coverage metric, comparing the metaheuristics two by two for all the instances, 50x50 instances, 100x100 instances, 200x200 instances and 300x300 instances. The *Percentage* field of this table shows the average set coverage regarding all other metaheuristics, where better values are shaded from darker to lighter tone.

As stated in Section 4.7.4, the set coverage is calculated by assuming the median Pareto fronts from the distribution of 31 samples. Note that the set coverage values shown in the table are the average metric for all the stop conditions, full values are in Section C.2 of Appendix C, specifically in Tables C.6, C.7, C.8, C.9, and C.10.

Analysing Table 5.9, we reach that MO-VNS* is the best algorithm for 50x50 instances, followed by MOEA/D and MO-ABC. For 100x100 instances, MO-VNS is the algorithm providing the best results, followed by MO-VNS* and MO-FA. In case of 200x200 instances, MO-FA is the best algorithm, followed by MOEA/D and SPEA2. For 300x300 instances, MO-FA is the best algorithm, followed by MOEA/D and MO-ABC. Finally, for all the instances, MO-FA is the algorithm providing the best behaviour, followed by MOEA/D and MO-VNS.

From this analysis, we notice that the conclusions obtained through hypervolume in Section 5.4.2 are similar to the obtained here by set coverage.

5.4.5 **Median Pareto Fronts**

Figures 5.3 and 5.4 show the median Pareto fronts obtained for 400 000 evaluations. Analysing these fronts, we reach similar conclusions as notice with hypervolume and set coverage. We do not include attainment surface due to this representation is not really clear for three objectives while comparing several fronts.

As stated for the bi-objective approach, we note that the distribution of the points in the objective space is not homogeneous, i.e. we find zones which were not covered by any algorithm. This could mean that the problem is not continuous.

As discussed before for hypervolume and set coverage, in case of 50x50_30(1), all the algorithms provide a similar behaviour because of the instance size. This way, we check that all the points are almost overlapped in this representation. On the other hand, we note that as the test case is harder, the number of points in such representation is greater.

Table 5.9: Average set coverage metric among all the metaheuristics, for all the instances, 50x50 instances, 100x100 instances, 200x200 instances, and 300x300 instances.

A dominates B (all the test cases)

A is dominated by B

A \ B	NSGA-II	SPEA2	MO-VNS	MO-VNS*	MO-ABC	MO-FA	MO-GSA	MOEA/D	Percentage
NSGA-II	#####	52,99%	13,42%	27,35%	17,18%	7,74%	53,46%	38,84%	30,14%
SPEA2	74,74%	#####	20,90%	30,64%	21,42%	12,68%	57,70%	40,18%	36,89%
MO-VNS	73,88%	65,02%	#####	52,55%	49,40%	35,07%	80,10%	69,61%	60,81%
MO-VNS*	63,20%	60,78%	36,22%	#####	53,27%	38,79%	71,61%	67,78%	55,95%
MO-ABC	65,72%	59,80%	30,54%	35,09%	#####	25,42%	56,74%	44,93%	45,46%
MO-FA	82,58%	78,65%	50,81%	51,26%	60,35%	#####	78,83%	79,09%	68,80%
MO-GSA	32,67%	31,00%	13,46%	21,20%	19,67%	15,52%	#####	40,72%	24,89%
MOEA/D	35,35%	32,25%	10,58%	14,13%	21,70%	6,22%	25,38%	#####	20,80%
Percentage	61,16%	54,36%	25,13%	33,18%	34,71%	20,21%	60,55%	54,45%	

A dominates B (50x50 test cases)

A is dominated by B

A \ B	NSGA-II	SPEA2	MO-VNS	MO-VNS*	MO-ABC	MO-FA	MO-GSA	MOEA/D	Percentage
NSGA-II	#####	100,00%	0,00%	7,55%	5,00%	2,04%	43,43%	2,13%	22,88%
SPEA2	100,00%	#####	0,00%	7,55%	5,00%	2,04%	43,43%	2,13%	22,88%
MO-VNS	100,00%	100,00%	#####	39,87%	65,45%	47,69%	98,99%	94,68%	78,10%
MO-VNS*	80,17%	80,08%	51,37%	#####	87,50%	75,51%	98,99%	82,98%	79,51%
MO-ABC	90,72%	90,68%	12,33%	16,98%	#####	10,20%	72,73%	34,04%	46,81%
MO-FA	100,00%	100,00%	41,78%	30,19%	92,50%	#####	96,97%	93,62%	79,29%
MO-GSA	51,13%	49,17%	0,34%	0,33%	7,27%	0,71%	#####	35,11%	20,58%
MOEA/D	90,72%	90,68%	1,71%	20,75%	57,50%	6,12%	32,32%	#####	42,83%
Percentage	87,53%	87,23%	15,36%	17,60%	45,75%	20,62%	69,55%	49,24%	

A dominates B (100x100 test cases)

A is dominated by B

A \ B	NSGA-II	SPEA2	MO-VNS	MO-VNS*	MO-ABC	MO-FA	MO-GSA	MOEA/D	Percentage
NSGA-II	#####	64,70%	14,17%	1,49%	16,97%	6,14%	75,17%	43,87%	31,79%
SPEA2	70,89%	#####	7,46%	0,37%	18,33%	6,39%	72,90%	47,39%	31,96%
MO-VNS	70,85%	76,75%	#####	40,96%	61,24%	42,27%	89,21%	88,83%	67,16%
MO-VNS*	93,48%	96,69%	42,70%	#####	63,03%	52,46%	96,61%	88,94%	76,27%
MO-ABC	54,64%	51,45%	17,51%	11,59%	#####	14,76%	53,46%	58,42%	37,40%
MO-FA	80,76%	82,72%	42,66%	29,85%	56,21%	#####	94,55%	81,39%	66,88%
MO-GSA	5,18%	15,68%	7,58%	5,08%	24,51%	0,13%	#####	44,44%	14,66%
MOEA/D	18,07%	16,58%	6,47%	1,27%	3,64%	1,90%	30,96%	#####	11,27%
Percentage	56,27%	57,79%	19,79%	12,94%	34,85%	17,72%	73,27%	64,75%	

A dominates B (200x200 test cases)

A is dominated by B

A \ B	NSGA-II	SPEA2	MO-VNS	MO-VNS*	MO-ABC	MO-FA	MO-GSA	MOEA/D	Percentage
NSGA-II	#####	33,07%	15,00%	40,22%	43,33%	3,18%	66,63%	66,67%	38,30%
SPEA2	59,94%	#####	34,04%	38,79%	51,12%	5,21%	79,86%	66,03%	47,86%
MO-VNS	67,71%	44,72%	#####	56,96%	47,84%	23,42%	85,65%	54,94%	54,46%
MO-VNS*	47,13%	49,91%	27,72%	#####	56,65%	9,60%	61,78%	60,37%	44,74%
MO-ABC	34,18%	23,19%	27,18%	26,70%	#####	9,06%	52,68%	37,44%	30,06%
MO-FA	84,58%	88,46%	56,53%	73,07%	78,95%	#####	75,48%	88,21%	77,90%
MO-GSA	17,13%	10,21%	3,39%	18,97%	13,46%	15,71%	#####	31,51%	15,77%
MOEA/D	8,35%	12,42%	10,70%	17,80%	14,60%	0,00%	29,91%	#####	13,40%
Percentage	45,57%	37,43%	24,94%	38,93%	43,71%	9,46%	64,57%	57,88%	

A dominates B (300x300 test cases)

A is dominated by B

A \ B	NSGA-II	SPEA2	MO-VNS	MO-VNS*	MO-ABC	MO-FA	MO-GSA	MOEA/D	Percentage
NSGA-II	#####	14,21%	24,52%	60,15%	3,42%	19,59%	28,61%	42,70%	27,60%
SPEA2	**68,12%**	#####	42,08%	75,86%	11,21%	37,09%	34,62%	45,18%	44,88%
MO-VNS	56,98%	38,63%	#####	72,42%	23,06%	26,90%	46,57%	39,99%	43,51%
MO-VNS*	**32,01%**	16,45%	23,08%	#####	5,91%	17,59%	29,07%	38,85%	23,28%
MO-ABC	**83,35%**	73,88%	65,13%	85,11%	#####	67,65%	48,10%	49,81%	67,57%
MO-FA	**64,98%**	43,42%	62,28%	71,92%	13,76%	#####	48,30%	53,16%	51,12%
MO-GSA	57,24%	48,94%	42,52%	60,44%	33,42%	45,52%	#####	51,83%	48,56%
MOEA/D	**24,26%**	9,31%	23,44%	16,71%	11,08%	16,87%	8,33%	#####	15,71%
Percentage	55,28%	34,98%	40,44%	63,23%	14,55%	33,03%	34,80%	45,93%	

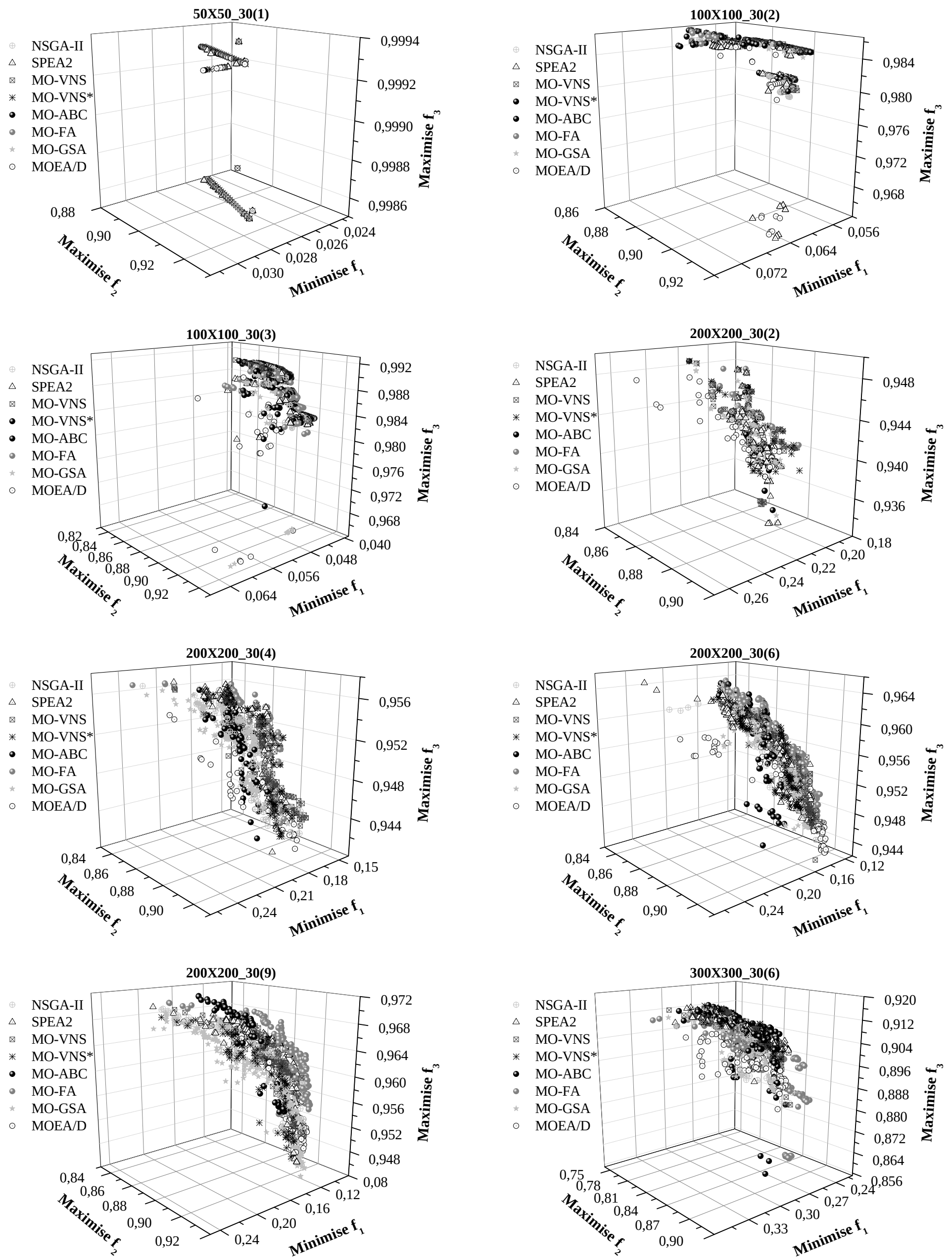

Figure 5.3: Convergence study based on the hypervolume metric. Part 1 of 2.

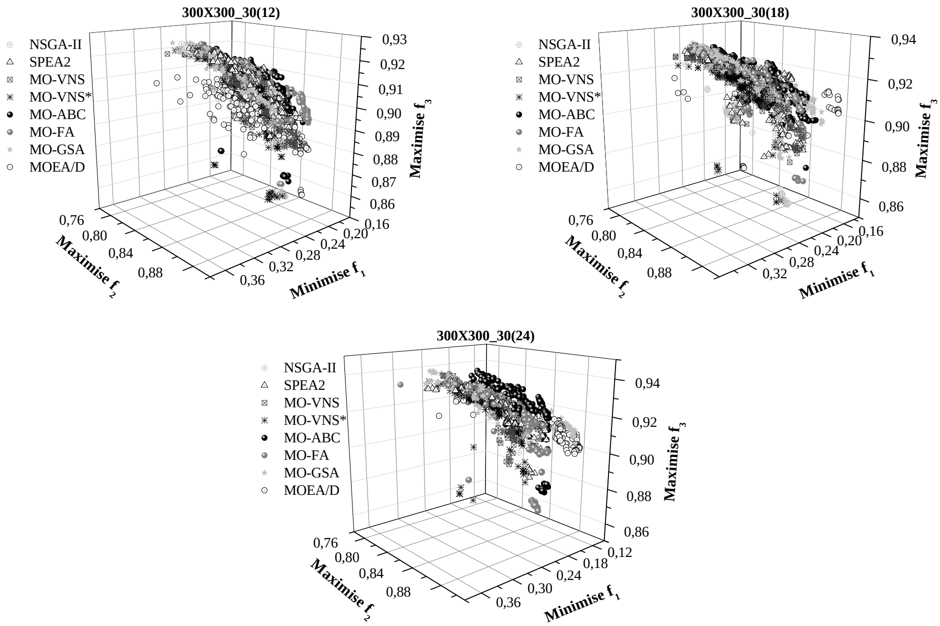

Figure 5.4: Convergence study based on the hypervolume metric. Part 2 of 2.

5.4.6 Impact of the Optimisation on the Fitness Functions

In this subsection, we analyse the impact of deploying RNs to traditional WSNs. Table 5.10 shows the extreme values obtained by MO-FA for 400 000 evaluations. Each extreme value is associated with the quality metrics I_G and I_{EF}. Both were discussed in Section 4.7.6.

According to this table, AEC is decreased up to 63.54% in 200x200_30(9), ASA is increased up to 16.36% in 300x300_30(24), and NR is increased up to 10.20% in 300x300_30(24). We notice that higher efficiency values are often obtained by assuming a reduced number of RNs. This way, the highest efficiency for AEC is 33.31% in 50x50_30(1), 2.64% for ASA in 300x300_-30(6), and 1.56% for NR in 100x100_30(2).

In conclusion, the addition of RNs seems to be a good way to optimise traditional WSNs, checking as AEC, ASA, and NR can be successfully optimised. However, the efficiency could be reduced if many RNs are deployed.

Table 5.10: Studying the extreme values of the median Pareto front obtained by MO-FA for 400 000 evaluations.

	max($f_1 : AEC$)		**min**($f_1 : AEC$)		**max**($f_2 : ASA$)		**min**($f_2 : ASA$)		**max**($f_3 : NR$)		**min**($f_3 : NR$)	
Instance($\tilde{\mathbf{s}}_\mathbf{r}$)	**value**	I_G,I_{EF}	**value**	I_G,I_{EF}	**value**	I_G,I_{EF}	**value**	I_G,I_{EF}	**value**	I_G,I_{EF}	**value**	I_G,I_{EF}
50x50_30(1)	0.0302	-14.39%,-14.39%	0.0235	-33.31%,**-33.31%**	92.07%	0.35%,0.35%	88.98%	-3.02%,-3.02%	99.93%	0.29%,0.29%	99.86%	0.22%,0.22%
100x100_30(2)	0.0712	-34.72%,-17.36%	0.0563	-48.38%,-24.19%	91.56%	2.60%,1.30%	87.34%	-2.13%,-1.06%	98.65%	3.11%,**1.56%**	98.06%	2.50%,1.25%
100x100_30(3)	0.0572	-47.54%,-15.85%	0.0430	-60.63%,-20.21%	91.61%	2.66%,0.89%	82.40%	-7.66%,-2.55%	99.21%	3.70%,1.23%	98.18%	2.63%,0.88%
200x200_30(2)	0.2381	-14.71%,-7.35%	0.1874	-32.87%,-16.44%	88.79%	1.94%,0.97%	85.46%	-1.88%,-0.94%	94.91%	1.81%,0.90%	94.00%	0.83%,0.41%
200x200_30(4)	0.2514	-9.92%,-2.48%	0.1631	-41.57%,-10.39%	89.44%	2.69%,0.67%	85.18%	-2.21%,-0.55%	95.73%	2.68%,0.67%	94.40%	1.26%,0.31%
200x200_30(6)	0.2075	-25.64%,-4.27%	0.1257	-54.96%,-9.16%	90.01%	3.34%,0.56%	86.39%	-0.82%,-0.14%	96.52%	3.53%,0.59%	94.58%	1.44%,0.24%
200x200_30(9)	0.2085	-25.29%,-2.81%	0.1018	**-63.54%**,-7.06%	90.67%	4.09%,0.45%	85.61%	-1.71%,-0.19%	97.07%	4.12%,0.46%	95.18%	2.09%,0.23%
300x300_30(6)	0.3474	-17.79%,-2.96%	0.2306	-45.41%,-7.57%	88.57%	15.86%,**2.64%**	78.20%	2.31%,0.38%	91.33%	7.09%,1.18%	85.95%	0.79%,0.13%
300x300_30(12)	0.3218	-23.84%,-1.99%	0.1962	-53.57%,-4.46%	88.73%	16.08%,1.34%	77.97%	2.00%,0.17%	92.54%	8.51%,0.71%	86.40%	1.31%,0.11%
300x300_30(18)	0.3146	-25.53%,-1.42%	0.1819	-56.94%,-3.16%	88.85%	16.23%,0.90%	78.04%	2.10%,0.12%	93.41%	9.54%,0.53%	86.84%	1.83%,0.10%
300x300_30(24)	0.3719	-11.97%,-0.50%	0.1591	-62.34%,-2.60%	88.95%	**16.36%**,0.68%	75.77%	-0.88%,-0.04%	93.98%	**10.20%**,0.43%	86.61%	1.56%,0.07%

Table 5.11: Solutions obtained through SPINDS heuristic.

	$f_1 : AEC$			$f_2 : ASA$			$f_3 : NR$		
Instance($\tilde{\mathbf{s}}_\mathbf{r}$)	**value**	I_G	I_{EF}	**value**	I_G	I_{EF}	**value**	I_G	I_{EF}
50x50_30(1)	0.0247	-29.89%	**-29.89%**	88.98%	-3.02%	-3.02%	99.86%	0.22%	0.22%
100x100_30(2)	0.0610	-44.11%	-22.06%	89.46%	0.25%	0.12%	98.54%	3.00%	**1.50%**
100x100_30(3)	0.0534	-51.06%	-17.02%	88.80%	-0.49%	-0.16%	98.95%	3.43%	1.14%
200x200_30(2)	0.2655	-4.89%	-2.44%	86.45%	-0.75%	-0.37%	94.13%	0.96%	0.48%
200x200_30(4)	0.1851	-33.69%	-8.42%	86.22%	-1.01%	-0.25%	94.46%	1.32%	0.33%
200x200_30(6)	0.1653	-40.77%	-6.80%	85.68%	-1.63%	-0.27%	94.46%	1.32%	0.22%
200x200_30(9)	0.1171	**-58.05%**	-6.45%	86.15%	-1.09%	-0.12%	94.65%	1.52%	0.17%
300x300_30(6)	0.3853	-8.80%	-1.47%	80.38%	**5.16%**	**0.86%**	90.16%	5.72%	0.95%
300x300_30(12)	0.3853	-8.80%	-0.73%	80.38%	**5.16%**	0.43%	90.17%	**5.74%**	0.48%
300x300_30(18)	0.3301	-21.86%	-1.21%	78.04%	2.10%	0.12%	89.62%	5.09%	0.28%
300x300_30(24)	0.3301	-21.86%	-0.91%	78.04%	2.10%	0.09%	89.62%	5.08%	0.21%

5.4.7 Comparisons to Other Approaches

In this subsection, we compare the results obtained by our approach to another authors approach. As stated in Section 4.7.7, we started this work by assuming an important limitation: we did not find any paper fitting this problem definition. As a way to attenuate this deficiency, we implemented the heuristic called SPINDS proposed by Hou et al. Specific details for implementing this heuristic were discussed in Section 4.7.7.

Comparing Tables 5.10 and 5.11, we note that MO-FA provides a better behaviour than SPINDS for all the test cases. In fact, all the results provided by SPINDS are dominated by MOFA. This way, we check that our proposal provides a better behaviour than another authors approach from the literature.

5.5 Scientific Achievements

In this chapter, we proposed and solved a three objective RNPP by assuming a wide range of MO metaheuristics. The following contributions were obtained from performing this task:

International journals (ISI-SCI):

- Jose M. Lanza-Gutierrez and Juan A. Gomez-Pulido. Assuming multiobjective metaheuristics to solve a three-objective optimisation problem for relay node deployment in wireless sensor networks. Applied Soft Computing, 30:675–687, 2015. Impact factor of 2.810 ($Q1$, $T1$). In [84], we apply NSGA-II, SPEA2, MO-VNS, MO-ABC, MO-FA, and MOEA/D for solving the problem.
- Jose M. Lanza-Gutierrez, Juan A. Gomez-Pulido, and Miguel A. Vega-Rodriguez. A new realistic approach for the relay node placement problem in wireless sensor networks by means of evolutionary computation. Ad Hoc and Sensor Wireless Networks, 26:193–209, 2015. Impact factor of 0.435 ($Q4$, $T3$). In [85], we apply NSGA-II and SPEA2 for solving the problem in 100x100, 200x200, and 300x300 instances.

International book chapters:

- Jose M. Lanza-Gutierrez, Juan A. Gomez-Pulido, and Miguel A. Vega-Rodriguez. A trajectory-based heuristic to solve a three-objective optimization problem for wireless sensor network deployment. In Applications of Evolutionary Computation, volume 8602 of Lecture Notes in Computer Science, pages 27–38. Springer Berlin / Heidelberg, 2014. In [86], we apply NSGA-II, SPEA2, and MO-VNS* for optimising 100x100, 200x200, and 300x300 instances.

National conferences:

- Jose M. Lanza-Gutierrez, Juan A. Gomez-Pulido, and Miguel A. Vega-Rodriguez. Un nuevo enfoque para el posicionamiento de routers sobre redes de sensores inalámbricos. In Actas del XV Conferencia de la Asociación Española para la Inteligencia Artificial (CAEPIA 13) - IX Congreso Español sobre Metaheurísticas, Algoritmos Evolutivos y Bioinspirados (MAEB 2013), pages 743–752, 2013. In [87], we apply NSGA-II and SPEA2 for optimising 100x100, 200x200, and 300x300 instances. This is a very preliminary work.

CHAPTER

6

Solving the RNPP: a Novel three-objective Indoor Approach

In this chapter, we propose and solve a novel approach of the RNPP, where we try to leverage existing infrastructure for indoor scenarios, while optimising three objectives. This approach is based on the knowledge obtained from Chapters 4 and 5. This chapter is structured as follows. The WSN model considered is presented in Section 6.1. The optimisation problem is defined in Section 6.2. Section 6.3 discusses the data set considered for comparing the metaheuristics while solving the problem. Chromosome definition and specific considerations for implementing the metaheuristics are detailed in Sections 6.4 and 6.5, respectively. Experimental results are discussed in Section 6.6. Finally, we list the scientific achievements obtained from solving this optimisation problem in Section 6.7.

6.1 The Wireless Sensor Network Model assumed

This section describes the WSN model considered in this three-objective indoor approach of the RNPP. The notation assumed is listed in Section 6.1.1. The general assumptions of the model are presented in Section 6.1.2. Connectivity is defined in Section 6.1.3. Finally, energy expenditure, coverage area, and network lifetime are discussed in Sections 6.1.4, 6.1.5, and 6.1.6, respectively.

6.1.1 Notation

The following notation is considered for modelling the WSN definition:

α path loss exponent, $\alpha \in [2, 4]$;

β	transmission quality parameter, $\beta > 0$;
τ	set of time periods, $\tau = \{0, 1, 2, \ldots\}$;
$A_{tp}(t)$	coverage area provided by the WSN at time $t > 0 \in \tau$, according to the transmission power level on the scenario;
$a_p^{tp}(t)$	variable assuming 1 if there is any sensor i such that the transmission power needed to reach the demand point p is lower than tp_{th}, and 0 otherwise, with $i \in S_b(t) \cup S_p(t)$ and $p \in \tilde{D}_p(t)$;
amp	energy cost per bit of the power amplifier, $amp > 0$;
$brick_{lost}$	attenuation caused by a red brick wall, when a signal passes through it, $brick_{lost} > 0$;
c	sink coordinates, $c = (x, y)$ where $x \in [0, d_x]$ and $y \in [0, d_y]$;
co_{th}	coverage threshold, $co_{th} \in [0, 1]$;
$\tilde{D}_p(t)$	set of demand points at time $t > 0$, $\forall p \in \tilde{D}_p,\ p = (x, y)$ where $x \in [0, d_x]$ and $y \in [0, d_y]$;
$\tilde{d}_p(t)$	number of demand points. It is the cardinal of $\tilde{D}_p(t)$;
d_{pn}	distance between two neighbouring demand points;
$djp_i^c(t)$	number of disjoint paths between the sensor $i \in S_b(t) \cup S_p(t)$ and the sink node at time $t > 0$;
d_x	width of the surface, $d_x > 0$;
d_y	height of the surface, $d_y > 0$;
$Ecb_i(t)$	energy charge of a sensor powered by batteries $i \in S_b(t)$ at time t;
$Eeb_i(t)$	energy expenditure of a sensor powered by batteries $i \in S_b(t)$ at time $t > 0$;
err	constant local channel error, $err \in [0, 1]$;
f_1	AEC of the sensors over the network lifetime;
f_2	ASA provided by the WSN over the network lifetime;
f_3	ANR provided by the WSN over the network lifetime;
$h_l^{i,c}(t)$	number of hops in the l-th disjoint path between $i \in S_b(t) \cup S_p(t)$ and the sink node at time $t > 0$;
iec	initial energy charge of the sensors powered by batteries, $iec > 0$;
k	information packet size in bits, $k > 0$;
t_n	network lifetime of the WSN based on the coverage threshold co_{th};
$Pb_i(t)$	number of packets sent by the sensor powered by batteries $i \in S_b(t)$ at time $t > 0$;
$\tilde{P}_l$	set of plugs on the scenario, $\forall p \in \tilde{P}_l$, $p = (x, y)$, where $x \in [0, d_x]$ and $y \in [0, d_y]$;
$re_i(t)$	reliability of the sensor $i \in S_b(t) \cup S_p(t)$ at time $t > 0$;

$Rpb_i(t)$	number of relayed packets sent by the sensor powered by batteries $i \in S_b(t)$ at time $t > 0$;
$tcst$	transmission constant, $tcst > 0$;
tp_{th}	transmission power threshold, it determines if the transmission power level is enough for receiving correctly a data packet;
$tpn_{i,j}(t)$	transmission power needed to send data from i to j at time $t > 0$, with $i, j \in S_b(t) \cup S_p(t) + c$ and $i \neq j$;
t_n^{tp}	network lifetime of the WSN based on the coverage threshold co_{th};
$\tilde{S}_b$	set of initial sensor coordinates powered by batteries, $\forall b \in \tilde{S}_b$, $b = (x, y)$ where $b \in [0, d_x]$ and $b \in [0, d_y]$;
$\tilde{s}_b$	number of sensor coordinates powered by batteries. It is the cardinal of $\tilde{S}_b$;
$\tilde{S}_p$	set of initial sensor coordinates plugged into the grid, $\forall p \in \tilde{S}_p$, $p = (x, y)$, where $p \in [0, d_x]$ and $p \in [0, d_y]$;
$\tilde{s}_p$	number of initial sensors plugged into the grid. It is the cardinal of $\tilde{S}_p$;
$S_b(t)$	set of sensor coordinates powered by batteries, holding that the energy charge is greater than 0 and that there is any path to the sink node, both at time $t > 0$, $S_b(t) \subseteq \tilde{S}_b$;
$s_b(t)$	number of sensors powered by batteries, holding that the energy charge is greater than 0 and that there is any path to the sink node, both at time $t > 0$. It is the cardinal of $S_b(t)$, $s_b(t) \leq \tilde{s}_b$;
$\tilde{s}_{bp}$	number of sensors (including both types), which will be deployed in the WSN, $\tilde{s}_{bp} > 0$;
$S_p(t)$	set of sensor coordinates plugged into the grid, holding that there is any path to the sink node at time $t > 0$, $S_p(t) \subseteq \tilde{S}_p$;
$s_p(t)$	number of sensors plugged into the grid, holding that there is any path to the sink node at time $t > 0$. It is the cardinal of $S_p(t)$, $s_p(t) \leq \tilde{s}_p$;
$w_i^c(t)$	variable which provides the next device in the minimum path between $i \in S_b(t) \cup S_p(t)$ and the sink node at $t > 0$, $w_i^c(t) \in \{S_b(t) \cup S_p(t)\} + c - i$;
$wlost_{i,j}(t)$	signal attenuation because of walls at $t > 0$, when sending data from i to j, with $i, j \in S_b(t) \cup S_p(t) + c$ and $i \neq j$;
$\tilde{W}_r$	set of red brick walls on the scenario, $\forall w \in \tilde{W}_r$, $w = (x, y)$, where $w \in [0, d_x]$ and $w \in [0, d_y]$;
$y_{i,j}^w(t)$	variable assuming 1 if the signal emitted by $i \in S_b(t) \cup S_p(t)$ has to necessarily pass through $w \in \tilde{W}_r$ to reach $j \in S_b(t) \cup S_p(t) + c$ at $t > 0$, and 0 otherwise;
$z_{j,i}^c(t)$	variable assuming 1 if $i \in S_b(t) \cup S_p(t)$ is in the minimum path between $j \in S_b(t) \cup S_p(t)$ and the sink node at $t > 0$, and 0 otherwise.

6.1.2 Assumptions of the Wireless Aensor Network Model

The general assumptions of the network model are:

1. The network is composed of three types of wireless static devices: a sink node plugged into the grid, $\tilde{s}_b$ sensors powered by batteries, and $\tilde{s}_p$ sensors plugged into the grid. They send messages by following a ST approach.

2. All the devices are placed on a same indoor 2D-surface of size d_x x d_y, which includes red brick walls whose coordinates are given by W_r. We consider that there are not interferences from other electronic devices.

3. We suppose that the sensors powered by batteries can be placed on anywhere of the surface, excepting on the walls. The sensors plugged into the grid can only be deployed in one of the plugs given by P_l. Such plugs are placed on the walls. Thus, we follow a constrained approach of the RNPP.

4. Initially, at time $t = 0$, all the sensors powered by batteries start with the same energy capacity iec in their batteries. If during operation, $t > 0$, a sensor is exhausted, it cannot be linked again.

5. The sink node is the only connection point of the network to the outside.

6. Both types of sensor capture information about the environment on a regular basis. Once the information is captured, it is immediately sent to the sink node.

7. Any two devices can be linked, if the transmission power needed is lower or equal than tp_{th}. In the case of sensors powered by batteries, the sensors must have enough energy capacity in their batteries.

8. The signal is attenuate, when it passes through a wall. The attenuation caused by a red brick is given by $brick_{lost}$.

9. All the devices consider the same multi-hop routing protocol provided by Dijsktra's Algorithm, for minimum path length among devices.

10. We suppose a perfect synchronisation among devices and the use of an efficient MAC protocol, such as S-MAC, which allows reducing energy cost on idle time.

6.1.3 Connectivity

In this chapter, we consider a more realistic approach, where connectivity is defined according to the transmission power needed to send data between any two devices, including attenuation because of walls. Thus, the transmission power needed $tpn_{i,j}(t)$ to send data from i to j at time $t > 0$, with $i, j \in S_b(t) \cup S_p(t) + c$ and $i \neq j$, is given by

$$tpn_{i,j}(t) = \frac{tcst}{||i-j||_d^2} 10^{wlost_{i,j}(t)10^{-1}}, \tag{6.1}$$

where $||\cdot||_d$ is the Euclidean distance between any two devices, $tcst$ is a transmission constant, and $wlost_{i,j}(t)$ is the signal attenuation because of walls at t, which is expressed as

$$wlost_{i,j}(t) = \sum_{w \in \tilde{W}_r} y_{i,j}^w(t)\ brick_{lost},$$

where $y^w_{i,j}(t)$ is a variable assuming 1 if the signal emitted by i has to necessarily pass through $w \in \tilde{W}_r$ to reach j at t, and 0 otherwise.

According to Equation (6.1), any two devices can be linked directly if the transmission power needed is lower than a certain threshold tp_{th} determined by the technical characteristics of the device. We assume that all the devices have a same value for this threshold.

6.1.4 Energy Expenditure

Following the approach presented in Chapter 4, we consider the same energy model proposed by Konstantinidis et al. [55] to simulate the energy expenditure of the sensors powered by batteries. We redefine this formulation because of the notation considered in this chapter is different.

Attending to this model, a sensor powered by batteries $i \in S_b(t)$, sends a number of data packets $Pb_i(t)$ at time $t \in \tau$ and $t > 0$ given by

$$Pb_i(t) = 1 + Rpb_i(t). \tag{6.2}$$

This means that Equation (6.2) is given by the sum of the number of data packets generated by i at t (in this case, we consider that each sensor captures a data packet per time period) and the number of relayed packets because of the multi-hop routing approach, which is expressed as

$$Rpb_i(t) = \sum_{j \in \{S_b(t) \cup S_p(t) - i\}} z^c_{j,i}(t). \tag{6.3}$$

Note that for calculating Equation (6.3), we consider that both types of sensor capture data. Moreover,we should mention that control packets from routing and MAC protocols were not simulated, because this is not the aim of this dissertation.

Based on this expression, the energy cost $Eeb_i(t)$ of a sensor powered by batteries i at time $t > 0$ is given by

$$Eeb_i(t) = Pb_i(t)\ \beta\ amp\ k\ (\|i - w^c_i(t)\|_d)^\alpha. \tag{6.4}$$

This way, the energy charge of a sensor powered by batteries i at time t is given by

$$Ecb_i(t) = \begin{cases} Ecb_i(t-1) - Eeb_i(t) & \text{if } t > 0 \\ iec & \text{if } t = 0 \end{cases}.$$

If this value equals zero, the sensor is out of energy; otherwise, it is active.

6.1.5 Coverage Area

In Chapters 4 and 5, we defined the coverage area of the WSN according to a constant sensitivity radius for all the sensors. In this chapter, we consider a more realistic approach, where the coverage is calculated based on the transmission power level on the scenario. Thus, we consider that an area of the surface is non-covered if the transmission power needed to reach any active device from this area is greater than the threshold tp_{th}.

As for the previous chapters, a set of demand points uniformly distributed on the surface $\tilde{D}_p(t)$ is assumed to approximate this area. Based on this idea, the coverage area provided by a WSN at time $t > 0$ is given by

$$A_{tp}(t) = \frac{\sum_{p \in \tilde{D}_p(t)} a^{tp}_p(t)}{\tilde{d}_p(t)}, \tag{6.5}$$

where $a_p^{tp}(t)$ is the indicator function expressed as

$$a_p^{tp}(t) = \begin{cases} 1 & \text{if } \exists i \in S_b(t) \cup S_p(t) : tpn_{i,p}(t) < tp_{th} \\ 0 & \text{otherwise} \end{cases},$$

where $tpn_{i,p}(t)$ is given by Equation (6.1). Thus, $a_p^{tp}(t)$ equals 1 if there is any sensor i such that the transmission power needed to reach the demand point p is lower than tp_{th}, and 0 otherwise. The accuracy of this metric was studied in Chapter 4, specifically in Section 4.1.4.

6.1.6 Network Lifetime

We consider the same criteria for calculating the network lifetime as in Chapters 4 and 5. Consequently, this value is defined according to the time until the information provided by the network is not enough. To this end, we consider the new formulation for calculating the coverage area. That is,

$$t_n^{tp} = ||\{t > 0 \in \tau : A_{tp}(t) > co_{th}\}||, \tag{6.6}$$

where $A_{tp}(t)$ is given by Equation (6.5) and co_{th} is the coverage threshold.

6.1.7 Network Reliability

As in Chapter 5, we assume that the reliability is calculated according to the number of disjoint paths between a given sensor and the sink node. However, in this approach, we consider that this metric depends on the time instant. Thus, given a sensor $i \in S_b \cup S_p$, the reliability $re_i^{tp}(t)$ of i at time $t > 0$ is denoted as

$$re_i^{tp}(t) = 1 - \prod_{l=1}^{djp_i^c(t)} \left(1 - (1 - err)^{h_l^{i,c}(t)}\right),$$

where $djp_i^c(t)$ is the number of disjoint paths between i and the sink node at t, $h_l^{i,c}(t)$ is the number of hops in the l-th disjoint path between both devices at t, and err is a constant local channel error. Note that the disjoint paths are calculated through Suurballe's Algorithm [82].

6.2 Problem Formulation

Let f_1 be the AEC of the sensors over the network lifetime. That is expressed as

$$f_1 = \frac{\sum_{t=1}^{t_n^{tp}} \left(\sum_{i \in S_b(t)} \frac{Eeb_i(t)}{s_b(t)} \right)}{t_n^{tp}}, \tag{6.7}$$

where $f_1 \in \mathbb{R}^+$ and both $Eeb_i(t)$ and t_n^{tp} are given by Equations (6.4) and (6.6), respectively.

Let f_2 be the ASA provided by the network, which is expressed as

$$f_2 = \frac{\sum_{t=1}^{t_n^{tp}} A_{tp}(t)}{t_n^{tp}}, \tag{6.8}$$

where $f_2 \in [0, 1]$ and $A_{tp}(t)$ is given by Equation (6.5).

Let f_3 be the ANR, showing the probability that the sensors successfully send information to the sink node over the network lifetime. That is

$$f_3 = \frac{\sum_{t=1}^{t_n^{tp}} \left(\sum_{i \in S_b(t) \cup S_p(t)} \frac{re_i^{tp}(t)}{s_b(t) + s_p(t)} \right)}{t_n^{tp}}, \quad (6.9)$$

where $f_3 \in [0, 1]$ and $re_i(t)$ is given by Equation (6.1.7).

This way, we define the constrained indoor RNPP as a three-objective optimisation problem, where given a scenario including walls and plugs, i.e. $\tilde{W}_r$ and $\tilde{P}_l$, the objective is to place $\tilde{s}_{bp}$ sensors (including both types) by assuming an ST network model to

$$\min(f_1), \max(f_2), \text{ and } \max(f_3),$$

subject to

$$\forall i \in \tilde{S}_b \cup \tilde{S}_p,\ i = (x, y),\ i \notin \tilde{W}_r : x \in [0, d_x]\ y \in [0, d_y],$$
$$\forall i \in \tilde{S}_p, i \in \tilde{P}_l,$$
$$\forall i \in \tilde{S}_b, i \notin \tilde{P}_l,$$
$$\tilde{s_b} + \tilde{s_p} = \tilde{s}_{bp}.$$

6.3 Description of the Dataset

As for the outdoor approach, we did not find any data set fitting this problem definition. This situation led us to define a new data set, with the purpose of providing a common framework for studying the indoor RNPP in future works. The new data set is composed of two different instances inspired by a real building with sizes 216.99m^2 and 577.28m^2, including walls and plugs, and is freely available in [65]

As stated before, this WSN model includes several parameters. We consider $\alpha = 2.00$, $\beta = 1.00$, $co_{th} = 0.70\%$, $k = 10$Kb, $iec = 0.005$J, $amp = 100$pJ/bit/m^2, $err = 0.10$, and $tcst = 100$ from [81] [61], [88], and [66]. Figures 6.1 and 6.2 show detailed information of these two instances according to the following criteria:

- **a) Main features:** We show the instance name, the position of the sink node, the reference points for calculating the hypervolume metric, which were obtained experimentally, and the test cases. Note that we consider that a test case is the total number or sensors (both types), which we deploy in the scenario. Being as adding such devices increases the network cost, we consider a reduced number of sensors but enough for covering all the surface. Thus, we define three test cases for 21.40x10.14 instance and seven for 32.80x17.60 instance.

- **b) Deployment details:** We include two tables and a figure. The tables detail plug coordinates and wall segments. The figure show the position of plugs and walls on the scenario. Note that for the definition of wall segments, we consider starting and ending points.

Instance name	Sink node	Reference points (f_1, f_2, f_3)		Test cases $(\tilde{s}_{bp})$
$(d_x \times d_y)$	(x-coordinate, y-coordinate)	ideal	nadir	
21.40x10.14	(10.70,5.07)	(0.00000,100.00,100.00)	(0.00006,50.00,80.00)	2, 3, 4

(a) Main features.

($\tilde{P}_1$) Plug coordinates: plugID , (x-coordinate, y-coordinate)							
#1	(0.10,6.90)	#3	(1.30,3.50)	#5	(21.30,6.70)	#7	(18.70,0.00)
#2	(9.70,5.70)	#4	(15.10,10.30)	#6	(15.50,3.50)	#8	(7.90,10.30)

($\tilde{P}_1$) Wall segments: wallID , (x-coordinate, y-coordinate)-(x-coordinate, y-coordinate)			
#1	(0.10,6.90)-(0.10,6.90)	#3	(0.10,6.90)-(0.10,6.90)

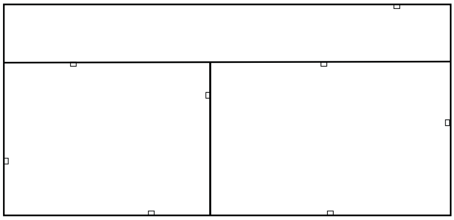

(b) Deployment details.

Figure 6.1: Instace 21.40x10.14.

Instance name	Sink node	Reference points (f_1, f_2, f_3)		Test cases $(\tilde{s}_{bp})$
$(d_x \times d_y)$	(x-coordinate, y-coordinate)	ideal	nadir	
32.80x17.60	(16.40,8.80)	(0.00000,100.00,100.00)	(0.00025,15.00,70.00)	2, 3, . . ., 8

(a) Main features.

($\tilde{P}_1$) Plug coordinates: plugID , (x-coordinate, y-coordinate)							
#1	(0.05,2.5)	#5	(14.25,6.1)	#9	(9.5,10.35)	#13	(25.5,10.65)
#2	(0.05,11.5)	#6	(19.9,0.05)	#10	(5.85,16.7)	#14	(27.15,16.5)
#3	(5.85,6.1)	#7	(27.15,1.1)	#11	(13.7,17.55)	#15	(32.75,3.5)
#4	(13.95,1.1)	#8	(26.3,7.25)	#12	(15.85,15.7)	#16	(32.75,15.1)

($\tilde{P}_1$) Wall segments: wallID , (x-coordinate, y-coordinate)-(x-coordinate, y-coordinate)					
#1	(0.10,6.90)-(0.10,6.90)	#3	(0.10,6.90)-(0.10,6.90)	#5	(0.10,6.90)-(0.10,6.90)
#2	(0.10,6.90)-(0.10,6.90)	#4	(0.10,6.90)-(0.10,6.90)	#6	(0.10,6.90)-(0.10,6.90)

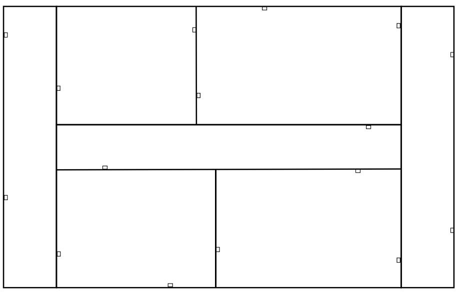

(b) Deployment details.

Figure 6.2: Instace 32.80x17.60.

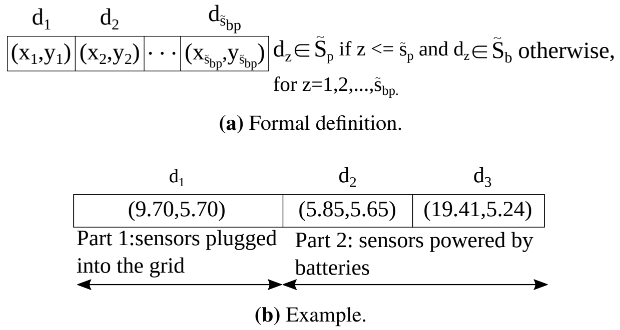

(a) Formal definition.

(b) Example.

Figure 6.3: Chromosome Statement.

6.4 Chromosome Definition

We consider a same chromosome structure for all the metaheuristics. As stated before, a chromosome is a possible solution to the optimisation problem and the objective of the RNPP defined in Section 6.2 is to place $\tilde{s}_{bp}$ sensors. This way, as Figure 6.3a shows, we assume that a chromosome consists of two parts, each one is composed of $\tilde{s}_p$ and $\tilde{s}_b$ genes, respectively. The sum of both parts equals $\tilde{s}_{bp}$ and a gene is bi-dimensional coordinate. We include an example of this encoding in Figure 6.3b by assuming the instance 21.40x10.14 and $\tilde{s}_b = 2$ and $\tilde{s}_p = 1$.

6.5 Scientific Achievements

In this chapter, we proposed and solved a novel three-objective indoor RNPP by considering the two classic MO metaheuristics. The following scientific achievements were obtained from performing this task:

International book chapters:

- Jose M. Lanza-Gutierrez, Juan A. Gomez-Pulido, S. Priem-Mendes, M. Ferreira, and J.S. Pereira. Planning the deployment of indoor wireless sensor networks through multiobjective evolutionary techniques. In *Applications of Evolutionary Computation*, volume 9028 of *Lecture Notes in Computer Science*, pages 128–139. Springer International Publishing, 2015. In [89], we apply NSGA-II and SPEA2 for solving the problem.

CHAPTER

7

Conclusions and Future Works

In this chapter, we include the conclusions obtained from performing the tasks presented in this PhD thesis and the future extension lines of this research. Both in Sections 7.1 and 7.2, respectively.

7.1 Conclusions

In this PhD thesis, we have studied three different approaches of the RNPP for WSNs These three approaches can be divided into two groups: outdoor and indoor networks. In the first two approaches (Chapters 4 and 5), we studied the deployment of RNs in traditional low-cost static previously-established outdoor WSNs, while optimising several relevant factors for the industry: ASA and AC in Chapter 4, and ASA, AC, and NR in Chapter 5. Thus, Chapter 5 is the natural evolution of the research line in Chapter 4 by including an additional conflicting objective function to optimise.

Because of the RNPP was defined as an NP-hard optimisation problem in the literature, it cannot be solved through exact techniques. Instead, we considered approximate techniques. Specifically MO metaheuristics, which ,in general, provide a good behaviour solving such type of problems. In this line, we assumed the two classic GAs NSGA-II and SPEA2, the trajectory algorithm MO-VNS, three swarm intelligence algorithms MO-GSA, MO-ABC, and MO-FA, and a state-of-the-art decomposition algorithm MOEA/D. Only four of these algorithms were MO in the original definition, which were NSGA-II, SPEA2, MO-VNS, and MOEA/D. Hence, the remainder algorithms were MO approaches proposed by ourselves, they are MO-GSA, MO-ABC, and MO-FA.

All these MO metaheuristics were applied for solving the two outdoor RNPP approaches by assuming a freely available data set. This benchmark was designed by ourselves at the beginning of this research lines, because we did not find any work fitting this problem definition. The results obtained were analysed by assuming three MO quality metrics (hypervolume, set coverage, and attainment surface) and a widely accepted statistical methodology. As a result, we checked that the swarm intelligence algorithm MO-FA provides the best significant average behaviour, when solving the first two outdoor approaches of the RNPP. Moreover, we studied the effects in the objective functions of adding RNs in traditional WNSs, checked that the addition of such devices was a good way to optimise previously established traditional WSNs, without replacing the all network, which is important of the industry.

From this study, we also noted that the addition of RNs in outdoor WSNs is a really hard problem, according to the instance size, as expected from an NP-hard problem. This means that the metaheuristics can exploit all their potential. In fact, we checked that the implemented methods provided better results than other approaches from the current literature.

Following with the second group (indoor networks). In Chapter 6, we proposed and solved a novel approach of the RNPP, where we tried to leverage existing infrastructure. This problem definition is interesting for industrial applications, whose aim is to provide localisation services for indoor environments. The goal of levering infrastructures allow reducing the deployment cost of the network, providing the benefit of assuming devices plugged into the grid.

This novel approach was defined by assuming the knowledge obtained by solving the two previous outdoor approaches. This way, this model incorporated some elements, involving that the computation cost of this problem was higher that the previous approach, such as the inclusion of signal attenuation because of walls. This means that this problem was harder than the other approaches, and then MO metaheuristics were good candidates to solve it. With this purpose, we considered the two classic MO metaheuristics NSGA-II and SPEA2 as a first approach in this research line, checking as these algorithms provided a good behaviour by solving such problem.

7.2 Future Works

According to the knowledge obtained from this PdH thesis, we can define several future lines of research. On the one hand, we could consider another optimisation problem and apply all the knowledge obtained in solving methods to enhance this field. At this moment, we are sharing our experiences in such MO algorithms with other researchers to solve a well-known NP-hard problem from a novel MO approach.

On the other hand, we could work with WSNs, applying the results obtained to real networks. Currently, we are exchanging experiences with an agriculture research center as a possible way to transfer this knowledge to the real world. Moreover, we could define more instances for all the approaches of the RNPP, including new solving method and simulating more realistic aspects of WSNs, such as MAC and routing protocols.

CHAPTER

8

Scientific Production

In this chapter, we present the scientific achievements obtained during the course of this PhD thesis. As we will discuss, we have obtained a total of 24 publications from 2011 to present, directly or indirectly related to this thesis, including 8 international indexed journals (ISI-SCI), 5 international book chapters, 3 international conferences, and 8 national conferences. These publications allow validating the quality and relevance of this thesis in the scientific literature.

This chapter is structured as follows. Section 8.1 details the scientific publications directly related to this dissertation. Section 8.2 includes all the contributions partially related to this thesis. Finally, Section 8.3 lists other merits obtained during this period.

8.1 Scientific Publications Directly Related to this Dissertation

In this section, we list the publications obtained directly related to this dissertation, including 6 international indexed journals (ISI-SCI), 5 international book chapters, 2 international conferences, and 6 national conferences.

International indexed journals (ISI-SCI):

- Juan A. Gomez-Pulido and Jose M. Lanza-Gutierrez. Reliability and efficiency in wireless sensor networks: heuristic approaches. *Journal of Heuristics*, 21(2): 141–143, 2015. Impact factor of 1.135 ($Q2$, $T2$). In [90], we provide a state-of-the-art of authors solving WSN problems by heuristic approaches.
- Jose M. Lanza-Gutierrez and Juan A. Gomez-Pulido. Assuming multiobjective metaheuristics to solve a three-objective optimisation problem for relay node deployment in wireless sensor networks. *Applied Soft Computing*, 30:675–687, 2015. Impact factor of 2.810 ($Q1$, $T1$). In [84], we apply NSGA-II, SPEA2, MO-VNS, MO-ABC, MO-FA, and MOEA/D for solving the problem in Chapter 5.

- Jose M. Lanza-Gutierrez, Juan A. Gomez-Pulido, and Miguel A. Vega-Rodriguez. A new realistic approach for the relay node placement problem in wireless sensor networks by means of evolutionary computation. *Ad Hoc and Sensor Wireless Networks*, 26:193–209, 2015. Impact factor of 0.435 ($Q4$, $T3$). In [85], we apply NSGA-II and SPEA2 for solving the problem in Chapter 5 for 100x100, 200x200, and 300x300 instances.
- Jose M. Lanza-Gutierrez and Juan A. Gomez-Pulido. A gravitational search algorithm for solving the relay node placement problem in wireless sensor networks. *International Journal of Communication Systems*, page n/a (on-line), 2015. Impact factor of 1.106 ($Q3$, $T2$). In [70], we apply NSGA-II, SPEA2, and MO-GSA for optimising the problem in Chapter 4 with 100x100 and 200x200 instances.
- Jose M. Lanza-Gutierrez and Juan A. Gomez-Pulido. Studying the multiobjective variable neighbourhood search algorithm when solving the relay node placement problem in wireless sensor networks. *Soft Computing*, page n/a (on-line), 2015. Impact factor of 1.271 ($Q3$, $T2$). In [71], we apply NSGA-II, SPEA2, MO-VNS, and MO-VNS* for optimising the problem in Chapter 4 with all the instances.
- Jose M Lanza-Gutierrez, Juan A Gomez-Pulido, and Miguel A Vega-Rodriguez. Intelligent relay node placement in heterogeneous wireless sensor networks for energy efficiency. *International Journal of Robotics and Automation*, 29:1–13, 2014. Impact factor of 0.408 ($Q4$, $T3$). In [72], we apply the metaheuristics NSGA-II, SPEA2, and MO-ABC for solving the problem in Chapter 4 with 100x100, 200x200, and 300x300 instances.

International book chapters:

- Jose M. Lanza-Gutierrez, Juan A. Gomez-Pulido, S. Priem-Mendes, M. Ferreira, and J.S. Pereira. Planning the deployment of indoor wireless sensor networks through multiobjective evolutionary techniques. In *Applications of Evolutionary Computation*, volume 9028 of *Lecture Notes in Computer Science*, pages 128–139. Springer International Publishing, 2015. In [89], we apply NSGA-II and SPEA2 for optimising the problem in Chapter 6.
- Jose M. Lanza-Gutierrez, Juan A. Gomez-Pulido, and Miguel A. Vega-Rodriguez. A trajectory-based heuristic to solve a three-objective optimization problem for wireless sensor network deployment. In *Applications of Evolutionary Computation*, volume 8602 of *Lecture Notes in Computer Science*, pages 27–38. Springer Berlin / Heidelberg, 2014. In [86], we apply NSGA-II, SPEA2, and MO-VNS* for optimising the problem in Chapter 5 with 100x100, 200x200, and 300x300 instances.
- Jose M. Lanza-Gutierrez, Juan A. Gomez-Pulido, and Miguel A. Vega-Rodriguez. A trajectory algorithm to solve the relay node placement problem in wireless sensor networks. In *Theory and Practice of Natural Computing*, volume 8273 of *Lecture Notes in Computer Science*, pages 145–156. Springer Berlin Heidelberg, 2013. In [73], we apply NSGA-II, SPEA2, and MO-VNS* for optimising the problem in Chapter 4 with 100x100, 200x200, and 300x300 instances.
- Jose M. Lanza-Gutierrez, Juan A. Gomez-Pulido, Miguel A. Vega-Rodriguez, and Juan M. Sanchez-Perez. Relay node positioning in wireless sensor networks by means of evolutionary techniques. In *Autonomous and Intelligent Systems*, volume

7326 of *Lecture Notes in Computer Science*, pages 18–25. Springer Berlin / Heidelberg, 2012. In [74], we apply NSGA-II and SPEA2 for optimising the problem in Chapter 4 with 100x100 and 200x200 instances. This is our first work exactly fitting this problem approach.

- Jose M. Lanza-Gutierrez, Juan A. Gomez-Pulido, Miguel A. Vega-Rodriguez, and Juan M. Sanchez-Perez. Optimizing energy consumption in heterogeneous wireless sensor networks by means of evolutionary algorithms. In *Applications of Evolutionary Computation*, volume 7248 of *Lecture Notes in Computer Science*, pages 1–10. Springer Berlin Heidelberg, 2012. In [75], we apply NSGA-II and SPEA2 for optimising 100x100 and 200x200 instances with 50 000 evaluations. In this contribution, we do not assume that the number of RNs should be significantly lower than the number of sensors. This paper can be considered as a very preliminary approach of the work in [74], belonging to Chapter 4.

International conferences:

- Jose M. Lanza-Gutierrez, Juan A. Gomez-Pulido, Miguel A. Vega-Rodriguez, and Juan M. Sanchez- Perez. A parallel evolutionary approach to solve the relay node placement problem in wireless sensor networks. In *Proceeding of GECCO*, pages 1157–1164, 2013. ACM conference. In [76], we apply NSGA-II and SPEA2 for solving the problem in Chapter 4 with 100x100 and 200x200 instances through OpenMP with 32 cores.
- Jose M Lanza-Gutierrez, Juan Gomez-Pulido, Miguel Vega-Rodriguez, Juan M Sanchez -Perez. Multi-objective evolutionary algorithms for energy-efficiency in heterogeneous wireless sensor networks. In *IEEE Sensors Applications Symposium (SAS)*, pages 1–6, 2012. IEEE conference. In [77], we apply NSGA-II and SPEA2 for solving a less realistic approach of work presented in Chapter 4. This contribution can be considered as one of our first steps in this research line and is a continuation of the work in [78].

National conferences:

- Jose M. Lanza-Gutierrez and Juan A. Gomez-Pulido. Optimización de redes de sensores inalámbricos mediante computación inteligente. In *Actas del XV Conferencia de la Asociación Española para la Inteligencia Artificial (CAEPIA 13) - Doctoral Consortium*, pages 1672–1676, 2013. In [91], we present the main objectives and tasks for getting this PhD dissertation.
- Jose M. Lanza-Gutierrez, Juan A. Gomez-Pulido, and Miguel A. Vega-Rodriguez. Un nuevo enfoque para el posicionamiento de routers sobre redes de sensores inalámbricos. In *Actas del XV Conferencia de la Asociación Española para la Inteligencia Artificial (CAEPIA 13) - IX Congreso Español sobre Metaheurísticas, Algoritmos Evolutivos y Bioinspirados (MAEB 2013)*, pages 743–752, 2013. In [87], we apply NSGA-II and SPEA2 for optimising the problem in Chapter 5 with 100x100, 200x200, and 300x300 instances. This is a very preliminary work.
- Jose M. Lanza-Gutierrez, Juan A. Gomez-Pulido, Miguel A. Vega-Rodriguez, and Juan M. Sanchez-Perez. Optimizando la eficiencia energética en redes de sensores

inalámbricos mediante computación evolutiva paralela. In *Actas de las XXIII Jornadas de Paralelismo (JP 2012), Servicio de Publicaciones. Universidad Miguel Hernández*, pages 163–168, 2012. In [79], we apply NSGA-II, SPEA2 for optimising the problem in Chapter 4 with 100x100 and 200x200 instances through OpenMP with 8 cores.

- Jose M. Lanza-Gutierrez, Juan A. Gomez-Pulido, Miguel A. Vega-Rodriguez, and Juan M. Sanchez-Perez. Posicionando routers en redes de sensores inalámbricos mediante algoritmos evolutivos para el incremento de la eficiencia energética. In *Actas de las III Jornadas de Computación Empotrada (JCE 2012), Servicio de Publicaciones. Univ. Miguel Hernandez*, pages 95–100, 2012. In [80], we apply NSGA-II and SPEA2 for optimising the problem in Chapter 4 with 100x100 and 200x200 instances with 50 000 evaluations. This is a very preliminary work before [74].
- Jose M Lanza-Gutierrez, Juan A Gomez-Pulido, Oscar Gutierrez-Blanco, Miguel A Vega- Rodriguez, and Juan M Sanchez. Diseño eficiente de redes heterogéneas de sensores inalámbricos mediante computación evolutiva multi-objetivo. In *Actas del VIII Congreso Español sobre Metaheurísticas, Algoritmos Evolutivos y Bioinspirados, Universidad de Castilla-La Mancha*, pages 337–344, 2012. In [78], we apply NSGA-II and SPEA2 for solving a less realistic approach of work performed in Chapter 4. This paper can be considered as one of our first steps in this line.
- Juan A Gomez Pulido, Francisco L Morcillo Garcia, Eloy J Diaz Alvarez, Jose M Lanza Gutierrez, Miguel A Vega Rodriguez, and Juan M Sanchez Perez. Experiencias con redes de sensores inalámbricos en la escuela politécnica de la universidad de extremadura. In *Actas de las III Jornadas de Computación Empotrada (JCE 2012), Servicio de Publicaciones. Universidad Miguel Hernández*, pages 114–119, 2012. In [92], we share experiences by deploying WSNs in the University of Extremadura.

8.2 Other Scientific Publications Partially Related to this Dissertation

This section lists other 5 scientific publications obtained partially related to this thesis, two of them are collaborations with other research groups. We include 2 international indexed journals (ISI-SCI), 1 international conference, and 2 national conferences.

International indexed journals (ISI-SCI):

- N.C. Caballe, I.T. Castro, C.J. Perez, and J.M. Lanza-Gutierrez. A condition-based maintenance of a dependent degradation-threshold-shock model in a system with multiple degradation processes. *Reliability Engineering & System Safety*, 134: 98–109, 2015. Impact factor of 2.410 ($Q1$, $T1$). The paper in [93] is a collaboration with Bayesian Inference and Decision Group of the University of Extremadura. Our contribution to this paper was to apply an GA for getting a set of parameters, which a system was subject to. This set allowed obtaining the maintenance strategy which minimised the total cost.
- M Ferreira, J Bagaric, Jose M Lanza-Gutierrez, S Priem-Mendes, JS Pereira, and Juan A Gomez-Pulido. On the use of perfect sequences and genetic algorithms for

estimating the indoor location of wireless sensors. *International Journal of Distributed Sensor Networks*, 2015, 2015. Impact factor of 0.665 ($Q4$, $T3$). The paper in [94] is a collaboration with both Polytechnic Institute of Leiria (Portugal) and Telecommunications Institute of Leiria (Portugal). Our contribution to this paper was to study the positioning of sensors in indoor environments through GAs. This paper is partially inspired in the work done in Chapter 6.

International conferences:

- Jose M. Lanza-Gutierrez, Juan A. Gomez-Pulido, Miguel A. Vega-Rodriguez, and Juan M. Sanchez-Perez. A multi-objective network design for real traffic models of the internet by means of a parallel framework for solving np-hard problems. In *Proceedings of the Third World Congress on Nature and Biologically Inspired Computing (NaBIC)*, pages 137–142, 2011. IEEE conference. In [95], we apply NSGA-II and SPEA2 for solving a multi-objective network design optimization problem for real traffic models of the Internet. In this paper, we also propose a parallel MPI version of a known framework for solving complex problems named PISA[1].

National conferences:

- Jose M Lanza-Gutierrez, Juan A Gomez-Pulido, Miguel A Vega-Rodriguez, and Juan M Sanchez. Paralelización de una plataforma para la resolución de problemas np-completos mediante algoritmos evolutivos. In *Actas de las XXII Jornadas de Paralelismo (JP2011), Servicio de Publicaciones. Universidad de La Laguna*, pages 63–68, 2011. In [96], we provide additional information of the parallelisation of PISA framework in [95].
- Jose M Lanza-Gutierrez, Juan A Gomez-Pulido, Miguel A Vega-Rodriguez, and Juan M Sanchez. Resolviendo el diseño de redes para modelos de tráfico reales de internet mediante optimización multiobjetivo en multiprocesadores. In *Actas de las XXII Jornadas de Paralelismo (JP2011), Servicio de Publicaciones. Universidad de La Laguna*, pages 95–100, 2011. In [97], we provide additional information by solving the multi-objective network design optimization problem for real traffic models of the Internet in [95].

8.3 Other Scientific Achievements

In this section, we list other scientific achievements obtained during this period, including 6 months and 1 week of international research stays, member of 1 international research group (besides of the group in the University of Extremadura), organisation of 5 international conferences/workshops, participation in 3 research projects, reviewer of 8 international indexed journals (ISI-SCI), reviewer of 2 international conferences, and associate editor of 1 international indexed journal (ISI-SCI).

[1] http://www.tik.ee.ethz.ch/sop/pisa/

International research stays:

- **Institution:** Pontificia Universidad Católica de Valparaiso (PUCV).
Country: Chile.
Duration: 24^{st} August 2015 to 24^{th} November 2015 (3 months.)
Funding entity: *Becas Santander Iberoamérica Jóvenes Profesores e Investigadores y Alumnos de Doctorado. España 2015.* (Santander Bank of Spain).
- **Institution:** Polytechnic Institute of Leiria.
Country: Portugal.
Duration: 1^{st} June 2015 to 30^{th} June 2015 (1 month).
Funding entity: *Visitas Docentes y Formativas ERASMUS+ 2014/2015* under Erasmus+ programme (European Commission).
- **Institution:** Polytechnic Institute of Leiria.
Country: Portugal.
Duration: 13^{th} January 2014 to 13^{th} March 2014 (2 months).
Funding entity: No funding.
- **Institution:** University of Coimbra.
Country: Portugal.
Duration: 17^{th} June 2013 to 21^{st} June 2014 (1 week).
Funding entity: *Visitas Formativas LLP/ERASMUS 2012/2013* under Erasmus programme (European Commission).

Member of international research groups

- **Institution:** Center for research in Informatics and Communications of Polytechnic Institute of Leiria.
Country: Portugal.
Position: Associate Member.

Organisation of conferences and workshops:

- **Title:** Third International Workshop on Parallelism in Bioinformatics (PBio) in 13^{th} IEEE International Symposium on Parallel and Distributed Processing with Applications (IEEE ISPA) conference.
Country: Finland.
City: Helsinki.
Position: Program committee.
Duration: 20^{th} August 2015 to 22^{nd} August 2015.
- **Title:** Second Congress on Multicore and GPU Programming (PPMG).
Country: Spain.
City: Cáceres.
Position: Local committee.
Duration: 5^{th} March 2015 to 6^{th} March 2015.
- **Title:** Second International Workshop on Parallelism in Bioinformatics (PBio) in IEEECluster 2014 conference.

Country: Spain.
City: Madrid.
Position: Program committee.
Duration: 24^{th} September 2014 to 26^{th} September 2014.

- **Title:** Second International Conference on the Theory and Practice of Natural Computing 2013 (TPNC).
Country: Spain.
City: Cáceres.
Position: Local committee.
Duration: 3^{rd} December 2013 to 5^{th} December 2013.

- **Title:** International Workshop on Parallelism in Bioinformatics (PBio) in EuroMPI 2013 conference.
Country: Spain.
City: Madrid.
Position: Program committee.
Duration: 15^{th} September 2013 to 18^{th} September 2013.

Participation in research projects:

- **Title:** *Optimización Multiobjetivo y Paralelismo en Bioinformática* (BIO).
Reference: TIN2012-30685.
Funding entity: *Ministerio de Economía y Competitividad. Plan Nacional de Investigación Científica, Desarrollo e Innovación Tecnológica 2012* (Spain).
Duration: 1^{st} January 2013 to 31^{st} December 2015 (3 years).
Budget: $110.823, 90$ euros.
Institutions: University of Extremadura.
Main researcher: Miguel A. Vega-Rodríguez.
Number of researchers: 12.

- **Title:** Multiobjective Metaheuristics and Parallelism in Communications (MSTAR).
Reference: TIN2008-06491-C04-04.
Funding entity: *Ministerio de Ciencia e Innovación. Plan Nacional de Investigación Científica, Desarrollo e Innovación Tecnológica 2008* (Spain).
Duration: 1^{st} January 2009 to 31^{st} December 2011 (3 years).
Budget: 110.110 euros.
Institutions: University of Extremadura, University of Malaga (Spain), University of La Laguna (Spain), and University Carlos III (Spain).
Main researcher: Miguel A. Vega-Rodríguez (University of Extremadura node) and E. Alba (coordinate project)
Number of researchers: 39.

- **Title:** *De Quatris IManager a VManager: Estrategias para el Almacenamiento y Búsqueda en Colecciones de Documentos de Video Digital.*
Reference: TIN2008-03063.
Funding entity: *Ministerio de Ciencia e Innovación. Plan Nacional de Investigación Científica, Desarrollo e Innovación Tecnológica 2008* (Spain).
Duration: 1^{st} January 2009 to 31^{st} December 2011 (3 years).
Institutions: University of Extremadura.

Main researcher: Manuel Barrena García.
Number of researchers: 14.

Reviewer of international journals (ISI-SCI) :

- Computers & Operations Research. Impact factor of 1.861 ($Q1$,$T1$).
- Parallel Computing: Systems & Applications. Impact factor of 1.511 ($Q1$,$T1$).
- Journal of Network and Computer Applications. Impact factor of 2.229 ($Q1$,$T1$).
- IEEE Transactions on Wireless Communications. Impact factor of 2.496 ($Q1$,$T1$).
- Expert system with applications. Impact factor of 2.240 ($Q1$,$T1$).
- IEEE sensors journal. Impact factor of 1.762 ($Q2$,$T1$).
- Autonomous Agents and MultiAgent Systems. Impact factor of 1.254 ($Q3$,$T2$).
- Journal of Heuristics. Impact factor of 1.135 ($Q2$,$T2$).

Reviewer of international conferences:

- 2014 IEEE International Symposium on Circuits and Systems (ISCAS).
- 2013 IEEE Wireless Communications and Networking Conference (WCNC).

Associate editor of international journals (ISI-SCI):

- Journal of Heuristics. Impact factor of 1.135 ($Q2$,$T2$).

APPENDIX

A

Additional Information for Implementing MOEA/D

In this appendix, we include additional information for implementing MOEA/D. In Section A.1, we provide the mathematical model needed for scaling the CHIM for two objectives. In Section A.3, we develop the model for scaling the CHIM for three objectives.

A.1 Scaling Procedure of the CHIM for two objectives

In this section, we provide the mathematical developed need for scaling the CHIM by assuming a problem with two objectives. The procedure is described below:

Let $F_1 = (x_1, y_1)$ and $F_2 = (x_2, y_2)$ be with $F_1 \neq F_2$, two given points delimiting the objective space $\mathbb{R}^2$ and let R_1 be the straight line which contains F_1 and F_2, expressed as

$$\frac{x - x_1}{x_2 - x_1} = \frac{y - y_1}{y_2 - y_1}.$$

Since x_1, y_1, x_2, and y_2 are constants and known, $(x_2 - x_1)$ and $(y_2 - y_1)$ are constants and known. We consider

$$m = (x_2 - x_1) \quad \text{and} \quad n = (y_2 - y_1).$$

Thus

$$\frac{x - x_1}{m} = \frac{y - y_1}{n}.$$

Hence, the straight line R_1 is given by the equation

$$x - \frac{m}{n}y + \frac{m}{n}y_1 - x_1 = 0. \tag{A.1}$$

Let $c = (x_c, y_c)$ be the midpoint between F_1 and F_2 contained in R_1, where x_c and y_c are given by

$$x_c = \frac{x_1 + x_2}{2} \quad \text{and} \quad y_c = \frac{y_1 + y_2}{2}.$$

Let $p = (x_p, y_p)$ be a point of R_1 which is located at a given distance d of the point c. By using the formula for the distance between two points, we have

$$d(c, p) = \sqrt{(x_p - x_c)^2 + (y_p - y_c)^2}, \tag{A.2}$$

where $d(c, p) = d$.

The point p is contained in R_1 and is located at a distance d if, and only if holds the following system of equations given by (A.1) and (A.2)

$$\begin{cases} d = \sqrt{(x_p - x_c)^2 + (y_p - y_c)^2} \\ x_p - \frac{m}{n} y_p + \frac{m}{n} y_1 - x_1 = 0 \end{cases}$$
$$\Rightarrow \begin{cases} d^2 = x_p^2 + x_c^2 - 2x_p x_c + y_p^2 + y_c^2 - 2y_p y_c \\ x_p = \frac{m}{n} y_p + t \end{cases},$$

where $t = x_1 - \frac{m}{n} y_1$.

Then, by using the substitution method for solving system of equations, we have

$$\begin{aligned} d^2 &= (x_p = \frac{m}{n} y_p + t)^2 + x_c^2 - 2x_c(x_p = \frac{m}{n} y_p + t) + y_p^2 + y_c^2 - 2y_p y_c \\ &= \left(\left(\frac{m}{n}\right)^2 + 1\right) y_p^2 + 2\left(\frac{m(t - x_c)}{n} - y_c\right) y_p + t^2 + x_c^2 - 2x_c t + y_c^2. \end{aligned}$$

That is

$$a y_p^2 + b y_p + u = 0,$$

where

$$a = \left(\frac{m}{n}\right)^2 + 1,$$

$$b = 2\left(\frac{m(t - x_c)}{n} - y_c\right),$$

and

$$u = t^2 + x_c^2 - 2x_c t + y_c^2 - d^2.$$

By using the method for solving the second grade equations

$$y_p = \frac{-b \pm \sqrt{b^2 - 4au}}{2a}.$$

Thus, we get two points $p_1 = (x_{p_1}, y_{p_1})$ and $p_2 = (x_{p_2}, y_{p_2})$ equidistant from the point c with a distance d and contained in the straight line R_1, which links F_1 and F_2, where

$$y_{p_1} = \frac{-b + \sqrt{b^2 - 4au}}{2a}; \quad y_{p_2} = \frac{-b - \sqrt{b^2 - 4au}}{2a},$$

and therefore

$$x_{p_1} = \frac{m}{n}\left(\frac{-b + \sqrt{b^2 - 4au}}{2a}\right) + t; \quad x_{p_2} = \frac{m}{n}\left(\frac{-b - \sqrt{b^2 - 4au}}{2a}\right) + t,$$

being $m = (x_2 - x_1)$, $n = (y_2 - y_1)$, $t = x_1 - \frac{m}{n} y_1$, $a = \left(\frac{m}{n}\right)^2 + 1$, $b = 2\left(\frac{m(t - x_c)}{n} - y_c\right)$, and $u = t^2 + x_c^2 - 2x_c t + y_c^2 - d^2$.

A.2 Normal Vector for two Objectives

Let $F_1 = (x_1, y_1)$ and $F_2 = (x_2, y_2)$ be with $F_1 \neq F_2$, two given points delimiting the objective space $\mathbb{R}^2$ and let R_1 be the straight line which contains F_1 and F_2, expressed as

$$\frac{x - x_1}{x_2 - x_1} = \frac{y - y_1}{y_2 - y_1}.$$

Based on Section A.1, the equation for the straight line R_1 is given by (A.1). That is,

$$x - \frac{m}{n}y + \frac{m}{n}y_1 - x_1 = 0,$$

where

$$m = (x_2 - x_1) \quad \text{and} \quad n = (y_2 - y_1).$$

Let $\overrightarrow{\mathbf{v_r}} = (-B, A)$ be the direction vector for a straight line with equation

$$Ax + By + C = 0,$$

and let $\overrightarrow{\mathbf{v_s}} = (A, B)$ be the perpendicular direction vector of $\overrightarrow{\mathbf{v_r}}$.

Then, for the straight line R_1,

$$\overrightarrow{\mathbf{v_r}} = \left(\frac{m}{n}, 1\right) \quad \text{and} \quad \overrightarrow{\mathbf{v_s}} = \left(1, -\frac{m}{n}\right).$$

A.3 Scaling Procedure of the CHIM for three objectives

In this section, we develop the scaling procedure of the CHIM for three objectives. In Section A.3.1, we provide a preliminary model. In Section A.3.2, we include the definitive model considered in this dissertation.

A.3.1 Preliminary Model

In this subsection, we provide a preliminary model for scaling the CHIM for three objectives. This model considers that we have three points in $\mathbb{R}^2$, defining a triangle. The objective of this procedure is to scale the triangle by assuming parallel lines at a given distance of the triangle centroid. This is a preliminary model which should be converted to $\mathbb{R}^3$.

Let $F_i^2 = (x_i, y_i)$ be the i-th extreme point delimiting the objective space $\mathbb{R}^2$ with $i = 1, 2, 3$, let $\overline{F_1^2 F_2^2}$, $\overline{F_2^2 F_3^2}$, and $\overline{F_1^2 F_3^2}$ be the straight lines which contain the points (F_1^2, F_2^2), (F_2^2, F_3^2), and (F_1^2, F_3^2), respectively, and let $C^2 = (x_c, y_c)$ be the centroid of the triangle generated by $\overline{F_1^2 F_2^2}$, $\overline{F_2^2 F_3^2}$, and $\overline{F_1^2 F_3^2}$.

A general straight line has a equation given by the expression

$$ax + by + c = 0.$$

Based on Section A.1, the straight line $\overline{F_1^2 F_2^2}$ is given by the expression (A.1). That is,

$$x - \frac{x_2 - x_1}{y_2 - y_1}y + \frac{y_1(x_2 - x_1)}{y_2 - y1} - x_1 = 0.$$

Then, for $\overline{F_1^2 F_2^2}$,

$$a = 1, \quad b = -\frac{x_2 - x_1}{y_2 - y_1}, \quad \text{and} \quad c = \frac{y_1(x_2 - x_1)}{y_2 - y1} - x_1. \tag{A.3}$$

Let $\overline{F_1^2 F_2^2}^{\,1}$ and$\overline{F_1^2 F_2^2}^{\,2}$ be the two possible parallel straight line which are located at a given distance d of $\overline{F_1^2 F_2^2}$. In a straight line parallel to $\overline{F_1^2 F_2^2}$, a and b will remain constant and c will vary and let c' be this variation of the parameter c. Then, the parallel straight line $\overline{F_1^2 F_2^2}^{u}$ of $\overline{F_1^2 F_2^2}$ for $u = 1, 2$ holds the following equation

$$x - \frac{x_2 - x_1}{y_2 - y_1} + c' = 0.$$

By applying the known formula for the distance between two parallel straight lines, we have

$$d\left(\overline{F_1^2 F_2^2}, \overline{F_1^2 F_2^2}^{\,u}\right) = \frac{|c - c'|}{\sqrt{a^2 + b^2}},$$

for $u = 1, 2$, and where a, b, and c are given by (A.3) and $d\left(\overline{F_1^2 F_2^2}, \overline{F_1^2 F_2^2}^{\,u}\right) = d$.

Then,

$$d = \frac{\left|\frac{y_1(x_2 - x_1)}{y_2 - y1} - x_1 - c'\right|}{\sqrt{1 + \left(-\frac{x_2 - x_1}{y_2 - y_1}\right)^2}}$$

$$\Rightarrow d\sqrt{1 + \left(-\frac{x_2 - x_1}{y_2 - y_1}\right)^2} = \left|\frac{y_1(x_2 - x_1)}{y_2 - y1} - x_1 - c'\right|$$

Hence, c' can have two values, c_1' and c_2' given by

$$c_1' = d\sqrt{1 + \left(\frac{x_2 - x_1}{y_2 - y_1}\right)^2} + \frac{y_1(x_2 - x_1)}{y_2 - y1} - x_1,$$

and

$$c_2' = -d\sqrt{1 + \left(\frac{x_2 - x_1}{y_2 - y_1}\right)^2} + \frac{y_1(x_2 - x_1)}{y_2 - y1} - x_1.$$

Thus, the expressions for $\overline{F_1^2 F_2^2}^{\,1}$ and$\overline{F_1^2 F_2^2}^{\,2}$ are given by

$$\overline{F_1^2 F_2^2}^{\,1} \equiv x + z_1 y + t_1 + h_1 = 0,$$

and

$$\overline{F_1^2 F_2^2}^{\,2} \equiv x + z_1 y - t_1 + h_1 = 0,$$

where

$$t_1 = d\sqrt{1 + z_1^2}, \quad \text{and} \quad h_1 = y_1\, z_1 - x_1,$$

being

$$z_1 = \frac{x_2 - x_1}{y_2 - y_1}.$$

Let $\overline{F_2^2 F_3^2}^{\,1}$ and$\overline{F_2^2 F_3^2}^{\,2}$ be the two possible parallel straight line which are located at a given distance d of $\overline{F_2^2 F_3^2}$ and let $\overline{F_1^2 F_3^2}^{\,1}$ and $\overline{F_1^2 F_3^2}^{\,2}$ be the two possible parallel straight line which are located at a given distance d of $\overline{F_1^2 F_3^2}$.

Based on the previous procedure, the corresponding parallel straight lines are given by the expressions

$$\overline{F_2^2 F_3^2}^{\,1} \equiv x + z_2 y - t_2 + h_2 = 0,$$

$$\overline{F_2^2 F_3^2}^{\,2} \equiv x + z_2 y - t_2 + h_2 = 0,$$

$$\overline{F_1^2 F_3^2}^{\,1} \equiv x + z_3 y - t_3 + h_3 = 0,$$

and

$$\overline{F_1^2 F_3^2}^{\,2} \equiv x + z_3 y - t_3 + h_3 = 0,$$

where

$$t_2 = d\sqrt{1 + z_2^2}, \quad \text{and} \quad h_2 = y_2\, z_2 - x_2,$$

and

$$t_3 = d\sqrt{1 + z_3^2}, \quad \text{and} \quad h_3 = y_1\, z_3 - x_1,$$

being

$$z_2 = \frac{x_3 - x_2}{y_3 - y_2} \quad \text{and} \quad z_3 = \frac{x_3 - x_1}{y_3 - y_1}.$$

Let $F_{i,uv}^2 = (x_{i,uv}, y_{i,uv})$ be the i-th point located at a distance d of its corresponding point $F_i^2 = (x_i, y_i)$ for $i = 1, 2, 3$ and generated by the cut-off point of the calculated parallel straight lines $\overline{F_i^2 F_j^2}^{\,u}$, $\overline{F_i^2 F_j^2}^{\,v}$ with $u, v = 1, 2$; $i, j = 1, 2, 3$, and $i < j$.

There are four possible cut-off points of the parallel straight lines $\overline{F_i^2 F_j^2}^{\,u}$ and $\overline{F_i^2 F_j^2}^{\,v}$ with $u, v = 1, 2$; $i, j = 1, 2, 3$, and $i < j$, corresponding to the four possible combinations for u and v. Thus,

- If $u = 1$ and $v = 1$, the cut-off point $F_{i,11}^2 = (x_{i,11}, y_{i,11})$ of the straight lines $\overline{F_i^2 F_j^2}^{\,1}$ and $\overline{F_i^2 F_j^2}^{\,1}$ with $i, j = 1, 2, 3$, and $i < j$ is given by the following system of equations

$$\begin{cases} x_{i,11} + z_i y_{i,11} + t_i + h_i = 0 \\ x_{i,11} + z_j y_{i,11} + t_j + h_j = 0 \end{cases}$$
$$\Rightarrow \begin{cases} x_{i,11} = -z_i y_{i,11} - t_i - h_i \\ x_{i,11} + z_j y_{i,11} + t_j + h_j = 0 \end{cases},$$

By using the substitution method for solving system of equations, we have

$$-z_i y_{i,11} - t_i - h_i + z_j y_{i,11} + t_j + h_j = 0.$$

Then

$$y_{i,11} = \frac{(t_i - t_j) + (h_i - h_j)}{z_j - z_i},$$

and

$$x_{i,11} = -z_i \left(\frac{(t_i - t_j) + (h_i - h_j)}{z_j - z_i} \right) - t_i - h_i.$$

- If $u = 1$ and $v = 2$, the cut-off point $F_{i,12}^2 = (x_{i,12}, y_{i,12})$ of the straight lines $\overline{F_i^2 F_j^2}^{\,1}$ and $\overline{F_i^2 F_j^2}^{\,2}$ with $i, j = 1, 2, 3$, and $i < j$ is given by the following system of equations

$$\begin{cases} x_{i,12} + z_i y_{i,12} + t_i + h_i = 0 \\ x_{i,12} + z_j y_{i,12} - t_j + h_j = 0 \end{cases}$$
$$\Rightarrow \begin{cases} x_{i,12} = -z_i y_{i,12} - t_i - h_i \\ x_{i,12} + z_j y_{i,12} - t_j + h_j = 0 \end{cases},$$

By using the substitution method for solving system of equations, we have

$$-z_i y_{i,12} - t_i - h_i + z_j y_{i,12} - t_j + h_j = 0.$$

Then

$$y_{i,12} = \frac{(t_i + t_j) + (h_i - h_j)}{z_j - z_i},$$

and

$$x_{i,12} = -z_i \left(\frac{(t_i + t_j) + (h_i - h_j)}{z_j - z_i} \right) - t_i - h_i.$$

- If $u = 2$ and $v = 1$, the cut-off point $F_{i,21}^2 = (x_{i,21}, y_{i,21})$ of the straight lines $\overline{F_i^2 F_j^2}^{\,2}$ and $\overline{F_i^2 F_j^2}^{\,1}$ with $i, j = 1, 2, 3$, and $i < j$ is given by the following system of equations

$$\begin{cases} x_{i,21} + z_i y_{i,21} - t_i + h_i = 0 \\ x_{i,21} + z_j y_{i,21} + t_j + h_j = 0 \end{cases}$$
$$\Rightarrow \begin{cases} x_{i,11} = -z_i y_{i,11} + t_i - h_i \\ x_{i,11} + z_j y_{i,11} + t_j + h_j = 0 \end{cases},$$

By using the substitution method for solving system of equations, we have

$$-z_i y_{i,11} + t_i - h_i + z_j y_{i,11} + t_j + h_j = 0.$$

Then

$$y_{i,11} = \frac{(-t_i - t_j) + (h_i - h_j)}{z_j - z_i},$$

and

$$x_{i,11} = -z_i \left(\frac{(-t_i - t_j) + (h_i - h_j)}{z_j - z_i} \right) + t_i - h_i.$$

- If $u = 2$ and $v = 2$, the cut-off point $F_{i,22}^2 = (x_{i,22}, y_{i,22})$ of the straight lines $\overline{F_i^2 F_j^2}^{\,2}$ and $\overline{F_i^2 F_j^2}^{\,2}$ with $i, j = 1, 2, 3$, and $i < j$ is given by the following system of equations

$$\begin{cases} x_{i,22} + z_i y_{i,22} - t_i + h_i = 0 \\ x_{i,22} + z_j y_{i,22} - t_j + h_j = 0 \end{cases}$$
$$\Rightarrow \begin{cases} x_{i,22} = -z_i y_{i,22} + t_i - h_i \\ x_{i,22} + z_j y_{i,22} - t_j + h_j = 0 \end{cases},$$

By using the substitution method for solving system of equations, we have

$$-z_i y_{i,11} + t_i - h_i + z_j y_{i,11} - t_j + h_j = 0.$$

Then

$$y_{i,11} = \frac{(-t_i + t_j) + (h_i - h_j)}{z_j - z_i},$$

and

$$x_{i,11} = -z_i \left(\frac{(-t_i + t_j) + (h_i - h_j)}{z_j - z_i} \right) + t_i - h_i.$$

Let $\overline{F_i^2 C^2}$ be for $i = 1, 2, 3$ the straight line which contains the points (F_i^2, C^2). Based on Section A.1, the general equation for $\overline{F_i^2 C^2}$ is given by

$$x - \frac{x_c - x_i}{y_c - y_i} y + \frac{y_c(x_c - x_i)}{y_c - y_1} - x_c = 0. \tag{A.4}$$

Then, the point E_i^2 searched for each F_i^2 will be the farthest from the centroid C^2 which holds the Equation (A.4) with $i = 1, 2, 3$.

A.3.2 **Definitive Model**

In this subsection, we provide the definitive model for scaling the CHIM for three objectives. In a first step, we decided to consider the approach in Section A.3.1. However, this procedure generates an infinite number of scaled triangles for three objectives. This situation led us to develop another approach based on the distance between centroid and vertices.

Let $F_i^3 = (x_i, y_i, z_i)$ be the i-th extreme point delimiting the objective space $\mathbb{R}^3$ with $i = 1, 2, 3$, let $C^3 = (x_c, y_c, z_c)$ be the centroid of the triangle generated by the points F_1^3, F_2^3, and F_3^3, and let $\overline{F_i^3 C^3}$ be the straight line which contain the points (F_i^2, C^3) for $i = 1, 2, 3$. The equation for the straight line $\overline{F_i^3 C^3}$ is expressed as

$$\frac{x - x_i}{x_c - x_i} = \frac{y - y_i}{y_c - y_i} = \frac{z - z_i}{z_c - z_i}. \tag{A.5}$$

Let $p_i = (x_{p_i}, y_{p_i}, z_{p_i})$ be a point of $\overline{F_i^3 C^3}$ for $i = 1, 2, 3$ which is located at a given distance d of the point C^3. By using the formula for the distance between two points, we have

$$d(C^3, p_i) = \sqrt{(x_{p_i} - x_c)^2 + (y_{p_i} - y_c)^2 + (z_{p_i} - z_c)^2}, \tag{A.6}$$

where $d(C^3, p_i) = d$.

The point p_i for $i = 1, 2, 3$ is contained in $\overline{F_i^3 C^3}$ and is located at a distance d if, and only if holds the following system of equations given by (A.5) and (A.6)

$$\begin{cases} \frac{x_{p_i} - x_i}{x_c - x_i} = \frac{y_{p_i} - y_i}{y_c - y_i} \\ \frac{x_{p_i} - x_i}{x_c - x_i} = \frac{z_{p_i} - z_i}{z_c - z_i} \\ d = \sqrt{(x_{p_i} - x_c)^2 + (y_{p_i} - y_c)^2 + (z_{p_i} - z_c)^2} \end{cases},$$

where $t = x_1 - \frac{m}{n} y_1$.

Since x_c, y_c, z_c, x_i, y_i, and z_i are constants and known, $(x_c - x_i)$, $(y_c - y_i)$, and $(z_c - z_i)$ are constants and known for $i = 1, 2, 3$. We consider

$$m = (x_c - x_i), \quad n = (y_c - y_i), \quad \text{and} \quad l = (z_c - z_i).$$

Then,

$$\left\{\begin{array}{l}(x_{p_i}-x_i)\,n=(y_{p_i}-y_i)\,m\\(x_{p_i}-x_i)\,l=(z_{p_i}-z_i)\,m\\d=\sqrt{(x_{p_i}-x_c)^2+(y_{p_i}-y_c)^2+(z_{p_i}-z_c)^2}\end{array}\right.$$
$$\Rightarrow\left\{\begin{array}{l}x_{p_i}=y_{p_i}\frac{m}{n}-j\\x_{p_i}=z_{p_i}\frac{m}{l}-k\\d=\sqrt{(x_{p_i}-x_c)^2+(y_{p_i}-y_c)^2+(z_{p_i}-z_c)^2}\end{array}\right.,$$

where

$$j=\frac{y_im}{n}-x_i \quad \text{and} \quad k=\frac{z_im}{l}-x_i.$$

Thus,

$$\left\{\begin{array}{l}y_{p_i}\frac{m}{n}-j=z_{p_i}\frac{m}{l}-k\\d^2=\left[\left(y_{p_i}\frac{m}{n}-j-x_c\right)\right]^2+(y_{p_i}-y_c)^2+(z_{p_i}-z_c)^2\end{array}\right.$$
$$\Rightarrow\left\{\begin{array}{l}y_{p_i}=\left(z_{p_i}\frac{m}{l}-k+j\right)\frac{n}{m}\\d^2=\left[\left(y_{p_i}\frac{m}{n}-j-x_c\right)\right]^2+(y_{p_i}-y_c)^2+(z_{p_i}-z_c)^2\end{array}\right.,$$

By using the substitution method for solving system of equations, we have

$$\begin{aligned}d^2&=\left(\left(z_{p_i}\frac{m}{l}-k+j\right)\frac{n}{m}\frac{m}{n}-j-x_c\right)^2+\left(\left(z_{p_i}\frac{m}{l}-k+j\right)\frac{n}{m}-y_c\right)^2+(z_{p_i}-z_c)^2\\&=\left(z_{p_i}\frac{m}{l}-k-x_c\right)^2+\left(z_{p_i}\frac{n}{l}+(j-k)\frac{n}{m}-y_c\right)^2+(z_{p_i}-z_c)^2\\&=z_{p_i}^2\left[\left(\frac{m}{l}\right)^2+\left(\frac{n}{l}\right)^2+1\right]+z_{p_i}\left[2b\frac{n}{l}-2a\frac{m}{l}-2z_c\right]+a^2+b^2+z_c^2,\end{aligned}$$

where

$$a=k+x_c \quad \text{and} \quad b=(j-k)\frac{n}{m}-y_c.$$

That is

$$rz_{p_i}^2+sz_{p_i}+t=0,$$

where

$$r=\left(\frac{m+n}{l}\right)^2+1,$$

$$s=2\left(\frac{bn-am}{l}-z_c\right),$$

and

$$t=a^2+b^2+z_c^2-d^2.$$

By using the method for solving the second grade equations

$$z_{p_i}=\frac{-s\pm\sqrt{s^2-4rt}}{2r}.$$

Thus, for each F_i^3 with $i=1,2,3$, we get two points $p_{i,1}=(x_{p_{i,1}},y_{p_{i,1}},z_{p_{i,1}})$ and $p_{i,2}=(x_{p_{i,2}},y_{p_{i,2}},z_{p_{i,2}})$ equidistant from the point C^3 with a distance d and contained in the straight line $\overline{F_i^3C^3}$, which links F_i^3 and C^3, where

$$z_{p_{i,1}}=\frac{-s+\sqrt{s^2-4rt}}{2r};\quad z_{p_{i,2}}=\frac{-s-\sqrt{s^2-4rt}}{2r},$$

and therefore

$$y_{p_{i,1}} = \left(z_{p_{i,1}}\frac{m}{l} - k + j\right)\frac{n}{m}; \quad y_{p_{i,2}} = \left(z_{p_{i,2}}\frac{m}{l} - k + j\right)\frac{n}{m},$$

and

$$x_{p_{i,1}} = y_{p_{i,1}}\frac{m}{n} - j; \quad x_{p_{i,2}} = y_{p_{i,2}}\frac{m}{n} - j.$$

Then, the point E_i^3 searched for each F_i^3 will be the farthest from the centroid C^3 between $p_{i,1}$ and $p_{i,2}$ with $i = 1, 2, 3$.

A.4 Normal Vector for Three Objectives

Let $F_1 = (x_1, y_1, z_1)$, $F_2 = (x_2, y_2, z_2)$, and $F_3 = (x_3, y_3, z_3)$ be with $F_1 \neq F_2 \neq F_3$, three given points delimiting the objective space $\mathbb{R}^3$ and let π be the plain which contains F_1, F_2, and F_3.

Let $P = (x, y, z)$ be an unknown point of the plain π. Since two points delimit a vector,

$$\overrightarrow{\mathbf{F_1P}} = (x - x_1, y - y_1, z - z_1),$$

$$\overrightarrow{\mathbf{F_1F_2}} = (x_2 - x_1, y_2 - y_1, z_2 - z_1),$$

and

$$\overrightarrow{\mathbf{F_1F_3}} = (x_3 - x_1, y_3 - y_1, z_3 - z_1).$$

We know that the implicit form of the equation of a plain is given by

$$\begin{vmatrix} x - x_1 & x_2 - x_1 & x_3 - x_1 \\ y - y_1 & y_2 - y_1 & y_3 - y_1 \\ z - z_1 & z_2 - z_1 & z_3 - z_1 \end{vmatrix} = 0$$

Developing the determinant, we have

$$A(x - x_1) + B(x - x_1) + C(z - z_1) = 0,$$

where

$$A = \begin{vmatrix} y_2 - y_1 & y_3 - y_1 \\ z_2 - z_1 & z_3 - z_1 \end{vmatrix}, \; B = -\begin{vmatrix} x_2 - x_1 & x_3 - x_1 \\ z_2 - z_1 & z_3 - z_1 \end{vmatrix}, \; C = \begin{vmatrix} x_2 - x_1 & x_3 - x_1 \\ y_2 - y_1 & y_3 - y_1 \end{vmatrix}. \tag{A.7}$$

Hence, the general equation of the plain π which contains the points F_1, F_2, F_3 and P is given by

$$Ax + By + Cz + D = 0,$$

where A, B, and C are given by (A.7) and D is defined as

$$D = -Ax_1 - By_1 - Cz_1.$$

In this way, a normal vector $\overrightarrow{\mathbf{v_n}}$ of the plain π is defined as

$$\overrightarrow{\mathbf{v_n}} = (A, B, C),$$

where A, B, and C are given by (A.7).

APPENDIX

B

Additional Information for Solving the RNPP: bi-objective Outdoor Approach

This appendix contains additional information for solving the bi-objective outdoor RNPP discussed in Chapter 4. Thus, Sections B.1 and B.2 include the p-values and set coverage metrics obtained by comparing the metaheuristics two by two, respectively.

B.1 Statistical Analysis Based on the Hypervolume Metric

In this section, we include all the p-values obtained by comparing the algorithms through Wilcoxon-Mann-Whitney's test and hypothesis $H_0 : \overline{Hyp_i} \leq \overline{Hyp_j}$ and $H_1 : \overline{Hyp_i} > \overline{Hyp_j}$, with $i, j = 1, 2, \ldots, 8$, 1=NSGA-II, 2=SPEA2, 3=MO-VNS, 4=MO-VNS*, 5=MO-ABC, 6=MO-FA, 7=MO-GSA, and 8=MOEA/D. Because of the symmetry observed in the p-values obtained, while comparing any two algorithms i and j, i.e. i vs j and j vs i. In the following tables, p-values lower than 0.05 means that $\overline{Hyp_i} > \overline{Hyp_j}$ (they appear shaded) and p-values higher than 0.95 means that $\overline{Hyp_j} > \overline{Hyp_i}$ (they appear in boldface). These p-values are in Tables B.1, B.2, B.3, B.4, B.5, B.6, and B.7.

B.2 Set Coverage Analysis

This section contains all the set coverage metrics obtained by comparing the metaheuristics two by two. These values are in Tables B.8, B.9, B.10, B.11, B.12, B.13, B.14, B.15, B.16, B.17, B.18, B.19, B.20, and B.21.

Table B.1: P-values obtained by comparing the metaheuristics through Wilcoxon-Mann-Whitney's test. Part 1 of 7.

	NSGA-II vs SPEA2					NSGA-II vs MO-VNS				
	Evaluations (Stop condition)					Evaluations (Stop condition)				
Instance($\tilde{s}_r$)	**50 000**	**100 000**	**200 000**	**300 000**	**400 000**	**50 000**	**100 000**	**200 000**	**300 000**	**400 000**
50x50_30(1)	0,5000	0,5000	0,5000	0,5000	0,5000	**0,9991**	**1,0000**	**1,0000**	**1,0000**	**1,0000**
50x50_60(1)	0,5000	0,5000	0,5000	0,5000	0,5000	**1,0000**	**1,0000**	**1,0000**	**1,0000**	**1,0000**
100x100_30(2)	0,0002	0,1520	0,0077	0,0000	0,0000	**1,0000**	**1,0000**	**1,0000**	**1,0000**	**1,0000**
100x100_30(3)	0,0000	0,0000	0,0000	0,0000	0,0000	**1,0000**	**1,0000**	**1,0000**	**1,0000**	**1,0000**
100x100_60(2)	0,0000	0,0000	0,0210	0,0067	0,0000	**1,0000**	**1,0000**	**1,0000**	**1,0000**	**1,0000**
100x100_60(3)	0,0000	0,0000	0,0000	0,0000	0,0000	**1,0000**	**1,0000**	**1,0000**	**1,0000**	**1,0000**
200x200_30(2)	0,2014	0,0034	0,0000	0,0000	0,0000	**1,0000**	**1,0000**	**1,0000**	**1,0000**	**1,0000**
200x200_30(4)	0,9235	0,7157	0,2138	0,0988	0,1064	**1,0000**	**1,0000**	**1,0000**	**1,0000**	**1,0000**
200x200_30(6)	0,8816	0,2458	0,0006	0,0007	0,0007	**1,0000**	**1,0000**	**0,9993**	**0,9998**	**0,9998**
200x200_30(9)	0,0000	0,0000	0,0000	0,0000	0,0000	**0,9643**	0,4200	0,3086	0,2795	0,4468
200x200_60(2)	**0,9999**	**0,9987**	**0,9991**	**0,9982**	**0,9938**	**1,0000**	**1,0000**	**1,0000**	**1,0000**	**1,0000**
200x200_60(4)	**1,0000**	**1,0000**	**0,9961**	**0,9979**	**0,9847**	**1,0000**	**1,0000**	**1,0000**	**1,0000**	**1,0000**
200x200_60(6)	0,0264	0,0000	0,0000	0,0000	0,0000	**1,0000**	**1,0000**	**1,0000**	**1,0000**	**1,0000**
200x200_60(9)	0,0000	0,0000	0,0000	0,0000	0,0000	**1,0000**	**1,0000**	**1,0000**	**1,0000**	**0,9999**
300x300_30(6)	**0,9978**	**0,9974**	**0,9669**	0,8829	0,6402	**1,0000**	**0,9997**	**0,9982**	**0,9968**	**0,9905**
300x300_30(12)	**0,9926**	**0,9873**	0,7304	0,7157	0,3206	**0,9676**	0,5630	0,0361	0,1933	0,0800
300x300_30(18)	**0,9985**	0,8831	0,1342	0,1513	0,0971	**0,9912**	0,0282	0,0000	0,0000	0,0000
300x300_30(24)	**1,0000**	**1,0000**	**0,9993**	0,9235	0,7658	**1,0000**	0,0178	0,0000	0,0000	0,0000
300x300_60(6)	**1,0000**	**1,0000**	**0,9994**	**0,9696**	0,9106	**1,0000**	**0,9990**	**0,9993**	**0,9977**	**0,9990**
300x300_60(12)	**1,0000**	**1,0000**	**1,0000**	**0,9997**	**0,9751**	0,9349	0,1710	0,0001	0,0000	0,0000
300x300_60(18)	**1,0000**	**1,0000**	**1,0000**	**0,9945**	**0,9879**	**0,9590**	0,0107	0,0000	0,0000	0,0000
300x300_60(24)	**1,0000**	**1,0000**	**1,0000**	**1,0000**	**0,9959**	**1,0000**	**0,9984**	0,0248	0,0000	0,0000

	NSGA-II vs MO-VNS*					NSGA-II vs MO-ABC				
	Evaluations (Stop condition)					Evaluations (Stop condition)				
Instance($\tilde{s}_r$)	**50 000**	**100 000**	**200 000**	**300 000**	**400 000**	**50 000**	**100 000**	**200 000**	**300 000**	**400 000**
50x50_30(1)	**1,0000**	**1,0000**	**1,0000**	**1,0000**	**1,0000**	**1,0000**	**1,0000**	**1,0000**	**1,0000**	**1,0000**
50x50_60(1)	**1,0000**	**1,0000**	**1,0000**	**1,0000**	**1,0000**	**1,0000**	**1,0000**	**1,0000**	**1,0000**	**1,0000**
100x100_30(2)	0,4209	0,7482	**0,9898**	**1,0000**	**1,0000**	**1,0000**	**1,0000**	**1,0000**	**1,0000**	**1,0000**
100x100_30(3)	**1,0000**	**1,0000**	**1,0000**	**1,0000**	**1,0000**	**1,0000**	**1,0000**	**1,0000**	**1,0000**	**1,0000**
100x100_60(2)	**1,0000**	**1,0000**	**1,0000**	**1,0000**	**1,0000**	**1,0000**	**1,0000**	**1,0000**	**1,0000**	**1,0000**
100x100_60(3)	**1,0000**	**1,0000**	**1,0000**	**1,0000**	**1,0000**	**1,0000**	**1,0000**	**1,0000**	**1,0000**	**1,0000**
200x200_30(2)	0,9235	**0,9977**	**0,9996**	**0,9992**	**0,9995**	**1,0000**	**1,0000**	**0,9999**	**0,9937**	**0,9553**
200x200_30(4)	**1,0000**	**1,0000**	**1,0000**	**1,0000**	**1,0000**	**1,0000**	**1,0000**	**1,0000**	**1,0000**	**1,0000**
200x200_30(6)	**1,0000**	**1,0000**	**1,0000**	**1,0000**	**1,0000**	**0,9899**	0,8691	**0,9976**	**1,0000**	**1,0000**
200x200_30(9)	**1,0000**	**1,0000**	**1,0000**	**1,0000**	**1,0000**	0,0547	0,0127	0,2011	**0,9889**	**1,0000**
200x200_60(2)	**1,0000**	**1,0000**	**1,0000**	**1,0000**	**1,0000**	**1,0000**	**1,0000**	**1,0000**	**1,0000**	**1,0000**
200x200_60(4)	**1,0000**	**1,0000**	**1,0000**	**1,0000**	**1,0000**	**1,0000**	**1,0000**	**1,0000**	**1,0000**	**1,0000**
200x200_60(6)	**1,0000**	**1,0000**	**1,0000**	**1,0000**	**1,0000**	**1,0000**	**1,0000**	**1,0000**	**1,0000**	**1,0000**
200x200_60(9)	**1,0000**	**1,0000**	**1,0000**	**0,9998**	**0,9867**	**0,9998**	0,8429	0,9331	**0,9998**	**1,0000**
300x300_30(6)	**1,0000**	**1,0000**	**1,0000**	**1,0000**	**0,9999**	**1,0000**	**1,0000**	**1,0000**	**1,0000**	**1,0000**
300x300_30(12)	**1,0000**	**1,0000**	**0,9949**	**0,9841**	0,6107	**1,0000**	**1,0000**	**1,0000**	**1,0000**	**1,0000**
300x300_30(18)	**1,0000**	**1,0000**	0,6080	0,3068	0,0922	**1,0000**	**1,0000**	**1,0000**	**1,0000**	**1,0000**
300x300_30(24)	**1,0000**	**1,0000**	**0,9918**	0,7701	0,4191	**1,0000**	**1,0000**	**1,0000**	**1,0000**	**0,9999**
300x300_60(6)	**1,0000**	**1,0000**	**1,0000**	**1,0000**	**1,0000**	**0,9995**	**0,9862**	**1,0000**	**1,0000**	**1,0000**
300x300_60(12)	**1,0000**	**1,0000**	**0,9999**	**0,9918**	0,6027	0,0291	0,0001	0,0000	0,0000	0,0000
300x300_60(18)	**1,0000**	**0,9699**	0,0000	0,0000	0,0000	**1,0000**	**0,9996**	0,8258	0,1199	0,0582
300x300_60(24)	**1,0000**	**1,0000**	0,8829	0,0000	0,0000	**1,0000**	**1,0000**	**1,0000**	**0,9885**	0,2748

Table B.2: P-values obtained by comparing the metaheuristics through Wilcoxon-Mann-Whitney's test. Part 2 of 7.

	NSGA-II vs MO-FA					NSGA-II vs MO-GSA				
	Evaluations (Stop condition)					Evaluations (Stop condition)				
Instance($\tilde{s}_r$)	50 000	100 000	200 000	300 000	400 000	50 000	100 000	200 000	300 000	400 000
50x50_30(1)	**1,0000**	**1,0000**	**1,0000**	**1,0000**	**1,0000**	**1,0000**	**1,0000**	**1,0000**	**1,0000**	**1,0000**
50x50_60(1)	**1,0000**	**1,0000**	**1,0000**	**1,0000**	**1,0000**	**1,0000**	**1,0000**	**1,0000**	**1,0000**	**1,0000**
100x100_30(2)	**1,0000**	**1,0000**	**1,0000**	**1,0000**	**1,0000**	**1,0000**	**1,0000**	**1,0000**	**1,0000**	**1,0000**
100x100_30(3)	**1,0000**	**1,0000**	**1,0000**	**1,0000**	**1,0000**	**0,9897**	**0,9999**	**1,0000**	**1,0000**	**1,0000**
100x100_60(2)	**1,0000**	**1,0000**	**1,0000**	**1,0000**	**1,0000**	**1,0000**	**1,0000**	**1,0000**	**1,0000**	**1,0000**
100x100_60(3)	**1,0000**	**1,0000**	**1,0000**	**1,0000**	**1,0000**	**1,0000**	**1,0000**	**1,0000**	**1,0000**	**1,0000**
200x200_30(2)	**1,0000**	**1,0000**	**1,0000**	**1,0000**	**1,0000**	**1,0000**	**1,0000**	**0,9999**	**1,0000**	**1,0000**
200x200_30(4)	**1,0000**	**1,0000**	**0,9998**	**0,9996**	**0,9992**	**1,0000**	**0,9999**	**0,9998**	**1,0000**	**1,0000**
200x200_30(6)	**1,0000**	**1,0000**	**1,0000**	**1,0000**	**1,0000**	**0,9991**	**0,9893**	0,9279	**0,9966**	**0,9994**
200x200_30(9)	**1,0000**	**1,0000**	**1,0000**	**1,0000**	**1,0000**	0,0078	0,0005	0,0103	0,0988	0,4655
200x200_60(2)	**1,0000**	**1,0000**	**1,0000**	**1,0000**	**1,0000**	0,5894	**0,9957**	**1,0000**	**1,0000**	**1,0000**
200x200_60(4)	**1,0000**	**1,0000**	**1,0000**	**1,0000**	**1,0000**	**1,0000**	**1,0000**	**1,0000**	**1,0000**	**1,0000**
200x200_60(6)	**1,0000**	**1,0000**	**1,0000**	**1,0000**	**0,9994**	**0,9669**	0,3865	0,9387	**0,9921**	**0,9912**
200x200_60(9)	**1,0000**	**1,0000**	**1,0000**	**1,0000**	**1,0000**	0,0000	0,0000	0,1376	0,6764	0,9191
300x300_30(6)	**1,0000**	**1,0000**	**0,9962**	**0,9775**	0,8818	0,0410	0,0264	0,1256	0,2386	0,3136
300x300_30(12)	**1,0000**	**1,0000**	**1,0000**	**1,0000**	**1,0000**	0,0579	0,0922	0,3808	0,8290	0,8997
300x300_30(18)	**1,0000**	**1,0000**	**1,0000**	**1,0000**	**1,0000**	**0,9972**	**0,9625**	**0,9923**	**0,9988**	**1,0000**
300x300_30(24)	**1,0000**	**1,0000**	**1,0000**	**1,0000**	**1,0000**	**1,0000**	**1,0000**	**1,0000**	**1,0000**	**1,0000**
300x300_60(6)	**1,0000**	**1,0000**	**1,0000**	**1,0000**	**1,0000**	0,6189	0,2299	**0,9680**	**0,9957**	**0,9988**
300x300_60(12)	**1,0000**	**1,0000**	**1,0000**	**1,0000**	**1,0000**	**0,9999**	**0,9992**	0,8715	0,8593	**0,9653**
300x300_60(18)	**1,0000**	**1,0000**	**1,0000**	**1,0000**	**0,9998**	**1,0000**	**0,9901**	**0,9999**	**0,9986**	**1,0000**
300x300_60(24)	**1,0000**	**1,0000**	**1,0000**	**1,0000**	**1,0000**	**0,9999**	**1,0000**	**1,0000**	**1,0000**	**1,0000**

	NSGA-II vs MO-MOEA/D					SPEA2 vs MO-VNS				
	Evaluations (Stop condition)					Evaluations (Stop condition)				
Instance($\tilde{s}_r$)	50 000	100 000	200 000	300 000	400 000	50 000	100 000	200 000	300 000	400 000
50x50_30(1)	**1,0000**	**1,0000**	**1,0000**	**1,0000**	**1,0000**	0,5849	0,7482	**0,9857**	**1,0000**	**1,0000**
50x50_60(1)	**1,0000**	**1,0000**	**1,0000**	**1,0000**	**1,0000**	**1,0000**	**1,0000**	**1,0000**	**1,0000**	**1,0000**
100x100_30(2)	**1,0000**	**1,0000**	**1,0000**	**1,0000**	**1,0000**	**1,0000**	**1,0000**	**1,0000**	**1,0000**	**1,0000**
100x100_30(3)	**1,0000**	**1,0000**	**1,0000**	**1,0000**	**1,0000**	**1,0000**	**1,0000**	**1,0000**	**1,0000**	**1,0000**
100x100_60(2)	**1,0000**	**1,0000**	**1,0000**	**1,0000**	**1,0000**	0,9314	**0,9992**	**0,9999**	**0,9998**	**1,0000**
100x100_60(3)	0,0000	0,0000	0,0000	0,0000	0,0000	**0,9998**	**1,0000**	**1,0000**	**1,0000**	**1,0000**
200x200_30(2)	**1,0000**	**1,0000**	**0,9998**	**0,9980**	**0,9975**	**1,0000**	**1,0000**	**1,0000**	**1,0000**	**1,0000**
200x200_30(4)	**0,9999**	**0,9998**	**0,9917**	**0,9852**	**0,9841**	**1,0000**	**1,0000**	**1,0000**	**1,0000**	**1,0000**
200x200_30(6)	**1,0000**	**0,9857**	0,0442	0,0245	0,0130	**0,9948**	**1,0000**	**1,0000**	**1,0000**	**1,0000**
200x200_30(9)	**0,9620**	0,2022	0,0066	0,0016	0,0004	**1,0000**	**1,0000**	**1,0000**	**1,0000**	**1,0000**
200x200_60(2)	**1,0000**	**1,0000**	**1,0000**	**1,0000**	**1,0000**	**1,0000**	**1,0000**	**1,0000**	**1,0000**	**1,0000**
200x200_60(4)	**0,9826**	0,8066	0,1857	0,0398	0,0133	**1,0000**	**1,0000**	**1,0000**	**1,0000**	**1,0000**
200x200_60(6)	0,0047	0,0000	0,0000	0,0000	0,0000	**1,0000**	**0,9999**	**0,9997**	**0,9997**	**0,9998**
200x200_60(9)	0,0000	0,0000	0,0000	0,0000	0,0000	**1,0000**	**0,9996**	0,9480	**0,9577**	0,8218
300x300_30(6)	0,0988	0,0007	0,0000	0,0000	0,0000	**1,0000**	**1,0000**	**0,9865**	0,6579	0,4468
300x300_30(12)	**0,9969**	0,6024	0,1776	0,2173	0,0767	**1,0000**	0,6189	0,1571	0,0765	0,0423
300x300_30(18)	**1,0000**	**1,0000**	**0,9998**	**0,9991**	**0,9887**	**1,0000**	**1,0000**	**1,0000**	**1,0000**	**1,0000**
300x300_30(24)	**1,0000**	**1,0000**	**0,9998**	0,8962	0,5532	**1,0000**	**0,9915**	0,1710	0,0163	0,0182
300x300_60(6)	**1,0000**	**1,0000**	**0,9999**	**0,9917**	0,9480	0,3338	0,0000	0,0000	0,0000	0,0000
300x300_60(12)	**1,0000**	**0,9992**	0,1605	0,0004	0,0000	**1,0000**	0,9194	0,0000	0,0000	0,0000
300x300_60(18)	**1,0000**	0,9060	0,0000	0,0000	0,0000	**1,0000**	**1,0000**	**1,0000**	**1,0000**	**1,0000**
300x300_60(24)	**1,0000**	**1,0000**	0,5698	0,0000	0,0000	**1,0000**	**1,0000**	**1,0000**	**1,0000**	**1,0000**

Table B.3: P-values obtained by comparing the metaheuristics through Wilcoxon-Mann-Whitney's test. Part 3 of 7.

	SPEA2 vs MO-VNS*					SPEA2 vs MO-ABC				
	Evaluations (Stop condition)					Evaluations (Stop condition)				
Instance($\tilde{s}_r$)	**50 000**	**100 000**	**200 000**	**300 000**	**400 000**	**50 000**	**100 000**	**200 000**	**300 000**	**400 000**
50x50_30(1)	0,5849	0,7482	**0,9857**	**1,0000**	**1,0000**	**1,0000**	**1,0000**	**1,0000**	**1,0000**	**1,0000**
50x50_60(1)	**1,0000**	**1,0000**	**1,0000**	**1,0000**	**1,0000**	**1,0000**	**1,0000**	**1,0000**	**1,0000**	**1,0000**
100x100_30(2)	**1,0000**	**1,0000**	**1,0000**	**1,0000**	**1,0000**	**1,0000**	**1,0000**	**1,0000**	**1,0000**	**1,0000**
100x100_30(3)	**1,0000**	**1,0000**	**1,0000**	**1,0000**	**1,0000**	**1,0000**	**1,0000**	**1,0000**	**1,0000**	**1,0000**
100x100_60(2)	0,9314	**0,9992**	**0,9999**	**0,9998**	**1,0000**	**1,0000**	**1,0000**	**1,0000**	**1,0000**	**1,0000**
100x100_60(3)	**0,9998**	**1,0000**	**1,0000**	**1,0000**	**1,0000**	**1,0000**	**1,0000**	**1,0000**	**1,0000**	**1,0000**
200x200_30(2)	**1,0000**	**1,0000**	**1,0000**	**1,0000**	**1,0000**	**0,9951**	**0,9973**	**1,0000**	**1,0000**	**1,0000**
200x200_30(4)	**1,0000**	**1,0000**	**1,0000**	**1,0000**	**1,0000**	**1,0000**	**0,9987**	**1,0000**	**1,0000**	**1,0000**
200x200_30(6)	**0,9948**	**1,0000**	**1,0000**	**1,0000**	**1,0000**	**1,0000**	**1,0000**	**1,0000**	**1,0000**	**1,0000**
200x200_30(9)	**1,0000**	**1,0000**	**1,0000**	**1,0000**	**1,0000**	**1,0000**	**1,0000**	**1,0000**	**1,0000**	**1,0000**
200x200_60(2)	**1,0000**	**1,0000**	**1,0000**	**1,0000**	**1,0000**	**1,0000**	**1,0000**	**1,0000**	**1,0000**	**1,0000**
200x200_60(4)	**1,0000**	**1,0000**	**1,0000**	**1,0000**	**1,0000**	**1,0000**	**1,0000**	**1,0000**	**1,0000**	**1,0000**
200x200_60(6)	**1,0000**	**0,9999**	**0,9997**	**0,9997**	**0,9998**	**1,0000**	**1,0000**	**1,0000**	**1,0000**	**1,0000**
200x200_60(9)	**1,0000**	**0,9996**	0,9480	**0,9577**	0,8218	**1,0000**	**1,0000**	**1,0000**	**1,0000**	**1,0000**
300x300_30(6)	**1,0000**	**1,0000**	**0,9865**	0,6579	0,4468	**1,0000**	**1,0000**	**1,0000**	**1,0000**	**1,0000**
300x300_30(12)	**1,0000**	0,6189	0,1571	0,0765	0,0423	**1,0000**	0,9495	**0,9918**	**1,0000**	**1,0000**
300x300_30(18)	**1,0000**	**1,0000**	**1,0000**	**1,0000**	**1,0000**	0,0001	0,0059	**0,9994**	**1,0000**	**1,0000**
300x300_30(24)	**1,0000**	**0,9915**	0,1710	0,0163	0,0182	0,0000	0,0000	0,0000	0,0000	0,0000
300x300_60(6)	0,3338	0,0000	0,0000	0,0000	0,0000	0,0001	0,0019	0,0021	0,0001	0,0002
300x300_60(12)	**1,0000**	0,9194	0,0000	0,0000	0,0000	**1,0000**	**1,0000**	0,5809	0,0030	0,0002
300x300_60(18)	**1,0000**	**1,0000**	**1,0000**	**1,0000**	**1,0000**	**1,0000**	**1,0000**	**1,0000**	**1,0000**	**1,0000**
300x300_60(24)	**1,0000**	**1,0000**	**1,0000**	**1,0000**	**1,0000**	**1,0000**	**1,0000**	**1,0000**	**1,0000**	**1,0000**

	SPEA2 vs MO-FA					SPEA2 vs MO-GSA				
	Evaluations (Stop condition)					Evaluations (Stop condition)				
Instance($\tilde{s}_r$)	**50 000**	**100 000**	**200 000**	**300 000**	**400 000**	**50 000**	**100 000**	**200 000**	**300 000**	**400 000**
50x50_30(1)	**1,0000**	**1,0000**	**1,0000**	**1,0000**	**1,0000**	1,0000	1,0000	1,0000	1,0000	1,0000
50x50_60(1)	**1,0000**	**1,0000**	**1,0000**	**1,0000**	**1,0000**	1,0000	1,0000	1,0000	1,0000	1,0000
100x100_30(2)	**1,0000**	**1,0000**	**1,0000**	**1,0000**	**1,0000**	1,0000	1,0000	1,0000	1,0000	1,0000
100x100_30(3)	**1,0000**	**1,0000**	**1,0000**	**1,0000**	**1,0000**	1,0000	1,0000	1,0000	1,0000	1,0000
100x100_60(2)	**1,0000**	**1,0000**	**1,0000**	**1,0000**	**1,0000**	1,0000	1,0000	1,0000	1,0000	1,0000
100x100_60(3)	**1,0000**	**1,0000**	**1,0000**	**1,0000**	**1,0000**	0,9999	1,0000	1,0000	1,0000	1,0000
200x200_30(2)	**1,0000**	**1,0000**	**1,0000**	**1,0000**	**1,0000**	0,9999	1,0000	1,0000	1,0000	1,0000
200x200_30(4)	**1,0000**	**1,0000**	**1,0000**	**1,0000**	**1,0000**	**0,9989**	0,9060	**0,9996**	**1,0000**	**1,0000**
200x200_30(6)	**1,0000**	**1,0000**	**1,0000**	**1,0000**	**1,0000**	0,0668	0,7879	**1,0000**	**1,0000**	**1,0000**
200x200_30(9)	**1,0000**	**1,0000**	**1,0000**	**1,0000**	**1,0000**	1,0000	1,0000	1,0000	1,0000	1,0000
200x200_60(2)	**1,0000**	**1,0000**	**1,0000**	**1,0000**	**1,0000**	0,9998	1,0000	1,0000	1,0000	1,0000
200x200_60(4)	**1,0000**	**1,0000**	**1,0000**	**1,0000**	**1,0000**	0,0765	0,7061	1,0000	1,0000	1,0000
200x200_60(6)	**1,0000**	**0,9953**	0,8594	0,8480	0,8525	0,0000	0,0000	0,0024	0,0248	0,0871
200x200_60(9)	**1,0000**	**1,0000**	**1,0000**	**1,0000**	**1,0000**	0,0001	0,0026	0,2132	0,7299	**0,9637**
300x300_30(6)	**1,0000**	**1,0000**	**1,0000**	**1,0000**	**1,0000**	0,4136	0,7254	**0,9998**	**1,0000**	**1,0000**
300x300_30(12)	**1,0000**	**1,0000**	**1,0000**	**1,0000**	**1,0000**	**1,0000**	**0,9999**	**0,9998**	**1,0000**	**1,0000**
300x300_30(18)	**1,0000**	**1,0000**	**1,0000**	**1,0000**	**1,0000**	0,0000	0,0000	0,0301	0,7701	**0,9590**
300x300_30(24)	**1,0000**	**1,0000**	**1,0000**	**1,0000**	**1,0000**	0,0000	0,0011	0,0002	0,0032	0,3565
300x300_60(6)	**1,0000**	**1,0000**	**1,0000**	**0,9999**	**0,9577**	0,0000	0,0000	0,6354	0,7646	**0,9836**
300x300_60(12)	**1,0000**	**1,0000**	**1,0000**	**1,0000**	**0,9995**	0,0000	0,0871	0,8496	**0,9990**	**0,9970**
300x300_60(18)	**1,0000**	**1,0000**	**1,0000**	**1,0000**	**1,0000**	**1,0000**	**1,0000**	**1,0000**	**1,0000**	**1,0000**
300x300_60(24)	**1,0000**	**1,0000**	**1,0000**	**1,0000**	**1,0000**	**1,0000**	**1,0000**	**1,0000**	**1,0000**	**1,0000**

Table B.4: P-values obtained by comparing the metaheuristics through Wilcoxon-Mann-Whitney's test. Part 4 of 7.

	SPEA2 vs MOEA/D					MO-VNS vs MO-VNS*				
	Evaluations (Stop condition)					Evaluations (Stop condition)				
Instance($\tilde{s}_r$)	50 000	100 000	200 000	300 000	400 000	50 000	100 000	200 000	300 000	400 000
50x50_30(1)	**1,0000**	**1,0000**	**1,0000**	**1,0000**	**1,0000**	0,0025	0,0005	0,0004	0,1377	0,0138
50x50_60(1)	**1,0000**	**1,0000**	**1,0000**	**1,0000**	**1,0000**	0,3677	0,1447	0,0004	0,0000	0,0000
100x100_30(2)	**1,0000**	**1,0000**	**1,0000**	**1,0000**	**1,0000**	0,0005	0,0009	0,0000	0,0000	0,0000
100x100_30(3)	0,2429	0,0183	0,0034	0,2173	0,0248	0,0616	0,0014	0,1064	0,5734	0,9232
100x100_60(2)	**1,0000**	**1,0000**	**1,0000**	**1,0000**	**1,0000**	0,0082	0,0117	0,0778	0,0075	0,0008
100x100_60(3)	**0,9998**	**0,9998**	**0,9999**	**1,0000**	**1,0000**	0,0024	0,0025	0,0019	0,0017	0,0326
200x200_30(2)	**0,9998**	**0,9999**	0,8066	0,7205	0,6687	**0,9944**	**0,9758**	**0,9741**	**0,9741**	**0,9520**
200x200_30(4)	**1,0000**	**0,9901**	0,9424	0,9022	0,8860	**1,0000**	**1,0000**	**1,0000**	**1,0000**	**1,0000**
200x200_30(6)	**1,0000**	**1,0000**	**1,0000**	**0,9982**	**0,9885**	0,0001	0,0067	0,0113	0,0415	0,1121
200x200_30(9)	0,5365	0,1439	0,0177	0,0010	0,0009	**0,9996**	**0,9722**	0,9404	0,7082	0,7325
200x200_60(2)	0,1064	0,0002	0,0000	0,0000	0,0000	**0,9995**	**0,9975**	**0,9577**	0,9172	0,9332
200x200_60(4)	0,1779	0,0000	0,0000	0,0000	0,0000	0,9255	0,8290	0,7061	0,4357	0,1895
200x200_60(6)	0,0000	0,0000	0,0000	0,0000	0,0000	**0,9996**	**0,9981**	**0,9912**	**0,9699**	**0,9768**
200x200_60(9)	0,8254	0,2299	0,1038	0,1013	0,0940	**1,0000**	**1,0000**	**1,0000**	**0,9998**	**0,9912**
300x300_30(6)	**1,0000**	**1,0000**	**1,0000**	**1,0000**	**0,9996**	**1,0000**	**1,0000**	**1,0000**	**1,0000**	**1,0000**
300x300_30(12)	**1,0000**	**0,9959**	0,5809	0,3037	0,2386	**1,0000**	**1,0000**	**1,0000**	**1,0000**	**1,0000**
300x300_30(18)	**1,0000**	**0,9637**	0,8987	0,7658	0,6559	**1,0000**	**0,9999**	**0,9974**	**0,9897**	**0,9538**
300x300_30(24)	0,0883	0,0004	0,0000	0,0000	0,0000	**1,0000**	**1,0000**	**1,0000**	**1,0000**	**1,0000**
300x300_60(6)	0,2257	0,0000	0,0000	0,0000	0,0000	**1,0000**	**0,9999**	0,7482	0,3236	0,1090
300x300_60(12)	**0,9999**	0,7252	0,0000	0,0000	0,0000	**1,0000**	**1,0000**	**0,9996**	**0,9985**	**0,9982**
300x300_60(18)	**1,0000**	**1,0000**	**1,0000**	**1,0000**	**1,0000**	0,1468	0,0001	0,0003	0,0117	0,2681
300x300_60(24)	**1,0000**	**1,0000**	**1,0000**	**1,0000**	**1,0000**	0,0000	0,0001	0,0143	0,5844	0,9061

	MO-VNS vs MO-ABC					MO-VNS vs MO-FA				
	Evaluations (Stop condition)					Evaluations (Stop condition)				
Instance($\tilde{s}_r$)	50 000	100 000	200 000	300 000	400 000	50 000	100 000	200 000	300 000	400 000
50x50_30(1)	0,8539	0,0000	0,0000	0,0000	0,0000	**0,9998**	0,8347	**0,9595**	**0,9995**	**0,9989**
50x50_60(1)	**1,0000**	**1,0000**	**0,9982**	0,7205	0,1227	**0,9956**	0,6925	0,2868	0,1503	0,0006
100x100_30(2)	0,0000	0,0000	0,0000	0,0000	0,0000	0,0000	0,0000	0,0000	0,0000	0,0000
100x100_30(3)	0,0765	0,0093	0,0000	0,0000	0,0000	0,0566	0,0001	0,0000	0,0000	0,0000
100x100_60(2)	0,0785	0,0025	0,0000	0,0000	0,0000	0,8685	0,6889	**0,9996**	0,9385	0,2027
100x100_60(3)	0,0000	0,0000	0,0000	0,0001	0,0000	0,0240	0,0291	0,0092	0,0070	0,0013
200x200_30(2)	0,0000	0,0000	0,1227	**0,9797**	**0,9970**	**0,9994**	**0,9970**	0,9458	0,9489	0,8628
200x200_30(4)	0,0017	0,1227	0,5140	**0,9927**	**1,0000**	**1,0000**	**1,0000**	**1,0000**	**1,0000**	**1,0000**
200x200_30(6)	**0,9947**	**0,9805**	0,6053	0,3273	0,2032	0,5973	0,2266	0,1100	0,1951	0,4057
200x200_30(9)	0,0000	**0,9608**	**1,0000**	**0,9974**	**0,9818**	**0,9835**	0,6456	0,0319	0,0005	0,0001
200x200_60(2)	0,0000	0,0000	0,0520	**0,9744**	**0,9995**	0,8966	0,6622	0,2173	0,0830	0,0304
200x200_60(4)	0,0000	0,0000	0,0000	0,1315	**0,9998**	**1,0000**	**1,0000**	**0,9989**	**0,9727**	0,8857
200x200_60(6)	**0,9835**	**0,9997**	**1,0000**	**1,0000**	**1,0000**	**0,9867**	0,9450	0,6422	0,4500	0,3082
200x200_60(9)	**1,0000**	**1,0000**	**1,0000**	**1,0000**	**1,0000**	**1,0000**	**1,0000**	**1,0000**	**1,0000**	**1,0000**
300x300_30(6)	**1,0000**	**1,0000**	**1,0000**	**1,0000**	**1,0000**	**1,0000**	**1,0000**	**1,0000**	**1,0000**	**1,0000**
300x300_30(12)	**1,0000**	**1,0000**	**1,0000**	**1,0000**	**1,0000**	**1,0000**	**1,0000**	**1,0000**	**1,0000**	**1,0000**
300x300_30(18)	0,0002	0,0085	0,9367	**1,0000**	**1,0000**	**1,0000**	**1,0000**	**1,0000**	**0,9990**	**0,9914**
300x300_30(24)	0,0031	0,0045	0,1199	0,4246	0,8936	**1,0000**	**1,0000**	**1,0000**	**1,0000**	**1,0000**
300x300_60(6)	**0,9989**	**1,0000**	**1,0000**	**1,0000**	**1,0000**	**1,0000**	**1,0000**	**1,0000**	**1,0000**	**1,0000**
300x300_60(12)	**1,0000**	**1,0000**	**1,0000**	**1,0000**	**1,0000**	**1,0000**	**1,0000**	**1,0000**	**1,0000**	**1,0000**
300x300_60(18)	**1,0000**	**1,0000**	**1,0000**	**1,0000**	**1,0000**	**1,0000**	**1,0000**	**1,0000**	**1,0000**	**1,0000**
300x300_60(24)	**1,0000**	**1,0000**	**1,0000**	**1,0000**	**1,0000**	**1,0000**	**1,0000**	**1,0000**	**1,0000**	**1,0000**

Table B.5: P-values obtained by comparing the metaheuristics through Wilcoxon-Mann-Whitney's test. Part 5 of 7.

	MO-VNS vs MO-GSA					**MO-VNS vs MOEA/D**				
	Evaluations (Stop condition)					**Evaluations (Stop condition)**				
Instance($\tilde{s}_r$)	**50 000**	**100 000**	**200 000**	**300 000**	**400 000**	**50 000**	**100 000**	**200 000**	**300 000**	**400 000**
50x50_30(1)	0,0013	0,0000	0,0000	0,0000	0,0000	0,0175	0,0000	0,0000	0,0000	0,0000
50x50_60(1)	0,0000	0,0000	0,0000	0,0000	0,0000	0,0258	0,0001	0,0000	0,0000	0,0000
100x100_30(2)	0,0000	0,0000	0,0000	0,0000	0,0000	0,0000	0,0000	0,0000	0,0000	0,0000
100x100_30(3)	0,0000	0,0000	0,0000	0,0000	0,0000	0,0000	0,0000	0,0000	0,0000	0,0000
100x100_60(2)	0,0256	0,0000	0,0000	0,0000	0,0000	0,0633	0,0014	0,0000	0,0000	0,0000
100x100_60(3)	0,0000	0,0000	0,0000	0,0000	0,0000	0,0001	0,0000	0,0000	0,0000	0,0000
200x200_30(2)	0,0000	0,0001	0,0043	0,0133	0,0535	0,0002	0,0002	0,0000	0,0000	0,0000
200x200_30(4)	0,0003	0,0189	0,1143	0,2939	0,5744	0,5324	0,3153	0,0373	0,0146	0,0032
200x200_30(6)	0,0000	0,0000	0,0000	0,0000	0,0003	0,0000	0,0000	0,0000	0,0000	0,0000
200x200_30(9)	0,0000	0,0000	0,0000	0,0000	0,0000	0,0000	0,0000	0,0000	0,0000	0,0000
200x200_60(2)	0,0000	0,0000	0,0000	0,0002	0,0013	0,0000	0,0000	0,0000	0,0000	0,0000
200x200_60(4)	0,0000	0,0000	0,0000	0,0000	0,0010	0,0000	0,0000	0,0000	0,0000	0,0000
200x200_60(6)	0,0000	0,0000	0,0002	0,0005	0,0027	0,0000	0,0000	0,0000	0,0000	0,0000
200x200_60(9)	0,0008	0,1117	0,8910	**0,9689**	**0,9970**	0,9294	0,6349	0,3864	0,2795	0,1895
300x300_30(6)	0,6662	**1,0000**	**1,0000**	**1,0000**	**1,0000**	**1,0000**	**1,0000**	**1,0000**	**1,0000**	**1,0000**
300x300_30(12)	**1,0000**	**1,0000**	**1,0000**	**1,0000**	**1,0000**	**1,0000**	**1,0000**	**1,0000**	**1,0000**	**1,0000**
300x300_30(18)	0,0000	0,0001	0,0153	0,1227	0,2299	**0,9590**	0,7701	0,5253	0,2386	0,0582
300x300_30(24)	**0,9524**	**0,9999**	**1,0000**	**1,0000**	**1,0000**	**0,9998**	**0,9995**	**0,9862**	0,8561	0,6136
300x300_60(6)	**0,9887**	**1,0000**	**1,0000**	**1,0000**	**1,0000**	**1,0000**	**0,9991**	0,8685	0,7157	0,6027
300x300_60(12)	0,0264	**0,9930**	**1,0000**	**1,0000**	**1,0000**	**1,0000**	**0,9995**	**0,9852**	**0,9776**	0,9465
300x300_60(18)	**1,0000**	**1,0000**	**1,0000**	**1,0000**	**1,0000**	**1,0000**	**1,0000**	**1,0000**	**1,0000**	**1,0000**
300x300_60(24)	**1,0000**	**1,0000**	**1,0000**	**1,0000**	**1,0000**	**1,0000**	**1,0000**	**1,0000**	**1,0000**	**1,0000**

	MO-VNS* vs MO-ABC					**MO-VNS vs MO-FA***				
	Evaluations (Stop condition)					**Evaluations (Stop condition)**				
Instance($\tilde{s}_r$)	**50 000**	**100 000**	**200 000**	**300 000**	**400 000**	**50 000**	**100 000**	**200 000**	**300 000**	**400 000**
50x50_30(1)	**1,0000**	0,8655	0,0694	0,0000	0,0000	**1,0000**	**0,9999**	**1,0000**	**1,0000**	**1,0000**
50x50_60(1)	**1,0000**	**1,0000**	**1,0000**	**1,0000**	**1,0000**	**0,9870**	**0,9943**	**1,0000**	**1,0000**	**1,0000**
100x100_30(2)	0,0186	0,0000	0,0000	0,0000	0,0000	0,0000	0,0000	0,0000	0,0000	0,0000
100x100_30(3)	0,6082	0,8181	0,1571	0,0000	0,0000	0,4972	0,4524	0,0745	0,0000	0,0000
100x100_60(2)	**0,9776**	0,3390	0,0177	0,0062	0,0016	**0,9976**	**0,9847**	**1,0000**	**0,9999**	**0,9967**
100x100_60(3)	0,3441	0,2386	0,5864	0,3493	0,0138	0,8561	0,7482	0,4691	0,3186	0,0596
200x200_30(2)	0,0000	0,0000	0,0002	0,6192	0,9407	0,6755	0,7487	0,6599	0,6013	0,4809
200x200_30(4)	0,0000	0,0000	0,0000	0,0001	0,0871	**0,9852**	**0,9947**	**0,9926**	**0,9953**	**0,9848**
200x200_30(6)	**1,0000**	**1,0000**	**0,9959**	0,9042	0,4942	**0,9998**	**0,9720**	0,8817	0,7326	0,6885
200x200_30(9)	0,0000	0,2055	**0,9946**	**0,9912**	0,9235	0,0135	0,0185	0,0010	0,0000	0,0000
200x200_60(2)	0,0000	0,0000	0,0001	0,7482	**0,9940**	0,0240	0,0301	0,0051	0,0016	0,0001
200x200_60(4)	0,0000	0,0000	0,0000	0,2011	**0,9988**	**1,0000**	**0,9993**	0,9450	0,9060	0,8801
200x200_60(6)	0,0079	0,2843	0,4136	0,6559	0,9036	0,1117	0,0725	0,0226	0,0182	0,0144
200x200_60(9)	0,8857	**1,0000**	**1,0000**	**1,0000**	**1,0000**	**1,0000**	**1,0000**	**1,0000**	**1,0000**	**1,0000**
300x300_30(6)	**0,9995**	**1,0000**	**1,0000**	**1,0000**	**1,0000**	**1,0000**	**1,0000**	**1,0000**	**1,0000**	**1,0000**
300x300_30(12)	0,0651	**0,9993**	**1,0000**	**1,0000**	**1,0000**	**1,0000**	**1,0000**	**1,0000**	**1,0000**	**1,0000**
300x300_30(18)	0,0000	0,0000	0,0423	**0,9945**	**1,0000**	**0,9889**	**0,9877**	**0,9858**	0,9164	0,8816
300x300_30(24)	0,0000	0,0000	0,0000	0,0000	0,0000	**1,0000**	**1,0000**	**1,0000**	**1,0000**	**1,0000**
300x300_60(6)	0,0004	**0,9590**	**1,0000**	**1,0000**	**1,0000**	**1,0000**	**1,0000**	**1,0000**	**1,0000**	**1,0000**
300x300_60(12)	0,0045	**0,9940**	**1,0000**	**1,0000**	**1,0000**	**1,0000**	**1,0000**	**1,0000**	**1,0000**	**1,0000**
300x300_60(18)	**1,0000**	**1,0000**	**1,0000**	**1,0000**	**1,0000**	**1,0000**	**1,0000**	**1,0000**	**1,0000**	**1,0000**
300x300_60(24)	**1,0000**	**1,0000**	**1,0000**	**1,0000**	**1,0000**	**1,0000**	**1,0000**	**1,0000**	**1,0000**	**1,0000**

Table B.6: P-values obtained by comparing the metaheuristics through Wilcoxon-Mann-Whitney's test. Part 6 of 7.

	MO-VNS* vs MO-GSA					**MO-VNS* vs MOEA/D**				
	Evaluations (Stop condition)					**Evaluations (Stop condition)**				
Instance($\tilde{s}_r$)	**50 000**	**100 000**	**200 000**	**300 000**	**400 000**	**50 000**	**100 000**	**200 000**	**300 000**	**400 000**
50x50_30(1)	0,7725	0,4598	0,0110	0,0000	0,0000	0,8417	0,4288	0,0081	0,0000	0,0000
50x50_60(1)	0,0000	0,0000	0,0000	0,0000	0,0000	0,0203	0,0000	0,0000	0,0000	0,0000
100x100_30(2)	0,0000	0,0000	0,0000	0,0000	0,0000	0,0000	0,0000	0,0000	0,0000	0,0000
100x100_30(3)	0,0687	0,0273	0,0177	0,0000	0,0000	0,0000	0,0000	0,0000	0,0000	0,0000
100x100_60(2)	**0,9614**	0,1117	0,0128	0,0076	0,0025	0,9434	0,2474	0,0196	0,0060	0,0016
100x100_60(3)	0,1143	0,0599	0,2257	0,1345	0,0025	0,2988	0,0988	0,0264	0,0011	0,0001
200x200_30(2)	0,0000	0,0000	0,0000	0,0000	0,0001	0,0000	0,0000	0,0000	0,0000	0,0000
200x200_30(4)	0,0000	0,0000	0,0000	0,0000	0,0000	0,0000	0,0000	0,0000	0,0000	0,0000
200x200_30(6)	0,0040	0,0000	0,0022	0,0008	0,0009	0,5744	0,0038	0,0000	0,0000	0,0000
200x200_30(9)	0,0000	0,0000	0,0000	0,0000	0,0000	0,0000	0,0000	0,0000	0,0000	0,0000
200x200_60(2)	0,0000	0,0000	0,0000	0,0000	0,0000	0,0000	0,0000	0,0000	0,0000	0,0000
200x200_60(4)	0,0000	0,0000	0,0000	0,0003	0,0746	0,0000	0,0000	0,0000	0,0000	0,0000
200x200_60(6)	0,0000	0,0000	0,0000	0,0000	0,0000	0,0000	0,0000	0,0000	0,0000	0,0000
200x200_60(9)	0,0000	0,0000	0,0058	0,2215	0,8962	0,0153	0,0177	0,0171	0,0291	0,0398
300x300_30(6)	0,0000	0,0010	**0,9942**	**1,0000**	**1,0000**	**0,9997**	**0,9997**	**0,9999**	**0,9998**	**0,9999**
300x300_30(12)	0,9274	**1,0000**	**1,0000**	**1,0000**	**1,0000**	**0,9999**	**0,9995**	**0,9983**	**0,9980**	**0,9927**
300x300_30(18)	0,0000	0,0000	0,0000	0,0001	0,0023	0,0006	0,0003	0,0023	0,0008	0,0004
300x300_30(24)	0,0000	0,0000	0,0016	0,0838	**0,9709**	0,0000	0,0000	0,0000	0,0000	0,0000
300x300_60(6)	0,0000	0,8582	**1,0000**	**1,0000**	**1,0000**	0,2988	0,4082	0,6027	0,6243	0,7571
300x300_60(12)	0,0000	0,0043	**1,0000**	**1,0000**	**1,0000**	0,3086	0,2132	0,1746	0,2386	0,2011
300x300_60(18)	**1,0000**	**1,0000**	**1,0000**	**1,0000**	**1,0000**	**1,0000**	**1,0000**	**1,0000**	**1,0000**	**1,0000**
300x300_60(24)	**1,0000**	**1,0000**	**1,0000**	**1,0000**	**1,0000**	**1,0000**	**1,0000**	**1,0000**	**1,0000**	**1,0000**

	MO-ABC vs MO-FA					**MO-ABC vs MO-GSA**				
	Evaluations (Stop condition)					**Evaluations (Stop condition)**				
Instance($\tilde{s}_r$)	**50 000**	**100 000**	**200 000**	**300 000**	**400 000**	**50 000**	**100 000**	**200 000**	**300 000**	**400 000**
50x50_30(1)	**0,9999**	**1,0000**	**1,0000**	**1,0000**	**1,0000**	0,0000	0,0000	0,0000	0,0000	0,0010
50x50_60(1)	0,0028	0,0000	0,0000	0,0000	0,0000	0,0000	0,0000	0,0000	0,0000	0,0000
100x100_30(2)	0,0000	0,0000	0,0003	0,1013	0,4302	0,0000	0,0000	0,0002	0,0512	0,3651
100x100_30(3)	0,4691	0,0210	0,3973	0,9376	**0,9963**	0,0000	0,0000	0,0000	0,0000	0,0002
100x100_60(2)	**0,9776**	**0,9835**	**1,0000**	**1,0000**	**1,0000**	0,2701	0,0828	0,4804	**0,9551**	**0,9912**
100x100_60(3)	**0,9727**	0,9255	0,6027	0,4747	0,3976	0,1013	0,0550	0,0196	0,0849	0,2609
200x200_30(2)	**1,0000**	**1,0000**	**0,9997**	0,5383	0,0684	**0,9551**	0,9453	0,1013	0,0000	0,0000
200x200_30(4)	**1,0000**	**1,0000**	**1,0000**	**1,0000**	**0,9998**	0,0894	0,1090	0,0363	0,0004	0,0000
200x200_30(6)	0,0161	0,0013	0,0339	0,1572	0,3781	0,0000	0,0000	0,0000	0,0000	0,0000
200x200_30(9)	**1,0000**	0,0242	0,0000	0,0000	0,0000	0,0000	0,0000	0,0000	0,0000	0,0000
200x200_60(2)	**1,0000**	**1,0000**	0,6764	0,0001	0,0000	0,0000	0,0000	0,0000	0,0000	0,0000
200x200_60(4)	**1,0000**	**1,0000**	**1,0000**	**0,9965**	0,0073	0,0000	0,0000	0,0111	0,0003	0,0000
200x200_60(6)	0,8529	0,1571	0,0014	0,0001	0,0000	0,0000	0,0000	0,0000	0,0000	0,0000
200x200_60(9)	**1,0000**	**0,9996**	**0,9889**	0,6610	0,4143	0,0000	0,0000	0,0000	0,0000	0,0000
300x300_30(6)	**1,0000**	**1,0000**	**1,0000**	**1,0000**	**1,0000**	0,0000	0,0000	0,0001	0,0026	0,0043
300x300_30(12)	**1,0000**	**1,0000**	**1,0000**	**1,0000**	**1,0000**	**0,9944**	**0,9942**	**0,9775**	0,8027	0,9029
300x300_30(18)	**1,0000**	**1,0000**	**1,0000**	0,1772	0,0002	0,0067	0,0018	0,0000	0,0000	0,0000
300x300_30(24)	**1,0000**	**1,0000**	**1,0000**	**1,0000**	**1,0000**	**1,0000**	**1,0000**	**1,0000**	**1,0000**	**1,0000**
300x300_60(6)	**1,0000**	**1,0000**	**1,0000**	**1,0000**	**1,0000**	0,1365	0,1140	**0,9964**	**0,9999**	**1,0000**
300x300_60(12)	**1,0000**	**1,0000**	**1,0000**	**1,0000**	**1,0000**	0,0000	0,0000	0,8028	**1,0000**	**1,0000**
300x300_60(18)	0,5000	0,5000	0,5000	0,5000	0,5000	0,5000	0,5000	0,5000	0,5000	0,5000
300x300_60(24)	0,5000	0,5000	0,5000	0,5000	0,5000	0,5000	0,5000	0,5000	0,5000	0,5000

Table B.7: P-values obtained by comparing the metaheuristics through Wilcoxon-Mann-Whitney's test. Part 7 of 7.

	MO-ABC vs MOEA/D					**MO-FA vs MO-GSA**				
	Evaluations (Stop condition)					**Evaluations (Stop condition)**				
Instance($\tilde{s}_r$)	**50 000**	**100 000**	**200 000**	**300 000**	**400 000**	**50 000**	**100 000**	**200 000**	**300 000**	**400 000**
50x50_30(1)	0,0000	0,0000	0,0000	0,0000	0,0000	0,0000	0,0000	0,0000	0,0000	0,0000
50x50_60(1)	0,0000	0,0000	0,0000	0,0000	0,0000	0,0000	0,0000	0,0000	0,0000	0,0000
100x100_30(2)	0,0000	0,0000	0,0000	0,0000	0,0000	0,0000	0,0005	0,2518	0,3211	0,3598
100x100_30(3)	0,0000	0,0000	0,0000	0,0000	0,0000	0,0000	0,0000	0,0000	0,0000	0,0000
100x100_60(2)	0,5140	0,5588	0,7989	0,8744	**0,9510**	0,0103	0,0031	0,0000	0,0000	0,0000
100x100_60(3)	0,4747	0,2299	0,0016	0,0004	0,0017	0,0053	0,0171	0,2609	0,4027	0,6245
200x200_30(2)	**0,9953**	0,9314	0,0003	0,0000	0,0000	0,0000	0,0000	0,0000	0,0000	0,0011
200x200_30(4)	**0,9974**	0,7003	0,0217	0,0000	0,0000	0,0000	0,0000	0,0000	0,0000	0,0000
200x200_30(6)	0,0000	0,0000	0,0000	0,0000	0,0000	0,0000	0,0000	0,0001	0,0000	0,0004
200x200_30(9)	0,0000	0,0000	0,0000	0,0000	0,0000	0,0000	0,0000	0,0000	0,0000	0,0188
200x200_60(2)	0,0000	0,0000	0,0000	0,0000	0,0000	0,0000	0,0000	0,0000	0,0109	0,1272
200x200_60(4)	0,0000	0,0000	0,0000	0,0000	0,0000	0,0000	0,0000	0,0000	0,0000	0,0001
200x200_60(6)	0,0000	0,0000	0,0000	0,0000	0,0000	0,0000	0,0000	0,0005	0,0051	0,0522
200x200_60(9)	0,0037	0,0000	0,0000	0,0000	0,0000	0,0000	0,0000	0,0000	0,0000	0,0000
300x300_30(6)	**0,9995**	0,2748	0,0006	0,0002	0,0000	0,0000	0,0000	0,0000	0,0000	0,0000
300x300_30(12)	**1,0000**	0,8593	0,0004	0,0000	0,0000	0,0000	0,0000	0,0000	0,0000	0,0000
300x300_30(18)	**1,0000**	**0,9998**	0,0633	0,0000	0,0000	0,0000	0,0000	0,0000	0,0000	0,0001
300x300_30(24)	**1,0000**	**1,0000**	**0,9996**	**0,9689**	0,3493	0,0000	0,0000	0,0000	0,0000	0,0000
300x300_60(6)	**0,9908**	0,0321	0,0000	0,0000	0,0000	0,0000	0,0000	0,0000	0,0006	0,7372
300x300_60(12)	0,8910	0,0111	0,0000	0,0000	0,0000	0,0000	0,0000	0,0000	0,0025	0,5448
300x300_60(18)	0,5000	0,5000	0,5000	0,5000	0,5000	0,5000	0,5000	0,5000	0,5000	0,5000
300x300_60(24)	0,5000	0,5000	0,5000	0,5000	0,5000	0,5000	0,5000	0,5000	0,5000	0,5000

	MO-FA vs MOEA/D					**MO-GSA vs MOEA/D**				
	Evaluations (Stop condition)					**Evaluations (Stop condition)**				
Instance($\tilde{s}_r$)	**50 000**	**100 000**	**200 000**	**300 000**	**400 000**	**50 000**	**100 000**	**200 000**	**300 000**	**400 000**
50x50_30(1)	0,0000	0,0000	0,0000	0,0000	0,0000	**0,9994**	0,5509	0,0000	0,0000	0,0000
50x50_60(1)	0,0000	0,0000	0,0000	0,0000	0,0000	**1,0000**	**1,0000**	**1,0000**	**1,0000**	**0,9995**
100x100_30(2)	0,0085	0,0596	0,0025	0,0000	0,0000	0,3390	0,3757	0,0067	0,0004	0,0000
100x100_30(3)	0,0000	0,0000	0,0000	0,0000	0,0000	0,0000	0,0000	0,0000	0,0000	0,0000
100x100_60(2)	0,0143	0,0053	0,0000	0,0000	0,0000	0,7658	0,9434	0,7658	0,3704	0,2215
100x100_60(3)	0,0410	0,0232	0,0398	0,0291	0,0922	0,7827	0,5864	0,0806	0,0076	0,0045
200x200_30(2)	0,0000	0,0000	0,0000	0,0000	0,0000	0,9450	0,4813	0,0051	0,0001	0,0000
200x200_30(4)	0,0000	0,0000	0,0000	0,0000	0,0000	**0,9996**	0,9189	0,2187	0,0241	0,0016
200x200_30(6)	0,0000	0,0000	0,0000	0,0000	0,0000	**0,9997**	**0,9979**	0,0411	0,0097	0,0000
200x200_30(9)	0,0000	0,0000	0,0000	0,0000	0,0000	0,0000	0,0000	0,0000	0,0000	0,0000
200x200_60(2)	0,0000	0,0000	0,0000	0,0000	0,0000	0,0000	0,0000	0,0000	0,0000	0,0000
200x200_60(4)	0,0000	0,0000	0,0000	0,0000	0,0000	0,6932	0,0000	0,0000	0,0000	0,0000
200x200_60(6)	0,0000	0,0000	0,0000	0,0000	0,0000	0,7252	0,0669	0,0009	0,0000	0,0000
200x200_60(9)	0,0000	0,0000	0,0000	0,0000	0,0000	**0,9999**	0,9151	0,2518	0,0940	0,0217
300x300_30(6)	0,0476	0,0000	0,0000	0,0000	0,0000	**1,0000**	**1,0000**	0,8857	0,5588	0,0331
300x300_30(12)	0,0073	0,0000	0,0000	0,0000	0,0000	**0,9775**	0,0547	0,0000	0,0000	0,0000
300x300_30(18)	0,0000	0,0000	0,0000	0,0000	0,0000	**1,0000**	**1,0000**	**0,9940**	0,5532	0,1376
300x300_30(24)	0,0000	0,0000	0,0000	0,0000	0,0000	**0,9942**	0,4860	0,0203	0,0000	0,0000
300x300_60(6)	0,0000	0,0000	0,0000	0,0000	0,0000	**0,9992**	0,2411	0,0000	0,0000	0,0000
300x300_60(12)	0,0000	0,0000	0,0000	0,0000	0,0000	**1,0000**	0,9129	0,0000	0,0000	0,0000
300x300_60(18)	0,5000	0,5000	0,5000	0,5000	0,5000	0,5000	0,5000	0,5000	0,5000	0,5000
300x300_60(24)	0,5000	0,5000	0,5000	0,5000	0,5000	0,5000	0,5000	0,5000	0,5000	0,5000

Table B.8: Set coverage metric by comparing all the metaheuristics two by two. Part 1 of 14.

	I_{SC}(NSGA-II,SPEA2)					I_{SC}(NSGA-II,MO-VNS)				
	Evaluations (Stop condition)					Evaluations (Stop condition)				
Instance($\tilde{s}_r$)	**50 000**	**100 000**	**200 000**	**300 000**	**400 000**	**50 000**	**100 000**	**200 000**	**300 000**	**400 000**
50x50_30(1)	56,52%	77,01%	96,81%	92,11%	96,49%	0,00%	0,00%	0,00%	0,00%	0,00%
50x50_60(1)	74,11%	92,97%	85,20%	99,97%	100,00%	0,00%	0,00%	0,00%	8,00%	5,00%
100x100_30(2)	54,00%	60,47%	77,46%	81,86%	91,87%	0,00%	0,00%	0,72%	0,00%	1,43%
100x100_30(3)	63,37%	90,72%	37,85%	78,19%	74,60%	0,00%	0,00%	0,00%	0,45%	0,00%
100x100_60(2)	98,67%	11,05%	97,62%	0,00%	100,00%	0,00%	0,00%	0,00%	0,00%	16,67%
100x100_60(3)	80,00%	92,60%	75,43%	100,00%	100,00%	0,00%	0,00%	0,00%	0,00%	0,00%
200x200_30(2)	91,67%	55,00%	0,00%	0,19%	100,00%	0,00%	0,00%	0,00%	0,00%	0,00%
200x200_30(4)	4,76%	97,06%	99,89%	100,00%	100,00%	9,09%	25,00%	12,50%	27,27%	83,33%
200x200_30(6)	16,67%	0,00%	10,71%	34,78%	54,55%	0,00%	0,00%	0,00%	0,00%	0,00%
200x200_30(9)	0,00%	35,71%	11,11%	0,00%	0,00%	0,00%	0,00%	0,00%	0,00%	0,00%
200x200_60(2)	92,59%	26,32%	93,22%	28,40%	28,57%	4,00%	3,13%	31,25%	14,71%	0,00%
200x200_60(4)	88,89%	64,29%	15,69%	30,56%	100,00%	0,00%	0,00%	21,43%	24,14%	0,00%
200x200_60(6)	5,45%	18,18%	0,55%	1,62%	0,15%	0,00%	18,18%	0,00%	45,00%	27,27%
200x200_60(9)	0,00%	92,07%	73,99%	96,35%	4,94%	38,46%	83,33%	69,23%	85,71%	53,85%
300x300_30(6)	20,33%	82,45%	99,88%	95,81%	100,00%	0,00%	41,67%	100,00%	100,00%	100,00%
300x300_30(12)	0,00%	0,00%	0,00%	0,00%	0,00%	0,00%	100,00%	100,00%	100,00%	100,00%
300x300_30(18)	0,00%	0,00%	0,00%	0,00%	6,67%	0,00%	0,00%	0,00%	0,00%	0,00%
300x300_30(24)	0,00%	16,67%	11,90%	13,16%	0,00%	37,50%	80,00%	100,00%	89,47%	92,86%
300x300_60(6)	0,00%	30,00%	0,00%	33,33%	77,08%	57,14%	68,75%	68,18%	75,76%	100,00%
300x300_60(12)	54,17%	26,92%	0,00%	0,00%	70,00%	61,11%	57,14%	19,05%	100,00%	100,00%
300x300_60(18)	100,00%	100,00%	100,00%	100,00%	100,00%	20,00%	20,00%	20,00%	20,00%	20,00%
300x300_60(24)	100,00%	100,00%	100,00%	100,00%	100,00%	20,00%	20,00%	20,00%	20,00%	20,00%

	I_{SC}(NSGA-II,MO-VNS*)					I_{SC}(NSGA-II,MO-ABC)				
	Evaluations (Stop condition)					Evaluations (Stop condition)				
Instance($\tilde{s}_r$)	**50 000**	**100 000**	**200 000**	**300 000**	**400 000**	**50 000**	**100 000**	**200 000**	**300 000**	**400 000**
50x50_30(1)	0,00%	0,00%	0,00%	0,00%	0,00%	0,00%	0,00%	0,67%	0,00%	16,06%
50x50_60(1)	0,00%	0,00%	0,00%	0,00%	5,88%	0,00%	0,00%	0,00%	16,34%	4,73%
100x100_30(2)	0,00%	0,00%	0,00%	0,00%	0,00%	1,89%	1,77%	0,92%	2,30%	2,39%
100x100_30(3)	0,00%	0,00%	0,00%	0,00%	0,00%	0,00%	0,00%	0,00%	0,00%	0,00%
100x100_60(2)	50,00%	50,00%	0,00%	40,00%	0,00%	31,36%	0,00%	0,29%	0,00%	42,59%
100x100_60(3)	0,00%	0,00%	0,00%	0,00%	0,00%	0,00%	0,00%	0,00%	0,00%	0,00%
200x200_30(2)	0,00%	0,00%	0,00%	0,00%	33,33%	0,00%	0,00%	0,00%	0,00%	0,00%
200x200_30(4)	0,00%	0,00%	0,00%	28,57%	0,00%	0,00%	91,67%	98,15%	24,56%	13,52%
200x200_30(6)	0,00%	0,00%	0,00%	0,00%	0,00%	0,00%	0,00%	0,00%	38,24%	0,00%
200x200_30(9)	0,00%	0,00%	5,26%	0,00%	0,00%	0,00%	0,00%	0,00%	0,00%	0,00%
200x200_60(2)	0,00%	0,00%	0,00%	0,00%	0,00%	2,44%	0,00%	0,89%	1,75%	0,00%
200x200_60(4)	0,00%	0,00%	0,00%	0,00%	0,00%	50,88%	35,29%	89,89%	9,38%	17,11%
200x200_60(6)	0,00%	0,00%	0,00%	0,00%	0,00%	0,00%	9,18%	0,00%	0,00%	0,00%
200x200_60(9)	27,27%	22,22%	44,44%	52,94%	50,00%	7,96%	0,59%	0,22%	0,34%	1,84%
300x300_30(6)	0,00%	14,29%	60,00%	0,00%	75,00%	9,38%	0,00%	4,81%	6,25%	20,51%
300x300_30(12)	0,00%	0,00%	28,57%	25,00%	100,00%	0,00%	33,33%	0,00%	0,00%	0,00%
300x300_30(18)	0,00%	0,00%	16,67%	0,00%	0,00%	8,33%	10,00%	0,00%	0,00%	0,00%
300x300_30(24)	0,00%	0,00%	16,67%	20,83%	0,00%	18,18%	100,00%	94,12%	100,00%	12,50%
300x300_60(6)	0,00%	87,50%	33,33%	100,00%	100,00%	3,85%	76,19%	40,00%	83,13%	92,86%
300x300_60(12)	0,00%	20,00%	0,00%	12,50%	9,09%	58,33%	61,98%	42,37%	60,37%	77,36%
300x300_60(18)	9,09%	9,09%	9,09%	9,09%	9,09%	11,11%	11,11%	11,11%	11,11%	11,11%
300x300_60(24)	9,09%	9,09%	9,09%	9,09%	9,09%	11,11%	11,11%	11,11%	11,11%	11,11%

Table B.9: Set coverage metric by comparing all the metaheuristics two by two. Part 2 of 14.

	I_{SC}(NSGA-II,MO-FA)					I_{SC}(NSGA-II,MO-GSA)				
	Evaluations (Stop condition)					Evaluations (Stop condition)				
Instance($\tilde{s}_r$)	**50 000**	**100 000**	**200 000**	**300 000**	**400 000**	**50 000**	**100 000**	**200 000**	**300 000**	**400 000**
50x50_30(1)	0,00%	0,00%	0,00%	0,00%	0,00%	9,09%	9,09%	0,00%	0,00%	9,09%
50x50_60(1)	6,67%	6,25%	0,00%	6,25%	11,76%	60,00%	40,00%	0,00%	0,00%	0,00%
100x100_30(2)	1,05%	0,00%	0,87%	0,00%	2,33%	1,23%	0,00%	1,85%	0,00%	1,85%
100x100_30(3)	0,00%	0,00%	0,00%	0,00%	0,00%	1,06%	0,00%	1,22%	0,00%	2,50%
100x100_60(2)	0,00%	20,00%	20,00%	0,00%	16,67%	44,44%	22,22%	20,00%	0,00%	25,00%
100x100_60(3)	0,00%	0,00%	0,00%	0,00%	0,00%	0,00%	0,00%	0,00%	0,00%	0,00%
200x200_30(2)	0,00%	0,00%	0,00%	0,00%	0,00%	0,00%	0,00%	0,00%	0,00%	33,33%
200x200_30(4)	0,00%	0,00%	0,00%	0,00%	0,00%	71,43%	0,00%	0,00%	100,00%	50,00%
200x200_30(6)	0,00%	0,00%	0,00%	0,00%	0,00%	0,00%	0,00%	0,00%	7,69%	9,09%
200x200_30(9)	0,00%	0,00%	0,00%	0,00%	0,00%	0,00%	0,00%	0,00%	0,00%	0,00%
200x200_60(2)	8,11%	3,51%	0,00%	13,46%	0,00%	70,00%	4,55%	34,48%	2,38%	25,00%
200x200_60(4)	0,00%	0,00%	0,00%	0,00%	0,00%	94,29%	86,67%	8,70%	9,00%	19,70%
200x200_60(6)	0,00%	12,50%	0,00%	0,00%	87,50%	50,00%	40,00%	46,67%	81,25%	58,82%
200x200_60(9)	0,00%	0,00%	0,00%	7,69%	11,11%	66,67%	45,45%	57,14%	57,14%	44,44%
300x300_30(6)	0,00%	0,00%	0,00%	0,00%	0,00%	40,00%	16,67%	38,46%	66,67%	16,67%
300x300_30(12)	0,00%	0,00%	0,00%	0,00%	0,00%	0,00%	0,00%	0,00%	0,00%	0,00%
300x300_30(18)	0,00%	0,00%	0,00%	0,00%	0,00%	44,44%	53,85%	7,14%	50,00%	0,00%
300x300_30(24)	0,00%	0,00%	0,00%	0,00%	0,00%	42,86%	63,16%	73,08%	33,33%	12,50%
300x300_60(6)	0,00%	0,00%	0,00%	0,00%	0,00%	14,29%	66,67%	27,66%	78,57%	26,67%
300x300_60(12)	0,00%	0,00%	0,00%	0,00%	0,00%	66,67%	0,00%	22,45%	19,05%	0,00%
300x300_60(18)	11,11%	11,11%	11,11%	11,11%	11,11%	11,11%	11,11%	11,11%	11,11%	11,11%
300x300_60(24)	11,11%	11,11%	11,11%	11,11%	11,11%	11,11%	11,11%	11,11%	11,11%	11,11%

	I_{SC}(NSGA-II,MOEA/D)					I_{SC}(SPEA2,NSGA-II)				
	Evaluations (Stop condition)					Evaluations (Stop condition)				
Instance($\tilde{s}_r$)	**50 000**	**100 000**	**200 000**	**300 000**	**400 000**	**50 000**	**100 000**	**200 000**	**300 000**	**400 000**
50x50_30(1)	7,69%	7,14%	13,33%	20,00%	0,00%	51,56%	57,78%	76,77%	79,17%	72,97%
50x50_60(1)	18,18%	25,00%	8,33%	16,67%	25,00%	35,64%	6,77%	70,63%	38,59%	50,50%
100x100_30(2)	6,52%	5,19%	9,76%	11,86%	8,33%	51,24%	69,09%	74,64%	63,54%	80,80%
100x100_30(3)	15,69%	18,87%	17,86%	12,77%	21,57%	20,42%	35,58%	42,58%	17,06%	39,80%
100x100_60(2)	16,67%	42,86%	0,00%	16,67%	50,00%	73,08%	97,69%	96,00%	0,00%	20,81%
100x100_60(3)	0,00%	12,50%	0,00%	28,57%	0,00%	44,39%	47,97%	48,59%	0,00%	0,00%
200x200_30(2)	0,00%	0,00%	0,00%	25,00%	75,00%	5,06%	67,86%	70,09%	72,32%	0,00%
200x200_30(4)	0,00%	0,00%	100,00%	100,00%	100,00%	94,78%	5,01%	0,00%	0,00%	0,00%
200x200_30(6)	0,00%	8,33%	0,00%	16,67%	28,57%	62,50%	85,71%	94,74%	76,47%	67,39%
200x200_30(9)	0,00%	20,00%	42,86%	64,00%	66,67%	90,00%	20,00%	58,33%	95,00%	47,06%
200x200_60(2)	71,43%	65,38%	85,71%	96,15%	81,25%	0,00%	58,43%	4,11%	1,35%	41,12%
200x200_60(4)	73,08%	81,82%	88,89%	68,97%	74,19%	21,21%	58,33%	19,74%	36,54%	0,00%
200x200_60(6)	22,22%	50,00%	61,54%	57,14%	62,50%	70,00%	0,54%	79,10%	57,75%	87,05%
200x200_60(9)	55,56%	72,73%	61,54%	66,67%	100,00%	99,41%	2,52%	52,46%	51,72%	92,82%
300x300_30(6)	0,00%	0,00%	30,77%	12,50%	10,00%	92,92%	15,89%	0,00%	12,36%	0,00%
300x300_30(12)	0,00%	0,00%	0,00%	0,00%	42,86%	100,00%	100,00%	100,00%	100,00%	100,00%
300x300_30(18)	14,29%	0,00%	20,00%	30,00%	52,63%	66,67%	100,00%	100,00%	41,18%	26,67%
300x300_30(24)	0,00%	62,50%	48,15%	52,00%	82,61%	100,00%	54,55%	36,84%	89,36%	95,83%
300x300_60(6)	50,00%	51,85%	100,00%	91,43%	97,14%	100,00%	40,00%	88,89%	21,52%	4,00%
300x300_60(12)	46,15%	74,42%	80,65%	78,95%	83,33%	44,44%	46,15%	86,79%	100,00%	13,64%
300x300_60(18)	11,11%	11,11%	11,11%	11,11%	11,11%	100,00%	100,00%	100,00%	100,00%	100,00%
300x300_60(24)	11,11%	11,11%	11,11%	11,11%	100,00%	100,00%	100,00%	100,00%	100,00%	100,00%

Table B.10: Set coverage metric by comparing all the metaheuristics two by two. Part 3 of 14.

	$\mathrm{I_{SC}}$(SPEA2,MO-VNS)					$\mathrm{I_{SC}}$(SPEA2,MO-VNS*)				
	Evaluations (Stop condition)					Evaluations (Stop condition)				
Instance($\tilde{s}_r$)	**50 000**	**100 000**	**200 000**	**300 000**	**400 000**	**50 000**	**100 000**	**200 000**	**300 000**	**400 000**
50x50_30(1)	0,00%	0,00%	0,00%	0,00%	0,00%	0,00%	0,00%	0,00%	0,00%	0,00%
50x50_60(1)	0,00%	0,00%	0,00%	8,00%	5,00%	0,00%	6,67%	0,00%	0,00%	5,88%
100x100_30(2)	0,00%	0,00%	0,00%	0,00%	0,00%	0,00%	0,00%	0,00%	0,00%	0,00%
100x100_30(3)	0,00%	0,00%	0,00%	0,00%	0,00%	0,00%	0,00%	0,00%	0,00%	0,00%
100x100_60(2)	0,00%	12,50%	0,00%	0,00%	16,67%	50,00%	50,00%	0,00%	0,00%	0,00%
100x100_60(3)	0,00%	0,00%	0,00%	0,00%	0,00%	0,00%	0,00%	0,00%	0,00%	0,00%
200x200_30(2)	0,00%	0,00%	0,00%	0,00%	0,00%	0,00%	0,00%	0,00%	0,00%	0,00%
200x200_30(4)	0,00%	16,67%	12,50%	18,18%	0,00%	0,00%	0,00%	0,00%	0,00%	0,00%
200x200_30(6)	0,00%	0,00%	0,00%	0,00%	0,00%	0,00%	0,00%	0,00%	0,00%	0,00%
200x200_30(9)	0,00%	0,00%	0,00%	0,00%	0,00%	0,00%	0,00%	10,53%	9,52%	0,00%
200x200_60(2)	0,00%	6,25%	9,38%	0,00%	0,00%	0,00%	0,00%	0,00%	0,00%	0,00%
200x200_60(4)	0,00%	0,00%	9,52%	13,79%	0,00%	0,00%	0,00%	0,00%	0,00%	0,00%
200x200_60(6)	0,00%	0,00%	14,29%	50,00%	54,55%	0,00%	0,00%	0,00%	0,00%	0,00%
200x200_60(9)	61,54%	91,67%	69,23%	85,71%	53,85%	45,45%	22,22%	66,67%	64,71%	40,00%
300x300_30(6)	22,22%	41,67%	72,73%	100,00%	90,00%	0,00%	0,00%	20,00%	0,00%	62,50%
300x300_30(12)	92,31%	100,00%	100,00%	100,00%	100,00%	13,33%	0,00%	100,00%	100,00%	100,00%
300x300_30(18)	42,86%	52,94%	73,33%	41,18%	0,00%	0,00%	0,00%	16,67%	43,75%	0,00%
300x300_30(24)	75,00%	100,00%	100,00%	100,00%	100,00%	0,00%	0,00%	8,33%	83,33%	30,00%
300x300_60(6)	95,24%	62,50%	95,45%	96,97%	100,00%	29,41%	87,50%	83,33%	100,00%	100,00%
300x300_60(12)	61,11%	64,29%	47,62%	100,00%	96,00%	17,65%	46,67%	0,00%	16,67%	9,09%
300x300_60(18)	20,00%	20,00%	20,00%	20,00%	20,00%	62,50%	12,50%	50,00%	55,56%	33,33%
300x300_60(24)	20,00%	20,00%	20,00%	20,00%	20,00%	50,00%	57,14%	25,00%	44,44%	20,00%

	$\mathrm{I_{SC}}$(SPEA2,MO-ABC)					$\mathrm{I_{SC}}$(SPEA2,MO-FA)				
	Evaluations (Stop condition)					Evaluations (Stop condition)				
Instance($\tilde{s}_r$)	**50 000**	**100 000**	**200 000**	**300 000**	**400 000**	**50 000**	**100 000**	**200 000**	**300 000**	**400 000**
50x50_30(1)	0,00%	0,00%	0,67%	0,00%	0,73%	0,00%	0,00%	0,00%	0,00%	0,00%
50x50_60(1)	0,00%	0,00%	0,00%	15,84%	4,73%	13,33%	6,25%	0,00%	6,25%	11,76%
100x100_30(2)	1,05%	1,77%	1,84%	0,00%	2,55%	1,05%	0,00%	0,00%	0,00%	0,00%
100x100_30(3)	0,00%	0,00%	0,00%	0,00%	0,00%	0,00%	0,00%	0,00%	0,00%	0,00%
100x100_60(2)	28,07%	0,11%	0,00%	0,00%	6,26%	0,00%	40,00%	20,00%	0,00%	0,00%
100x100_60(3)	0,00%	0,00%	0,00%	0,00%	0,00%	0,00%	0,00%	0,00%	0,00%	0,00%
200x200_30(2)	0,00%	0,00%	87,34%	0,00%	0,00%	0,00%	0,00%	0,00%	0,00%	0,00%
200x200_30(4)	0,00%	11,67%	3,70%	0,00%	0,00%	0,00%	0,00%	0,00%	0,00%	0,00%
200x200_30(6)	0,00%	0,00%	0,00%	47,06%	18,18%	0,00%	0,00%	0,00%	0,00%	0,00%
200x200_30(9)	0,00%	0,00%	0,00%	0,00%	0,00%	0,00%	0,00%	0,00%	0,00%	0,00%
200x200_60(2)	0,00%	0,00%	0,00%	0,00%	0,87%	0,00%	3,51%	0,00%	13,46%	0,00%
200x200_60(4)	7,02%	37,25%	52,81%	0,00%	1,32%	0,00%	0,00%	0,00%	0,00%	0,00%
200x200_60(6)	0,00%	0,00%	0,00%	0,00%	0,00%	0,00%	0,00%	0,00%	42,86%	93,75%
200x200_60(9)	45,13%	0,59%	0,22%	3,40%	19,20%	0,00%	0,00%	0,00%	7,69%	22,22%
300x300_30(6)	14,06%	0,00%	0,39%	6,25%	0,00%	0,00%	0,00%	0,00%	0,00%	0,00%
300x300_30(12)	27,27%	33,33%	0,00%	0,00%	0,00%	0,00%	0,00%	0,00%	0,00%	0,00%
300x300_30(18)	91,67%	95,00%	10,71%	0,00%	0,00%	0,00%	0,00%	7,69%	0,00%	0,00%
300x300_30(24)	100,00%	100,00%	100,00%	100,00%	100,00%	0,00%	0,00%	0,00%	0,00%	0,00%
300x300_60(6)	61,54%	90,48%	96,67%	83,13%	90,48%	0,00%	0,00%	0,00%	0,00%	0,00%
300x300_60(12)	29,17%	61,98%	96,05%	99,39%	77,36%	0,00%	0,00%	0,00%	0,00%	0,00%
300x300_60(18)	11,11%	11,11%	11,11%	11,11%	11,11%	11,11%	11,11%	11,11%	11,11%	11,11%
300x300_60(24)	11,11%	11,11%	11,11%	11,11%	11,11%	11,11%	11,11%	11,11%	11,11%	11,11%

Table B.11: Set coverage metric by comparing all the metaheuristics two by two. Part 4 of 14.

	I_{SC}(SPEA2,MO-GSA)					I_{SC}(SPEA2,MOEA/D)				
	Evaluations (Stop condition)					Evaluations (Stop condition)				
Instance($\tilde{s}_r$)	**50 000**	**100 000**	**200 000**	**300 000**	**400 000**	**50 000**	**100 000**	**200 000**	**300 000**	**400 000**
50x50_30(1)	9,09%	9,09%	0,00%	0,00%	0,00%	0,00%	7,14%	13,33%	13,33%	0,00%
50x50_60(1)	53,33%	0,00%	0,00%	0,00%	0,00%	18,18%	8,33%	8,33%	16,67%	16,67%
100x100_30(2)	1,23%	0,00%	0,00%	0,00%	0,00%	4,35%	5,19%	9,76%	11,86%	8,33%
100x100_30(3)	0,00%	0,00%	0,00%	0,00%	0,83%	7,84%	11,32%	14,29%	10,64%	19,61%
100x100_60(2)	22,22%	44,44%	0,00%	0,00%	0,00%	16,67%	42,86%	0,00%	0,00%	50,00%
100x100_60(3)	0,00%	0,00%	0,00%	0,00%	0,00%	0,00%	12,50%	0,00%	0,00%	0,00%
200x200_30(2)	0,00%	0,00%	14,29%	0,00%	22,22%	0,00%	0,00%	40,00%	50,00%	25,00%
200x200_30(4)	0,00%	0,00%	0,00%	75,00%	33,33%	0,00%	0,00%	66,67%	33,33%	0,00%
200x200_30(6)	0,00%	0,00%	0,00%	15,38%	9,09%	0,00%	58,33%	0,00%	16,67%	28,57%
200x200_30(9)	8,33%	0,00%	0,00%	0,00%	4,76%	7,69%	10,00%	57,14%	100,00%	91,67%
200x200_60(2)	0,00%	0,00%	3,45%	2,38%	5,77%	57,14%	80,77%	85,71%	96,15%	90,63%
200x200_60(4)	48,57%	70,00%	6,52%	5,00%	9,09%	53,85%	84,85%	80,56%	68,97%	70,97%
200x200_60(6)	71,43%	46,67%	60,00%	81,25%	82,35%	33,33%	50,00%	61,54%	64,29%	87,50%
200x200_60(9)	88,89%	54,55%	64,29%	57,14%	33,33%	55,56%	63,64%	69,23%	71,43%	81,82%
300x300_30(6)	86,67%	0,00%	23,08%	50,00%	0,00%	0,00%	0,00%	0,00%	12,50%	10,00%
300x300_30(12)	0,00%	0,00%	0,00%	0,00%	0,00%	0,00%	0,00%	50,00%	50,00%	100,00%
300x300_30(18)	100,00%	100,00%	100,00%	0,00%	56,25%	42,86%	50,00%	45,00%	45,00%	52,63%
300x300_30(24)	92,86%	100,00%	65,38%	80,95%	75,00%	31,25%	62,50%	48,15%	80,00%	95,65%
300x300_60(6)	85,71%	61,90%	53,19%	76,19%	18,33%	90,00%	70,37%	100,00%	74,29%	100,00%
300x300_60(12)	100,00%	17,95%	28,57%	52,38%	0,00%	65,38%	81,40%	87,10%	100,00%	92,59%
300x300_60(18)	11,11%	11,11%	11,11%	11,11%	11,11%	11,11%	11,11%	11,11%	11,11%	11,11%
300x300_60(24)	11,11%	11,11%	11,11%	11,11%	11,11%	11,11%	11,11%	11,11%	11,11%	100,00%

	I_{SC}(MO-VNS,NSGA-II)					I_{SC}(MO-VNS,SPEA2)				
	Evaluations (Stop condition)					Evaluations (Stop condition)				
Instance($\tilde{s}_r$)	**50 000**	**100 000**	**200 000**	**300 000**	**400 000**	**50 000**	**100 000**	**200 000**	**300 000**	**400 000**
50x50_30(1)	100,00%	56,67%	100,00%	100,00%	100,00%	91,30%	90,80%	100,00%	100,00%	100,00%
50x50_60(1)	29,70%	87,22%	100,00%	79,35%	45,71%	72,32%	92,97%	100,00%	99,97%	6,33%
100x100_30(2)	95,02%	99,55%	96,58%	98,25%	94,80%	99,00%	100,00%	100,00%	100,00%	100,00%
100x100_30(3)	100,00%	100,00%	96,65%	94,88%	100,00%	100,00%	98,97%	100,00%	99,47%	100,00%
100x100_60(2)	96,15%	99,23%	100,00%	99,50%	34,77%	100,00%	83,14%	100,00%	0,00%	99,68%
100x100_60(3)	100,00%	100,00%	100,00%	100,00%	100,00%	100,00%	100,00%	100,00%	100,00%	100,00%
200x200_30(2)	100,00%	98,21%	99,11%	100,00%	100,00%	100,00%	100,00%	100,00%	100,00%	100,00%
200x200_30(4)	99,13%	3,34%	0,63%	0,00%	0,00%	100,00%	14,71%	0,00%	0,00%	100,00%
200x200_30(6)	100,00%	92,86%	94,74%	100,00%	100,00%	100,00%	92,86%	100,00%	95,65%	90,91%
200x200_30(9)	100,00%	100,00%	100,00%	100,00%	100,00%	100,00%	100,00%	100,00%	100,00%	100,00%
200x200_60(2)	72,22%	85,39%	52,05%	86,49%	87,85%	100,00%	23,68%	77,97%	30,25%	94,81%
200x200_60(4)	93,94%	88,89%	88,16%	66,03%	97,62%	100,00%	100,00%	90,20%	22,22%	100,00%
200x200_60(6)	100,00%	80,65%	99,75%	37,75%	95,68%	69,09%	83,64%	44,99%	3,78%	0,63%
200x200_60(9)	31,95%	0,19%	0,07%	4,31%	44,50%	11,76%	17,07%	0,21%	0,88%	6,46%
300x300_30(6)	92,92%	38,32%	0,00%	0,00%	0,00%	25,20%	23,94%	0,59%	0,00%	0,00%
300x300_30(12)	88,64%	0,00%	0,00%	0,00%	0,00%	0,00%	0,00%	0,00%	0,00%	0,00%
300x300_30(18)	100,00%	100,00%	88,89%	100,00%	100,00%	66,67%	5,26%	0,00%	0,00%	46,67%
300x300_30(24)	40,00%	0,00%	0,00%	23,40%	0,00%	0,00%	0,00%	0,00%	0,00%	0,00%
300x300_60(6)	35,71%	20,00%	7,41%	0,00%	0,00%	0,00%	13,33%	0,00%	0,00%	0,00%
300x300_60(12)	33,33%	0,00%	47,17%	0,00%	0,00%	33,33%	11,54%	21,21%	0,00%	0,00%
300x300_60(18)	88,89%	88,89%	88,89%	88,89%	88,89%	88,89%	88,89%	88,89%	88,89%	88,89%
300x300_60(24)	88,89%	88,89%	88,89%	88,89%	88,89%	88,89%	88,89%	88,89%	88,89%	88,89%

Table B.12: Set coverage metric by comparing all the metaheuristics two by two. Part 5 of 14.

	I_{SC}(MO-VNS,MO-VNS*)					I_{SC}(MO-VNS,MO-ABC)				
	Evaluations (Stop condition)					Evaluations (Stop condition)				
Instance($\tilde{s}_r$)	**50 000**	**100 000**	**200 000**	**300 000**	**400 000**	**50 000**	**100 000**	**200 000**	**300 000**	**400 000**
50x50_30(1)	75,00%	81,82%	92,86%	92,86%	100,00%	70,86%	52,59%	95,97%	97,88%	97,08%
50x50_60(1)	66,67%	66,67%	83,33%	76,92%	88,24%	50,65%	97,58%	95,50%	90,84%	79,59%
100x100_30(2)	95,28%	97,76%	97,81%	100,00%	99,28%	99,37%	99,65%	96,31%	99,84%	99,84%
100x100_30(3)	7,37%	51,05%	65,87%	59,05%	79,45%	54,95%	42,21%	53,76%	54,72%	86,81%
100x100_60(2)	100,00%	100,00%	75,00%	100,00%	100,00%	64,04%	99,89%	100,00%	99,91%	99,91%
100x100_60(3)	100,00%	100,00%	100,00%	100,00%	60,00%	100,00%	100,00%	100,00%	100,00%	100,00%
200x200_30(2)	0,00%	0,00%	42,86%	0,00%	33,33%	100,00%	100,00%	100,00%	8,82%	0,00%
200x200_30(4)	0,00%	0,00%	0,00%	0,00%	0,00%	100,00%	51,67%	68,52%	0,00%	0,77%
200x200_30(6)	100,00%	100,00%	90,91%	87,50%	100,00%	81,82%	45,00%	82,35%	82,35%	95,45%
200x200_30(9)	0,00%	36,36%	31,58%	71,43%	0,00%	100,00%	45,45%	0,00%	31,82%	7,41%
200x200_60(2)	0,00%	0,00%	0,00%	14,81%	0,00%	46,34%	69,57%	20,54%	14,04%	35,65%
200x200_60(4)	0,00%	0,00%	0,00%	0,00%	86,96%	94,74%	96,08%	56,18%	12,50%	53,95%
200x200_60(6)	20,00%	11,11%	0,00%	6,67%	5,26%	0,00%	33,67%	5,19%	0,00%	47,97%
200x200_60(9)	45,45%	0,00%	0,00%	29,41%	20,00%	8,85%	0,59%	0,00%	0,00%	0,32%
300x300_30(6)	0,00%	0,00%	0,00%	0,00%	25,00%	6,25%	0,00%	0,00%	0,00%	0,00%
300x300_30(12)	0,00%	0,00%	0,00%	0,00%	0,00%	0,00%	33,33%	0,00%	0,00%	0,00%
300x300_30(18)	0,00%	0,00%	16,67%	0,00%	0,00%	41,67%	20,00%	0,00%	8,33%	1,82%
300x300_30(24)	0,00%	0,00%	0,00%	8,33%	0,00%	18,18%	93,33%	47,06%	96,55%	0,00%
300x300_60(6)	5,88%	43,75%	8,33%	11,76%	27,78%	0,00%	64,29%	41,67%	2,41%	26,19%
300x300_60(12)	0,00%	0,00%	0,00%	0,00%	0,00%	45,83%	14,05%	3,39%	6,71%	13,21%
300x300_60(18)	87,50%	87,50%	83,33%	88,89%	83,33%	88,89%	88,89%	88,89%	88,89%	88,89%
300x300_60(24)	75,00%	85,71%	75,00%	88,89%	80,00%	88,89%	88,89%	88,89%	88,89%	88,89%

	I_{SC}(MO-VNS,MO-FA)					I_{SC}(MO-VNS,MO-GSA)				
	Evaluations (Stop condition)					Evaluations (Stop condition)				
Instance($\tilde{s}_r$)	**50 000**	**100 000**	**200 000**	**300 000**	**400 000**	**50 000**	**100 000**	**200 000**	**300 000**	**400 000**
50x50_30(1)	57,14%	93,33%	92,86%	93,33%	93,33%	72,73%	100,00%	100,00%	100,00%	100,00%
50x50_60(1)	53,33%	68,75%	80,00%	81,25%	82,35%	80,00%	80,00%	100,00%	83,33%	85,71%
100x100_30(2)	92,63%	98,20%	96,52%	100,00%	99,22%	100,00%	100,00%	97,22%	99,14%	97,22%
100x100_30(3)	73,87%	84,13%	56,80%	80,29%	85,12%	92,55%	98,48%	96,34%	87,50%	94,17%
100x100_60(2)	0,00%	80,00%	80,00%	66,67%	83,33%	88,89%	88,89%	100,00%	83,33%	75,00%
100x100_60(3)	100,00%	100,00%	100,00%	0,00%	0,00%	100,00%	100,00%	100,00%	100,00%	100,00%
200x200_30(2)	0,00%	0,00%	33,33%	0,00%	50,00%	100,00%	90,91%	100,00%	100,00%	66,67%
200x200_30(4)	7,14%	0,00%	0,00%	0,00%	0,00%	100,00%	0,00%	0,00%	50,00%	50,00%
200x200_30(6)	33,33%	100,00%	50,00%	61,54%	100,00%	100,00%	100,00%	50,00%	76,92%	72,73%
200x200_30(9)	0,00%	13,33%	0,00%	25,00%	0,00%	100,00%	92,31%	47,37%	78,57%	90,48%
200x200_60(2)	8,11%	43,86%	9,52%	15,38%	70,15%	95,00%	36,36%	51,72%	66,67%	100,00%
200x200_60(4)	0,00%	0,00%	0,00%	0,00%	0,00%	91,43%	93,33%	80,43%	5,00%	89,39%
200x200_60(6)	0,00%	0,00%	9,09%	28,57%	93,75%	57,14%	100,00%	86,67%	87,50%	64,71%
200x200_60(9)	0,00%	0,00%	0,00%	0,00%	0,00%	88,89%	9,09%	14,29%	42,86%	22,22%
300x300_30(6)	0,00%	0,00%	0,00%	0,00%	0,00%	40,00%	16,67%	0,00%	0,00%	0,00%
300x300_30(12)	0,00%	0,00%	0,00%	0,00%	0,00%	0,00%	0,00%	0,00%	0,00%	0,00%
300x300_30(18)	0,00%	0,00%	0,00%	0,00%	0,00%	77,78%	92,31%	71,43%	50,00%	81,25%
300x300_30(24)	0,00%	0,00%	0,00%	0,00%	0,00%	28,57%	65,79%	0,00%	0,00%	0,00%
300x300_60(6)	0,00%	0,00%	0,00%	0,00%	0,00%	0,00%	61,90%	4,26%	0,00%	0,00%
300x300_60(12)	0,00%	0,00%	0,00%	0,00%	0,00%	62,96%	0,00%	0,00%	0,00%	0,00%
300x300_60(18)	88,89%	88,89%	88,89%	88,89%	88,89%	88,89%	88,89%	88,89%	88,89%	88,89%
300x300_60(24)	88,89%	88,89%	88,89%	88,89%	88,89%	88,89%	88,89%	88,89%	88,89%	88,89%

Table B.13: Set coverage metric by comparing all the metaheuristics two by two. Part 6 of 14.

	I_{SC}(MO-VNS,MOEA/D)					I_{SC}(MO-VNS*,NSGA-II)				
	Evaluations (Stop condition)					Evaluations (Stop condition)				
Instance($\tilde{s}_r$)	**50 000**	**100 000**	**200 000**	**300 000**	**400 000**	**50 000**	**100 000**	**200 000**	**300 000**	**400 000**
50x50_30(1)	100,00%	100,00%	100,00%	100,00%	100,00%	71,88%	98,89%	100,00%	100,00%	100,00%
50x50_60(1)	100,00%	91,67%	100,00%	100,00%	91,67%	29,70%	83,46%	91,14%	100,00%	15,77%
100x100_30(2)	100,00%	97,40%	98,78%	100,00%	100,00%	95,02%	99,55%	96,58%	96,51%	94,80%
100x100_30(3)	64,71%	88,68%	82,14%	100,00%	98,04%	97,89%	100,00%	94,74%	100,00%	100,00%
100x100_60(2)	83,33%	100,00%	100,00%	83,33%	100,00%	30,77%	1,54%	98,00%	30,20%	33,76%
100x100_60(3)	100,00%	100,00%	100,00%	100,00%	100,00%	20,56%	100,00%	100,00%	100,00%	100,00%
200x200_30(2)	100,00%	71,43%	100,00%	100,00%	100,00%	100,00%	100,00%	100,00%	100,00%	0,00%
200x200_30(4)	0,00%	0,00%	66,67%	0,00%	100,00%	100,00%	100,00%	100,00%	0,00%	3,41%
200x200_30(6)	100,00%	100,00%	100,00%	83,33%	100,00%	100,00%	92,86%	94,74%	100,00%	100,00%
200x200_30(9)	100,00%	100,00%	100,00%	100,00%	91,67%	100,00%	100,00%	83,33%	100,00%	100,00%
200x200_60(2)	71,43%	65,38%	85,71%	88,46%	84,38%	94,44%	83,15%	58,90%	89,19%	80,37%
200x200_60(4)	73,08%	90,91%	83,33%	68,97%	70,97%	100,00%	86,11%	98,68%	98,08%	99,21%
200x200_60(6)	88,89%	80,00%	76,92%	100,00%	50,00%	100,00%	100,00%	100,00%	100,00%	100,00%
200x200_60(9)	55,56%	0,00%	0,00%	42,86%	40,91%	73,96%	7,75%	2,39%	5,17%	53,42%
300x300_30(6)	0,00%	0,00%	0,00%	0,00%	0,00%	100,00%	72,90%	1,55%	39,01%	0,00%
300x300_30(12)	0,00%	0,00%	0,00%	0,00%	0,00%	100,00%	100,00%	1,61%	1,22%	0,00%
300x300_30(18)	42,86%	50,00%	45,00%	50,00%	63,16%	100,00%	100,00%	83,33%	100,00%	100,00%
300x300_30(24)	18,75%	50,00%	40,74%	56,00%	78,26%	100,00%	100,00%	78,95%	65,96%	93,75%
300x300_60(6)	53,33%	40,74%	68,00%	31,43%	80,00%	100,00%	0,00%	25,93%	0,00%	0,00%
300x300_60(12)	42,31%	72,09%	61,29%	68,42%	64,81%	100,00%	92,31%	47,17%	83,02%	59,09%
300x300_60(18)	88,89%	88,89%	88,89%	88,89%	88,89%	33,33%	88,89%	66,67%	33,33%	44,44%
300x300_60(24)	88,89%	88,89%	88,89%	88,89%	100,00%	22,22%	22,22%	55,56%	77,78%	77,78%

	I_{SC}(MO-VNS*,SPEA2)					I_{SC}(MO-VNS*,MO-VNS)				
	Evaluations (Stop condition)					Evaluations (Stop condition)				
Instance($\tilde{s}_r$)	**50 000**	**100 000**	**200 000**	**300 000**	**400 000**	**50 000**	**100 000**	**200 000**	**300 000**	**400 000**
50x50_30(1)	65,22%	80,46%	100,00%	100,00%	100,00%	0,00%	0,00%	92,86%	92,86%	100,00%
50x50_60(1)	72,32%	96,62%	96,55%	100,00%	0,63%	90,00%	92,86%	64,29%	60,00%	50,00%
100x100_30(2)	99,00%	100,00%	100,00%	99,85%	99,88%	89,31%	91,97%	96,38%	99,29%	98,57%
100x100_30(3)	99,42%	98,97%	100,00%	100,00%	100,00%	91,72%	70,39%	74,63%	90,54%	79,30%
100x100_60(2)	1,77%	1,16%	89,88%	0,00%	92,60%	0,00%	0,00%	66,67%	50,00%	83,33%
100x100_60(3)	95,00%	100,00%	100,00%	100,00%	100,00%	0,00%	0,00%	0,00%	0,00%	40,00%
200x200_30(2)	100,00%	100,00%	100,00%	100,00%	82,79%	83,33%	87,50%	50,00%	25,00%	12,50%
200x200_30(4)	100,00%	100,00%	100,00%	99,85%	99,83%	100,00%	100,00%	100,00%	100,00%	50,00%
200x200_30(6)	100,00%	85,71%	100,00%	95,65%	90,91%	0,00%	72,73%	83,33%	72,73%	100,00%
200x200_30(9)	100,00%	100,00%	88,89%	68,75%	91,67%	100,00%	38,46%	72,73%	37,50%	76,47%
200x200_60(2)	100,00%	31,58%	57,63%	25,31%	57,14%	100,00%	96,88%	78,13%	50,00%	91,89%
200x200_60(4)	100,00%	100,00%	100,00%	100,00%	100,00%	96,30%	96,97%	95,24%	74,14%	6,82%
200x200_60(6)	100,00%	100,00%	100,00%	100,00%	100,00%	87,50%	72,73%	85,71%	70,00%	77,27%
200x200_60(9)	97,65%	99,70%	1,50%	0,83%	9,51%	61,54%	100,00%	76,92%	57,14%	38,46%
300x300_30(6)	100,00%	89,36%	13,65%	99,19%	11,04%	66,67%	91,67%	100,00%	100,00%	60,00%
300x300_30(12)	76,92%	25,00%	0,00%	0,00%	0,00%	100,00%	100,00%	100,00%	100,00%	100,00%
300x300_30(18)	100,00%	100,00%	62,50%	42,86%	53,33%	85,71%	100,00%	93,33%	76,47%	90,00%
300x300_30(24)	81,82%	38,89%	59,52%	0,00%	43,40%	100,00%	100,00%	100,00%	78,95%	100,00%
300x300_60(6)	52,63%	0,00%	11,90%	0,00%	0,00%	95,24%	43,75%	81,82%	54,55%	66,67%
300x300_60(12)	70,83%	65,38%	75,76%	20,69%	63,33%	94,44%	85,71%	100,00%	81,82%	88,00%
300x300_60(18)	33,33%	88,89%	66,67%	33,33%	44,44%	40,00%	80,00%	50,00%	40,00%	40,00%
300x300_60(24)	22,22%	22,22%	55,56%	77,78%	77,78%	30,00%	40,00%	40,00%	60,00%	60,00%

Table B.14: Set coverage metric by comparing all the metaheuristics two by two. Part 7 of 14.

	I_{SC}(MO-VNS*,MO-ABC)					I_{SC}(MO-VNS*,MO-FA)				
	Evaluations (Stop condition)					Evaluations (Stop condition)				
Instance($\tilde{s}_r$)	**50 000**	**100 000**	**200 000**	**300 000**	**400 000**	**50 000**	**100 000**	**200 000**	**300 000**	**400 000**
50x50_30(1)	30,46%	34,07%	98,66%	100,00%	97,08%	14,29%	6,67%	92,86%	93,33%	93,33%
50x50_60(1)	51,95%	97,58%	91,50%	96,53%	60,65%	60,00%	81,25%	66,67%	87,50%	64,71%
100x100_30(2)	94,76%	96,99%	96,31%	99,84%	99,84%	88,42%	91,89%	95,65%	100,00%	97,67%
100x100_30(3)	80,22%	53,90%	50,18%	86,94%	80,49%	95,50%	92,06%	44,80%	94,89%	61,98%
100x100_60(2)	0,00%	0,34%	99,90%	99,35%	99,91%	0,00%	20,00%	60,00%	33,33%	83,33%
100x100_60(3)	28,07%	0,00%	96,27%	100,00%	100,00%	0,00%	0,00%	0,00%	0,00%	0,00%
200x200_30(2)	100,00%	100,00%	100,00%	47,06%	1,41%	75,00%	28,57%	66,67%	40,00%	0,00%
200x200_30(4)	100,00%	100,00%	100,00%	17,54%	1,63%	42,86%	33,33%	0,00%	0,00%	0,00%
200x200_30(6)	0,00%	35,00%	44,12%	82,35%	95,45%	0,00%	72,73%	50,00%	61,54%	100,00%
200x200_30(9)	100,00%	54,55%	28,57%	27,27%	77,78%	15,38%	13,33%	31,25%	62,50%	81,25%
200x200_60(2)	97,56%	82,61%	34,82%	42,11%	36,52%	8,11%	100,00%	100,00%	26,92%	100,00%
200x200_60(4)	94,74%	68,63%	59,55%	57,81%	55,26%	1,30%	79,41%	0,00%	0,00%	0,00%
200x200_60(6)	75,00%	100,00%	98,52%	34,84%	39,02%	54,55%	75,00%	36,36%	100,00%	100,00%
200x200_60(9)	71,68%	1,78%	43,67%	0,00%	12,88%	0,00%	0,00%	0,00%	0,00%	0,00%
300x300_30(6)	29,69%	5,14%	3,55%	6,25%	0,00%	0,00%	0,00%	0,00%	0,00%	0,00%
300x300_30(12)	100,00%	33,33%	0,00%	0,00%	0,00%	0,00%	0,00%	0,00%	0,00%	0,00%
300x300_30(18)	100,00%	100,00%	64,29%	27,78%	12,73%	0,00%	5,88%	0,00%	0,00%	0,00%
300x300_30(24)	100,00%	100,00%	100,00%	96,55%	100,00%	0,00%	0,00%	0,00%	0,00%	0,00%
300x300_60(6)	76,92%	14,29%	33,33%	4,82%	50,00%	0,00%	0,00%	0,00%	0,00%	0,00%
300x300_60(12)	79,17%	64,46%	8,47%	21,34%	49,06%	0,00%	0,00%	0,00%	0,00%	0,00%
300x300_60(18)	33,33%	66,67%	44,44%	33,33%	33,33%	33,33%	66,67%	44,44%	33,33%	33,33%
300x300_60(24)	11,11%	22,22%	33,33%	55,56%	55,56%	11,11%	22,22%	33,33%	55,56%	55,56%

	I_{SC}(MO-VNS*,MO-GSA)					I_{SC}(MO-VNS*,MOEA/D)				
	Evaluations (Stop condition)					Evaluations (Stop condition)				
Instance($\tilde{s}_r$)	**50 000**	**100 000**	**200 000**	**300 000**	**400 000**	**50 000**	**100 000**	**200 000**	**300 000**	**400 000**
50x50_30(1)	27,27%	9,09%	100,00%	100,00%	100,00%	15,38%	21,43%	100,00%	100,00%	100,00%
50x50_60(1)	80,00%	90,00%	72,73%	91,67%	71,43%	100,00%	100,00%	91,67%	100,00%	91,67%
100x100_30(2)	96,30%	98,78%	98,15%	99,14%	97,22%	100,00%	98,70%	98,78%	100,00%	100,00%
100x100_30(3)	97,87%	80,30%	84,15%	97,50%	90,00%	76,47%	77,36%	60,71%	100,00%	100,00%
100x100_60(2)	0,00%	33,33%	80,00%	83,33%	75,00%	0,00%	100,00%	75,00%	66,67%	100,00%
100x100_60(3)	57,14%	50,00%	50,00%	80,00%	100,00%	80,00%	87,50%	100,00%	100,00%	100,00%
200x200_30(2)	100,00%	100,00%	100,00%	100,00%	100,00%	100,00%	100,00%	100,00%	100,00%	25,00%
200x200_30(4)	100,00%	100,00%	100,00%	100,00%	100,00%	50,00%	100,00%	100,00%	100,00%	100,00%
200x200_30(6)	27,27%	78,57%	50,00%	61,54%	72,73%	33,33%	91,67%	100,00%	100,00%	100,00%
200x200_30(9)	100,00%	84,62%	89,47%	42,86%	100,00%	100,00%	70,00%	85,71%	100,00%	91,67%
200x200_60(2)	100,00%	63,64%	89,66%	85,71%	90,38%	92,86%	76,92%	85,71%	88,46%	81,25%
200x200_60(4)	94,29%	83,33%	100,00%	99,00%	28,79%	76,92%	87,88%	83,33%	68,97%	74,19%
200x200_60(6)	92,86%	100,00%	100,00%	100,00%	100,00%	100,00%	70,00%	76,92%	92,86%	87,50%
200x200_60(9)	77,78%	72,73%	42,86%	42,86%	22,22%	55,56%	81,82%	61,54%	76,19%	86,36%
300x300_30(6)	100,00%	33,33%	15,38%	66,67%	0,00%	0,00%	7,14%	0,00%	25,00%	0,00%
300x300_30(12)	11,11%	0,00%	0,00%	0,00%	0,00%	0,00%	8,33%	0,00%	50,00%	14,29%
300x300_30(18)	100,00%	100,00%	92,86%	50,00%	100,00%	71,43%	70,00%	60,00%	65,00%	73,68%
300x300_30(24)	100,00%	78,95%	96,15%	28,57%	87,50%	56,25%	62,50%	51,85%	96,00%	82,61%
300x300_60(6)	28,57%	9,52%	0,00%	0,00%	0,00%	63,33%	51,85%	80,00%	48,57%	68,57%
300x300_60(12)	85,19%	58,97%	81,63%	46,03%	0,00%	57,69%	74,42%	77,42%	78,95%	66,67%
300x300_60(18)	33,33%	66,67%	44,44%	33,33%	33,33%	33,33%	66,67%	44,44%	33,33%	33,33%
300x300_60(24)	11,11%	22,22%	33,33%	55,56%	55,56%	11,11%	22,22%	33,33%	55,56%	100,00%

Table B.15: Set coverage metric by comparing all the metaheuristics two by two. Part 8 of 14.

	I_{SC}(MO-ABC,NSGA-II)					I_{SC}(MO-ABC,SPEA2)				
	Evaluations (Stop condition)					Evaluations (Stop condition)				
Instance($\tilde{s}_r$)	50 000	100 000	200 000	300 000	400 000	50 000	100 000	200 000	300 000	400 000
50x50_30(1)	100,00%	100,00%	100,00%	100,00%	94,59%	100,00%	100,00%	98,94%	100,00%	98,25%
50x50_60(1)	86,14%	100,00%	100,00%	75,54%	46,31%	100,00%	100,00%	100,00%	99,93%	6,38%
100x100_30(2)	95,02%	99,55%	96,58%	96,51%	94,80%	99,00%	100,00%	100,00%	99,85%	99,88%
100x100_30(3)	100,00%	100,00%	100,00%	95,56%	100,00%	100,00%	100,00%	100,00%	100,00%	100,00%
100x100_60(2)	96,15%	100,00%	97,00%	100,00%	78,68%	100,00%	66,28%	100,00%	0,00%	100,00%
100x100_60(3)	100,00%	100,00%	100,00%	100,00%	98,09%	100,00%	100,00%	100,00%	100,00%	100,00%
200x200_30(2)	100,00%	95,54%	97,77%	100,00%	100,00%	100,00%	100,00%	0,80%	100,00%	100,00%
200x200_30(4)	99,13%	50,36%	0,00%	36,67%	3,86%	85,71%	64,71%	98,44%	0,12%	100,00%
200x200_30(6)	100,00%	92,86%	94,74%	88,24%	97,83%	100,00%	92,86%	100,00%	95,65%	86,36%
200x200_30(9)	100,00%	100,00%	100,00%	100,00%	100,00%	80,00%	100,00%	100,00%	100,00%	100,00%
200x200_60(2)	88,89%	93,26%	97,26%	89,19%	100,00%	100,00%	100,00%	98,31%	100,00%	76,62%
200x200_60(4)	30,30%	44,44%	6,58%	96,15%	62,70%	88,89%	64,29%	0,00%	100,00%	87,76%
200x200_60(6)	100,00%	98,39%	100,00%	100,00%	100,00%	98,18%	100,00%	100,00%	47,03%	100,00%
200x200_60(9)	67,46%	6,59%	2,60%	17,24%	95,13%	97,65%	81,25%	2,04%	0,91%	15,21%
300x300_30(6)	76,99%	100,00%	1,55%	40,66%	0,00%	56,91%	100,00%	94,59%	18,29%	100,00%
300x300_30(12)	100,00%	2,33%	2,41%	100,00%	92,31%	15,38%	25,00%	12,82%	3,23%	6,14%
300x300_30(18)	50,00%	28,57%	100,00%	100,00%	100,00%	0,00%	0,00%	87,50%	100,00%	86,67%
300x300_30(24)	0,00%	0,00%	0,00%	0,00%	66,67%	0,00%	0,00%	0,00%	0,00%	0,00%
300x300_60(6)	89,29%	33,33%	51,85%	11,39%	0,00%	15,79%	3,33%	2,38%	20,51%	0,00%
300x300_60(12)	44,44%	0,00%	28,30%	0,00%	11,36%	66,67%	15,38%	3,03%	0,00%	6,67%
300x300_60(18)	100,00%	100,00%	100,00%	100,00%	100,00%	100,00%	100,00%	100,00%	100,00%	100,00%
300x300_60(24)	100,00%	100,00%	100,00%	100,00%	100,00%	100,00%	100,00%	100,00%	100,00%	100,00%

	I_{SC}(MO-ABC,MO-VNS)					I_{SC}(MO-ABC,MO-VNS*)				
	Evaluations (Stop condition)					Evaluations (Stop condition)				
Instance($\tilde{s}_r$)	50 000	100 000	200 000	300 000	400 000	50 000	100 000	200 000	300 000	400 000
50x50_30(1)	41,67%	35,71%	50,00%	64,29%	50,00%	100,00%	100,00%	57,14%	71,43%	50,00%
50x50_60(1)	40,00%	85,71%	85,71%	44,00%	70,00%	33,33%	80,00%	88,89%	76,92%	94,12%
100x100_30(2)	49,62%	59,12%	52,90%	44,29%	44,29%	52,76%	59,70%	54,01%	44,60%	44,60%
100x100_30(3)	31,36%	46,37%	56,22%	53,60%	30,84%	4,74%	38,82%	55,95%	45,26%	37,15%
100x100_60(2)	16,67%	0,00%	0,00%	0,00%	16,67%	100,00%	66,67%	0,00%	40,00%	0,00%
100x100_60(3)	0,00%	0,00%	0,00%	0,00%	0,00%	0,00%	80,00%	0,00%	0,00%	0,00%
200x200_30(2)	0,00%	0,00%	0,00%	50,00%	100,00%	0,00%	0,00%	0,00%	20,00%	33,33%
200x200_30(4)	0,00%	16,67%	12,50%	81,82%	66,67%	0,00%	0,00%	0,00%	0,00%	16,67%
200x200_30(6)	75,00%	81,82%	83,33%	63,64%	72,73%	100,00%	100,00%	90,91%	50,00%	72,73%
200x200_30(9)	0,00%	46,15%	100,00%	56,25%	58,82%	0,00%	9,09%	68,42%	66,67%	29,63%
200x200_60(2)	8,00%	28,13%	50,00%	64,71%	37,84%	0,00%	0,00%	0,00%	38,89%	0,00%
200x200_60(4)	0,00%	0,00%	21,43%	32,76%	0,00%	0,00%	0,00%	0,00%	0,00%	0,00%
200x200_60(6)	75,00%	54,55%	57,14%	85,00%	77,27%	20,00%	0,00%	0,00%	53,33%	42,11%
200x200_60(9)	61,54%	91,67%	92,31%	85,71%	84,62%	18,18%	44,44%	44,44%	88,24%	70,00%
300x300_30(6)	44,44%	91,67%	81,82%	81,25%	100,00%	57,14%	57,14%	80,00%	42,86%	100,00%
300x300_30(12)	100,00%	50,00%	100,00%	100,00%	100,00%	0,00%	66,67%	85,71%	100,00%	100,00%
300x300_30(18)	42,86%	35,29%	93,33%	88,24%	90,00%	0,00%	0,00%	16,67%	43,75%	66,67%
300x300_30(24)	62,50%	10,00%	60,00%	0,00%	92,86%	0,00%	0,00%	0,00%	0,00%	0,00%
300x300_60(6)	100,00%	12,50%	36,36%	63,64%	52,38%	17,65%	56,25%	41,67%	70,59%	38,89%
300x300_60(12)	66,67%	28,57%	47,62%	18,18%	52,00%	17,65%	26,67%	0,00%	0,00%	4,55%
300x300_60(18)	100,00%	100,00%	100,00%	100,00%	100,00%	100,00%	100,00%	100,00%	100,00%	100,00%
300x300_60(24)	100,00%	100,00%	100,00%	100,00%	100,00%	100,00%	100,00%	100,00%	100,00%	100,00%

Table B.16: Set coverage metric by comparing all the metaheuristics two by two. Part 9 of 14.

	I_{SC}(MO-ABC,MO-FA)					I_{SC}(MO-ABC,MO-GSA)				
	Evaluations (Stop condition)					Evaluations (Stop condition)				
Instance($\tilde{s}_r$)	**50 000**	**100 000**	**200 000**	**300 000**	**400 000**	**50 000**	**100 000**	**200 000**	**300 000**	**400 000**
50x50_30(1)	50,00%	40,00%	50,00%	66,67%	53,33%	100,00%	72,73%	80,00%	93,33%	100,00%
50x50_60(1)	40,00%	87,50%	80,00%	75,00%	82,35%	100,00%	100,00%	100,00%	75,00%	92,86%
100x100_30(2)	73,68%	73,87%	68,70%	57,72%	60,47%	74,07%	76,83%	67,59%	52,59%	53,70%
100x100_30(3)	47,75%	77,78%	68,80%	78,10%	51,24%	85,11%	92,42%	90,24%	78,33%	50,83%
100x100_60(2)	0,00%	40,00%	40,00%	0,00%	0,00%	77,78%	77,78%	90,00%	50,00%	0,00%
100x100_60(3)	0,00%	0,00%	0,00%	0,00%	0,00%	42,86%	100,00%	50,00%	80,00%	80,00%
200x200_30(2)	0,00%	0,00%	0,00%	0,00%	83,33%	25,00%	36,36%	42,86%	100,00%	100,00%
200x200_30(4)	0,00%	0,00%	0,00%	0,00%	0,00%	85,71%	0,00%	0,00%	100,00%	100,00%
200x200_30(6)	33,33%	90,91%	60,00%	84,62%	72,73%	100,00%	100,00%	50,00%	92,31%	72,73%
200x200_30(9)	0,00%	0,00%	31,25%	37,50%	68,75%	75,00%	92,31%	94,74%	85,71%	90,48%
200x200_60(2)	8,11%	3,51%	1,19%	25,00%	37,31%	85,00%	77,27%	86,21%	97,62%	96,15%
200x200_60(4)	0,00%	0,00%	0,00%	0,00%	0,00%	97,14%	96,67%	8,70%	11,00%	19,70%
200x200_60(6)	18,18%	37,50%	36,36%	100,00%	100,00%	85,71%	100,00%	86,67%	93,75%	100,00%
200x200_60(9)	0,00%	20,00%	27,27%	38,46%	44,44%	66,67%	63,64%	50,00%	71,43%	88,89%
300x300_30(6)	7,14%	11,76%	0,00%	38,46%	0,00%	53,33%	100,00%	30,77%	83,33%	50,00%
300x300_30(12)	0,00%	0,00%	0,00%	0,00%	0,00%	0,00%	72,73%	0,00%	0,00%	15,38%
300x300_30(18)	0,00%	0,00%	7,69%	0,00%	18,75%	77,78%	76,92%	100,00%	100,00%	100,00%
300x300_30(24)	0,00%	0,00%	0,00%	0,00%	0,00%	28,57%	5,26%	19,23%	0,00%	12,50%
300x300_60(6)	0,00%	0,00%	0,00%	0,00%	0,00%	42,86%	23,81%	31,91%	21,43%	0,00%
300x300_60(12)	0,00%	0,00%	0,00%	0,00%	0,00%	92,59%	0,00%	16,33%	0,00%	0,00%
300x300_60(18)	100,00%	100,00%	100,00%	100,00%	100,00%	100,00%	100,00%	100,00%	100,00%	100,00%
300x300_60(24)	100,00%	100,00%	100,00%	100,00%	100,00%	100,00%	100,00%	100,00%	100,00%	100,00%

	I_{SC}(MO-ABC,MOEA/D)					I_{SC}(MO-FA,NSGA-II)				
	Evaluations (Stop condition)					Evaluations (Stop condition)				
Instance($\tilde{s}_r$)	**50 000**	**100 000**	**200 000**	**300 000**	**400 000**	**50 000**	**100 000**	**200 000**	**300 000**	**400 000**
50x50_30(1)	92,31%	78,57%	100,00%	100,00%	93,33%	100,00%	56,67%	100,00%	100,00%	100,00%
50x50_60(1)	63,64%	91,67%	100,00%	91,67%	91,67%	53,47%	79,32%	98,49%	75,54%	15,77%
100x100_30(2)	91,30%	83,12%	70,73%	57,63%	58,33%	95,02%	99,55%	96,58%	96,51%	94,80%
100x100_30(3)	70,59%	81,13%	83,93%	100,00%	100,00%	100,00%	100,00%	100,00%	100,00%	100,00%
100x100_60(2)	50,00%	57,14%	25,00%	16,67%	66,67%	96,15%	85,38%	98,00%	99,50%	97,72%
100x100_60(3)	0,00%	87,50%	90,91%	100,00%	100,00%	100,00%	100,00%	100,00%	1,67%	32,06%
200x200_30(2)	0,00%	42,86%	20,00%	100,00%	100,00%	100,00%	100,00%	100,00%	100,00%	100,00%
200x200_30(4)	0,00%	0,00%	55,56%	100,00%	100,00%	100,00%	100,00%	100,00%	100,00%	100,00%
200x200_30(6)	100,00%	91,67%	100,00%	100,00%	100,00%	100,00%	92,86%	94,74%	94,12%	100,00%
200x200_30(9)	53,85%	80,00%	100,00%	100,00%	91,67%	100,00%	100,00%	100,00%	100,00%	100,00%
200x200_60(2)	92,86%	80,77%	85,71%	100,00%	90,63%	66,67%	78,65%	53,42%	62,16%	80,37%
200x200_60(4)	80,77%	84,85%	91,67%	68,97%	100,00%	100,00%	88,89%	98,68%	98,08%	97,62%
200x200_60(6)	100,00%	60,00%	69,23%	100,00%	87,50%	100,00%	93,01%	100,00%	95,50%	2,88%
200x200_60(9)	66,67%	72,73%	69,23%	90,48%	86,36%	99,41%	100,00%	100,00%	37,93%	96,87%
300x300_30(6)	0,00%	21,43%	38,46%	75,00%	60,00%	100,00%	100,00%	100,00%	100,00%	100,00%
300x300_30(12)	0,00%	50,00%	50,00%	50,00%	57,14%	100,00%	100,00%	100,00%	100,00%	100,00%
300x300_30(18)	42,86%	20,00%	60,00%	55,00%	100,00%	100,00%	100,00%	83,33%	100,00%	100,00%
300x300_30(24)	0,00%	0,00%	48,15%	36,00%	78,26%	100,00%	100,00%	100,00%	100,00%	100,00%
300x300_60(6)	70,00%	66,67%	80,00%	74,29%	85,71%	100,00%	100,00%	74,07%	39,24%	84,00%
300x300_60(12)	61,54%	86,05%	77,42%	71,05%	77,78%	100,00%	100,00%	100,00%	100,00%	97,73%
300x300_60(18)	100,00%	100,00%	100,00%	100,00%	100,00%	100,00%	100,00%	100,00%	100,00%	100,00%
300x300_60(24)	100,00%	100,00%	100,00%	100,00%	100,00%	100,00%	100,00%	100,00%	100,00%	100,00%

Table B.17: Set coverage metric by comparing all the metaheuristics two by two. Part 10 of 14.

	I_{SC}(MO-FA,SPEA2)					I_{SC}(MO-FA,MO-VNS)				
	Evaluations (Stop condition)					Evaluations (Stop condition)				
Instance($\tilde{s}_r$)	**50 000**	**100 000**	**200 000**	**300 000**	**400 000**	**50 000**	**100 000**	**200 000**	**300 000**	**400 000**
50x50_30(1)	100,00%	90,80%	100,00%	100,00%	100,00%	75,00%	100,00%	100,00%	100,00%	92,86%
50x50_60(1)	72,32%	92,88%	99,94%	0,15%	0,63%	90,00%	85,71%	85,71%	44,00%	55,00%
100x100_30(2)	99,00%	100,00%	100,00%	99,85%	100,00%	32,82%	50,36%	56,52%	48,57%	57,86%
100x100_30(3)	99,42%	100,00%	100,00%	100,00%	100,00%	23,08%	29,61%	23,88%	25,23%	13,66%
100x100_60(2)	100,00%	1,16%	89,88%	0,00%	92,60%	100,00%	37,50%	16,67%	100,00%	83,33%
100x100_60(3)	100,00%	100,00%	100,00%	100,00%	100,00%	0,00%	0,00%	0,00%	0,00%	20,00%
200x200_30(2)	100,00%	100,00%	100,00%	100,00%	100,00%	83,33%	100,00%	0,00%	25,00%	50,00%
200x200_30(4)	100,00%	100,00%	100,00%	100,00%	100,00%	63,64%	100,00%	100,00%	100,00%	100,00%
200x200_30(6)	100,00%	92,86%	100,00%	95,65%	90,91%	33,33%	90,91%	75,00%	54,55%	100,00%
200x200_30(9)	100,00%	100,00%	88,89%	81,25%	83,33%	81,82%	76,92%	86,36%	56,25%	52,94%
200x200_60(2)	77,78%	30,26%	57,63%	11,73%	55,84%	72,00%	62,50%	68,75%	55,88%	13,51%
200x200_60(4)	100,00%	100,00%	100,00%	61,11%	97,96%	100,00%	100,00%	97,62%	87,93%	95,45%
200x200_60(6)	100,00%	97,27%	100,00%	2,43%	0,00%	87,50%	63,64%	71,43%	60,00%	4,55%
200x200_60(9)	100,00%	100,00%	99,20%	64,34%	15,21%	100,00%	100,00%	100,00%	100,00%	100,00%
300x300_30(6)	100,00%	100,00%	100,00%	100,00%	100,00%	100,00%	91,67%	100,00%	100,00%	100,00%
300x300_30(12)	100,00%	100,00%	100,00%	100,00%	100,00%	100,00%	100,00%	100,00%	100,00%	100,00%
300x300_30(18)	100,00%	94,74%	62,50%	100,00%	53,33%	100,00%	100,00%	93,33%	100,00%	100,00%
300x300_30(24)	81,82%	44,44%	80,95%	93,42%	88,68%	100,00%	100,00%	100,00%	100,00%	100,00%
300x300_60(6)	63,16%	46,67%	73,81%	53,85%	72,92%	100,00%	100,00%	100,00%	100,00%	100,00%
300x300_60(12)	100,00%	100,00%	100,00%	93,10%	83,33%	100,00%	100,00%	100,00%	100,00%	100,00%
300x300_60(18)	100,00%	100,00%	100,00%	100,00%	100,00%	100,00%	100,00%	100,00%	100,00%	100,00%
300x300_60(24)	100,00%	100,00%	100,00%	100,00%	100,00%	100,00%	100,00%	100,00%	100,00%	100,00%

	I_{SC}(MO-FA,MO-VNS*)					I_{SC}(MO-FA,MO-ABC)				
	Evaluations (Stop condition)					Evaluations (Stop condition)				
Instance($\tilde{s}_r$)	**50 000**	**100 000**	**200 000**	**300 000**	**400 000**	**50 000**	**100 000**	**200 000**	**300 000**	**400 000**
50x50_30(1)	100,00%	90,91%	100,00%	100,00%	92,86%	99,34%	52,59%	99,33%	100,00%	100,00%
50x50_60(1)	100,00%	80,00%	88,89%	84,62%	88,24%	57,14%	97,58%	95,00%	67,08%	60,36%
100x100_30(2)	36,22%	52,24%	57,66%	48,92%	56,83%	80,71%	89,89%	93,09%	96,22%	96,50%
100x100_30(3)	0,00%	13,50%	36,90%	3,88%	26,88%	27,47%	14,94%	23,66%	8,89%	42,58%
100x100_60(2)	100,00%	66,67%	25,00%	100,00%	100,00%	100,00%	0,46%	99,90%	99,91%	99,91%
100x100_60(3)	100,00%	100,00%	83,33%	0,00%	0,00%	100,00%	100,00%	99,25%	0,51%	0,00%
200x200_30(2)	80,00%	20,00%	57,14%	0,00%	33,33%	100,00%	100,00%	92,41%	41,18%	0,00%
200x200_30(4)	0,00%	66,67%	75,00%	100,00%	100,00%	100,00%	100,00%	100,00%	100,00%	100,00%
200x200_30(6)	100,00%	100,00%	63,64%	37,50%	100,00%	68,18%	45,00%	88,24%	85,29%	95,45%
200x200_30(9)	45,45%	50,00%	63,16%	76,19%	40,74%	100,00%	72,73%	42,86%	40,91%	59,26%
200x200_60(2)	56,67%	0,00%	0,00%	38,89%	0,00%	29,27%	82,61%	34,82%	45,61%	14,78%
200x200_60(4)	94,74%	16,67%	96,15%	93,10%	95,65%	100,00%	100,00%	59,55%	53,13%	48,68%
200x200_60(6)	40,00%	22,22%	53,85%	0,00%	0,00%	51,67%	55,10%	25,19%	0,00%	0,00%
200x200_60(9)	100,00%	100,00%	100,00%	100,00%	100,00%	100,00%	98,82%	87,72%	6,80%	25,04%
300x300_30(6)	100,00%	100,00%	100,00%	100,00%	100,00%	98,44%	99,36%	99,92%	6,25%	100,00%
300x300_30(12)	100,00%	100,00%	100,00%	100,00%	100,00%	100,00%	100,00%	100,00%	100,00%	100,00%
300x300_30(18)	71,43%	28,57%	83,33%	100,00%	100,00%	100,00%	85,00%	67,86%	41,67%	40,00%
300x300_30(24)	100,00%	100,00%	100,00%	83,33%	100,00%	100,00%	100,00%	100,00%	100,00%	100,00%
300x300_60(6)	100,00%	100,00%	100,00%	100,00%	100,00%	100,00%	97,62%	95,00%	30,12%	88,10%
300x300_60(12)	100,00%	100,00%	100,00%	100,00%	100,00%	100,00%	100,00%	100,00%	61,59%	100,00%
300x300_60(18)	100,00%	100,00%	100,00%	100,00%	100,00%	100,00%	100,00%	100,00%	100,00%	100,00%
300x300_60(24)	100,00%	100,00%	100,00%	100,00%	100,00%	100,00%	100,00%	100,00%	100,00%	100,00%

Table B.18: Set coverage metric by comparing all the metaheuristics two by two. Part 11 of 11 of 14.

	I_{SC}(MO-FA,MO-GSA)					I_{SC}(MO-FA,MOEA/D)				
	Evaluations (Stop condition)					Evaluations (Stop condition)				
Instance($\tilde{s}_r$)	**50 000**	**100 000**	**200 000**	**300 000**	**400 000**	**50 000**	**100 000**	**200 000**	**300 000**	**400 000**
50x50_30(1)	100,00%	100,00%	100,00%	100,00%	100,00%	100,00%	100,00%	100,00%	100,00%	100,00%
50x50_60(1)	80,00%	80,00%	81,82%	83,33%	92,86%	100,00%	100,00%	100,00%	91,67%	91,67%
100x100_30(2)	60,49%	80,49%	76,85%	56,90%	72,22%	65,22%	61,04%	70,73%	67,80%	70,00%
100x100_30(3)	76,60%	75,76%	68,29%	41,67%	48,33%	62,75%	47,17%	83,93%	89,36%	86,27%
100x100_60(2)	88,89%	66,67%	80,00%	83,33%	75,00%	83,33%	85,71%	75,00%	83,33%	100,00%
100x100_60(3)	100,00%	100,00%	100,00%	40,00%	60,00%	100,00%	87,50%	100,00%	85,71%	80,00%
200x200_30(2)	100,00%	100,00%	100,00%	100,00%	88,89%	100,00%	100,00%	100,00%	100,00%	100,00%
200x200_30(4)	100,00%	66,67%	100,00%	100,00%	100,00%	25,00%	75,00%	100,00%	100,00%	100,00%
200x200_30(6)	81,82%	100,00%	75,00%	100,00%	72,73%	55,56%	91,67%	91,67%	100,00%	100,00%
200x200_30(9)	100,00%	92,31%	94,74%	78,57%	90,48%	100,00%	90,00%	100,00%	100,00%	91,67%
200x200_60(2)	60,00%	50,00%	82,76%	78,57%	90,38%	57,14%	73,08%	85,71%	73,08%	78,13%
200x200_60(4)	100,00%	100,00%	100,00%	96,00%	95,45%	88,46%	93,94%	83,33%	68,97%	70,97%
200x200_60(6)	92,86%	100,00%	93,33%	81,25%	11,76%	88,89%	60,00%	92,31%	71,43%	12,50%
200x200_60(9)	100,00%	100,00%	85,71%	85,71%	100,00%	88,89%	100,00%	92,31%	90,48%	90,91%
300x300_30(6)	100,00%	100,00%	100,00%	100,00%	100,00%	40,00%	57,14%	100,00%	87,50%	100,00%
300x300_30(12)	100,00%	100,00%	100,00%	100,00%	100,00%	100,00%	58,33%	100,00%	100,00%	100,00%
300x300_30(18)	100,00%	100,00%	92,86%	75,00%	100,00%	57,14%	100,00%	100,00%	100,00%	100,00%
300x300_30(24)	100,00%	92,11%	100,00%	100,00%	100,00%	75,00%	62,50%	70,37%	76,00%	86,96%
300x300_60(6)	71,43%	100,00%	70,21%	78,57%	83,33%	73,33%	55,56%	84,00%	65,71%	80,00%
300x300_60(12)	100,00%	100,00%	100,00%	96,83%	93,02%	65,38%	86,05%	90,32%	84,21%	77,78%
300x300_60(18)	100,00%	100,00%	100,00%	100,00%	100,00%	100,00%	100,00%	100,00%	100,00%	100,00%
300x300_60(24)	100,00%	100,00%	100,00%	100,00%	100,00%	100,00%	100,00%	100,00%	100,00%	100,00%

	I_{SC}(MO-GSA,NSGA-II)					I_{SC}(MO-GSA,SPEA2)				
	Evaluations (Stop condition)					Evaluations (Stop condition)				
Instance($\tilde{s}_r$)	**50 000**	**100 000**	**200 000**	**300 000**	**400 000**	**50 000**	**100 000**	**200 000**	**300 000**	**400 000**
50x50_30(1)	87,50%	38,89%	66,67%	98,96%	94,59%	69,57%	77,01%	94,68%	99,12%	98,25%
50x50_60(1)	10,89%	30,08%	93,52%	100,00%	100,00%	4,46%	97,08%	100,00%	100,00%	100,00%
100x100_30(2)	90,55%	99,55%	95,73%	95,85%	94,80%	92,50%	99,36%	100,00%	99,56%	100,00%
100x100_30(3)	96,48%	99,52%	94,74%	93,86%	97,28%	98,84%	100,00%	100,00%	98,94%	99,50%
100x100_60(2)	73,08%	98,46%	96,00%	91,58%	97,72%	92,04%	50,00%	95,24%	0,00%	92,60%
100x100_60(3)	20,56%	100,00%	100,00%	100,00%	98,09%	95,00%	100,00%	100,00%	100,00%	100,00%
200x200_30(2)	100,00%	100,00%	100,00%	100,00%	0,00%	91,67%	100,00%	0,80%	100,00%	0,00%
200x200_30(4)	97,39%	96,42%	97,49%	0,00%	0,00%	57,14%	97,06%	100,00%	0,00%	0,07%
200x200_30(6)	100,00%	92,86%	100,00%	88,24%	89,13%	100,00%	85,71%	92,86%	95,65%	72,73%
200x200_30(9)	90,00%	100,00%	100,00%	100,00%	100,00%	40,00%	100,00%	100,00%	100,00%	75,00%
200x200_60(2)	44,44%	88,76%	54,79%	86,49%	57,01%	100,00%	100,00%	67,80%	21,60%	64,94%
200x200_60(4)	0,00%	13,89%	86,84%	78,21%	78,57%	38,89%	7,14%	82,35%	27,78%	32,65%
200x200_60(6)	45,00%	2,69%	14,68%	1,00%	67,63%	1,82%	9,09%	22,59%	2,16%	0,13%
200x200_60(9)	1,18%	1,36%	0,07%	3,45%	44,84%	8,24%	18,60%	0,21%	0,75%	14,45%
300x300_30(6)	76,99%	92,52%	1,55%	39,29%	45,50%	51,22%	86,70%	94,82%	81,95%	99,86%
300x300_30(12)	100,00%	100,00%	100,00%	100,00%	100,00%	100,00%	100,00%	100,00%	3,23%	100,00%
300x300_30(18)	50,00%	14,29%	77,78%	35,29%	93,33%	0,00%	0,00%	0,00%	14,29%	46,67%
300x300_30(24)	40,00%	0,00%	0,00%	61,70%	93,75%	0,00%	0,00%	30,95%	0,00%	0,00%
300x300_60(6)	89,29%	33,33%	59,26%	60,76%	48,00%	36,84%	13,33%	23,81%	23,08%	64,58%
300x300_60(12)	33,33%	76,92%	47,17%	84,91%	100,00%	0,00%	46,15%	45,45%	27,59%	90,00%
300x300_60(18)	100,00%	100,00%	100,00%	100,00%	100,00%	100,00%	100,00%	100,00%	100,00%	100,00%
300x300_60(24)	100,00%	100,00%	100,00%	100,00%	100,00%	100,00%	100,00%	100,00%	100,00%	100,00%

Table B.19: Set coverage metric by comparing all the metaheuristics two by two. Part 12 of 14.

	$\mathrm{I_{SC}}$(MO-GSA,MO-VNS)					$\mathrm{I_{SC}}$(MO-GSA,MO-VNS*)				
	Evaluations (Stop condition)					Evaluations (Stop condition)				
Instance($\tilde{s}_r$)	**50 000**	**100 000**	**200 000**	**300 000**	**400 000**	**50 000**	**100 000**	**200 000**	**300 000**	**400 000**
50x50_30(1)	0,00%	28,57%	0,00%	14,29%	28,57%	25,00%	54,55%	0,00%	14,29%	28,57%
50x50_60(1)	0,00%	7,14%	0,00%	12,00%	15,00%	0,00%	6,67%	16,67%	0,00%	23,53%
100x100_30(2)	15,27%	5,84%	30,43%	57,86%	50,00%	14,96%	5,22%	31,39%	58,27%	51,08%
100x100_30(3)	2,96%	0,00%	1,00%	5,86%	6,17%	0,53%	10,13%	24,60%	0,86%	17,00%
100x100_60(2)	16,67%	0,00%	0,00%	0,00%	0,00%	100,00%	50,00%	0,00%	40,00%	0,00%
100x100_60(3)	0,00%	0,00%	0,00%	0,00%	0,00%	0,00%	0,00%	50,00%	0,00%	0,00%
200x200_30(2)	0,00%	0,00%	0,00%	0,00%	0,00%	0,00%	0,00%	0,00%	0,00%	0,00%
200x200_30(4)	0,00%	16,67%	12,50%	9,09%	0,00%	0,00%	0,00%	0,00%	0,00%	0,00%
200x200_30(6)	0,00%	27,27%	33,33%	27,27%	0,00%	68,75%	36,36%	27,27%	0,00%	0,00%
200x200_30(9)	0,00%	0,00%	31,82%	6,25%	11,76%	0,00%	9,09%	21,05%	19,05%	0,00%
200x200_60(2)	0,00%	28,13%	21,88%	20,59%	0,00%	0,00%	0,00%	0,00%	16,67%	0,00%
200x200_60(4)	0,00%	0,00%	19,05%	46,55%	6,82%	0,00%	0,00%	0,00%	0,00%	62,32%
200x200_60(6)	12,50%	0,00%	0,00%	0,00%	31,82%	0,00%	0,00%	0,00%	0,00%	0,00%
200x200_60(9)	0,00%	75,00%	53,85%	71,43%	15,38%	9,09%	22,22%	44,44%	47,06%	30,00%
300x300_30(6)	22,22%	41,67%	100,00%	100,00%	100,00%	0,00%	14,29%	60,00%	14,29%	100,00%
300x300_30(12)	100,00%	100,00%	100,00%	100,00%	100,00%	66,67%	100,00%	100,00%	100,00%	100,00%
300x300_30(18)	42,86%	0,00%	0,00%	17,65%	0,00%	0,00%	0,00%	0,00%	25,00%	0,00%
300x300_30(24)	62,50%	0,00%	100,00%	94,74%	100,00%	0,00%	0,00%	8,33%	41,67%	0,00%
300x300_60(6)	85,71%	50,00%	95,45%	75,76%	100,00%	29,41%	75,00%	100,00%	88,24%	100,00%
300x300_60(12)	27,78%	85,71%	95,24%	100,00%	100,00%	0,00%	46,67%	0,00%	37,50%	63,64%
300x300_60(18)	100,00%	100,00%	100,00%	100,00%	100,00%	100,00%	100,00%	100,00%	100,00%	100,00%
300x300_60(24)	100,00%	100,00%	100,00%	100,00%	100,00%	100,00%	100,00%	100,00%	100,00%	100,00%

	$\mathrm{I_{SC}}$(MO-GSA,MO-ABC)					$\mathrm{I_{SC}}$(MO-GSA,MO-FA)				
	Evaluations (Stop condition)					Evaluations (Stop condition)				
Instance($\tilde{s}_r$)	**50 000**	**100 000**	**200 000**	**300 000**	**400 000**	**50 000**	**100 000**	**200 000**	**300 000**	**400 000**
50x50_30(1)	0,00%	20,00%	72,48%	56,08%	59,12%	0,00%	26,67%	0,00%	13,33%	26,67%
50x50_60(1)	0,00%	0,00%	2,50%	28,22%	53,25%	0,00%	12,50%	0,00%	18,75%	11,76%
100x100_30(2)	38,78%	47,87%	70,05%	82,92%	88,69%	32,63%	17,12%	44,35%	66,67%	65,89%
100x100_30(3)	12,09%	4,55%	2,15%	5,56%	22,53%	10,81%	22,22%	14,40%	40,88%	27,27%
100x100_60(2)	0,44%	0,00%	21,84%	97,85%	99,36%	50,00%	20,00%	20,00%	0,00%	16,67%
100x100_60(3)	28,07%	0,00%	15,67%	1,03%	23,35%	0,00%	0,00%	0,00%	0,00%	0,00%
200x200_30(2)	10,00%	20,00%	87,34%	0,00%	0,00%	0,00%	0,00%	0,00%	0,00%	0,00%
200x200_30(4)	45,33%	95,00%	37,04%	0,00%	0,00%	0,00%	8,33%	0,00%	0,00%	0,00%
200x200_30(6)	0,00%	30,00%	14,71%	17,65%	13,64%	33,33%	27,27%	10,00%	30,77%	0,00%
200x200_30(9)	26,67%	13,64%	4,76%	0,00%	0,00%	0,00%	0,00%	0,00%	0,00%	0,00%
200x200_60(2)	0,00%	13,04%	0,00%	12,28%	1,74%	8,11%	3,51%	0,00%	15,38%	0,00%
200x200_60(4)	0,00%	0,00%	53,93%	29,69%	34,21%	0,00%	0,00%	0,00%	0,00%	0,00%
200x200_60(6)	0,00%	0,00%	4,44%	0,00%	0,00%	9,09%	0,00%	9,09%	14,29%	87,50%
200x200_60(9)	3,54%	0,59%	0,22%	0,34%	0,48%	0,00%	0,00%	0,00%	0,00%	0,00%
300x300_30(6)	9,38%	0,00%	4,81%	0,00%	0,48%	0,00%	0,00%	0,00%	0,00%	0,00%
300x300_30(12)	100,00%	33,33%	90,48%	7,69%	1,64%	0,00%	0,00%	0,00%	0,00%	0,00%
300x300_30(18)	41,67%	10,00%	0,00%	0,00%	0,00%	0,00%	0,00%	0,00%	0,00%	0,00%
300x300_30(24)	36,36%	93,33%	58,82%	100,00%	50,00%	0,00%	0,00%	0,00%	0,00%	0,00%
300x300_60(6)	69,23%	76,19%	95,00%	81,93%	90,48%	0,00%	0,00%	0,00%	0,00%	0,00%
300x300_60(12)	0,00%	61,16%	93,22%	100,00%	88,68%	0,00%	0,00%	0,00%	0,00%	0,00%
300x300_60(18)	100,00%	100,00%	100,00%	100,00%	100,00%	100,00%	100,00%	100,00%	100,00%	100,00%
300x300_60(24)	100,00%	100,00%	100,00%	100,00%	100,00%	100,00%	100,00%	100,00%	100,00%	100,00%

Table B.20: Set coverage metric by comparing all the metaheuristics two by two. Part 13 of 14.

	$\mathbf{I_{SC}}$(MO-GSA,MOEA/D)					$\mathbf{I_{SC}}$(MOEA/D,NSGA-II)				
	Evaluations (Stop condition)					Evaluations (Stop condition)				
Instance($\tilde{s}_r$)	50 000	100 000	200 000	300 000	400 000	50 000	100 000	200 000	300 000	400 000
50x50_30(1)	23,08%	78,57%	46,67%	66,67%	73,33%	62,50%	38,89%	39,39%	28,13%	86,49%
50x50_60(1)	18,18%	16,67%	25,00%	33,33%	33,33%	19,80%	71,43%	18,14%	27,72%	24,55%
100x100_30(2)	56,52%	50,65%	60,98%	62,71%	68,33%	76,62%	80,00%	75,50%	76,42%	82,80%
100x100_30(3)	62,75%	58,49%	62,50%	100,00%	74,51%	45,07%	28,37%	59,81%	54,27%	58,16%
100x100_60(2)	16,67%	57,14%	25,00%	16,67%	83,33%	73,08%	0,00%	73,00%	29,70%	13,20%
100x100_60(3)	40,00%	62,50%	100,00%	100,00%	100,00%	13,55%	61,68%	30,92%	99,97%	32,24%
200x200_30(2)	0,00%	28,57%	60,00%	100,00%	25,00%	100,00%	98,21%	61,22%	24,22%	8,75%
200x200_30(4)	0,00%	0,00%	77,78%	0,00%	33,33%	99,13%	99,76%	0,00%	0,00%	0,00%
200x200_30(6)	44,44%	91,67%	66,67%	50,00%	42,86%	87,50%	57,14%	78,95%	82,35%	82,61%
200x200_30(9)	38,46%	70,00%	100,00%	100,00%	91,67%	90,00%	40,00%	25,00%	15,00%	5,88%
200x200_60(2)	85,71%	80,77%	85,71%	80,77%	84,38%	22,22%	42,70%	41,10%	0,00%	14,02%
200x200_60(4)	76,92%	81,82%	80,56%	68,97%	74,19%	0,00%	25,00%	0,00%	0,00%	0,00%
200x200_60(6)	77,78%	40,00%	69,23%	57,14%	62,50%	35,00%	0,54%	3,48%	1,00%	9,71%
200x200_60(9)	55,56%	45,45%	53,85%	80,95%	77,27%	72,78%	68,02%	2,39%	3,45%	0,00%
300x300_30(6)	0,00%	0,00%	23,08%	12,50%	30,00%	100,00%	99,53%	1,55%	40,66%	15,30%
300x300_30(12)	0,00%	58,33%	100,00%	50,00%	100,00%	100,00%	100,00%	100,00%	100,00%	46,15%
300x300_30(18)	42,86%	0,00%	30,00%	45,00%	63,16%	50,00%	57,14%	55,56%	58,82%	20,00%
300x300_30(24)	0,00%	0,00%	51,85%	48,00%	86,96%	80,00%	0,00%	0,00%	6,38%	0,00%
300x300_60(6)	66,67%	51,85%	100,00%	100,00%	100,00%	32,14%	0,00%	0,00%	0,00%	0,00%
300x300_60(12)	53,85%	81,40%	83,87%	94,74%	90,74%	44,44%	0,00%	0,00%	0,00%	0,00%
300x300_60(18)	100,00%	100,00%	100,00%	100,00%	100,00%	100,00%	100,00%	100,00%	100,00%	100,00%
300x300_60(24)	100,00%	100,00%	100,00%	100,00%	100,00%	100,00%	100,00%	100,00%	100,00%	0,00%

	$\mathbf{I_{SC}}$(MOEA/D,SPEA2)					$\mathbf{I_{SC}}$(MOEA/D,MO-VNS)				
	Evaluations (Stop condition)					Evaluations (Stop condition)				
Instance($\tilde{s}_r$)	50 000	100 000	200 000	300 000	400 000	50 000	100 000	200 000	300 000	400 000
50x50_30(1)	86,96%	77,01%	87,23%	85,96%	78,95%	25,00%	28,57%	28,57%	28,57%	14,29%
50x50_60(1)	72,32%	0,55%	0,27%	99,82%	1,67%	30,00%	42,86%	57,14%	32,00%	45,00%
100x100_30(2)	82,50%	86,97%	91,55%	86,65%	89,93%	0,00%	0,73%	2,17%	12,14%	12,14%
100x100_30(3)	22,09%	22,68%	87,69%	60,64%	53,55%	15,98%	2,79%	1,99%	0,00%	2,64%
100x100_60(2)	95,58%	1,16%	67,86%	0,00%	0,32%	16,67%	0,00%	0,00%	0,00%	0,00%
100x100_60(3)	20,00%	1,08%	72,77%	100,00%	100,00%	0,00%	0,00%	0,00%	0,00%	0,00%
200x200_30(2)	100,00%	100,00%	0,68%	8,74%	99,81%	0,00%	0,00%	0,00%	0,00%	0,00%
200x200_30(4)	100,00%	100,00%	0,56%	0,06%	0,14%	63,64%	33,33%	6,25%	27,27%	0,00%
200x200_30(6)	83,33%	14,29%	85,71%	78,26%	72,73%	0,00%	0,00%	0,00%	9,09%	9,09%
200x200_30(9)	60,00%	71,43%	11,11%	0,00%	16,67%	0,00%	0,00%	0,00%	0,00%	17,65%
200x200_60(2)	14,81%	1,32%	37,29%	0,00%	0,00%	0,00%	3,13%	18,75%	0,00%	0,00%
200x200_60(4)	16,67%	7,14%	0,00%	0,00%	0,00%	3,70%	0,00%	0,00%	15,52%	0,00%
200x200_60(6)	10,91%	6,36%	0,55%	2,16%	0,06%	0,00%	18,18%	14,29%	0,00%	27,27%
200x200_60(9)	97,65%	82,01%	1,29%	0,53%	4,56%	61,54%	91,67%	84,62%	50,00%	30,77%
300x300_30(6)	100,00%	92,55%	94,82%	88,56%	98,53%	55,56%	58,33%	100,00%	100,00%	100,00%
300x300_30(12)	92,31%	100,00%	82,05%	0,00%	0,00%	100,00%	100,00%	100,00%	100,00%	100,00%
300x300_30(18)	33,33%	5,26%	0,00%	0,00%	0,00%	42,86%	47,06%	20,00%	41,18%	0,00%
300x300_30(24)	36,36%	5,56%	64,29%	0,00%	0,00%	62,50%	20,00%	30,00%	0,00%	0,00%
300x300_60(6)	0,00%	0,00%	0,00%	20,51%	0,00%	4,76%	6,25%	9,09%	12,12%	0,00%
300x300_60(12)	0,00%	11,54%	0,00%	0,00%	0,00%	33,33%	14,29%	14,29%	9,09%	12,00%
300x300_60(18)	100,00%	100,00%	100,00%	100,00%	100,00%	100,00%	100,00%	100,00%	100,00%	100,00%
300x300_60(24)	100,00%	100,00%	100,00%	100,00%	0,00%	100,00%	100,00%	100,00%	100,00%	0,00%

Table B.21: Set coverage metric by comparing all the metaheuristics two by two. Part 14 of 14.

	I_{SC}(MOEA/D,MO-VNS*					I_{SC}(MOEA/D,MO-ABC)				
	Evaluations (Stop condition)					Evaluations (Stop condition)				
Instance($\tilde{s}_r$)	**50 000**	**100 000**	**200 000**	**300 000**	**400 000**	**50 000**	**100 000**	**200 000**	**300 000**	**400 000**
50x50_30(1)	25,00%	36,36%	28,57%	28,57%	14,29%	29,80%	19,26%	46,31%	42,86%	54,01%
50x50_60(1)	25,00%	40,00%	44,44%	61,54%	52,94%	44,16%	79,03%	87,00%	80,45%	60,06%
100x100_30(2)	0,00%	1,49%	2,19%	12,23%	12,23%	8,39%	10,99%	8,29%	3,94%	5,41%
100x100_30(3)	9,47%	11,39%	20,24%	0,00%	2,77%	12,09%	1,30%	0,72%	0,00%	3,85%
100x100_60(2)	87,50%	0,00%	0,00%	0,00%	0,00%	0,66%	0,34%	0,29%	0,37%	0,09%
100x100_60(3)	0,00%	0,00%	0,00%	0,00%	0,00%	15,79%	0,00%	0,00%	0,00%	0,00%
200x200_30(2)	0,00%	0,00%	0,00%	0,00%	22,22%	60,00%	40,00%	87,34%	0,00%	0,00%
200x200_30(4)	0,00%	0,00%	0,00%	0,00%	0,00%	100,00%	100,00%	66,67%	0,00%	0,00%
200x200_30(6)	50,00%	0,00%	0,00%	12,50%	9,09%	0,00%	0,00%	0,00%	5,88%	9,09%
200x200_30(9)	0,00%	9,09%	10,53%	0,00%	0,00%	13,33%	18,18%	0,00%	0,00%	0,00%
200x200_60(2)	0,00%	0,00%	0,00%	0,00%	0,00%	0,00%	0,00%	4,46%	0,00%	0,87%
200x200_60(4)	0,00%	0,00%	0,00%	0,00%	0,00%	0,00%	31,37%	0,00%	0,00%	0,00%
200x200_60(6)	0,00%	11,11%	0,00%	0,00%	0,00%	0,00%	6,12%	0,00%	0,00%	25,20%
200x200_60(9)	36,36%	11,11%	22,22%	17,65%	10,00%	75,22%	0,59%	0,07%	0,34%	0,00%
300x300_30(6)	71,43%	57,14%	80,00%	42,86%	100,00%	100,00%	17,68%	4,81%	6,25%	0,32%
300x300_30(12)	93,33%	0,00%	57,14%	37,50%	46,67%	100,00%	33,33%	0,00%	0,00%	0,00%
300x300_30(18)	0,00%	0,00%	0,00%	0,00%	0,00%	33,33%	10,00%	0,00%	2,78%	0,00%
300x300_30(24)	0,00%	0,00%	0,00%	0,00%	0,00%	100,00%	93,33%	52,94%	68,97%	0,00%
300x300_60(6)	11,76%	6,25%	0,00%	11,76%	11,11%	7,69%	0,00%	10,00%	0,00%	0,00%
300x300_60(12)	17,65%	20,00%	0,00%	0,00%	4,55%	0,00%	2,48%	89,27%	38,41%	0,00%
300x300_60(18)	100,00%	100,00%	100,00%	100,00%	100,00%	100,00%	100,00%	100,00%	100,00%	100,00%
300x300_60(24)	100,00%	100,00%	100,00%	100,00%	0,00%	100,00%	100,00%	100,00%	100,00%	0,00%

	I_{SC}(MOEA/D,MO-FA)					I_{SC}(MOEA/D,MO-GSA)				
	Evaluations (Stop condition)					Evaluations (Stop condition)				
Instance($\tilde{s}_r$)	**50 000**	**100 000**	**200 000**	**300 000**	**400 000**	**50 000**	**100 000**	**200 000**	**300 000**	**400 000**
50x50_30(1)	14,29%	26,67%	28,57%	26,67%	13,33%	36,36%	54,55%	30,00%	46,67%	27,27%
50x50_60(1)	20,00%	37,50%	53,33%	50,00%	52,94%	73,33%	60,00%	36,36%	66,67%	57,14%
100x100_30(2)	5,26%	16,22%	11,30%	12,20%	12,40%	14,81%	15,85%	20,37%	9,48%	10,19%
100x100_30(3)	19,82%	23,02%	5,60%	2,19%	4,13%	40,43%	13,64%	7,32%	0,00%	8,33%
100x100_60(2)	50,00%	0,00%	20,00%	0,00%	0,00%	77,78%	11,11%	10,00%	50,00%	50,00%
100x100_60(3)	0,00%	0,00%	0,00%	0,00%	0,00%	28,57%	0,00%	0,00%	0,00%	0,00%
200x200_30(2)	0,00%	0,00%	0,00%	0,00%	0,00%	100,00%	63,64%	0,00%	0,00%	11,11%
200x200_30(4)	28,57%	8,33%	0,00%	0,00%	0,00%	100,00%	66,67%	0,00%	50,00%	33,33%
200x200_30(6)	33,33%	0,00%	0,00%	7,69%	9,09%	18,18%	0,00%	0,00%	23,08%	45,45%
200x200_30(9)	0,00%	0,00%	0,00%	0,00%	0,00%	25,00%	23,08%	0,00%	0,00%	4,76%
200x200_60(2)	2,70%	3,51%	0,00%	13,46%	0,00%	0,00%	0,00%	3,45%	2,38%	0,00%
200x200_60(4)	0,00%	0,00%	0,00%	0,00%	0,00%	2,86%	16,67%	0,00%	4,00%	0,00%
200x200_60(6)	0,00%	0,00%	0,00%	28,57%	81,25%	0,00%	46,67%	26,67%	18,75%	5,88%
200x200_60(9)	0,00%	0,00%	0,00%	0,00%	11,11%	77,78%	63,64%	50,00%	28,57%	0,00%
300x300_30(6)	14,29%	17,65%	0,00%	0,00%	0,00%	100,00%	100,00%	61,54%	66,67%	33,33%
300x300_30(12)	0,00%	0,00%	0,00%	0,00%	0,00%	33,33%	0,00%	0,00%	0,00%	0,00%
300x300_30(18)	0,00%	0,00%	0,00%	0,00%	0,00%	44,44%	69,23%	64,29%	50,00%	18,75%
300x300_30(24)	0,00%	0,00%	0,00%	0,00%	0,00%	92,86%	84,21%	3,85%	28,57%	0,00%
300x300_60(6)	0,00%	0,00%	0,00%	0,00%	0,00%	42,86%	4,76%	0,00%	0,00%	0,00%
300x300_60(12)	0,00%	0,00%	0,00%	0,00%	0,00%	33,33%	0,00%	0,00%	0,00%	0,00%
300x300_60(18)	100,00%	100,00%	100,00%	100,00%	100,00%	100,00%	100,00%	100,00%	100,00%	100,00%
300x300_60(24)	100,00%	100,00%	100,00%	100,00%	0,00%	100,00%	100,00%	100,00%	100,00%	0,00%

APPENDIX

C

Additional Information for Solving the RNPP: three-objective Outdoor Approach

This appendix includes additional information for solving the three-objective outdoor RNPP discussed in Chapter 5. Thus, Sections C.1 and C.2 include the p-values and set coverage metrics obtained by comparing the metaheuristics two by two, respectively.

C.1 Statistical Analysis Based on the Hypervolume Metric

This section includes all the p-values obtained by comparing the algorithms through Wilcoxon-Mann-Whitney's test and hypothesis $H_0 : \overline{Hyp_i} \leq \overline{Hyp_j}$ and $H_1 : \overline{Hyp_i} > \overline{Hyp_j}$, with $i, j = 1, 2, \ldots, 8$, 1=NSGA-II, 2=SPEA2, 3=MO-VNS, 4=MO-VNS*, 5=MO-ABC, 6=MO-FA, 7=MO-GSA, and 8=MOEA/D. Because of the symmetry observed in the p-values obtained, while comparing any two algorithms i and j, i.e. i vs j and j vs i. In the following tables, p-values lower than 0.05 means that $\overline{Hyp_i} > \overline{Hyp_j}$ (they appear shaded) and p-values higher than 0.95 means that $\overline{Hyp_j} > \overline{Hyp_i}$ (they appear in boldface). These p-values are in Tables C.1, C.2, C.3, C.4, and C.5.

C.2 Set Coverage Analysis

This section contains all the set coverage metrics obtained by comparing the metaheuristics two by two. These values are in Tables C.6, C.7, C.8, C.9, C.10, C.11, C.12, C.13, C.14, and C.15.

Table C.1: P-values obtained by comparing the metaheuristics through Wilcoxon-Mann-Whitney's test. Part 1 of 5.

	NSGA-II vs SPEA2					NSGA-II vs MO-VNS				
	Evaluations (Stop condition)					Evaluations (Stop condition)				
Instance($\tilde{s}_r$)	**50 000**	**100 000**	**200 000**	**300 000**	**400 000**	**50 000**	**100 000**	**200 000**	**300 000**	**400 000**
50x50_30(1)	0.5000	0.5000	0.5000	0.5000	0.5000	**1.0000**	**1.0000**	**1.0000**	**1.0000**	**1.0000**
100x100_30(2)	**0.9930**	0.5000	0.8333	0.0004	0.0001	**1.0000**	**1.0000**	**1.0000**	**1.0000**	**1.0000**
100x100_30(3)	**0.9960**	**0.9976**	**0.9976**	0.9489	**0.9999**	**1.0000**	**1.0000**	**1.0000**	**1.0000**	**1.0000**
200x200_30(2)	0.7391	0.4412	0.0616	0.0257	0.0071	0.4082	**0.9852**	**1.0000**	**1.0000**	**1.0000**
200x200_30(4)	0.3493	0.1782	0.2891	0.1171	0.0785	0.0047	0.0535	0.1710	0.2051	0.3918
200x200_30(6)	**0.9811**	**0.9524**	0.9418	0.9465	**0.9602**	0.1038	0.1227	0.4524	0.6082	0.7989
200x200_30(9)	**0.9984**	**0.9999**	**0.9996**	**0.9998**	**0.9998**	0.3757	0.1782	0.0616	0.0988	0.2518
300x300_30(6)	**0.9752**	0.9083	**0.9876**	**0.9841**	**0.9679**	**0.9736**	0.5560	0.8429	0.8655	0.8744
300x300_30(12)	**0.9988**	**0.9993**	**1.0000**	**1.0000**	**1.0000**	**0.9995**	**0.9963**	**0.9867**	**0.9908**	**0.9841**
300x300_30(18)	**1.0000**	**1.0000**	**1.0000**	**1.0000**	**1.0000**	**1.0000**	**1.0000**	**1.0000**	**0.9998**	**0.9999**
300x300_30(24)	**0.9999**	**1.0000**	**1.0000**	**1.0000**	**1.0000**	**1.0000**	**1.0000**	**1.0000**	**1.0000**	**1.0000**

	NSGA-II vs MO-VNS*					NSGA-II vs MO-ABC				
	Evaluations (Stop condition)					Evaluations (Stop condition)				
Instance($\tilde{s}_r$)	**50 000**	**100 000**	**200 000**	**300 000**	**400 000**	**50 000**	**100 000**	**200 000**	**300 000**	**400 000**
50x50_30(1)	**0.9998**	**1.0000**	**1.0000**	**1.0000**	**1.0000**	**1.0000**	**1.0000**	**1.0000**	**1.0000**	**1.0000**
100x100_30(2)	**1.0000**	**1.0000**	**1.0000**	**1.0000**	**1.0000**	**0.9999**	**0.9989**	**0.9970**	**0.9963**	**0.9993**
100x100_30(3)	**1.0000**	**1.0000**	**1.0000**	**1.0000**	**1.0000**	**1.0000**	**1.0000**	**1.0000**	**0.9998**	**0.9998**
200x200_30(2)	0.6559	**1.0000**	**1.0000**	**1.0000**	**1.0000**	0.4302	0.0341	0.0001	0.0000	0.0000
200x200_30(4)	0.1285	0.3390	0.2215	0.2173	0.2795	0.0000	0.0000	0.0000	0.0000	0.0000
200x200_30(6)	0.7820	0.8106	0.1140	0.0093	0.0015	0.0000	0.0000	0.0000	0.0000	0.0000
200x200_30(9)	0.4860	0.0000	0.0000	0.0000	0.0000	0.0000	0.0000	0.0000	0.0000	0.0000
300x300_30(6)	**0.9907**	0.4804	0.0547	0.0079	0.0027	0.3136	0.3236	0.4468	0.2474	0.3037
300x300_30(12)	**0.9997**	0.8496	0.3598	0.0917	0.0148	**1.0000**	**1.0000**	**1.0000**	**1.0000**	**1.0000**
300x300_30(18)	**1.0000**	**1.0000**	**0.9985**	0.8272	0.3545	**1.0000**	**1.0000**	**1.0000**	**1.0000**	**1.0000**
300x300_30(24)	**1.0000**	**1.0000**	**0.9999**	**0.9824**	0.8884	**1.0000**	**1.0000**	**1.0000**	**1.0000**	**1.0000**

	NSGA-II vs MO-FA					NSGA-II vs MO-GSA				
	Evaluations (Stop condition)					Evaluations (Stop condition)				
Instance($\tilde{s}_r$)	**50 000**	**100 000**	**200 000**	**300 000**	**400 000**	**50 000**	**100 000**	**200 000**	**300 000**	**400 000**
50x50_30(1)	**1.0000**	**1.0000**	**1.0000**	**1.0000**	**1.0000**	**1.0000**	**1.0000**	**1.0000**	**1.0000**	**1.0000**
100x100_30(2)	**1.0000**	**1.0000**	**1.0000**	**1.0000**	**1.0000**	0.0000	0.0000	0.0000	0.0000	0.0000
100x100_30(3)	**1.0000**	**1.0000**	**1.0000**	**1.0000**	**1.0000**	0.0000	0.0000	0.0000	0.0000	0.0000
200x200_30(2)	**1.0000**	**1.0000**	**1.0000**	**1.0000**	**1.0000**	0.6533	0.0785	0.0331	0.1396	0.2535
200x200_30(4)	0.6864	0.5140	0.1471	0.0725	0.0785	0.0000	0.0006	0.0088	0.0582	0.0449
200x200_30(6)	**0.9992**	**0.9918**	**0.9915**	**0.9940**	**0.9973**	0.0000	0.0000	0.0000	0.0025	0.0217
200x200_30(9)	**1.0000**	**1.0000**	**1.0000**	**0.9993**	**0.9993**	0.0003	0.0000	0.0047	0.7658	0.7277
300x300_30(6)	0.9012	**0.9577**	**0.9997**	**0.9999**	**0.9999**	0.0000	0.0000	0.0005	0.0047	0.0070
300x300_30(12)	**1.0000**	**1.0000**	**1.0000**	**1.0000**	**1.0000**	**0.9648**	**0.9551**	**0.9999**	**1.0000**	**1.0000**
300x300_30(18)	**1.0000**	**1.0000**	**1.0000**	**1.0000**	**1.0000**	**1.0000**	**1.0000**	**1.0000**	**1.0000**	**1.0000**
300x300_30(24)	**1.0000**	**1.0000**	**1.0000**	**1.0000**	**1.0000**	**1.0000**	**1.0000**	**1.0000**	**1.0000**	**1.0000**

Table C.2: P-values obtained by comparing the metaheuristics through Wilcoxon-Mann-Whitney's test. Part 2 of 5.

	NSGA-II vs MOEA/D					SPEA2 vs MO-VNS				
	Evaluations (Stop condition)					Evaluations (Stop condition)				
Instance($\tilde{s}_r$)	50 000	100 000	200 000	300 000	400 000	50 000	100 000	200 000	300 000	400 000
50x50_30(1)	**1.0000**	**1.0000**	**1.0000**	**1.0000**	**1.0000**	**1.0000**	**1.0000**	**1.0000**	**1.0000**	**1.0000**
100x100_30(2)	0.7743	0.0119	0.0088	0.0000	0.0000	**1.0000**	**1.0000**	**1.0000**	**1.0000**	**1.0000**
100x100_30(3)	**1.0000**	**1.0000**	**1.0000**	**1.0000**	**1.0000**	**1.0000**	**1.0000**	**1.0000**	**1.0000**	**1.0000**
200x200_30(2)	0.6864	0.3704	0.1171	0.3170	0.4541	0.2891	**0.9897**	**1.0000**	**1.0000**	**1.0000**
200x200_30(4)	0.9434	**0.9510**	**0.9868**	**0.9875**	0.9480	0.0079	0.1605	0.3186	0.5196	0.7012
200x200_30(6)	**1.0000**	**1.0000**	**1.0000**	**1.0000**	**1.0000**	0.0067	0.0119	0.0806	0.1285	0.2051
200x200_30(9)	**1.0000**	**1.0000**	**1.0000**	**1.0000**	**1.0000**	0.0015	0.0000	0.0000	0.0001	0.0003
300x300_30(6)	**0.9992**	**0.9804**	**0.9905**	**0.9551**	**0.9502**	0.4972	0.0964	0.0745	0.1256	0.1782
300x300_30(12)	**1.0000**	**1.0000**	**1.0000**	**1.0000**	**1.0000**	0.6296	0.3287	0.0633	0.0490	0.0210
300x300_30(18)	**1.0000**	**1.0000**	**1.0000**	**1.0000**	**1.0000**	**0.9669**	0.5973	0.4246	0.1972	0.1047
300x300_30(24)	**1.0000**	**1.0000**	**1.0000**	**1.0000**	**1.0000**	**1.0000**	**0.9997**	**0.9885**	0.7701	0.8027

	SPEA2 vs MO-VNS*					SPEA2 vs MO-ABC				
	Evaluations (Stop condition)					Evaluations (Stop condition)				
Instance($\tilde{s}_r$)	50 000	100 000	200 000	300 000	400 000	50 000	100 000	200 000	300 000	400 000
50x50_30(1)	**0.9998**	**1.0000**	**1.0000**	**1.0000**	**1.0000**	**1.0000**	**1.0000**	**1.0000**	**1.0000**	**1.0000**
100x100_30(2)	**1.0000**	**1.0000**	**1.0000**	**1.0000**	**1.0000**	**0.9969**	**0.9988**	**0.9875**	**0.9969**	**0.9994**
100x100_30(3)	**1.0000**	**1.0000**	**1.0000**	**1.0000**	**1.0000**	**1.0000**	**1.0000**	**0.9991**	**0.9975**	**0.9905**
200x200_30(2)	0.6349	**1.0000**	**1.0000**	**1.0000**	**1.0000**	0.2891	0.0375	0.0055	0.0010	0.0004
200x200_30(4)	0.2655	0.6189	0.3973	0.5864	0.7482	0.0000	0.0000	0.0000	0.0000	0.0000
200x200_30(6)	0.2309	0.2552	0.0035	0.0001	0.0000	0.0000	0.0000	0.0000	0.0000	0.0000
200x200_30(9)	0.0012	0.0000	0.0000	0.0000	0.0000	0.0000	0.0000	0.0000	0.0000	0.0000
300x300_30(6)	0.4541	0.0687	0.0005	0.0000	0.0000	0.0321	0.0894	0.0232	0.0094	0.0107
300x300_30(12)	0.3484	0.0035	0.0000	0.0000	0.0000	**0.9996**	**0.9999**	**1.0000**	**0.9993**	**0.9829**
300x300_30(18)	**1.0000**	0.4916	0.0018	0.0000	0.0000	**1.0000**	**1.0000**	**1.0000**	**1.0000**	**1.0000**
300x300_30(24)	**1.0000**	**0.9999**	0.0616	0.0000	0.0000	**1.0000**	**1.0000**	**1.0000**	**1.0000**	**1.0000**

	SPEA2 vs MO-FA					SPEA2 vs MO-GSA				
	Evaluations (Stop condition)					Evaluations (Stop condition)				
Instance($\tilde{s}_r$)	50 000	100 000	200 000	300 000	400 000	50 000	100 000	200 000	300 000	400 000
50x50_30(1)	**1.0000**	**1.0000**	**1.0000**	**1.0000**	**1.0000**	**1.0000**	**1.0000**	**1.0000**	**1.0000**	**1.0000**
100x100_30(2)	**1.0000**	**1.0000**	**1.0000**	**1.0000**	**1.0000**	0.0000	0.0000	0.0000	0.0000	0.0000
100x100_30(3)	**1.0000**	**1.0000**	**1.0000**	**1.0000**	**1.0000**	0.0000	0.0000	0.0000	0.0000	0.0000
200x200_30(2)	**1.0000**	**1.0000**	**1.0000**	**1.0000**	**1.0000**	0.4804	0.0669	0.3598	0.8254	**0.9510**
200x200_30(4)	0.7827	0.7701	0.2748	0.2429	0.4468	0.0000	0.0086	0.0264	0.3651	0.4860
200x200_30(6)	**0.9953**	**0.9709**	**0.9679**	**0.9674**	**0.9776**	0.0000	0.0000	0.0000	0.0000	0.0000
200x200_30(9)	0.9215	0.7109	0.9418	0.9151	0.8593	0.0000	0.0000	0.0000	0.0013	0.0013
300x300_30(6)	0.3864	0.7252	**0.9959**	**0.9974**	**0.9969**	0.0000	0.0000	0.0000	0.0000	0.0001
300x300_30(12)	**0.9857**	**0.9970**	**0.9998**	**0.9996**	**1.0000**	0.0706	0.0248	0.2386	0.9480	0.7949
300x300_30(18)	**1.0000**	**1.0000**	**1.0000**	**1.0000**	**1.0000**	**1.0000**	**0.9987**	**1.0000**	**1.0000**	**1.0000**
300x300_30(24)	**1.0000**	**1.0000**	**1.0000**	**1.0000**	**1.0000**	**1.0000**	**1.0000**	**1.0000**	**1.0000**	**1.0000**

Table C.3: P-values obtained by comparing the metaheuristics through Wilcoxon-Mann-Whitney's test. Part 3 of 5.

	SPEA2 vs MOEA/D					MO-VNS vs MO-VNS*				
	Evaluations (Stop condition)					Evaluations (Stop condition)				
Instance($\tilde{s}_r$)	**50 000**	**100 000**	**200 000**	**300 000**	**400 000**	**50 000**	**100 000**	**200 000**	**300 000**	**400 000**
50x50_30(1)	**1.0000**	**1.0000**	**1.0000**	**1.0000**	**1.0000**	**0.9790**	**0.9988**	**1.0000**	**1.0000**	**1.0000**
100x100_30(2)	0.0183	0.0103	0.0000	0.0000	0.0000	0.9170	0.7909	0.6687	0.6998	0.2820
100x100_30(3)	**1.0000**	**1.0000**	**1.0000**	**1.0000**	**1.0000**	0.5913	0.4471	0.0823	0.5973	0.6764
200x200_30(2)	0.4916	0.3287	0.3651	0.7205	0.8857	0.4357	0.8741	0.6243	0.2946	0.9172
200x200_30(4)	**0.9835**	**0.9841**	**0.9957**	**0.9990**	**0.9973**	**0.9538**	0.8529	0.6027	0.5973	0.5365
200x200_30(6)	**1.0000**	**1.0000**	**1.0000**	**1.0000**	**1.0000**	**0.9643**	**0.9534**	0.2016	0.0132	0.0004
200x200_30(9)	**1.0000**	**1.0000**	**1.0000**	**1.0000**	**1.0000**	0.6136	0.0036	0.0000	0.0000	0.0000
300x300_30(6)	0.8181	0.5196	0.3572	0.2215	0.3037	0.5230	0.4468	0.0122	0.0008	0.0001
300x300_30(12)	**1.0000**	**1.0000**	**1.0000**	**1.0000**	**1.0000**	0.2628	0.0196	0.0030	0.0001	0.0000
300x300_30(18)	**1.0000**	**1.0000**	**1.0000**	**1.0000**	**1.0000**	**0.9669**	0.3313	0.0040	0.0001	0.0000
300x300_30(24)	**1.0000**	**1.0000**	**1.0000**	**1.0000**	**1.0000**	**0.9699**	0.3646	0.0001	0.0000	0.0000

	MO-VNS vs MO-ABC					MO-VNS vs MO-FA				
	Evaluations (Stop condition)					Evaluations (Stop condition)				
Instance($\tilde{s}_r$)	**50 000**	**100 000**	**200 000**	**300 000**	**400 000**	**50 000**	**100 000**	**200 000**	**300 000**	**400 000**
50x50_30(1)	**1.0000**	**1.0000**	**1.0000**	**1.0000**	**1.0000**	**1.0000**	**1.0000**	**1.0000**	**1.0000**	**1.0000**
100x100_30(2)	0.0001	0.0000	0.0000	0.0000	0.0000	0.0002	0.0000	0.0000	0.0000	0.0000
100x100_30(3)	0.0490	0.1779	0.0138	0.0011	0.0010	0.5588	0.5804	0.0417	0.0153	0.0291
200x200_30(2)	0.6082	0.0041	0.0000	0.0000	0.0000	**1.0000**	**1.0000**	**1.0000**	**1.0000**	**1.0000**
200x200_30(4)	0.0002	0.0000	0.0000	0.0000	0.0000	**0.9977**	0.9450	0.5643	0.4082	0.2725
200x200_30(6)	0.0000	0.0000	0.0000	0.0000	0.0000	**0.9998**	**0.9986**	**0.9930**	**0.9885**	**0.9915**
200x200_30(9)	0.0000	0.0000	0.0000	0.0000	0.0000	**0.9999**	**1.0000**	**1.0000**	**0.9998**	**0.9995**
300x300_30(6)	0.0189	0.3390	0.1746	0.0651	0.0651	0.4191	0.9367	**0.9990**	**0.9996**	**0.9991**
300x300_30(12)	**0.9976**	**1.0000**	**1.0000**	**1.0000**	**1.0000**	**0.9659**	**0.9989**	**1.0000**	**1.0000**	**1.0000**
300x300_30(18)	**1.0000**	**1.0000**	**1.0000**	**1.0000**	**1.0000**	**0.9997**	**1.0000**	**1.0000**	**1.0000**	**1.0000**
300x300_30(24)	**1.0000**	**1.0000**	**1.0000**	**1.0000**	**1.0000**	**0.9988**	**1.0000**	**1.0000**	**1.0000**	**1.0000**

	MO-VNS vs MO-GSA					MO-VNS vs MOEA/D				
	Evaluations (Stop condition)					Evaluations (Stop condition)				
Instance($\tilde{s}_r$)	**50 000**	**100 000**	**200 000**	**300 000**	**400 000**	**50 000**	**100 000**	**200 000**	**300 000**	**400 000**
50x50_30(1)	0.0000	0.0000	0.0000	0.0000	0.0000	**1.0000**	**1.0000**	**1.0000**	**1.0000**	**1.0000**
100x100_30(2)	0.0000	0.0000	0.0000	0.0000	0.0000	0.0000	0.0000	0.0000	0.0000	0.0000
100x100_30(3)	0.0000	0.0000	0.0000	0.0000	0.0000	0.1117	0.0430	0.0894	0.0331	0.0256
200x200_30(2)	0.7012	0.0045	0.0000	0.0000	0.0000	0.7061	0.0273	0.0000	0.0000	0.0000
200x200_30(4)	0.0206	0.0668	0.1439	0.3918	0.2429	**0.9991**	**0.9835**	**0.9910**	**0.9870**	0.8829
200x200_30(6)	0.0041	0.0001	0.0012	0.0043	0.0017	**1.0000**	**1.0000**	**1.0000**	**1.0000**	**1.0000**
200x200_30(9)	0.0018	0.0017	0.4136	0.9313	0.8667	**1.0000**	**1.0000**	**1.0000**	**1.0000**	**1.0000**
300x300_30(6)	0.0000	0.0000	0.0000	0.0003	0.0005	0.8624	0.9401	0.8496	0.7571	0.7345
300x300_30(12)	0.0273	0.0725	0.8987	**0.9985**	**0.9985**	**1.0000**	**1.0000**	**1.0000**	**1.0000**	**1.0000**
300x300_30(18)	**0.9942**	**0.9977**	**1.0000**	**1.0000**	**1.0000**	**1.0000**	**1.0000**	**1.0000**	**1.0000**	**1.0000**
300x300_30(24)	**1.0000**	**1.0000**	**1.0000**	**1.0000**	**1.0000**	**1.0000**	**1.0000**	**1.0000**	**1.0000**	**1.0000**

Table C.4: P-values obtained by comparing the metaheuristics through Wilcoxon-Mann-Whitney's test. Part 4 of 5.

	MO-VNS* vs MO-ABC					MO-VNS* vs MO-FA				
	Evaluations (Stop condition)					Evaluations (Stop condition)				
Instance($\tilde{s}_r$)	**50 000**	**100 000**	**200 000**	**300 000**	**400 000**	**50 000**	**100 000**	**200 000**	**300 000**	**400 000**
50x50_30(1)	**1.0000**	**1.0000**	**0.9966**	0.9084	0.3036	**1.0000**	**1.0000**	**1.0000**	**1.0000**	**1.0000**
100x100_30(2)	0.0000	0.0000	0.0000	0.0000	0.0000	0.0000	0.0000	0.0000	0.0000	0.0000
100x100_30(3)	0.0324	0.1598	0.2351	0.0008	0.0002	0.4313	0.6759	0.5662	0.0148	0.0048
200x200_30(2)	0.3545	0.0000	0.0000	0.0000	0.0000	**1.0000**	**1.0000**	**1.0000**	**1.0000**	**0.9986**
200x200_30(4)	0.0000	0.0000	0.0000	0.0000	0.0000	0.9215	0.7157	0.4246	0.2342	0.2748
200x200_30(6)	0.0000	0.0000	0.0000	0.0000	0.0000	**0.9962**	**0.9893**	**0.9986**	**0.9995**	**1.0000**
200x200_30(9)	0.0000	0.0032	0.0005	0.0002	0.0000	**1.0000**	**1.0000**	**1.0000**	**1.0000**	**1.0000**
300x300_30(6)	0.0063	0.3086	0.8047	0.9331	**0.9699**	0.4712	**0.9551**	**0.9999**	**1.0000**	**1.0000**
300x300_30(12)	**1.0000**	**1.0000**	**1.0000**	**1.0000**	**1.0000**	**0.9959**	**1.0000**	**1.0000**	**1.0000**	**1.0000**
300x300_30(18)	**1.0000**	**1.0000**	**1.0000**	**1.0000**	**1.0000**	**0.9993**	**1.0000**	**1.0000**	**1.0000**	**1.0000**
300x300_30(24)	**1.0000**	**1.0000**	**1.0000**	**1.0000**	**1.0000**	**0.9564**	**1.0000**	**1.0000**	**1.0000**	**1.0000**

	MO-VNS* vs MO-GSA					MO-VNS* vs MOEA/D				
	Evaluations (Stop condition)					Evaluations (Stop condition)				
Instance($\tilde{s}_r$)	**50 000**	**100 000**	**200 000**	**300 000**	**400 000**	**50 000**	**100 000**	**200 000**	**300 000**	**400 000**
50x50_30(1)	0.0009	0.0003	0.0000	0.0000	0.0000	**1.0000**	**1.0000**	**0.9998**	**0.9977**	0.9285
100x100_30(2)	0.0000	0.0000	0.0000	0.0000	0.0000	0.0000	0.0000	0.0000	0.0000	0.0000
100x100_30(3)	0.0000	0.0000	0.0000	0.0000	0.0000	0.1302	0.1128	0.5288	0.0256	0.0171
200x200_30(2)	0.3598	0.0000	0.0000	0.0000	0.0000	0.5028	0.0000	0.0000	0.0000	0.0000
200x200_30(4)	0.0002	0.0056	0.0706	0.2748	0.2386	**0.9897**	0.9480	**0.9940**	**0.9951**	0.9465
200x200_30(6)	0.0000	0.0000	0.0007	0.3755	0.9083	**1.0000**	**1.0000**	**1.0000**	**1.0000**	**1.0000**
200x200_30(9)	0.0001	0.2055	**1.0000**	**1.0000**	**1.0000**	**1.0000**	**1.0000**	**1.0000**	**1.0000**	**1.0000**
300x300_30(6)	0.0000	0.0000	0.0136	0.4691	0.7785	0.9191	**0.9790**	**1.0000**	**1.0000**	**1.0000**
300x300_30(12)	0.0500	0.8378	**1.0000**	**1.0000**	**1.0000**	**1.0000**	**1.0000**	**1.0000**	**1.0000**	**1.0000**
300x300_30(18)	0.9172	**0.9993**	**1.0000**	**1.0000**	**1.0000**	**1.0000**	**1.0000**	**1.0000**	**1.0000**	**1.0000**
300x300_30(24)	**1.0000**	**1.0000**	**1.0000**	**1.0000**	**1.0000**	**1.0000**	**1.0000**	**1.0000**	**1.0000**	**1.0000**

	MO-ABC vs MO-FA					MO-ABC vs MO-GSA				
	Evaluations (Stop condition)					Evaluations (Stop condition)				
Instance($\tilde{s}_r$)	**50 000**	**100 000**	**200 000**	**300 000**	**400 000**	**50 000**	**100 000**	**200 000**	**300 000**	**400 000**
50x50_30(1)	**1.0000**	**1.0000**	**1.0000**	**1.0000**	**1.0000**	0.0000	0.0000	0.0000	0.0000	0.0000
100x100_30(2)	**0.9751**	**0.9879**	**0.9987**	**0.9997**	**1.0000**	0.0000	0.0000	0.0000	0.0000	0.0000
100x100_30(3)	0.9349	0.7039	0.7180	0.9036	0.9313	0.0000	0.0000	0.0000	0.0000	0.0000
200x200_30(2)	**1.0000**	**1.0000**	**1.0000**	**1.0000**	**1.0000**	0.7345	0.6296	**0.9852**	**0.9999**	**1.0000**
200x200_30(4)	**1.0000**	**1.0000**	**1.0000**	**1.0000**	**1.0000**	**0.9951**	**1.0000**	**1.0000**	**1.0000**	**1.0000**
200x200_30(6)	**1.0000**	**1.0000**	**1.0000**	**1.0000**	**1.0000**	**1.0000**	**1.0000**	**1.0000**	**1.0000**	**1.0000**
200x200_30(9)	**1.0000**	**1.0000**	**1.0000**	**1.0000**	**1.0000**	**0.9847**	**0.9776**	**1.0000**	**1.0000**	**1.0000**
300x300_30(6)	0.9106	0.9313	**0.9992**	**0.9998**	**0.9998**	0.0000	0.0000	0.0024	0.0599	0.0745
300x300_30(12)	0.3186	0.3864	0.8655	0.8883	**0.9999**	0.0000	0.0000	0.0000	0.0128	0.0633
300x300_30(18)	0.0001	0.0000	0.0000	0.0000	0.0000	0.0000	0.0000	0.0014	0.1227	0.1156
300x300_30(24)	0.0000	0.0000	0.0000	0.0000	0.0000	0.1227	0.2091	**0.9985**	**1.0000**	**1.0000**

Table C.5: P-values obtained by comparing the metaheuristics through Wilcoxon-Mann-Whitney's test. Part 5 of 5.

	MO-ABC vs MOEA/D					MO-FA vs MO-GSA				
	Evaluations (Stop condition)					Evaluations (Stop condition)				
Instance($\tilde{s}_r$)	**50 000**	**100 000**	**200 000**	**300 000**	**400 000**	**50 000**	**100 000**	**200 000**	**300 000**	**400 000**
50x50_30(1)	0.0000	0.0006	0.9297	**0.9988**	**1.0000**	0.0000	0.0000	0.0000	0.0000	0.0000
100x100_30(2)	0.0006	0.0004	0.0025	0.0005	0.0005	0.0000	0.0000	0.0000	0.0000	0.0000
100x100_30(3)	0.8028	0.6082	**0.9625**	**0.9862**	**0.9940**	0.0000	0.0000	0.0000	0.0000	0.0000
200x200_30(2)	0.6764	0.7743	0.9418	**0.9962**	**0.9996**	0.0000	0.0000	0.0000	0.0000	0.0000
200x200_30(4)	**1.0000**	**1.0000**	**1.0000**	**1.0000**	**1.0000**	0.0000	0.0010	0.1143	0.6814	0.5973
200x200_30(6)	**1.0000**	**1.0000**	**1.0000**	**1.0000**	**1.0000**	0.0000	0.0000	0.0001	0.0002	0.0001
200x200_30(9)	**1.0000**	**1.0000**	**1.0000**	**1.0000**	**1.0000**	0.0000	0.0000	0.0000	0.0013	0.0013
300x300_30(6)	**0.9989**	**0.9689**	**0.9867**	**0.9893**	**0.9935**	0.0000	0.0000	0.0000	0.0000	0.0000
300x300_30(12)	**1.0000**	**0.9998**	**0.9987**	**0.9955**	**0.9982**	0.0002	0.0000	0.0001	0.0051	0.0000
300x300_30(18)	**0.9994**	**0.9993**	**0.9999**	**0.9999**	**0.9999**	0.1143	0.0159	0.7526	**0.9970**	**0.9920**
300x300_30(24)	**1.0000**	**1.0000**	**1.0000**	**1.0000**	**1.0000**	**0.9995**	**0.9998**	**1.0000**	**1.0000**	**1.0000**

	MO-FA vs MOEA/D					MO-GSA vs MOEA/D				
	Evaluations (Stop condition)					Evaluations (Stop condition)				
Instance($\tilde{s}_r$)	**50 000**	**100 000**	**200 000**	**300 000**	**400 000**	**50 000**	**100 000**	**200 000**	**300 000**	**400 000**
50x50_30(1)	0.0000	0.0000	0.0000	0.0000	0.0000	**1.0000**	**1.0000**	**1.0000**	**1.0000**	**1.0000**
100x100_30(2)	0.0000	0.0000	0.0000	0.0000	0.0000	**1.0000**	**1.0000**	**1.0000**	**1.0000**	**0.9987**
100x100_30(3)	0.0633	0.0217	0.6726	0.5643	0.5809	**1.0000**	**1.0000**	**1.0000**	**1.0000**	**1.0000**
200x200_30(2)	0.0000	0.0000	0.0000	0.0000	0.0000	0.5309	0.5698	0.4136	0.4747	0.6507
200x200_30(4)	0.8801	0.8962	**0.9968**	**0.9983**	**0.9918**	**1.0000**	**0.9997**	**0.9999**	**0.9997**	**0.9987**
200x200_30(6)	0.9210	0.8801	0.7482	0.7109	0.6914	**1.0000**	**1.0000**	**1.0000**	**1.0000**	**1.0000**
200x200_30(9)	**1.0000**	**1.0000**	**1.0000**	**1.0000**	**1.0000**	**1.0000**	**1.0000**	**1.0000**	**1.0000**	**1.0000**
300x300_30(6)	0.8218	0.2748	0.0040	0.0004	0.0003	**1.0000**	**1.0000**	**1.0000**	**1.0000**	**1.0000**
300x300_30(12)	**1.0000**	**0.9997**	0.8829	0.8624	0.3629	**1.0000**	**1.0000**	**1.0000**	**1.0000**	**1.0000**
300x300_30(18)	**1.0000**	**1.0000**	**1.0000**	**1.0000**	**1.0000**	**1.0000**	**1.0000**	**1.0000**	**0.9994**	**0.9995**
300x300_30(24)	**1.0000**	**1.0000**	**1.0000**	**1.0000**	**1.0000**	**1.0000**	**1.0000**	**1.0000**	**0.9960**	**0.9995**

Table C.6: Set coverage metric by comparing all the metaheuristics two by two. Part 1 of 10.

	I_{SC}(NSGA-II,SPEA2)					I_{SC}(NSGA-II,MO-VNS)				
	Evaluations (Stop condition)					Evaluations (Stop condition)				
Instance($\tilde{s}_r$)	**50 000**	**100 000**	**200 000**	**300 000**	**400 000**	**50 000**	**100 000**	**200 000**	**300 000**	**400 000**
50x50_30(1)	56,52%	77,01%	96,81%	92,11%	96,49%	0,00%	0,00%	0,00%	0,00%	0,00%
100x100_30(2)	54,00%	60,47%	77,46%	81,86%	91,87%	0,00%	0,00%	0,72%	0,00%	1,43%
100x100_30(3)	63,37%	90,72%	37,85%	78,19%	74,60%	0,00%	0,00%	0,00%	0,45%	0,00%
200x200_30(2)	91,67%	55,00%	0,00%	0,19%	100,00%	0,00%	0,00%	0,00%	0,00%	0,00%
200x200_30(4)	4,76%	97,06%	99,89%	100,00%	100,00%	9,09%	25,00%	12,50%	27,27%	83,33%
200x200_30(6)	16,67%	0,00%	10,71%	34,78%	54,55%	0,00%	0,00%	0,00%	0,00%	0,00%
200x200_30(9)	0,00%	35,71%	11,11%	0,00%	0,00%	0,00%	0,00%	0,00%	0,00%	0,00%
300x300_30(6)	20,33%	82,45%	99,88%	95,81%	100,00%	0,00%	41,67%	100,00%	100,00%	100,00%
300x300_30(12)	0,00%	0,00%	0,00%	0,00%	0,00%	0,00%	100,00%	100,00%	100,00%	100,00%
300x300_30(18)	0,00%	0,00%	0,00%	0,00%	6,67%	0,00%	0,00%	0,00%	0,00%	0,00%
300x300_30(24)	0,00%	16,67%	11,90%	13,16%	0,00%	37,50%	80,00%	100,00%	89,47%	92,86%

	I_{SC}(NSGA-II,MO-VNS*)					I_{SC}(NSGA-II,MO-ABC)				
	Evaluations (Stop condition)					Evaluations (Stop condition)				
Instance($\tilde{s}_r$)	**50 000**	**100 000**	**200 000**	**300 000**	**400 000**	**50 000**	**100 000**	**200 000**	**300 000**	**400 000**
50x50_30(1)	0,00%	0,00%	0,00%	0,00%	0,00%	0,00%	0,00%	0,67%	0,00%	16,06%
100x100_30(2)	0,00%	0,00%	0,00%	0,00%	0,00%	1,89%	1,77%	0,92%	2,30%	2,39%
100x100_30(3)	0,00%	0,00%	0,00%	0,00%	0,00%	0,00%	0,00%	0,00%	0,00%	0,00%
200x200_30(2)	0,00%	0,00%	0,00%	0,00%	33,33%	0,00%	0,00%	0,00%	0,00%	0,00%
200x200_30(4)	0,00%	0,00%	0,00%	28,57%	0,00%	0,00%	91,67%	98,15%	24,56%	13,52%
200x200_30(6)	0,00%	0,00%	0,00%	0,00%	0,00%	0,00%	0,00%	0,00%	38,24%	0,00%
200x200_30(9)	0,00%	0,00%	5,26%	0,00%	0,00%	0,00%	0,00%	0,00%	0,00%	0,00%
300x300_30(6)	0,00%	14,29%	60,00%	0,00%	75,00%	9,38%	0,00%	4,81%	6,25%	20,51%
300x300_30(12)	0,00%	0,00%	28,57%	25,00%	100,00%	0,00%	33,33%	0,00%	0,00%	0,00%
300x300_30(18)	0,00%	0,00%	16,67%	0,00%	0,00%	8,33%	10,00%	0,00%	0,00%	0,00%
300x300_30(24)	0,00%	0,00%	16,67%	20,83%	0,00%	18,18%	100,00%	94,12%	100,00%	12,50%

	I_{SC}(NSGA-II,MO-FA)					I_{SC}(NSGA-II,MO-GSA)				
	Evaluations (Stop condition)					Evaluations (Stop condition)				
Instance($\tilde{s}_r$)	**50 000**	**100 000**	**200 000**	**300 000**	**400 000**	**50 000**	**100 000**	**200 000**	**300 000**	**400 000**
50x50_30(1)	0,00%	0,00%	0,00%	0,00%	0,00%	9,09%	9,09%	0,00%	0,00%	9,09%
100x100_30(2)	1,05%	0,00%	0,87%	0,00%	2,33%	1,23%	0,00%	1,85%	0,00%	1,85%
100x100_30(3)	0,00%	0,00%	0,00%	0,00%	0,00%	1,06%	0,00%	1,22%	0,00%	2,50%
200x200_30(2)	0,00%	0,00%	0,00%	0,00%	0,00%	0,00%	0,00%	0,00%	0,00%	33,33%
200x200_30(4)	0,00%	0,00%	0,00%	0,00%	0,00%	71,43%	0,00%	0,00%	100,00%	50,00%
200x200_30(6)	0,00%	0,00%	0,00%	0,00%	0,00%	0,00%	0,00%	0,00%	7,69%	9,09%
200x200_30(9)	0,00%	0,00%	0,00%	0,00%	0,00%	0,00%	0,00%	0,00%	0,00%	0,00%
300x300_30(6)	0,00%	0,00%	0,00%	0,00%	0,00%	40,00%	16,67%	38,46%	66,67%	16,67%
300x300_30(12)	0,00%	0,00%	0,00%	0,00%	0,00%	0,00%	0,00%	0,00%	0,00%	0,00%
300x300_30(18)	0,00%	0,00%	0,00%	0,00%	0,00%	44,44%	53,85%	7,14%	50,00%	0,00%
300x300_30(24)	0,00%	0,00%	0,00%	0,00%	0,00%	42,86%	63,16%	73,08%	33,33%	12,50%

Table C.7: Set coverage metric by comparing all the metaheuristics two by two. Part 2 of 10.

	I_{SC}(NSGA-II,MOEA/D)					I_{SC}(SPEA2,NSGA-II)				
	Evaluations (Stop condition)					Evaluations (Stop condition)				
Instance($\tilde{s}_r$)	**50 000**	**100 000**	**200 000**	**300 000**	**400 000**	**50 000**	**100 000**	**200 000**	**300 000**	**400 000**
50x50_30(1)	7,69%	7,14%	13,33%	20,00%	0,00%	51,56%	57,78%	76,77%	79,17%	72,97%
100x100_30(2)	6,52%	5,19%	9,76%	11,86%	8,33%	51,24%	69,09%	74,64%	63,54%	80,80%
100x100_30(3)	15,69%	18,87%	17,86%	12,77%	21,57%	20,42%	35,58%	42,58%	17,06%	39,80%
200x200_30(2)	0,00%	0,00%	0,00%	25,00%	75,00%	5,06%	67,86%	70,09%	72,32%	0,00%
200x200_30(4)	0,00%	0,00%	100,00%	100,00%	100,00%	94,78%	5,01%	0,00%	0,00%	0,00%
200x200_30(6)	0,00%	8,33%	0,00%	16,67%	28,57%	62,50%	85,71%	94,74%	76,47%	67,39%
200x200_30(9)	0,00%	20,00%	42,86%	64,00%	66,67%	90,00%	20,00%	58,33%	95,00%	47,06%
300x300_30(6)	0,00%	0,00%	30,77%	12,50%	10,00%	92,92%	15,89%	0,00%	12,36%	0,00%
300x300_30(12)	0,00%	0,00%	0,00%	0,00%	42,86%	100,00%	100,00%	100,00%	100,00%	100,00%
300x300_30(18)	14,29%	0,00%	20,00%	30,00%	52,63%	66,67%	100,00%	100,00%	41,18%	26,67%
300x300_30(24)	0,00%	62,50%	48,15%	52,00%	82,61%	100,00%	54,55%	36,84%	89,36%	95,83%

	I_{SC}(SPEA2,MO-VNS)					I_{SC}(SPEA2,MO-VNS*)				
	Evaluations (Stop condition)					Evaluations (Stop condition)				
Instance($\tilde{s}_r$)	**50 000**	**100 000**	**200 000**	**300 000**	**400 000**	**50 000**	**100 000**	**200 000**	**300 000**	**400 000**
50x50_30(1)	0,00%	0,00%	0,00%	0,00%	0,00%	0,00%	0,00%	0,00%	0,00%	0,00%
100x100_30(2)	0,00%	0,00%	0,00%	0,00%	0,00%	0,00%	0,00%	0,00%	0,00%	0,00%
100x100_30(3)	0,00%	0,00%	0,00%	0,00%	0,00%	0,00%	0,00%	0,00%	0,00%	0,00%
200x200_30(2)	0,00%	0,00%	0,00%	0,00%	0,00%	0,00%	0,00%	0,00%	0,00%	0,00%
200x200_30(4)	0,00%	16,67%	12,50%	18,18%	0,00%	0,00%	0,00%	0,00%	0,00%	0,00%
200x200_30(6)	0,00%	0,00%	0,00%	0,00%	0,00%	0,00%	0,00%	0,00%	0,00%	0,00%
200x200_30(9)	0,00%	0,00%	0,00%	0,00%	0,00%	0,00%	0,00%	10,53%	9,52%	0,00%
300x300_30(6)	22,22%	41,67%	72,73%	100,00%	90,00%	0,00%	0,00%	20,00%	0,00%	62,50%
300x300_30(12)	92,31%	100,00%	100,00%	100,00%	100,00%	13,33%	0,00%	100,00%	100,00%	100,00%
300x300_30(18)	42,86%	52,94%	73,33%	41,18%	0,00%	0,00%	0,00%	16,67%	43,75%	0,00%
300x300_30(24)	75,00%	100,00%	100,00%	100,00%	100,00%	0,00%	0,00%	8,33%	83,33%	30,00%

	I_{SC}(SPEA2,MO-ABC)					I_{SC}(SPEA2,MO-FA)				
	Evaluations (Stop condition)					Evaluations (Stop condition)				
Instance($\tilde{s}_r$)	**50 000**	**100 000**	**200 000**	**300 000**	**400 000**	**50 000**	**100 000**	**200 000**	**300 000**	**400 000**
50x50_30(1)	0,00%	0,00%	0,67%	0,00%	0,73%	0,00%	0,00%	0,00%	0,00%	0,00%
100x100_30(2)	1,05%	1,77%	1,84%	0,00%	2,55%	1,05%	0,00%	0,00%	0,00%	0,00%
100x100_30(3)	0,00%	0,00%	0,00%	0,00%	0,00%	0,00%	0,00%	0,00%	0,00%	0,00%
200x200_30(2)	0,00%	0,00%	87,34%	0,00%	0,00%	0,00%	0,00%	0,00%	0,00%	0,00%
200x200_30(4)	0,00%	11,67%	3,70%	0,00%	0,00%	0,00%	0,00%	0,00%	0,00%	0,00%
200x200_30(6)	0,00%	0,00%	0,00%	47,06%	18,18%	0,00%	0,00%	0,00%	0,00%	0,00%
200x200_30(9)	0,00%	0,00%	0,00%	0,00%	0,00%	0,00%	0,00%	0,00%	0,00%	0,00%
300x300_30(6)	14,06%	0,00%	0,39%	6,25%	0,00%	0,00%	0,00%	0,00%	0,00%	0,00%
300x300_30(12)	27,27%	33,33%	0,00%	0,00%	0,00%	0,00%	0,00%	0,00%	0,00%	0,00%
300x300_30(18)	91,67%	95,00%	10,71%	0,00%	0,00%	0,00%	0,00%	7,69%	0,00%	0,00%
300x300_30(24)	100,00%	100,00%	100,00%	100,00%	100,00%	0,00%	0,00%	0,00%	0,00%	0,00%

Table C.8: Set coverage metric by comparing all the metaheuristics two by two. Part 3 of 10.

	I_{SC}(SPEA2,MO-GSA)					I_{SC}(SPEA2,MOEA/D)				
	Evaluations (Stop condition)					Evaluations (Stop condition)				
Instance($\tilde{s}_r$)	**50 000**	**100 000**	**200 000**	**300 000**	**400 000**	**50 000**	**100 000**	**200 000**	**300 000**	**400 000**
50x50_30(1)	9,09%	9,09%	0,00%	0,00%	0,00%	0,00%	7,14%	13,33%	13,33%	0,00%
100x100_30(2)	1,23%	0,00%	0,00%	0,00%	0,00%	4,35%	5,19%	9,76%	11,86%	8,33%
100x100_30(3)	0,00%	0,00%	0,00%	0,00%	0,83%	7,84%	11,32%	14,29%	10,64%	19,61%
200x200_30(2)	0,00%	0,00%	14,29%	0,00%	22,22%	0,00%	0,00%	40,00%	50,00%	25,00%
200x200_30(4)	0,00%	0,00%	0,00%	75,00%	33,33%	0,00%	0,00%	66,67%	33,33%	0,00%
200x200_30(6)	0,00%	0,00%	0,00%	15,38%	9,09%	0,00%	58,33%	0,00%	16,67%	28,57%
200x200_30(9)	8,33%	0,00%	0,00%	0,00%	4,76%	7,69%	10,00%	57,14%	100,00%	91,67%
300x300_30(6)	86,67%	0,00%	23,08%	50,00%	0,00%	0,00%	0,00%	0,00%	12,50%	10,00%
300x300_30(12)	0,00%	0,00%	0,00%	0,00%	0,00%	0,00%	0,00%	50,00%	50,00%	100,00%
300x300_30(18)	100,00%	100,00%	100,00%	0,00%	56,25%	42,86%	50,00%	45,00%	45,00%	52,63%
300x300_30(24)	92,86%	100,00%	65,38%	80,95%	75,00%	31,25%	62,50%	48,15%	80,00%	95,65%

	I_{SC}(MO-VNS,NSGA-II)					I_{SC}(MO-VNS,SPEA2)				
	Evaluations (Stop condition)					Evaluations (Stop condition)				
Instance($\tilde{s}_r$)	**50 000**	**100 000**	**200 000**	**300 000**	**400 000**	**50 000**	**100 000**	**200 000**	**300 000**	**400 000**
50x50_30(1)	100,00%	56,67%	100,00%	100,00%	100,00%	91,30%	90,80%	100,00%	100,00%	100,00%
100x100_30(2)	95,02%	99,55%	96,58%	98,25%	94,80%	99,00%	100,00%	100,00%	100,00%	100,00%
100x100_30(3)	100,00%	100,00%	96,65%	94,88%	100,00%	100,00%	98,97%	100,00%	99,47%	100,00%
200x200_30(2)	100,00%	98,21%	99,11%	100,00%	100,00%	100,00%	100,00%	100,00%	100,00%	100,00%
200x200_30(4)	99,13%	3,34%	0,63%	0,00%	0,00%	100,00%	14,71%	0,00%	0,00%	100,00%
200x200_30(6)	100,00%	92,86%	94,74%	100,00%	100,00%	100,00%	92,86%	100,00%	95,65%	90,91%
200x200_30(9)	100,00%	100,00%	100,00%	100,00%	100,00%	100,00%	100,00%	100,00%	100,00%	100,00%
300x300_30(6)	92,92%	38,32%	0,00%	0,00%	0,00%	25,20%	23,94%	0,59%	0,00%	0,00%
300x300_30(12)	88,64%	0,00%	0,00%	0,00%	0,00%	0,00%	0,00%	0,00%	0,00%	0,00%
300x300_30(18)	100,00%	100,00%	88,89%	100,00%	100,00%	66,67%	5,26%	0,00%	0,00%	46,67%
300x300_30(24)	40,00%	0,00%	0,00%	23,40%	0,00%	0,00%	0,00%	0,00%	0,00%	0,00%

	I_{SC}(MO-VNS,MO-VNS*)					I_{SC}(MO-VNS,MO-ABC)				
	Evaluations (Stop condition)					Evaluations (Stop condition)				
Instance($\tilde{s}_r$)	**50 000**	**100 000**	**200 000**	**300 000**	**400 000**	**50 000**	**100 000**	**200 000**	**300 000**	**400 000**
50x50_30(1)	75,00%	81,82%	92,86%	92,86%	100,00%	70,86%	52,59%	95,97%	97,88%	97,08%
100x100_30(2)	95,28%	97,76%	97,81%	100,00%	99,28%	99,37%	99,65%	96,31%	99,84%	99,84%
100x100_30(3)	7,37%	51,05%	65,87%	59,05%	79,45%	54,95%	42,21%	53,76%	54,72%	86,81%
200x200_30(2)	0,00%	0,00%	42,86%	0,00%	33,33%	100,00%	100,00%	100,00%	8,82%	0,00%
200x200_30(4)	0,00%	0,00%	0,00%	0,00%	0,00%	100,00%	51,67%	68,52%	0,00%	0,77%
200x200_30(6)	100,00%	100,00%	90,91%	87,50%	100,00%	81,82%	45,00%	82,35%	82,35%	95,45%
200x200_30(9)	0,00%	36,36%	31,58%	71,43%	0,00%	100,00%	45,45%	0,00%	31,82%	7,41%
300x300_30(6)	0,00%	0,00%	0,00%	0,00%	25,00%	6,25%	0,00%	0,00%	0,00%	0,00%
300x300_30(12)	0,00%	0,00%	0,00%	0,00%	0,00%	0,00%	33,33%	0,00%	0,00%	0,00%
300x300_30(18)	0,00%	0,00%	16,67%	0,00%	0,00%	41,67%	20,00%	0,00%	8,33%	1,82%
300x300_30(24)	0,00%	0,00%	0,00%	8,33%	0,00%	18,18%	93,33%	47,06%	96,55%	0,00%

Table C.9: Set coverage metric by comparing all the metaheuristics two by two. Part 4 of 10.

	I_{SC}(MO-VNS,MO-FA)				
	Evaluations (Stop condition)				
Instance($\tilde{s}_r$)	50 000	100 000	200 000	300 000	400 000
50x50_30(1)	57,14%	93,33%	92,86%	93,33%	93,33%
100x100_30(2)	92,63%	98,20%	96,52%	100,00%	99,22%
100x100_30(3)	73,87%	84,13%	56,80%	80,29%	85,12%
200x200_30(2)	0,00%	0,00%	33,33%	0,00%	50,00%
200x200_30(4)	7,14%	0,00%	0,00%	0,00%	0,00%
200x200_30(6)	33,33%	100,00%	50,00%	61,54%	100,00%
200x200_30(9)	0,00%	13,33%	0,00%	25,00%	0,00%
300x300_30(6)	0,00%	0,00%	0,00%	0,00%	0,00%
300x300_30(12)	0,00%	0,00%	0,00%	0,00%	0,00%
300x300_30(18)	0,00%	0,00%	0,00%	0,00%	0,00%
300x300_30(24)	0,00%	0,00%	0,00%	0,00%	0,00%

	I_{SC}(MO-VNS,MO-GSA)				
	Evaluations (Stop condition)				
Instance($\tilde{s}_r$)	50 000	100 000	200 000	300 000	400 000
50x50_30(1)	72,73%	100,00%	100,00%	100,00%	100,00%
100x100_30(2)	100,00%	100,00%	97,22%	99,14%	97,22%
100x100_30(3)	92,55%	98,48%	96,34%	87,50%	94,17%
200x200_30(2)	100,00%	90,91%	100,00%	100,00%	66,67%
200x200_30(4)	100,00%	0,00%	0,00%	50,00%	50,00%
200x200_30(6)	100,00%	100,00%	50,00%	76,92%	72,73%
200x200_30(9)	100,00%	92,31%	47,37%	78,57%	90,48%
300x300_30(6)	40,00%	16,67%	0,00%	0,00%	0,00%
300x300_30(12)	0,00%	0,00%	0,00%	0,00%	0,00%
300x300_30(18)	77,78%	92,31%	71,43%	50,00%	81,25%
300x300_30(24)	28,57%	65,79%	0,00%	0,00%	0,00%

	I_{SC}(MO-VNS,MOEA/D)				
	Evaluations (Stop condition)				
Instance($\tilde{s}_r$)	50 000	100 000	200 000	300 000	400 000
50x50_30(1)	100,00%	100,00%	100,00%	100,00%	100,00%
100x100_30(2)	100,00%	97,40%	98,78%	100,00%	100,00%
100x100_30(3)	64,71%	88,68%	82,14%	100,00%	98,04%
200x200_30(2)	100,00%	71,43%	100,00%	100,00%	100,00%
200x200_30(4)	0,00%	0,00%	66,67%	0,00%	100,00%
200x200_30(6)	100,00%	100,00%	100,00%	83,33%	100,00%
200x200_30(9)	100,00%	100,00%	100,00%	100,00%	91,67%
300x300_30(6)	0,00%	0,00%	0,00%	0,00%	0,00%
300x300_30(12)	0,00%	0,00%	0,00%	0,00%	0,00%
300x300_30(18)	42,86%	50,00%	45,00%	50,00%	63,16%
300x300_30(24)	18,75%	50,00%	40,74%	56,00%	78,26%

	I_{SC}(MO-VNS*,NSGA-II)				
	Evaluations (Stop condition)				
Instance($\tilde{s}_r$)	50 000	100 000	200 000	300 000	400 000
50x50_30(1)	71,88%	98,89%	100,00%	100,00%	100,00%
100x100_30(2)	95,02%	99,55%	96,58%	96,51%	94,80%
100x100_30(3)	97,89%	100,00%	94,74%	100,00%	100,00%
200x200_30(2)	100,00%	100,00%	100,00%	100,00%	0,00%
200x200_30(4)	100,00%	100,00%	100,00%	0,00%	3,41%
200x200_30(6)	100,00%	92,86%	94,74%	100,00%	100,00%
200x200_30(9)	100,00%	100,00%	83,33%	100,00%	100,00%
300x300_30(6)	100,00%	72,90%	1,55%	39,01%	0,00%
300x300_30(12)	100,00%	100,00%	1,61%	1,22%	0,00%
300x300_30(18)	100,00%	100,00%	83,33%	100,00%	100,00%
300x300_30(24)	100,00%	100,00%	78,95%	65,96%	93,75%

	I_{SC}(MO-VNS*,SPEA2)				
	Evaluations (Stop condition)				
Instance($\tilde{s}_r$)	50 000	100 000	200 000	300 000	400 000
50x50_30(1)	65,22%	80,46%	100,00%	100,00%	100,00%
100x100_30(2)	99,00%	100,00%	100,00%	99,85%	99,88%
100x100_30(3)	99,42%	98,97%	100,00%	100,00%	100,00%
200x200_30(2)	100,00%	100,00%	100,00%	100,00%	82,79%
200x200_30(4)	100,00%	100,00%	100,00%	99,85%	99,83%
200x200_30(6)	100,00%	85,71%	100,00%	95,65%	90,91%
200x200_30(9)	100,00%	100,00%	88,89%	68,75%	91,67%
300x300_30(6)	100,00%	89,36%	13,65%	99,19%	11,04%
300x300_30(12)	76,92%	25,00%	0,00%	0,00%	0,00%
300x300_30(18)	100,00%	100,00%	62,50%	42,86%	53,33%
300x300_30(24)	81,82%	38,89%	59,52%	0,00%	43,40%

	I_{SC}(MO-VNS*,MO-VNS)				
	Evaluations (Stop condition)				
Instance($\tilde{s}_r$)	50 000	100 000	200 000	300 000	400 000
50x50_30(1)	0,00%	0,00%	92,86%	92,86%	100,00%
100x100_30(2)	89,31%	91,97%	96,38%	99,29%	98,57%
100x100_30(3)	91,72%	70,39%	74,63%	90,54%	79,30%
200x200_30(2)	83,33%	87,50%	50,00%	25,00%	12,50%
200x200_30(4)	100,00%	100,00%	100,00%	100,00%	50,00%
200x200_30(6)	0,00%	72,73%	83,33%	72,73%	100,00%
200x200_30(9)	100,00%	38,46%	72,73%	37,50%	76,47%
300x300_30(6)	66,67%	91,67%	100,00%	100,00%	60,00%
300x300_30(12)	100,00%	100,00%	100,00%	100,00%	100,00%
300x300_30(18)	85,71%	100,00%	93,33%	76,47%	90,00%
300x300_30(24)	100,00%	100,00%	100,00%	78,95%	100,00%

Table C.10: Set coverage metric by comparing all the metaheuristics two by two. Part 5 of 10.

	I_{SC}(MO-VNS*,MO-ABC)					I_{SC}(MO-VNS*,MO-FA)				
	Evaluations (Stop condition)					Evaluations (Stop condition)				
Instance($\tilde{s}_r$)	**50 000**	**100 000**	**200 000**	**300 000**	**400 000**	**50 000**	**100 000**	**200 000**	**300 000**	**400 000**
50x50_30(1)	30,46%	34,07%	98,66%	100,00%	97,08%	14,29%	6,67%	92,86%	93,33%	93,33%
100x100_30(2)	94,76%	96,99%	96,31%	99,84%	99,84%	88,42%	91,89%	95,65%	100,00%	97,67%
100x100_30(3)	80,22%	53,90%	50,18%	86,94%	80,49%	95,50%	92,06%	44,80%	94,89%	61,98%
200x200_30(2)	100,00%	100,00%	100,00%	47,06%	1,41%	75,00%	28,57%	66,67%	40,00%	0,00%
200x200_30(4)	100,00%	100,00%	100,00%	17,54%	1,63%	42,86%	33,33%	0,00%	0,00%	0,00%
200x200_30(6)	0,00%	35,00%	44,12%	82,35%	95,45%	0,00%	72,73%	50,00%	61,54%	100,00%
200x200_30(9)	100,00%	54,55%	28,57%	27,27%	77,78%	15,38%	13,33%	31,25%	62,50%	81,25%
300x300_30(6)	29,69%	5,14%	3,55%	6,25%	0,00%	0,00%	0,00%	0,00%	0,00%	0,00%
300x300_30(12)	100,00%	33,33%	0,00%	0,00%	0,00%	0,00%	0,00%	0,00%	0,00%	0,00%
300x300_30(18)	100,00%	100,00%	64,29%	27,78%	12,73%	0,00%	5,88%	0,00%	0,00%	0,00%
300x300_30(24)	100,00%	100,00%	100,00%	96,55%	100,00%	0,00%	0,00%	0,00%	0,00%	0,00%

	I_{SC}(MO-VNS*,MO-GSA)					I_{SC}(MO-VNS*,MOEA/D)				
	Evaluations (Stop condition)					Evaluations (Stop condition)				
Instance($\tilde{s}_r$)	**50 000**	**100 000**	**200 000**	**300 000**	**400 000**	**50 000**	**100 000**	**200 000**	**300 000**	**400 000**
50x50_30(1)	27,27%	9,09%	100,00%	100,00%	100,00%	15,38%	21,43%	100,00%	100,00%	100,00%
100x100_30(2)	96,30%	98,78%	98,15%	99,14%	97,22%	100,00%	98,70%	98,78%	100,00%	100,00%
100x100_30(3)	97,87%	80,30%	84,15%	97,50%	90,00%	76,47%	77,36%	60,71%	100,00%	100,00%
200x200_30(2)	100,00%	100,00%	100,00%	100,00%	100,00%	100,00%	100,00%	100,00%	100,00%	25,00%
200x200_30(4)	100,00%	100,00%	100,00%	100,00%	100,00%	50,00%	100,00%	100,00%	100,00%	100,00%
200x200_30(6)	27,27%	78,57%	50,00%	61,54%	72,73%	33,33%	91,67%	100,00%	100,00%	100,00%
200x200_30(9)	100,00%	84,62%	89,47%	42,86%	100,00%	100,00%	70,00%	85,71%	100,00%	91,67%
300x300_30(6)	100,00%	33,33%	15,38%	66,67%	0,00%	0,00%	7,14%	0,00%	25,00%	0,00%
300x300_30(12)	11,11%	0,00%	0,00%	0,00%	0,00%	0,00%	8,33%	0,00%	50,00%	14,29%
300x300_30(18)	100,00%	100,00%	92,86%	50,00%	100,00%	71,43%	70,00%	60,00%	65,00%	73,68%
300x300_30(24)	100,00%	78,95%	96,15%	28,57%	87,50%	56,25%	62,50%	51,85%	96,00%	82,61%

	I_{SC}(MO-ABC,NSGA-II)					I_{SC}(MO-ABC,SPEA2)				
	Evaluations (Stop condition)					Evaluations (Stop condition)				
Instance($\tilde{s}_r$)	**50 000**	**100 000**	**200 000**	**300 000**	**400 000**	**50 000**	**100 000**	**200 000**	**300 000**	**400 000**
50x50_30(1)	100,00%	100,00%	100,00%	100,00%	94,59%	100,00%	100,00%	98,94%	100,00%	98,25%
100x100_30(2)	95,02%	99,55%	96,58%	96,51%	94,80%	99,00%	100,00%	100,00%	99,85%	99,88%
100x100_30(3)	100,00%	100,00%	100,00%	95,56%	100,00%	100,00%	100,00%	100,00%	100,00%	100,00%
200x200_30(2)	100,00%	95,54%	97,77%	100,00%	100,00%	100,00%	100,00%	0,80%	100,00%	100,00%
200x200_30(4)	99,13%	50,36%	0,00%	36,67%	3,86%	85,71%	64,71%	98,44%	0,12%	100,00%
200x200_30(6)	100,00%	92,86%	94,74%	88,24%	97,83%	100,00%	92,86%	100,00%	95,65%	86,36%
200x200_30(9)	100,00%	100,00%	100,00%	100,00%	100,00%	80,00%	100,00%	100,00%	100,00%	100,00%
300x300_30(6)	76,99%	100,00%	1,55%	40,66%	0,00%	56,91%	100,00%	94,59%	18,29%	100,00%
300x300_30(12)	100,00%	2,33%	2,41%	100,00%	92,31%	15,38%	25,00%	12,82%	3,23%	6,14%
300x300_30(18)	50,00%	28,57%	100,00%	100,00%	100,00%	0,00%	0,00%	87,50%	100,00%	86,67%
300x300_30(24)	0,00%	0,00%	0,00%	0,00%	66,67%	0,00%	0,00%	0,00%	0,00%	0,00%

Table C.11: Set coverage metric by comparing all the metaheuristics two by two. Part 6 of 10.

	I_{SC}(MO-ABC,MO-VNS)					I_{SC}(MO-ABC,MO-VNS*)				
	Evaluations (Stop condition)					Evaluations (Stop condition)				
Instance($\tilde{s}_r$)	**50 000**	**100 000**	**200 000**	**300 000**	**400 000**	**50 000**	**100 000**	**200 000**	**300 000**	**400 000**
50x50_30(1)	41,67%	35,71%	50,00%	64,29%	50,00%	100,00%	100,00%	57,14%	71,43%	50,00%
100x100_30(2)	49,62%	59,12%	52,90%	44,29%	44,29%	52,76%	59,70%	54,01%	44,60%	44,60%
100x100_30(3)	31,36%	46,37%	56,22%	53,60%	30,84%	4,74%	38,82%	55,95%	45,26%	37,15%
200x200_30(2)	0,00%	0,00%	0,00%	50,00%	100,00%	0,00%	0,00%	0,00%	20,00%	33,33%
200x200_30(4)	0,00%	16,67%	12,50%	81,82%	66,67%	0,00%	0,00%	0,00%	0,00%	16,67%
200x200_30(6)	75,00%	81,82%	83,33%	63,64%	72,73%	100,00%	100,00%	90,91%	50,00%	72,73%
200x200_30(9)	0,00%	46,15%	100,00%	56,25%	58,82%	0,00%	9,09%	68,42%	66,67%	29,63%
300x300_30(6)	44,44%	91,67%	81,82%	81,25%	100,00%	57,14%	57,14%	80,00%	42,86%	100,00%
300x300_30(12)	100,00%	50,00%	100,00%	100,00%	100,00%	0,00%	66,67%	85,71%	100,00%	100,00%
300x300_30(18)	42,86%	35,29%	93,33%	88,24%	90,00%	0,00%	0,00%	16,67%	43,75%	66,67%
300x300_30(24)	62,50%	10,00%	60,00%	0,00%	92,86%	0,00%	0,00%	0,00%	0,00%	0,00%

	I_{SC}(MO-ABC,MO-FA)					I_{SC}(MO-ABC,MO-GSA)				
	Evaluations (Stop condition)					Evaluations (Stop condition)				
Instance($\tilde{s}_r$)	**50 000**	**100 000**	**200 000**	**300 000**	**400 000**	**50 000**	**100 000**	**200 000**	**300 000**	**400 000**
50x50_30(1)	50,00%	40,00%	50,00%	66,67%	53,33%	100,00%	72,73%	80,00%	93,33%	100,00%
100x100_30(2)	73,68%	73,87%	68,70%	57,72%	60,47%	74,07%	76,83%	67,59%	52,59%	53,70%
100x100_30(3)	47,75%	77,78%	68,80%	78,10%	51,24%	85,11%	92,42%	90,24%	78,33%	50,83%
200x200_30(2)	0,00%	0,00%	0,00%	0,00%	83,33%	25,00%	36,36%	42,86%	100,00%	100,00%
200x200_30(4)	0,00%	0,00%	0,00%	0,00%	0,00%	85,71%	0,00%	0,00%	100,00%	100,00%
200x200_30(6)	33,33%	90,91%	60,00%	84,62%	72,73%	100,00%	100,00%	50,00%	92,31%	72,73%
200x200_30(9)	0,00%	0,00%	31,25%	37,50%	68,75%	75,00%	92,31%	94,74%	85,71%	90,48%
300x300_30(6)	7,14%	11,76%	0,00%	38,46%	0,00%	53,33%	100,00%	30,77%	83,33%	50,00%
300x300_30(12)	0,00%	0,00%	0,00%	0,00%	0,00%	0,00%	72,73%	0,00%	0,00%	15,38%
300x300_30(18)	0,00%	0,00%	7,69%	0,00%	18,75%	77,78%	76,92%	100,00%	100,00%	100,00%
300x300_30(24)	0,00%	0,00%	0,00%	0,00%	0,00%	28,57%	5,26%	19,23%	0,00%	12,50%

	I_{SC}(MO-ABC,MOEA/D)					I_{SC}(MO-FA,NSGA-II)				
	Evaluations (Stop condition)					Evaluations (Stop condition)				
Instance($\tilde{s}_r$)	**50 000**	**100 000**	**200 000**	**300 000**	**400 000**	**50 000**	**100 000**	**200 000**	**300 000**	**400 000**
50x50_30(1)	92,31%	78,57%	100,00%	100,00%	93,33%	100,00%	56,67%	100,00%	100,00%	100,00%
100x100_30(2)	91,30%	83,12%	70,73%	57,63%	58,33%	95,02%	99,55%	96,58%	96,51%	94,80%
100x100_30(3)	70,59%	81,13%	83,93%	100,00%	100,00%	100,00%	100,00%	100,00%	100,00%	100,00%
200x200_30(2)	0,00%	42,86%	20,00%	100,00%	100,00%	100,00%	100,00%	100,00%	100,00%	100,00%
200x200_30(4)	0,00%	0,00%	55,56%	100,00%	100,00%	100,00%	100,00%	100,00%	100,00%	100,00%
200x200_30(6)	100,00%	91,67%	100,00%	100,00%	100,00%	100,00%	92,86%	94,74%	94,12%	100,00%
200x200_30(9)	53,85%	80,00%	100,00%	100,00%	91,67%	100,00%	100,00%	100,00%	100,00%	100,00%
300x300_30(6)	0,00%	21,43%	38,46%	75,00%	60,00%	100,00%	100,00%	100,00%	100,00%	100,00%
300x300_30(12)	0,00%	50,00%	50,00%	50,00%	57,14%	100,00%	100,00%	100,00%	100,00%	100,00%
300x300_30(18)	42,86%	20,00%	60,00%	55,00%	100,00%	100,00%	100,00%	83,33%	100,00%	100,00%
300x300_30(24)	0,00%	0,00%	48,15%	36,00%	78,26%	100,00%	100,00%	100,00%	100,00%	100,00%

Table C.12: Set coverage metric by comparing all the metaheuristics two by two. Part 7 of 10.

	I_{SC}(MO-FA,SPEA2)					I_{SC}(MO-FA,MO-VNS)				
	Evaluations (Stop condition)					Evaluations (Stop condition)				
Instance($\tilde{s}_r$)	50 000	100 000	200 000	300 000	400 000	50 000	100 000	200 000	300 000	400 000
50x50_30(1)	100,00%	90,80%	100,00%	100,00%	100,00%	75,00%	100,00%	100,00%	100,00%	92,86%
100x100_30(2)	99,00%	100,00%	100,00%	99,85%	100,00%	32,82%	50,36%	56,52%	48,57%	57,86%
100x100_30(3)	99,42%	100,00%	100,00%	100,00%	100,00%	23,08%	29,61%	23,88%	25,23%	13,66%
200x200_30(2)	100,00%	100,00%	100,00%	100,00%	100,00%	83,33%	100,00%	0,00%	25,00%	50,00%
200x200_30(4)	100,00%	100,00%	100,00%	100,00%	100,00%	63,64%	100,00%	100,00%	100,00%	100,00%
200x200_30(6)	100,00%	92,86%	100,00%	95,65%	90,91%	33,33%	90,91%	75,00%	54,55%	100,00%
200x200_30(9)	100,00%	100,00%	88,89%	81,25%	83,33%	81,82%	76,92%	86,36%	56,25%	52,94%
300x300_30(6)	100,00%	100,00%	100,00%	100,00%	100,00%	100,00%	91,67%	100,00%	100,00%	100,00%
300x300_30(12)	100,00%	100,00%	100,00%	100,00%	100,00%	100,00%	100,00%	100,00%	100,00%	100,00%
300x300_30(18)	100,00%	94,74%	62,50%	100,00%	53,33%	100,00%	100,00%	93,33%	100,00%	100,00%
300x300_30(24)	81,82%	44,44%	80,95%	93,42%	88,68%	100,00%	100,00%	100,00%	100,00%	100,00%

	I_{SC}(MO-FA,MO-VNS*)					I_{SC}(MO-FA,MO-ABC)				
	Evaluations (Stop condition)					Evaluations (Stop condition)				
Instance($\tilde{s}_r$)	50 000	100 000	200 000	300 000	400 000	50 000	100 000	200 000	300 000	400 000
50x50_30(1)	100,00%	90,91%	100,00%	100,00%	92,86%	99,34%	52,59%	99,33%	100,00%	100,00%
100x100_30(2)	36,22%	52,24%	57,66%	48,92%	56,83%	80,71%	89,89%	93,09%	96,22%	96,50%
100x100_30(3)	0,00%	13,50%	36,90%	3,88%	26,88%	27,47%	14,94%	23,66%	8,89%	42,58%
200x200_30(2)	80,00%	20,00%	57,14%	0,00%	33,33%	100,00%	100,00%	92,41%	41,18%	0,00%
200x200_30(4)	0,00%	66,67%	75,00%	100,00%	100,00%	100,00%	100,00%	100,00%	100,00%	100,00%
200x200_30(6)	100,00%	100,00%	63,64%	37,50%	100,00%	68,18%	45,00%	88,24%	85,29%	95,45%
200x200_30(9)	45,45%	50,00%	63,16%	76,19%	40,74%	100,00%	72,73%	42,86%	40,91%	59,26%
300x300_30(6)	100,00%	100,00%	100,00%	100,00%	100,00%	98,44%	99,36%	99,92%	6,25%	100,00%
300x300_30(12)	100,00%	100,00%	100,00%	100,00%	100,00%	100,00%	100,00%	100,00%	100,00%	100,00%
300x300_30(18)	71,43%	28,57%	83,33%	100,00%	100,00%	100,00%	85,00%	67,86%	41,67%	40,00%
300x300_30(24)	100,00%	100,00%	100,00%	83,33%	100,00%	100,00%	100,00%	100,00%	100,00%	100,00%

	I_{SC}(MO-FA,MO-GSA)					I_{SC}(MO-FA,MOEA/D)				
	Evaluations (Stop condition)					Evaluations (Stop condition)				
Instance($\tilde{s}_r$)	50 000	100 000	200 000	300 000	400 000	50 000	100 000	200 000	300 000	400 000
50x50_30(1)	100,00%	100,00%	100,00%	100,00%	100,00%	100,00%	100,00%	100,00%	100,00%	100,00%
100x100_30(2)	60,49%	80,49%	76,85%	56,90%	72,22%	65,22%	61,04%	70,73%	67,80%	70,00%
100x100_30(3)	76,60%	75,76%	68,29%	41,67%	48,33%	62,75%	47,17%	83,93%	89,36%	86,27%
200x200_30(2)	100,00%	100,00%	100,00%	100,00%	88,89%	100,00%	100,00%	100,00%	100,00%	100,00%
200x200_30(4)	100,00%	66,67%	100,00%	100,00%	100,00%	25,00%	75,00%	100,00%	100,00%	100,00%
200x200_30(6)	81,82%	100,00%	75,00%	100,00%	72,73%	55,56%	91,67%	91,67%	100,00%	100,00%
200x200_30(9)	100,00%	92,31%	94,74%	78,57%	90,48%	100,00%	90,00%	100,00%	100,00%	91,67%
300x300_30(6)	100,00%	100,00%	100,00%	100,00%	100,00%	40,00%	57,14%	100,00%	87,50%	100,00%
300x300_30(12)	100,00%	100,00%	100,00%	100,00%	100,00%	100,00%	58,33%	100,00%	100,00%	100,00%
300x300_30(18)	100,00%	100,00%	92,86%	75,00%	100,00%	57,14%	100,00%	100,00%	100,00%	100,00%
300x300_30(24)	100,00%	92,11%	100,00%	100,00%	100,00%	75,00%	62,50%	70,37%	76,00%	86,96%

Table C.13: Set coverage metric by comparing all the metaheuristics two by two. Part 8 of 10.

	I_{SC}(MO-GSA,NSGA-II)					I_{SC}(MO-GSA,SPEA2)				
	Evaluations (Stop condition)					Evaluations (Stop condition)				
Instance($\tilde{s}_r$)	**50 000**	**100 000**	**200 000**	**300 000**	**400 000**	**50 000**	**100 000**	**200 000**	**300 000**	**400 000**
50x50_30(1)	87,50%	38,89%	66,67%	98,96%	94,59%	69,57%	77,01%	94,68%	99,12%	98,25%
100x100_30(2)	90,55%	99,55%	95,73%	95,85%	94,80%	92,50%	99,36%	100,00%	99,56%	100,00%
100x100_30(3)	96,48%	99,52%	94,74%	93,86%	97,28%	98,84%	100,00%	100,00%	98,94%	99,50%
200x200_30(2)	100,00%	100,00%	100,00%	100,00%	0,00%	91,67%	100,00%	0,80%	100,00%	0,00%
200x200_30(4)	97,39%	96,42%	97,49%	0,00%	0,00%	57,14%	97,06%	100,00%	0,00%	0,07%
200x200_30(6)	100,00%	92,86%	100,00%	88,24%	89,13%	100,00%	85,71%	92,86%	95,65%	72,73%
200x200_30(9)	90,00%	100,00%	100,00%	100,00%	100,00%	40,00%	100,00%	100,00%	100,00%	75,00%
300x300_30(6)	76,99%	92,52%	1,55%	39,29%	45,50%	51,22%	86,70%	94,82%	81,95%	99,86%
300x300_30(12)	100,00%	100,00%	100,00%	100,00%	100,00%	100,00%	100,00%	100,00%	3,23%	100,00%
300x300_30(18)	50,00%	14,29%	77,78%	35,29%	93,33%	0,00%	0,00%	0,00%	14,29%	46,67%
300x300_30(24)	40,00%	0,00%	0,00%	61,70%	93,75%	0,00%	0,00%	30,95%	0,00%	0,00%

	I_{SC}(MO-GSA,MO-VNS)					I_{SC}(MO-GSA,MO-VNS*)				
	Evaluations (Stop condition)					Evaluations (Stop condition)				
Instance($\tilde{s}_r$)	**50 000**	**100 000**	**200 000**	**300 000**	**400 000**	**50 000**	**100 000**	**200 000**	**300 000**	**400 000**
50x50_30(1)	0,00%	28,57%	0,00%	14,29%	28,57%	25,00%	54,55%	0,00%	14,29%	28,57%
100x100_30(2)	15,27%	5,84%	30,43%	57,86%	50,00%	14,96%	5,22%	31,39%	58,27%	51,08%
100x100_30(3)	2,96%	0,00%	1,00%	5,86%	6,17%	0,53%	10,13%	24,60%	0,86%	17,00%
200x200_30(2)	0,00%	0,00%	0,00%	0,00%	0,00%	0,00%	0,00%	0,00%	0,00%	0,00%
200x200_30(4)	0,00%	16,67%	12,50%	9,09%	0,00%	0,00%	0,00%	0,00%	0,00%	0,00%
200x200_30(6)	0,00%	27,27%	33,33%	27,27%	0,00%	68,75%	36,36%	27,27%	0,00%	0,00%
200x200_30(9)	0,00%	0,00%	31,82%	6,25%	11,76%	0,00%	9,09%	21,05%	19,05%	0,00%
300x300_30(6)	22,22%	41,67%	100,00%	100,00%	100,00%	0,00%	14,29%	60,00%	14,29%	100,00%
300x300_30(12)	100,00%	100,00%	100,00%	100,00%	100,00%	66,67%	100,00%	100,00%	100,00%	100,00%
300x300_30(18)	42,86%	0,00%	0,00%	17,65%	0,00%	0,00%	0,00%	0,00%	25,00%	0,00%
300x300_30(24)	62,50%	0,00%	100,00%	94,74%	100,00%	0,00%	0,00%	8,33%	41,67%	0,00%

	I_{SC}(MO-GSA,MO-ABC)					I_{SC}(MO-GSA,MO-FA)				
	Evaluations (Stop condition)					Evaluations (Stop condition)				
Instance($\tilde{s}_r$)	**50 000**	**100 000**	**200 000**	**300 000**	**400 000**	**50 000**	**100 000**	**200 000**	**300 000**	**400 000**
50x50_30(1)	0,00%	20,00%	72,48%	56,08%	59,12%	0,00%	26,67%	0,00%	13,33%	26,67%
100x100_30(2)	38,78%	47,87%	70,05%	82,92%	88,69%	32,63%	17,12%	44,35%	66,67%	65,89%
100x100_30(3)	12,09%	4,55%	2,15%	5,56%	22,53%	10,81%	22,22%	14,40%	40,88%	27,27%
200x200_30(2)	10,00%	20,00%	87,34%	0,00%	0,00%	0,00%	0,00%	0,00%	0,00%	0,00%
200x200_30(4)	45,33%	95,00%	37,04%	0,00%	0,00%	0,00%	8,33%	0,00%	0,00%	0,00%
200x200_30(6)	0,00%	30,00%	14,71%	17,65%	13,64%	33,33%	27,27%	10,00%	30,77%	0,00%
200x200_30(9)	26,67%	13,64%	4,76%	0,00%	0,00%	0,00%	0,00%	0,00%	0,00%	0,00%
300x300_30(6)	9,38%	0,00%	4,81%	0,00%	0,48%	0,00%	0,00%	0,00%	0,00%	0,00%
300x300_30(12)	100,00%	33,33%	90,48%	7,69%	1,64%	0,00%	0,00%	0,00%	0,00%	0,00%
300x300_30(18)	41,67%	10,00%	0,00%	0,00%	0,00%	0,00%	0,00%	0,00%	0,00%	0,00%
300x300_30(24)	36,36%	93,33%	58,82%	100,00%	50,00%	0,00%	0,00%	0,00%	0,00%	0,00%

Table C.14: Set coverage metric by comparing all the metaheuristics two by two. Part 9 of 10.

	I_{SC}(MO-GSA,MOEA/D)					I_{SC}(MOEA/D,NSGA-II)				
	Evaluations (Stop condition)					Evaluations (Stop condition)				
Instance($\tilde{s}_r$)	**50 000**	**100 000**	**200 000**	**300 000**	**400 000**	**50 000**	**100 000**	**200 000**	**300 000**	**400 000**
50x50_30(1)	23,08%	78,57%	46,67%	66,67%	73,33%	62,50%	38,89%	39,39%	28,13%	86,49%
100x100_30(2)	56,52%	50,65%	60,98%	62,71%	68,33%	76,62%	80,00%	75,50%	76,42%	82,80%
100x100_30(3)	62,75%	58,49%	62,50%	100,00%	74,51%	45,07%	28,37%	59,81%	54,27%	58,16%
200x200_30(2)	0,00%	28,57%	60,00%	100,00%	25,00%	100,00%	98,21%	61,22%	24,22%	8,75%
200x200_30(4)	0,00%	0,00%	77,78%	0,00%	33,33%	99,13%	99,76%	0,00%	0,00%	0,00%
200x200_30(6)	44,44%	91,67%	66,67%	50,00%	42,86%	87,50%	57,14%	78,95%	82,35%	82,61%
200x200_30(9)	38,46%	70,00%	100,00%	100,00%	91,67%	90,00%	40,00%	25,00%	15,00%	5,88%
300x300_30(6)	0,00%	0,00%	23,08%	12,50%	30,00%	100,00%	99,53%	1,55%	40,66%	15,30%
300x300_30(12)	0,00%	58,33%	100,00%	50,00%	100,00%	100,00%	100,00%	100,00%	100,00%	46,15%
300x300_30(18)	42,86%	0,00%	30,00%	45,00%	63,16%	50,00%	57,14%	55,56%	58,82%	20,00%
300x300_30(24)	0,00%	0,00%	51,85%	48,00%	86,96%	80,00%	0,00%	0,00%	6,38%	0,00%

	I_{SC}(MOEA/D,SPEA2)					I_{SC}(MOEA/D,MO-VNS)				
	Evaluations (Stop condition)					Evaluations (Stop condition)				
Instance($\tilde{s}_r$)	**50 000**	**100 000**	**200 000**	**300 000**	**400 000**	**50 000**	**100 000**	**200 000**	**300 000**	**400 000**
50x50_30(1)	86,96%	77,01%	87,23%	85,96%	78,95%	25,00%	28,57%	28,57%	28,57%	14,29%
100x100_30(2)	82,50%	86,97%	91,55%	86,65%	89,93%	0,00%	0,73%	2,17%	12,14%	12,14%
100x100_30(3)	22,09%	22,68%	87,69%	60,64%	53,55%	15,98%	2,79%	1,99%	0,00%	2,64%
200x200_30(2)	100,00%	100,00%	0,68%	8,74%	99,81%	0,00%	0,00%	0,00%	0,00%	0,00%
200x200_30(4)	100,00%	100,00%	0,56%	0,06%	0,14%	63,64%	33,33%	6,25%	27,27%	0,00%
200x200_30(6)	83,33%	14,29%	85,71%	78,26%	72,73%	0,00%	0,00%	0,00%	9,09%	9,09%
200x200_30(9)	60,00%	71,43%	11,11%	0,00%	16,67%	0,00%	0,00%	0,00%	0,00%	17,65%
300x300_30(6)	100,00%	92,55%	94,82%	88,56%	98,53%	55,56%	58,33%	100,00%	100,00%	100,00%
300x300_30(12)	92,31%	100,00%	82,05%	0,00%	0,00%	100,00%	100,00%	100,00%	100,00%	100,00%
300x300_30(18)	33,33%	5,26%	0,00%	0,00%	0,00%	42,86%	47,06%	20,00%	41,18%	0,00%
300x300_30(24)	36,36%	5,56%	64,29%	0,00%	0,00%	62,50%	20,00%	30,00%	0,00%	0,00%

	I_{SC}(MOEA/D,MO-VNS*)					I_{SC}(MOEA/D,MO-ABC)				
	Evaluations (Stop condition)					Evaluations (Stop condition)				
Instance($\tilde{s}_r$)	**50 000**	**100 000**	**200 000**	**300 000**	**400 000**	**50 000**	**100 000**	**200 000**	**300 000**	**400 000**
50x50_30(1)	25,00%	36,36%	28,57%	28,57%	14,29%	29,80%	19,26%	46,31%	42,86%	54,01%
100x100_30(2)	0,00%	1,49%	2,19%	12,23%	12,23%	8,39%	10,99%	8,29%	3,94%	5,41%
100x100_30(3)	9,47%	11,39%	20,24%	0,00%	2,77%	12,09%	1,30%	0,72%	0,00%	3,85%
200x200_30(2)	0,00%	0,00%	0,00%	0,00%	22,22%	60,00%	40,00%	87,34%	0,00%	0,00%
200x200_30(4)	0,00%	0,00%	0,00%	0,00%	0,00%	100,00%	100,00%	66,67%	0,00%	0,00%
200x200_30(6)	50,00%	0,00%	0,00%	12,50%	9,09%	0,00%	0,00%	0,00%	5,88%	9,09%
200x200_30(9)	0,00%	9,09%	10,53%	0,00%	0,00%	13,33%	18,18%	0,00%	0,00%	0,00%
300x300_30(6)	71,43%	57,14%	80,00%	42,86%	100,00%	100,00%	17,68%	4,81%	6,25%	0,32%
300x300_30(12)	93,33%	0,00%	57,14%	37,50%	46,67%	100,00%	33,33%	0,00%	0,00%	0,00%
300x300_30(18)	0,00%	0,00%	0,00%	0,00%	0,00%	33,33%	10,00%	0,00%	2,78%	0,00%
300x300_30(24)	0,00%	0,00%	0,00%	0,00%	0,00%	100,00%	93,33%	52,94%	68,97%	0,00%

Table C.15: Set coverage metric by comparing all the metaheuristics two by two. Part 10 of 10.

	I_{SC}(MOEA/D,MO-FA)					I_{SC}(MOEA/D,MO-GSA)				
	Evaluations (Stop condition)					Evaluations (Stop condition)				
Instance($\tilde{s}_r$)	**50 000**	**100 000**	**200 000**	**300 000**	**400 000**	**50 000**	**100 000**	**200 000**	**300 000**	**400 000**
50x50_30(1)	14,29%	26,67%	28,57%	26,67%	13,33%	36,36%	54,55%	30,00%	46,67%	27,27%
100x100_30(2)	5,26%	16,22%	11,30%	12,20%	12,40%	14,81%	15,85%	20,37%	9,48%	10,19%
100x100_30(3)	19,82%	23,02%	5,60%	2,19%	4,13%	40,43%	13,64%	7,32%	0,00%	8,33%
200x200_30(2)	0,00%	0,00%	0,00%	0,00%	0,00%	100,00%	63,64%	0,00%	0,00%	11,11%
200x200_30(4)	28,57%	8,33%	0,00%	0,00%	0,00%	100,00%	66,67%	0,00%	50,00%	33,33%
200x200_30(6)	33,33%	0,00%	0,00%	7,69%	9,09%	18,18%	0,00%	0,00%	23,08%	45,45%
200x200_30(9)	0,00%	0,00%	0,00%	0,00%	0,00%	25,00%	23,08%	0,00%	0,00%	4,76%
300x300_30(6)	14,29%	17,65%	0,00%	0,00%	0,00%	100,00%	100,00%	61,54%	66,67%	33,33%
300x300_30(12)	0,00%	0,00%	0,00%	0,00%	0,00%	33,33%	0,00%	0,00%	0,00%	0,00%
300x300_30(18)	0,00%	0,00%	0,00%	0,00%	0,00%	44,44%	69,23%	64,29%	50,00%	18,75%
300x300_30(24)	0,00%	0,00%	0,00%	0,00%	0,00%	92,86%	84,21%	3,85%	28,57%	0,00%

References

[1] Jennifer Yick Biswanath Mukherjee and Dipak Ghosal. Wireless sensor network survey. *Computer Networks*, 52:2292–2330, 2008. 1

[2] Xiuzhen Cheng, B. Narahari, R. Simha, M.X. Cheng, and D. Liu. Strong minimum energy topology in wireless sensor networks: Np-completeness and heuristics. *IEEE Transactions on Mobile Computing*, 2:248–256, 2003. 1

[3] Jae-Hwan Chang and L. Tassiulas. Maximum lifetime routing in wireless sensor networks. *IEEE/ACM Transactions on Networking*, 12:609–619, 2004. 1

[4] Ilhem Boussaïd, Julien Lepagnot, and Patrick Siarry. A survey on optimization metaheuristics. *Information Sciences*, 237(0):82–117, 2013. 1

[5] I.F. Akyildiz, Weilian Su, Y. Sankarasubramaniam, and E. Cayirci. A survey on sensor networks. *IEEE Communications Magazine*, 40:102–114, 2002. 2

[6] Y.T. Hou, Yi Shi, H.D. Sherali, and S.F. Midkiff. On energy provisioning and relay node placement for wireless sensor networks. *IEEE Transactions on Wireless Communications*, 4:2579–2590, 2005. 2, 85

[7] Michael R. Garey and David S. Johnson. *Computers and Intractability: A Guide to the Theory of NP-Completeness*. W. H. Freeman & Co., 1979. 3

[8] Kalyanmoy Deb, Amrit Pratap, Sameer Agarwal, and T. Meyarivan. A fast elitist multi-objective genetic algorithm: Nsga-ii. *IEEE Transactions on Evolutionary Computation*, 6:182–197, 2000. 5, 19, 29

[9] Eckart Zitzler, Marco Laumanns, and Lothar Thiele. Spea2: Improving the strength pareto evolutionary algorithm. Technical report, Computer Engineering and Networks Laboratory (TIK), ETH Zurich, 2001. 5, 31

[10] Qingfu Zhang and Hui Li. Moea/d: A multiobjective evolutionary algorithm based on decomposition. *IEEE Transactions on Evolutionary Computation*, 11(6):712–731, 2007. 5, 44

[11] N. MladenoviÄ‡ and P. Hansen. Variable neighborhood search. *Computers and Operations Research*, 24:1097–1100, 1997. 5, 33

[12] Esmat Rashedi, Hossein Nezamabadi-pour, and Saeid Saryazdi. Gsa: A gravitational search algorithm. *Information Sciences*, 179:2232–2248, 2009. 5, 40

[13] Xin-She Yang. Firefly algorithms for multimodal optimization. In *Stochastic Algorithms: Foundations and Applications*, volume 5792 of *Lecture Notes in Computer Science*, pages 169–178. Springer Berlin Heidelberg, 2009. 5, 37

[14] Dervis Karaboga and Bahriye Basturk. A powerful and efficient algorithm for numerical function optimization: artificial bee colony (abc) algorithm. *Journal of Global Optimization*, 39:459–471, 2007. 5, 35

[15] Eckart Zitzler. *Evolutionary Algorithms for Multiobjective Optimization: Methods and Applications.(Doctoral dissertation)*. Swiss Federal Institute of Technology (ETH), 1999. 7, 18, 54, 92

[16] J. Knowles, L. Thiele, and E. Zitzler. A tutorial on the performance assessment of stochastic multiobjective optimizers. Technical report, Computer Engineering and Networks Laboratory (TIK), ETH Zurich, Switzerland, 2006. 9, 16

[17] Alexander Schrijver. *Theory of Linear and Integer Programming*. John Wiley & Sons, Inc., 1986. 10

[18] Francesca Rossi, Peter Van Beek, and Toby Walsh. *Handbook of constraint programming*. Elsevier, 2006. 10

[19] Vijay V. Vazirani. *Approximation Algorithms*. Springer-Verlag New York, Inc., New York, NY, USA, 2001. 10

[20] Fred Glover. Future paths for integer programming and links to artificial intelligence. *Computers and Operations Research*, 13(5):533–549, 1986. 10

[21] IbrahimH. Osman and Gilbert Laporte. Metaheuristics: A bibliography. *Annals of Operations Research*, 63(5):511–623, 1996. 11

[22] *Meta-Heuristics: Advances and Trends in Local Search Paradigms for Optimization*. Kluwer Academic Publishers, Norwell, MA, USA, 1999. 11

[23] Thomas G Stützle. *Local search algorithms for combinatorial problems: analysis, improvements, and new applications*, volume 220. Infix Sankt Augustin, Germany, 1999. 11

[24] Marco Dorigo, Mauro Birattari, and Thomas Stützle. Metaheuristic. In *Encyclopedia of Machine Learning*, pages 662–662. Springer US, 2010. 11

[25] T. Back. *Evolutionary Algorithms in Theory and Practice: Evolution Strategies, Evolutionary Programming, Genetic Algorithms*. Oxford University Press, 1996. 12, 13

[26] J. Kennedy and R. Eberhart. Particle swarm optimization. In *Neural Networks, 1995. Proceedings., IEEE International Conference on*, volume 4, pages 1942–1948, 1995. 14

[27] Marco Dorigo, Vittorio Maniezzo, and Alberto Colorni. Ant system: optimization by a colony of cooperating agents. *IEEE Transactions on Systems, Man, and Cybernetics, Part B: Cybernetics*, 26(1):29–41, 1996. 14

[28] V. Granville, M. Krivánek, and J. P. Rasson. Simulated annealing: A proof of convergence. *IEEE Transactions on Pattern Analysis and Machine Intelligence*, 16(6):652–656, 1994. 14

[29] Fred Glover. Future paths for integer programming and links to artificial intelligence. *Computers and Operations Research*, 13(5):533–549, 1986. 14

[30] Thomas A Feo and Mauricio GC Resende. Greedy randomized adaptive search procedures. *Journal of global optimization*, 6(2):109–133, 1995. 14

[31] Chris Voudouris and Edward Tsang. Function optimization using guided local search. *University of Essex, Technical Report CSM-249, Colchester, UK*, 1995. 14

[32] Helena R Lourenço, Olivier C Martin, and Thomas Stützle. *Iterated local search*. Springer, 2003. 14

[33] El-Ghazali Talbi. *Metaheuristics: From Design to Implementation*. Wiley Publishing, 2009. 15

[34] Christian Blum and Andrea Roli. Metaheuristics in combinatorial optimization: Overview and conceptual comparison. *ACM COMPUTING SURVEYS*, pages 268–308, 2003. 15

[35] R. Chiong. *Nature-Inspired Algorithms for Optimisation*. Studies in Computational Intelligence. Springer Berlin Heidelberg, 2009. 15

[36] Carlos Coello Coello, Gary B Lamont, and David A Van Veldhuizen. *Evolutionary algorithms for solving multi-objective problems*. Springer Science & Business Media, 2007. 16

[37] E. Zitzler and L. Thiele. Multiobjective evolutionary algorithms: a comparative case study and the strength pareto approach. *IEEE Transactions on Evolutionary Computation*, 3:257–271, 1999. 17, 31

[38] E. Zitzler, L. Thiele, M. Laumanns, C.M. Fonseca, and V.G. da Fonseca. Performance assessment of multiobjective optimizers: an analysis and review. *IEEE Transactions on Evolutionary Computation*, 7(2):117–132, 2003. 17, 18

[39] David Allen Van Veldhuizen. *Multiobjective Evolutionary Algorithms: Classifications, Analyses, and New Innovations*. PhD thesis, Wright Patterson AFB, OH, USA, 1999. 19

[40] CarlosA.Coello Coello and NareliCruz Cortes. Solving multiobjective optimization problems using an artificial immune system. *Genetic Programming and Evolvable Machines*, 6(2):163–190, 2005. 19

[41] Carlos M. Fonseca and Peter J. Fleming. On the performance assessment and comparison of stochastic multiobjective optimizers. In *Proceedings of PPNS IV*, pages 584–593, 1996. 20

[42] G. S. Almasi and A. Gottlieb. *Highly Parallel Computing*. Benjamin-Cummings Publishing Co., Inc., Redwood City, CA, USA, 1989. 20

[43] Blaise Barney et al. Introduction to parallel computing. *Lawrence Livermore National Laboratory*, 6(13):10, 2010. 20

[44] M. Flynn. Some computer organizations and their effectiveness. *IEEE Transactions on Computers*, C-21(9):948–960, 1972. 23

[45] David A Patterson and John L Hennessy. *Computer organization and design: the hardware/software interface*. Newnes, 2013. 23

[46] Ted G. Lewis and Hesham El-Rewini. *Introduction to Parallel Computing*. Prentice-Hall, Inc., Upper Saddle River, NJ, USA, 1992. 26

[47] Gene M. Amdahl. Validity of the single processor approach to achieving large scale computing capabilities. In *Proceedings of the April 18-20, 1967, Spring Joint Computer Conference*, pages 483–485, 1967. 27

[48] N. Srinivas and Kalyanmoy Deb. Multiobjective optimization using nondominated sorting in genetic algorithms. *Evolutionary Computation*, 2:221–248, 1994. 29

[49] Martin Josef Geiger. Randomised variable neighbourhood search for multi objective optimisation. In *Proceedings of EU/ME Workshop*, volume 0809.0271, pages 34–42, 2008. 33, 35

[50] I. Das and J. Dennis. Normal-boundary intersection: A new method for generating the pareto surface in nonlinear multicriteria optimization problems. *Journal on Optimization*, 8(3):631–657, 1998. 44

[51] Qingfu Zhang, Hui Li, D. Maringer, and E. Tsang. Moea/d with nbi-style tchebycheff approach for portfolio management. In *IEEE Congress on Evolutionary Computation (CEC)*, pages 1–8, 2010. 44

[52] Alvaro Rubio-Largo, Qingfu Zhang, and Miguel A. Vega-Rodriguez. A multiobjective evolutionary algorithm based on decomposition with normal boundary intersection for traffic grooming in optical networks. *Information Sciences*, 289(0):91–116, 2014. 44

[53] Thomas H Cormen, Charles E Leiserson, Ronald L Rivest, and Clifford Stein. *Introduction to Algorithms(Third Edition)*. The MIT Press, 2009. 51

[54] Wei Ye, J. Heidemann, and D. Estrin. An energy-efficient mac protocol for wireless sensor networks. In *Proceedings of INFOCOM*, volume 3, pages 1567–1576, 2002. 51

[55] A. Konstantinidis, Kun Yang, and Qingfu Zhang. An evolutionary algorithm to a multiobjective deployment and power assignment problem in wireless sensor networks. In *Proceedings of IEEE GLOBECOM*, pages 1–6, 2008. 51, 54, 92, 113

[56] MP Fewell. Area of common overlap of three circles. Technical report, DTIC Document, 2006. 52

[57] Bang Wang. Coverage problems in sensor networks: A survey. *ACM Computing Surveys*, 43:32:1–32:53, 2011. 52

[58] Isabel Dietrich and Falko Dressler. On the lifetime of wireless sensor networks. *ACM Transactions on Sensor Networks*, 5:1–39, 2009. 53

[59] Giuseppe Anastasi, Marco Conti, Mario Di Francesco, and Andrea Passarella. Energy conservation in wireless sensor networks: A survey. *Ad Hoc Networks*, 7(3):537–568, 2009. 54, 92

[60] Chuan Zhu, Chunlin Zheng, Lei Shu, and Guangjie Han. A survey on coverage and connectivity issues in wireless sensor networks. *Journal of Network and Computer Applications*, 35(2):619–632, 2012. 54, 92

[61] Andreas Konstantinidis and Kun Yang. Multi-objective k-connected deployment and power assignment in wsns using a problem-specific constrained evolutionary algorithm based on decomposition. *Computer Communications*, 34:83–98, 2011. 54, 55, 92, 115

[62] M. Le Berre, F. Hnaien, and H. Snoussi. Multi-objective optimization in wireless sensors networks. In *Proceedings of ICM*, volume 1, pages 1–4, 2011. 54, 92

[63] Andreas Konstantinidis and Kun Yang. Multi-objective energy-efficient dense deployment in wireless sensor networks using a hybrid problem-specific moea/d. *Applied Soft Computing*, 11:4117–4134, 2011. 54, 92

[64] Andreas Konstantinidis, Kun Yang, Qingfu Zhang, and Demetrios Zeinalipour-Yazti. A multi-objective evolutionary algorithm for the deployment and power assignment problem in wireless sensor networks. *Computer Networks*, 54:960–976, 2010. 54, 92

[65] Jose M. Lanza-Gutierrez, Juan A. Gomez-Pulido, Miguel A. Vega-Rodriguez, and Juan M. Sanchez-Perez. Instance sets for optimization in wireless sensor networks. http://arco.unex.es/wsnopt, 2011. 54, 115

[66] F.V.C. Martins, E.G. Carrano, E.F. Wanner, R.H.C. Takahashi, and G.R. Mateus. A hybrid multiobjective evolutionary approach for improving the performance of wireless sensor networks. *IEEE Sensors Journal*, 11:545–554, 2011. 55, 115

[67] Hubert W Lilliefors. On the kolmogorov-smirnov test for normality with mean and variance unknown. *Journal of the American Statistical Association*, 62:399–402, 1967. 67, 98

[68] S. S. Shapiro and M. B. Wilk. An analysis of variance test for normality (complete samples). *Biometrika*, 52:591–611, 1965. 67, 98

[69] H. B. Mann and D. R. Whitney. On a test of whether one of two random variables is stochastically larger than the other. *Annals of Mathematical Statistics*, 1:50–60, 1947. 67, 98

[70] Jose M. Lanza-Gutierrez and Juan A. Gomez-Pulido. A gravitational search algorithm for solving the relay node placement problem in wireless sensor networks. *International Journal of Communication Systems*, page online, 2015. 86, 122

[71] Jose M. Lanza-Gutierrez and Juan A. Gomez-Pulido. Studying the multiobjective variable neighbourhood search algorithm when solving the relay node placement problem in wireless sensor networks. *Soft Computing*, page online, 2015. 87, 122

[72] Jose M Lanza-Gutierrez, Juan A Gomez-Pulido, and Miguel A Vega-Rodriguez. Intelligent relay node placement in heterogeneous wireless sensor networks for energy efficiency. *International Journal of Robotics and Automation*, 29:1–13, 2014. 87, 122

[73] Jose M. Lanza-Gutierrez, Juan A. Gomez-Pulido, and Miguel A. Vega-Rodriguez. A trajectory algorithm to solve the relay node placement problem in wireless sensor networks. In *Theory and Practice of Natural Computing*, volume 8273 of *Lecture Notes in Computer Science*, pages 145–156. Springer Berlin Heidelberg, 2013. 87, 122

[74] Jose M. Lanza-Gutierrez, Juan A. Gomez-Pulido, Miguel A. Vega-Rodriguez, and Juan M. Sanchez-Perez. Relay node positioning in wireless sensor networks by means of evolutionary techniques. In *Autonomous and Intelligent Systems*, volume 7326 of *Lecture Notes in Computer Science*, pages 18–25. Springer Berlin / Heidelberg, 2012. 87, 88, 123, 124

[75] Jose M. Lanza-Gutierrez, Juan A. Gomez-Pulido, Miguel A. Vega-Rodriguez, and Juan M. Sanchez-Perez. Optimizing energy consumption in heterogeneous wireless sensor networks by means of evolutionary algorithms. In *Applications of Evolutionary Computation*, volume 7248 of *Lecture Notes in Computer Science*, pages 1–10. Springer Berlin Heidelberg, 2012. 87, 123

[76] Jose M. Lanza-Gutierrez, Juan A. Gomez-Pulido, Miguel A. Vega-Rodriguez, and Juan M. Sanchez-Perez. A parallel evolutionary approach to solve the relay node placement problem in wireless sensor networks. In *Proceeding of GECCO*, pages 1157–1164, 2013. 87, 123

[77] Jose M Lanza-Gutierrez, Juan Gomez-Pulido, Miguel Vega-Rodriguez, and Juan M Sanchez-Perez. Multi-objective evolutionary algorithms for energy-efficiency in heterogeneous wireless sensor networks. In *IEEE Sensors Applications Symposium (SAS)*, pages 1–6, 2012. 87, 123

[78] Jose M Lanza-Gutierrez, Juan A Gomez-Pulido, Oscar Gutierrez-Blanco, Miguel A Vega-Rodriguez, and Juan M Sanchez. Diseño eficiente de redes heterogéneas de sensores inalámbricos mediante computación evolutiva multi-objetivo. In *Actas del VIII Congreso Español sobre Metaheurísticas, Algoritmos Evolutivos y Bioinspirados, Universidad de Castilla-La Mancha*, pages 337–344, 2012. 87, 88, 123, 124

[79] Jose M. Lanza-Gutierrez, Juan A. Gomez-Pulido, Miguel A. Vega-Rodriguez, and Juan M. Sanchez-Perez. Optimizando la eficiencia energética en redes de sensores inalámbricos mediante computación evolutiva paralela. In *Actas de las XXIII Jornadas de Paralelismo (JP 2012), Servicio de Publicaciones. Universidad Miguel Hernandez*, pages 163–168, 2012. 88, 124

[80] Jose M. Lanza-Gutierrez, Juan A. Gomez-Pulido, Miguel A. Vega-Rodriguez, and Juan M. Sanchez-Perez. Posicionando routers en redes de sensores inalámbricos mediante algoritmos evolutivos para el incremento de la eficiencia energética. In *Actas de las III Jornadas de Computación Empotrada (JCE 2012), Servicio de Publicaciones. Univ. Miguel Hernandez*, pages 95–100, 2012. 88, 124

[81] Budhaditya Deb, Sudeept Bhatnagar, and Badri Nath. Reliable information forwarding using multiple paths in sensor networks. In *Proceedings of IEEE LCN*, pages 406–415, 2003. 91, 115

[82] J. W. Suurballe. Disjoint paths in a network. *Networks*, 4:125–145, 1974. 91, 114

[83] K. Islam, Weiming Shen, and Xianbin Wang. Wireless sensor network reliability and security in factory automation: A survey. *IEEE Transactions on Systems, Man, and Cybernetics, Part C: Applications and Reviews*, 42(6):1243–1256, 2012. 92

[84] Jose M. Lanza-Gutierrez and Juan A. Gomez-Pulido. Assuming multiobjective metaheuristics to solve a three-objective optimisation problem for relay node deployment in wireless sensor networks. *Applied Soft Computing*, 30:675–687, 2015. 107, 121

[85] Jose M. Lanza-Gutierrez, Juan A. Gomez-Pulido, and Miguel A. Vega-Rodriguez. A new realistic approach for the relay node placement problem in wireless sensor networks by means of evolutionary computation (accepted). *Ad Hoc and Sensor Wireless Networks*, 26:193–209, 2015. 107, 122

[86] Jose M. Lanza-Gutierrez, Juan A. Gomez-Pulido, and Miguel A. Vega-Rodriguez. A trajectory-based heuristic to solve a three-objective optimization problem for wireless sensor network deployment. In *Applications of Evolutionary Computation*, volume 8602 of *Lecture Notes in Computer Science*, pages 27–38. Springer Berlin / Heidelberg, 2014. 107, 122

[87] Jose M. Lanza-Gutierrez, Juan A. Gomez-Pulido, and Miguel A. Vega-Rodriguez. Un nuevo enfoque para el posicionamiento de routers sobre redes de sensores inalámbricos. In *Actas del XV Conferencia de la Asociación Española para la Inteligencia Artificial (CAEPIA 13) - IX Congreso Español sobre Metaheurísticas, Algoritmos Evolutivos y Bioinspirados (MAEB 2013)*, pages 743–752, 2013. 107, 123

[88] H. Mahboubi, K. Moezzi, AG. Aghdam, K. Sayrafian-Pour, and V. Marbukh. Distributed deployment algorithms for improved coverage in a network of wireless mobile sensors. *IEEE Transactions on Industrial Informatics*, 10:163–174, 2014. 115

[89] Jose M. Lanza-Gutierrez, Juan A. Gomez-Pulido, S. Priem-Mendes, M. Ferreira, and J.S. Pereira. Planning the deployment of indoor wireless sensor networks through multiobjective evolutionary techniques. In *Applications of Evolutionary Computation*, volume 9028 of *Lecture Notes in Computer Science*, pages 128–139. Springer International Publishing, 2015. 117, 122

[90] Juan A. Gomez-Pulido and Jose M. Lanza-Gutierrez. Reliability and efficiency in wireless sensor networks: heuristic approaches. *Journal of Heuristics*, 21(2):141–143, 2015. 121

[91] Jose M. Lanza-Gutierrez and Juan A. Gomez-Pulido. Optimización de redes de sensores inalámbricos mediante computación inteligente. In *Actas del XV Conferencia de la Asociación Española para la Inteligencia Artificial (CAEPIA 13) - Doctoral Consortium*, pages 1672–1676, 2013. 123

[92] Juan A Gomez Pulido, Francisco L Morcillo Garcia, Eloy J Diaz Alvarez, Jose M Lanza Gutierrez, Miguel A Vega Rodriguez, and Juan M Sanchez Perez. Experiencias con redes de sensores inalámbricos en la escuela politécnica de la universidad de extremadura. In *Actas de las III Jornadas de Computación Empotrada (JCE 2012), Servicio de Publicaciones. Universidad Miguel Hernández*, pages 114–119, 2012. 124

[93] N.C. Caballe, I.T. Castro, C.J. Perez, and J.M. Lanza-Gutierrez. A condition-based maintenance of a dependent degradation-threshold-shock model in a system with multiple degradation processes. *Reliability Engineering & System Safety*, 134:98–109, 2015. 124

[94] M Ferreira, J Bagarić, Jose M Lanza-Gutierrez, S Priem-Mendes, JS Pereira, and Juan A Gomez-Pulido. On the use of perfect sequences and genetic algorithms for estimating the indoor location of wireless sensors. *International Journal of Distributed Sensor Networks*, 2015, 2015. 125

[95] Jose M. Lanza-Gutierrez, Juan A. Gomez-Pulido, Miguel A. Vega-Rodriguez, and Juan M. Sanchez-Perez. A multi-objective network design for real traffic models of the internet by means of a parallel framework for solving np-hard problems. In *Proceedings of the Third World Congress on Nature and Biologically Inspired Computing (NaBIC), IEEE*, pages 137–142, 2011. 125

[96] Jose M Lanza-Gutierrez, Juan A Gomez-Pulido, Miguel A Vega-Rodriguez, and Juan M Sanchez. Paralelización de una plataforma para la resolución de problemas np-completos mediante algoritmos evolutivos. In *Actas de las XXII Jornadas de Paralelismo (JP2011), Servicio de Publicaciones. Universidad de La Laguna*, pages 63–68, 2011. 125

[97] Jose M Lanza-Gutierrez, Juan A Gomez-Pulido, Miguel A Vega-Rodriguez, and Juan M Sanchez. Resolviendo el diseño de redes para modelos de tráfico reales de internet mediante optimización multiobjetivo en multiprocesadores. In *Actas de las XXII Jornadas de Paralelismo (JP2011), Servicio de Publicaciones. Universidad de La Laguna*, pages 95–100, 2011. 125

Declaration

I herewith declare that I have produced this work without the prohibited assistance of third parties and without making use of aids other than those specified; notions taken over directly or indirectly from other sources have been identified as such. This work has not previously been presented in identical or similar form to any examination board.

The dissertation work was conducted from 2011 to 2015 under the supervision of Prof. Dr. Juan A. and Gómez-Pulido at the University of Extremadura (Spain).

Cáceres,

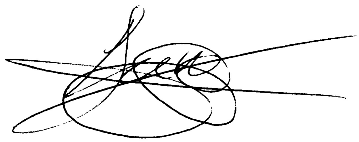

José M. Lanza-Gutiérrez

This dissertation was finished writing in Cáceres (Spain) on Friday 9th October, 2015

This page is intentionally left blank